**ELSEVIER**

# The influence of of cross-linking process on the physicochemical properties of new copolyesters containing xylitol

Marta Piątek-Hnat*, Kuba Bomba

*West Pomeranian University of Technology, Faculty of Chemical Technology and Engineering, Department of Polymer and Biomaterials Science, Piastów Ave. 42, 71-065 Szczecin, Poland*

ABSTRACT

The goal of this research was developing biodegradable and biocompatibile xylitol-based copolymers with improved mechanical properties, and investigating the change in their thermal and chemical properties with progress of the cross-linking process. Using a raw material of natural origin such as xylitol, a prepolymer was obtained by esterification and polycondensation. Then, at subsequent stages of the crosslinking process in a vacuum dryer, samples of materials were taken to determine the progress of the process using Fourier transform infrared spectroscopy. The method of differential scanning calorimetry also defined changes in the ranges of phase changes occurring at each stage of the crosslinking process. After the crosslinking process, ester materials based on sebacic and succinic acid were characterized in terms of mechanical and surface properties.

## 1. Introduction

Polyester materials are very popular among many research teams in the world. This is due to the fact that these materials can be obtained from easily available raw materials and the method of their synthesis allows you to modify them in the direction of the desired properties. Among many types of polyesters, succinic acid copolyesters and sebacic acid copolyesters deserve attention. These copolymers belong to the group of biodegradable aliphatic polyesters.

Despite many advantages, widespread use of biodegradable polyesters is limited due to the limited range of mechanical properties and the difficulty of their modification due to the lack of reactive functional groups. In this paper [1] describes a new class of multiblock copolymers composed of PBF poly (butylene fumarate and PBS poly (butylene succinate. The obtained materials have good thermal and mechanical properties, and as the authors describe the increase in biodegradability. The rate of copolymer degradation was significantly accelerated by copolymerization of PBF with PBS, especially at 50% and higher its share in the copolymer. It has been found that both segments are compatible in both the amorphous and crystalline region, and isomorphic co-crystallization between PBF and PBS occurs in the crystal region, which was the first time. It is noteworthy that the reactive C−C bond found in the copolymer backbone allows the physicochemical properties to be modified as needed.

The article [2] describes the method of preparation and properties of multiblock copolymers composed of poly (butylene succinate) PBS and poly (ε-caprolactone) PCL and with hexamethylene diisocyanate (HDI) as a chain extender. According to the authors, such copolymers could be used in the field of biodegradable polymeric materials. PBS and PCL do not show miscibility in the amorphous phase. However, in the high temperature area two melting temperature of the crystalline phase can be observed. The thermal stability of the copolymers increases with the increase of PBS. However, the mechanical properties can be well regulated by changing the proportion of PBS and PCL, obtaining rigid materials characterized by a high value of stress to break, to elastic elastomers, which is characterized by a high value of strain to break. The authors emphasize that copolymers with 10–30% PCL are characterized by optimal mechanical properties and impact resistance.

Examples of multiblock copolymers are those consisting of crystalline poly (butylene succinate) (PBS) and amorphous poly (1,2-propylene succinate) (PPSu), which were synthesized by chain elongation using hexamethylene diisocyanate (HDI) [3]. Authors of studies ^{13}C NMR confirmed the receipt of copolymers with a sequential structure. They also confirmed that block copolymers have very good mechanical and thermal properties as well as excellent impact strength. The use of the amorphous soft PPSu segment not only gives the copolymers higher impact resistance without lowering the melting point, but also increases the rate of enzymatic degradation.

In the article [4], the authors describe a biodegradable copolymer of

---

* Corresponding author.
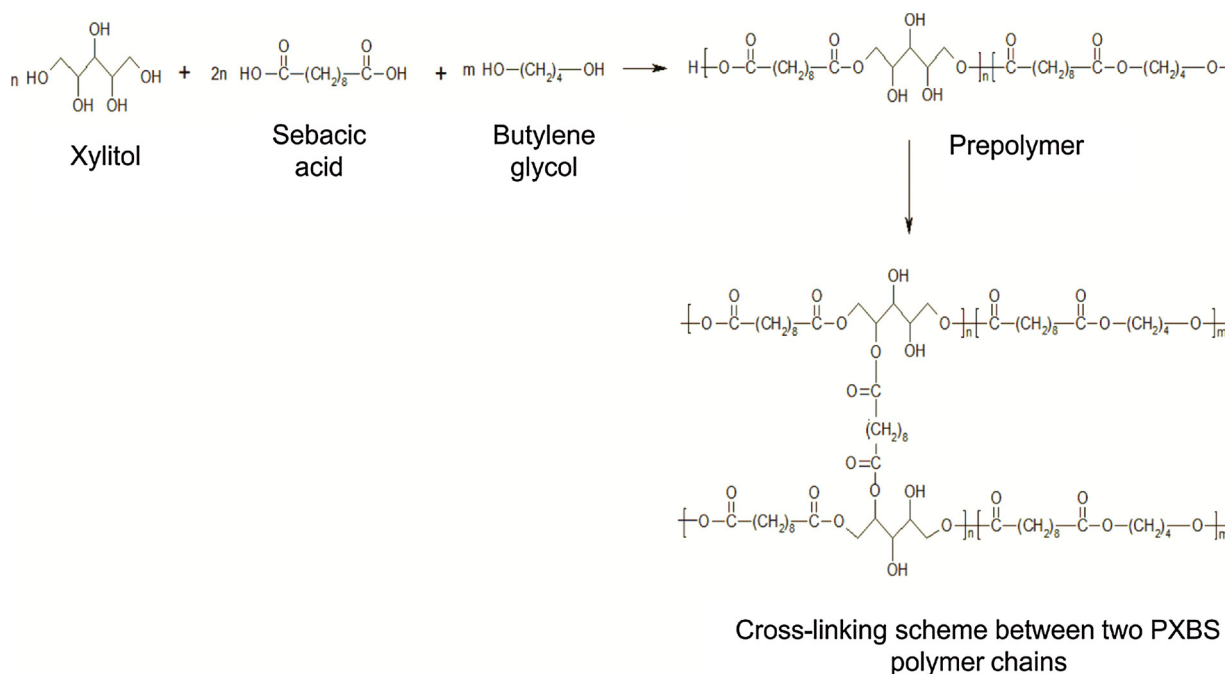 *E-mail address:* marp@zut.edu.pl (M. Piątek-Hnat).

Fig. 1. Scheme of poly(xylitol sebacate-co-butylene sebacate)PXBS structure.
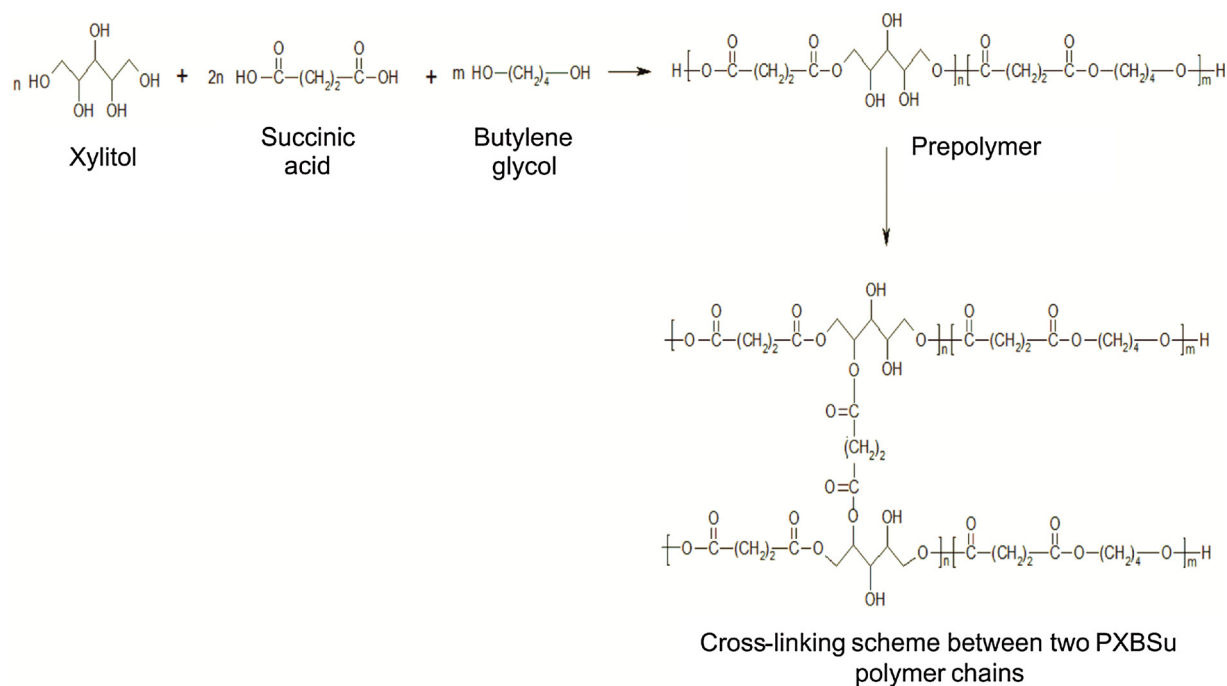


Fig. 2. Scheme of poly(xylitol succinate-co-butylene succinate)PXBSu structure.

**Table 1**
Composition and selected properties of poly(xylitol sebacate-co-butylene sebacate) PXBS after 288 h crosslinking.

| Polymer sample | Molar Composition [mol] | | | H ShA | $\sigma_r$ MPa | $\varepsilon_r$ % | X % | CA |
|---|---|---|---|---|---|---|---|---|
| | Sebacic acid | Xylitol | Butylene glycol | | | | | |
| poly(xylitol sebacate-*co*-butylene sebacate) PXBS | 2 | 1 | 1 | 36 +/−0.42 | 0.93 +/−0.25 | 306 +/−63 | 91 | 46 |

where: H - Hardness, $\sigma_r$ - Stress in break, $\varepsilon$ - Elongation, X - Gel fraction, CA - Contact angle.

**Table 2**
Composition and selected properties of poly(xylitol succinate-co-butylene succinate) PXBSu after 288 h crosslinking.

| Polymer sample | Molar Composition [mol] | | | H ShA | $\sigma_r$ MPa | $\varepsilon_r$ % | X % | CA |
|---|---|---|---|---|---|---|---|---|
| | Succinic acid | Xylitol | Butylene glycol | | | | | |
| poly(xylitol sebacate-*co*-butylene sebacate) PXBSu | 2 | 1 | 1 | 46 +/− 0.68 | 1.5 +/− 0.19 | 248 +/− 83 | 96 | 69 |

where: H - Hardness, $\sigma_r$ - Stress in break, $\varepsilon$ - Elongation, X - Gel fraction, CA - Contact angle.
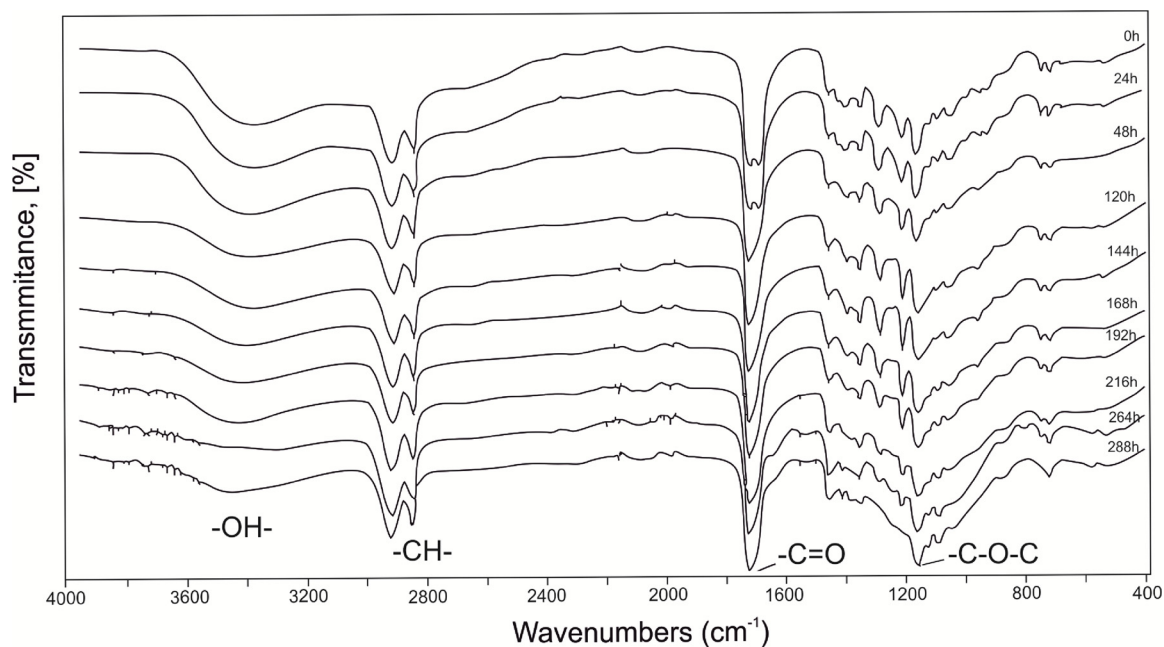


**Fig. 3.** Spectrum ATR-FTIR spectra of pre- PXBS (0 h) and PXBS during the crosslinking process (24 h–288 h).
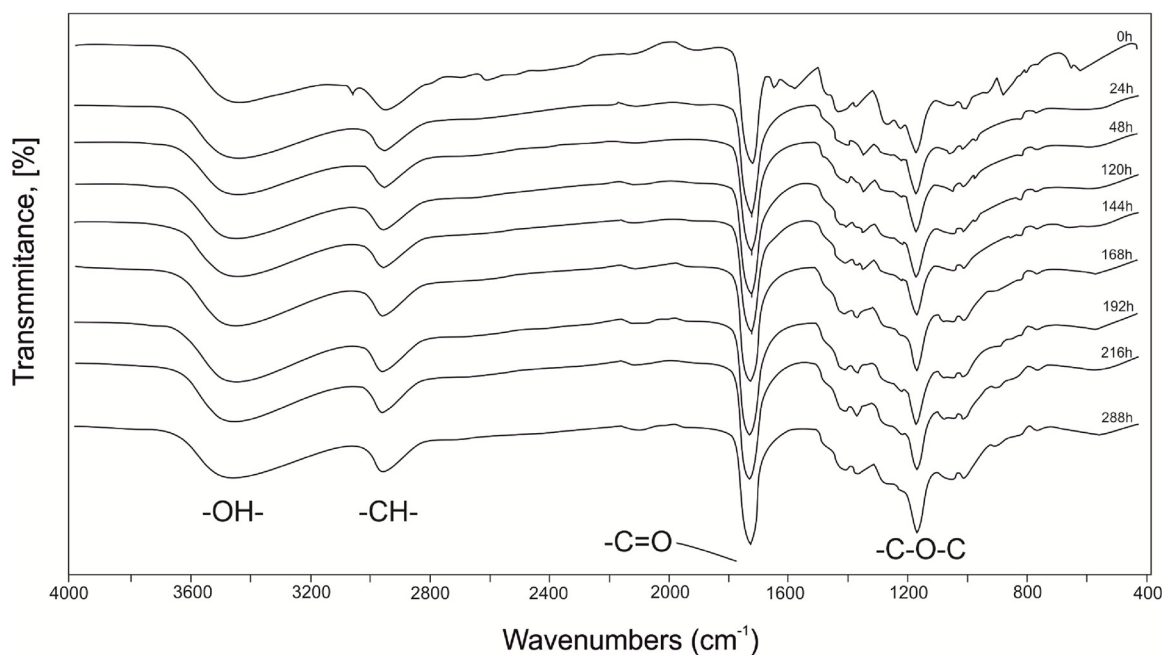


**Fig. 4.** Spectrum ATR-FTIR spectra of pre- PXBSu (0 h) and PXBSu during the crosslinking process (24 h–288 h).

poly (butylene succinate) and a butylene ester of dilinoleic acid (PBS/DLA), which were the coating for multi-component controlled release fertilizer (NPK). It has been shown that the studied PBS/DLA are very interesting materials in the processes of nutrient release due to their biodegradability, which can be extremely important in agricultural cultivation.

Poly(polyol sebacate) polyesters are biocompatible and biodegradable elastomers exhibiting a wide range of potential biomedical applications like scaffolds for treating cartilage defects [5] vascular tissue engineering [6], myocardial tissue engineering [7], and retinal

**Table 3**
Thermal properties of the poly(xylitol sebacate-co-butylene sebacate) PXBS.

| Cross-linking time | First heating | | | | Cooling | | Second heating | | | | | |
|---|---|---|---|---|---|---|---|---|---|---|---|---|
| | $T_{m1}$ [°C] | $\Delta H_{m1}$ [J/g] | $T_{m2}$ [°C] | $\Delta H_{m2}$ [J/g] | $T_{c1}$ [°C] | $\Delta H_{c1}$ [J/g] | $T_{g1}$ [°C] | $\Delta c_p$ [J/g°C] | $T_{m3}$ [°C] | $\Delta H_{m3}$ [J/g] | $T_{m4}$ [°C] | $\Delta H_{m4}$ [J/g] |
| 0 h | 19 | 24.17 | 44.9 | 50.89 | −3.9 | 65.87 | −13.1 | 0.558 | 22.6 | 61.3 | 50.7 | 3.17 |
| 24 h | 18.5 | 28.29 | 42 | 34.38 | −5 | 54.27 | −12 | 0.292 | 21.4 | 61.2 | n.o. | n.o. |
| 48 h | 19.5 | 23.28 | 43.5 | 41.56 | −6.3 | 47.16 | −12.8 | 0.128 | 21.1 | 53.15 | n.o. | n.o. |
| 120 h | 15.8 | 40.09 | 39.9 | 10.86 | −7.4 | 46.93 | −18.4 | 0.339 | 17.5 | 49.84 | n.o. | n.o. |
| 144 h | 17.2 | 34.1 | 41 | 18.18 | −8.8 | 42.77 | −19.3 | 0.426 | 18.3 | 48.41 | n.o. | n.o. |
| 168 h | 16.4 | 36.8 | 40.7 | 10.28 | −10.9 | 39.12 | −21.7 | 0.371 | 17.5 | 45.74 | n.o. | n.o. |
| 192 h | 18.9 | 28.67 | 42.9 | 9.76 | −13.3 | 30.3 | −20.5 | 0.264 | 19.9 | 35.52 | n.o. | n.o. |
| 216 h | 16.5 | 34.35 | 40.6 | 6.42 | −14.3 | 27.87 | −22.9 | 0.209 | 18.2 | 36.04 | n.o. | n.o. |
| 264 h | 19.5 | 32.15 | 43.3 | 3.54 | −18.7 | 25.42 | −26.3 | 0.336 | 20.3 | 34.48 | n.o. | n.o. |
| 288 h | 17.5 | 24.01 | 41.2 | 0.66 | −19 | 15.87 | −28 | 0.248 | 17.6 | 23.18 | n.o. | n.o. |

n.o. - not observed, where: $T_{g1}$ - glass transition temperatures; $\Delta c_p$ - change of the heat capacity at glass transition, $T_{m1}$, $T_{m2}$, $T_{m3}$, $T_{m4}$ - melting temperature; $T_{c1}$ - crystallization temperatures; $\Delta H_{m1}$, $\Delta H_{m2}$, $\Delta H_{m3}$, $\Delta H_{m4}$, - heat of melting at $T_{m1}$, $T_{m2}$, $T_{m3}$, $T_{m4}$; $\Delta H_{c1}$ - crystallization heat in $T_{c1}$.
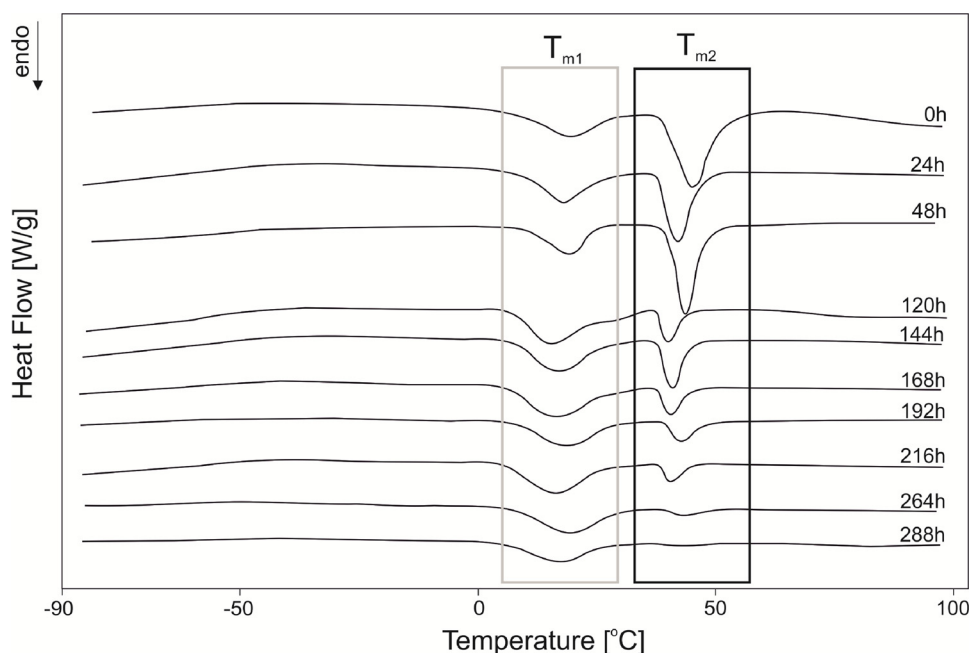


**Fig. 5.** DSC thermograms of poly(xylitol sebacate-co-butylene sebacate) PXBS at the crosslinking stages subjected to first heating.

progenitor cell grafting [8]. They also have potential applications as contact guidance materials [9], hollow conduit neural guides [10], and drug delivery [11]. Polyesters with similar properties to poly(glycerol sebacate) can be synthesized by substituting glycerol with natural polyols like mannitol, sorbitol and xylitol [12]. One of the possible monomers for biodegradable polyester synthesis, xylitol is a sugar alcohol found naturally in fruits and vegetables like lettuce, cauliflower, raspberry, grape, banana and strawberry. It can also be found in yeast, lichens, mushrooms, and seaweed. It is an intermediate in human carbohydrate metabolism, produced by human adults between 5 and 15 g/day [13]. Xylitol-based polymers are of great interest to biomaterials science due to their biocompatibility, and biodegradability. Poly(xylitol sebacate) has been shown to possess in vitro and in vivo biocompatibility comparable to poly(L-lactic-co-glycolic acid) (PLGA) [14–16]. Furthermore, both mechanical properties and degradation rate of polyesters containing xylitol can be fine-tuned by adjusting xylitol: dicarboxylic acid ratio [15,17]. Those properties can also be fine-tuned by adjusting curing time and dicarboxylic acid chain length. [17]. To the best of our knowledge, poly(xylitol sebacate-co-butylene sebacate) and poly(xylitol succinate-co-butylene succinate) have not been previously synthesized by other authors, and are novelty materials. Using butylene glycol as an additional monomer in polyester synthesis

allowed us to obtain copolyesters with improved mechanical properties compared to polyesters synthesized using only polyol and dicarboxylic acid.

## 2. Material and experimental methods

### 2.1. Synthesis and characterization of xylitol-based copolymers

All chemicals except xylitol were purchased from Sigma–Aldrich (St. Louis, MO, USA). Two copolymers containing xylitol were synthesized: poly(xylitol sebacate-*co*-butylene sebacate) with sebacic acid: butylene glycol: xylitol ratio of 2:1:1 (PXBS), and poly(xylitol succinate-co-butylene succinate) with succinic acid: butylene glycol: xylitol ratio of 2:1:1 (PXBSu) Monomers were melted in a round bottom flask in a temperature above 100 °C under a blanket of $N_2$. Following that, esterification reaction was performed for 13,5 h in 150 °C under a blanket of $N_2$, catalyzed by Ti(OBu)$_4$. Then, polycondensation reaction was conducted in 150 °C under vacuum. Prepolymers were then cross-linked in a vacuum-dryer in 100 °C under 100 mBar for 288 h. Samples were taken directly after polycondensation reaction ended, and at consecutive stages of cross-linking process.
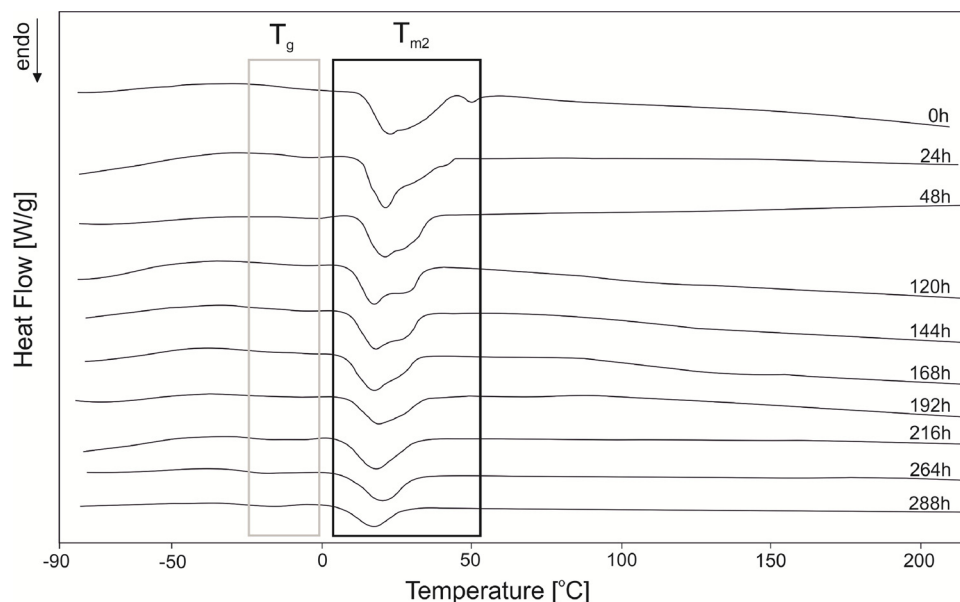
**Fig. 7.** DSC thermograms of poly(xylitol sebacate-co-butylene sebacate) PXBS at the crosslinking stages subjected to second heating.
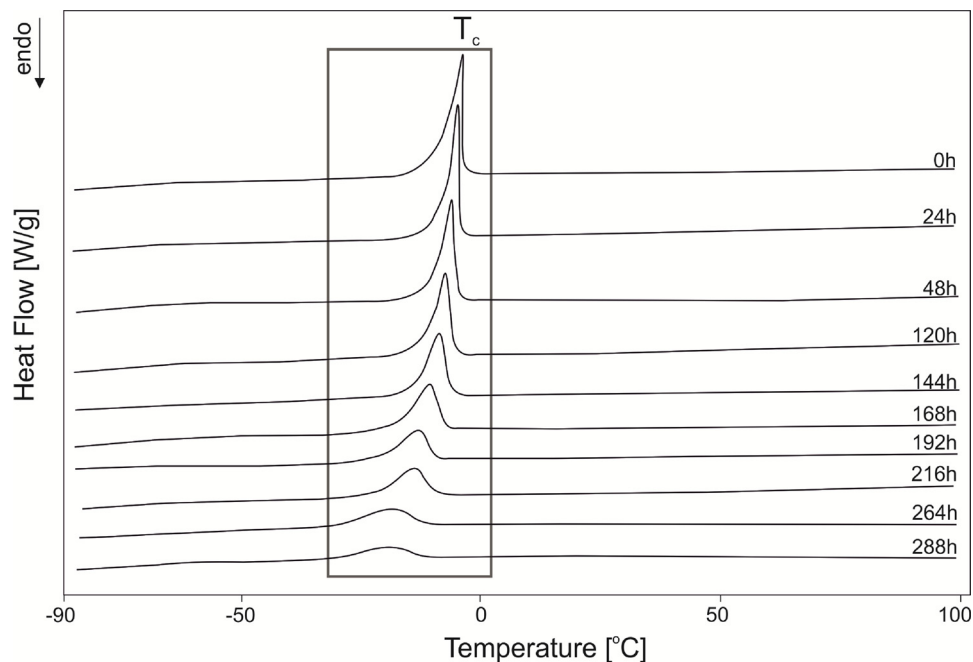


**Fig. 6.** DSC thermograms of poly(xylitol sebacate-co-butylene sebacate PXBS) at the crosslinking stages subjected to cooling.

**Table 4**
Thermal properties of the poly(xylitol succinate-co-butylene succinate)) PXBSu.

| Cross-linking time | First heating | | | | Cooling | | Second heating | |
|---|---|---|---|---|---|---|---|---|
| | Tg$_1$ [°C] | $\Delta$c$_{p1}$ [J/g°C] | Tm$_1$ [°C] | $\Delta$Hm$_1$ [J/g] | Tg$_2$ [°C] | $\Delta$c$_{p2}$ [J/g°C] | T$_{g3}$ [°C] | $\Delta$c$_{p3}$ [J/g°C] |
| 0 h | −19.9 | 0.522 | 46.8 | 15.41 | −26.4 | 0.84 | −15.7 | 0.57 |
| 24 h | −19.2 | 0.48 | 48.1 | 12.82 | −23.5 | 0.606 | −16.9 | 0.519 |
| 48 h | −18.6 | 0.533 | 48.4 | 13.92 | −24.8 | 0.542 | −18.8 | 0.651 |
| 120 h | −17.8 | 0.533 | 47.8 | 12.12 | −23.4 | 0.7 | −17.6 | 0.617 |
| 144 h | −17.6 | 0.596 | 48.5 | 12.32 | −22.5 | 0.668 | −17.5 | 0.719 |
| 168 h | −14.2 | 0.588 | 49.8 | 8.52 | −18 | 0.709 | −10.4 | 0.596 |
| 192 h | −12.2 | 0.449 | 50.9 | 7.77 | −18.9 | 0.897 | −5.2 | 0.475 |
| 216 h | −12 | 0.604 | 53.2 | 4.14 | −18.2 | 0.695 | −9.8 | 0.612 |
| 288 h | −7 | 0.572 | n.o. | n.o. | −18.6 | 0.624 | −2.8 | 0.543 |

n.o. - not observed, where: T$_{g1,2,3}$ - glass transition temperatures; $\Delta$c$_{p1,2,3}$ - change of the heat capacity at glass transition T$_{g1}$, T$_{g2}$, T$_{g3}$; T$_{m1}$ - melting temperature; $\Delta$H$_{m1}$ - heat of melting at T$_{m1}$.
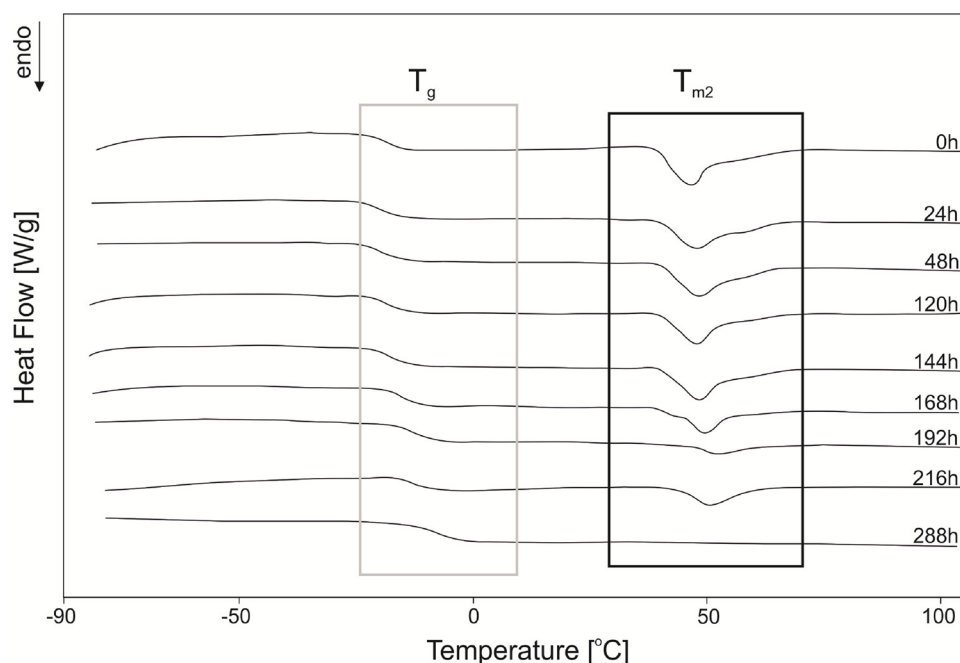
**Fig. 8.** DSC thermograms of poly(xylitol succinate-co-butylene succinate) PXBSu at the crosslinking stages subjected to first heating.
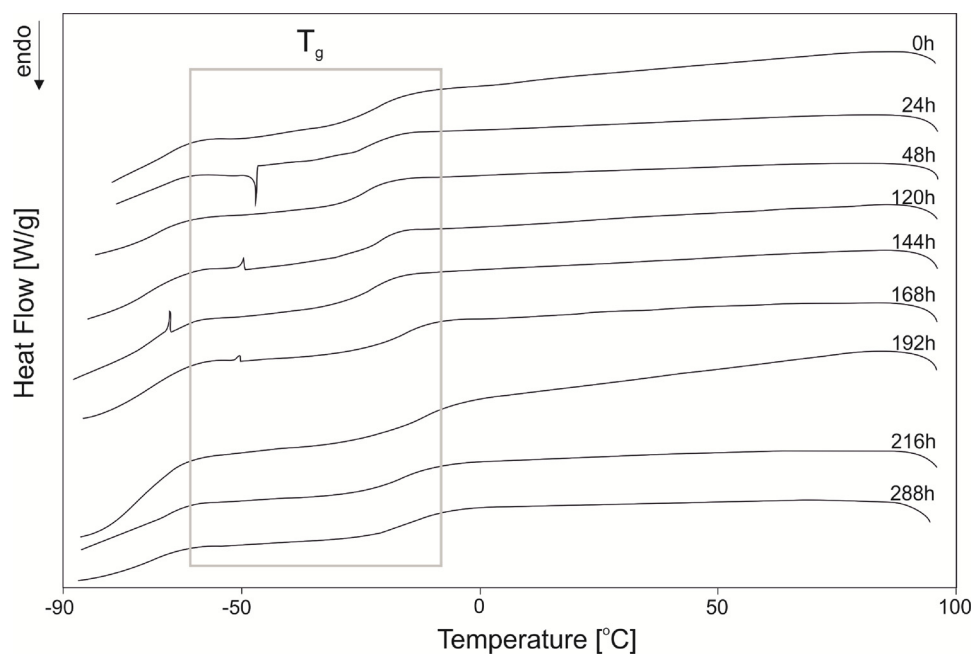


**Fig. 9.** DSC thermograms of poly(xylitol succinate-co-butylene succinate) PXBSu at the crosslinking stages subjected to cooling.

## 2.2. Experimental methods

### 2.2.1. Fourier transform infrared spectroscopy (FTIR)

Fourier transform infrared spectrometry (ATR FTIR Alpha spectrometer, Bruker) was used to examine the chemical structure of all materials obtained at subsequent stages of the crosslinking process. FTIR transmission spectra were recorded between 400 and 4000 cm$^{-1}$, with 2 cm$^{-1}$ resolution. The test results were developed using Omnic software.

### 2.2.2. Differential scanning calorimetry (DSC)

Thermal properties were determined using differential scanning calorimetry (DSC) (Q100, TA Instruments apparatus). The measurement was carried out in a cycle heating in the temperature range from

$-100$ to $200\,^\circ$C.

### 2.2.3. Mechanical properties

Mechanical tests were carried out with an Instron 3366 instrunents equipped with a 500 N load cell in accordance with standard PN-EN-ISO 527/1:1996 (crosshead speed of 100 mm/min, at 25 °C and 50% of relative humidity).

### 2.2.4. Hardness

Hardness (H) for materials after 288 h was measured using a Zwick/ Material Testing 3100 Shore A hardness tester.

### 2.2.5. Water contact angle

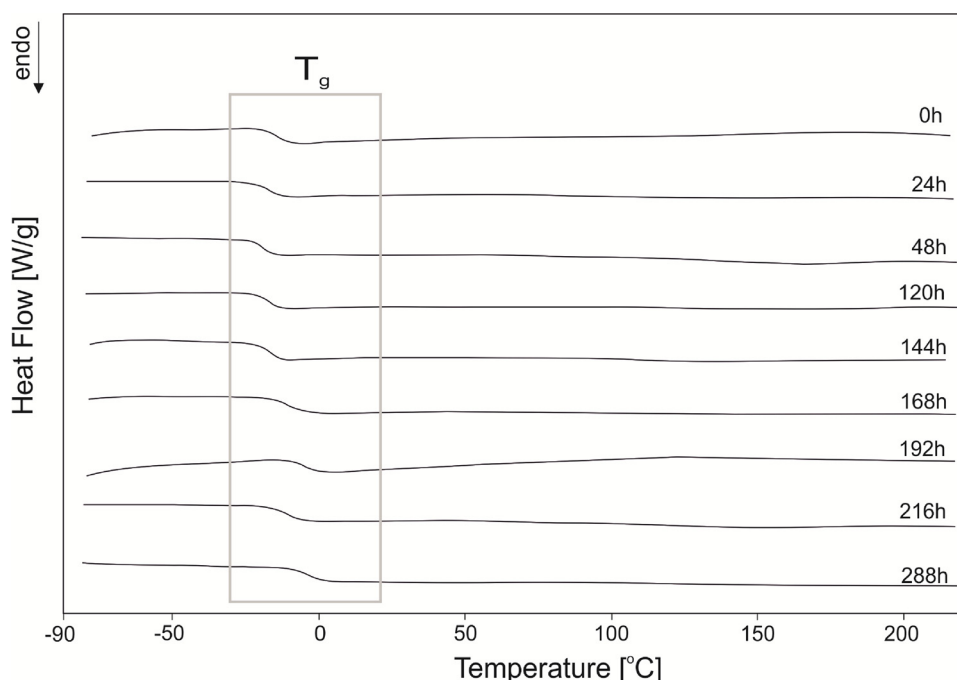The water contact angle was measured by using a KRUSS DSA100

**Fig. 10.** DSC thermograms of poly(xylitol succinate-co-butylene succinate) PXBSu at the crosslinking stages subjected to second heating.

digital goniometer. Static contact angle measurements were performed on the surface of degreased materials after 288 h croslinking by placing a 2 µL droplet of deionized water using the automatic dispenser of the goniometer. Contact angle was calculated using Kruss drop shape analysis software (DSA4).

### 2.2.6. Gel fraction

Determination of gel fraction of elastomers after 288 was made by the extraction method. PN-EN 579: 2001. Material samples after 288 h croslinking (about 1 g) were placed in Schott type P2 crucible and subjected to extraction in boiling tetrahydrofuran (100 cm$^3$) for 3 h. After extraction, the samples were dried in a vacuum oven at 25 °C for 3 h and then in a desiccator. Three determinations were made for each elastomer. The content of gel fractions was calculated from formula (1) as the mean of three measurements:

X = m1/m0 100% (1)

where: m1 - sample mass after extraction, m0 - sample mass before extraction.

## 3. Results and discussion

As a result of the described synthesis, two ester elastomers were obtained, the reactions of which are shown in Figs. 1 and 2. In Tables 1 and 2 the basic physicochemical properties of PXBS and PXBS were compared after 288 h of crosslinking (the third stage of the preparation process - crosslinking).

### 3.1. Fourier transform infrared spectroscopy (FTIR)

The obtained spectra show bands typical for polyester structure. For both materials four transmittance peaks can be observed (Fig. 3 (PXBS) and Fig. 4 (PXBSu)): −C−O−C group at about 1150 cm$^{-1}$ wavelenght, −C=O group at about 1706 cm$^{-1}$ wavelenght, −CH at about 2944 cm$^{-1}$ wavelght, and intermolecularly associated −OH groups at about 3435 cm$^{-1}$ wavelenght. Peak intensity of −OH groups decreases, and peak intensity of −C−O−C groups increases with the cross-linking progress. It is the result of bonding between molecules in the adjacent polymer chains.

### 3.2. Differential scanning calorimetry (DSC)

#### 3.2.1. Poly(xylitol sebacate-co-butylene sebacate)

Table 3 contains the values of the characteristic temperatures of phase transitions with thermal effects at subsequent stages of PXBS crosslinking.

On the first-heating thermograms (Fig. 5) two melting temperatures can be observed, $T_{m1}$ is the result of melting of poly(xylitol sebacate), and $T_{m2}$ is the result of melting of poly(butylene sebacate). Second melting enthalpy value decreases with the cross-linking progress. On the second-heating thermograms (Fig. 7) $T_{m2}$ can only be observed for the non-crosslinked polymer. Glass transition temperature can be observed on the second-heating thermograms. Cooling thermograms (Fig. 6) show crystallization temperatures. Both the temperatures and enthalpies of crystallization decrease with the cross-linking progress.

#### 3.2.2. Poly(xylitol succinate-co-butylene succinate) PXBSu

Table 4 contains the values of the characteristic temperatures of phase transitions with thermal effects at subsequent stages of PXBSu crosslinking.

On the first-heating thermogram glass transition temperature and melting temperature can be observed. Glass transition temperature increases with the cross-linking progress. Melting temperature increases, and melting enthalpy decreases with the cross-linking progress. For the completely cross-linked material melting temperature cannot be observed (Fig. 8). On the cooling thermograms (Fig. 9) glass transition temperature can be observed. Fig. 9 shows a wide range of glass transition, which is probably associated with the overlap of certain effects associated with the crystallization of other crystalline forms. On the second-heating thermograms (Fig. 10) thermogram only glass transition temperature can be observed. Melting temperature cannot be observed which is probably the result of thermal cross-linking that occurred during DSC analysis.

### 3.3. Mechanical properties

The mechanical properties of the PXBS and PXBSu elastomers after 288 h of crosslinking are shown in Tables 1 and 2. An elastomer based on succinic acid (PXBSu) 288 h after the crosslinking process has a

much higher value of tensile strength of 1.5 MPa than the elastomer PXBS (0.93 MPa). Elongation material PXBS is higher relative to the material as is evident PXBSu the observed values of tensile strength.

### 3.4. Hardness

Tables 1 and 2 show the hardness results for PXBS and PXBS after 288 h of crosslinking. It can be observed that both materials have a very low Shore A value and can be included in soft elastomers similar to cross-linked silicone rubber.

### 3.5. Water contact angle

Wetting properties of polymeric materials are very important for their applications in medicine. Therefore, it is important that the designed materials determine their hydrophilicity or hydrophobicity. Hydrophilic surfaces potentially improve biocompatibility. To investigate the wetting characteristics of the surfaces of our materials, the water contact angle measurements were made for ester elastomers after 288 h of the crosslinking process and the results are presented in Tables 1 and 2. Both the PXBS and PXBS material are characterized by a hydrophilic surface. However, for an ester elastomer based on sebacic acid, the surface of the material exhibits a significantly higher wettability compared to an elastomer based on succinic acid.

### 3.6. Gel fraction

The results of the gel fraction for ester materials presented in Table 1 and 2 after 288 h of cross-linking indicate obtaining materials characterized by a high degree of cross-linking. Both PXBS and PXBSu achieved gel fraction values of 91 and 96%, respectively. Slightly lower value can be observed for the PXBS material, which is directly related to the fact that the material shows an endothermic melting transformation visible on DSC thermograms after the crosslinking process (Figs. 5, 7). The PXBSu material does not show such a conversion, while DSC thermograms show the glass transition temperature, which is typical for elastomeric materials.

### 4. Conclusions

Copolymers synthesized by us exhibit better mechanical properties than materials synthesized using only xylitol and dicarboxylic acid, while retaining their biocompatibility and biodegradability. Mechanical properties, and change in thermal and chemical properties with progress of the cross-linking process were investigated. Different temperatures and thermal effects corresponding to various phase transitions were recored at consecutive stages of the cross-linking process. Bonding between adjacent polymer chains lead to decreasing peak intensity of intermolecularly associated −OH groups and increasing peak intensity of −C−O−C groups in FTIR analysis with progress of the cross-linking process.

### Conflicts of interest

The authors declared that they have no conflict of interest.

### References

[1] L. Zheng, Z. Wang, S. Wu, Ch. Li, D. Zhang, Y. Xiao, Novel poly(butylene fumarate) and poly(butylene succinate) multiblock copolymers bearing reactive carbon-carbon double bonds: synthesis, characterization, cocrystallization, and properties, Ind. Eng. Chem. Res. 52 (2013) 6147–6155, https://doi.org/10.1021/ie303573d.

[2] L. Zheng, Li Ch, Z. Wang, J. Wang, Y. Xiao, D. Zhang, G. Guan, Novel biodegradable and double crystalline multiblock copolymers comprising of poly(butylene succinate) and poly(ε-caprolactone): synthesis, characterization, and properties, Ind. Eng. Chem. Res. 51 (2012) 7264–7272, https://doi.org/10.1021/ie300576z.

[3] L. Zheng, Ch. Li, W. Huang, X. Huang, D. Zhang, G. Guan, Y. Xiao, D. Wang, Synthesis of high-impact biodegradable multiblock copolymers comprising of poly(butylene succinate) and poly(1,2-propylene succinate) with hexamethylene diisocyanate as chain extender, Polym. Adv. Technol. 22 (2011) 279–285, https://doi.org/10.1002/pat.1530.

[4] K. Lubkowski, A. Smorowska, B. Grzmil, A. Kozłowska, Controlled-release fertilizer prepared using a biodegradable aliphatic copolyester of poly(butylene succinate) and dimerized fatty acid, J. Agric. Food Chem. 63 (2015) 2597–2605, https://doi.org/10.1021/acs.jafc.5b00518.

[5] J.M. Kemppainen, S.J. Hollister, Tailoring the mechanical properties of 3D-designed poly(glycerol sebacate cartilage applications) scaffolds for, J. Biomed. Mater. Res. - Part A 94 (2010) 9–18, https://doi.org/10.1002/jbm.a.3265.

[6] D. Motlagh, J. Yang, K.Y. Lui, A.R. Webb, G.A. Ameer, Hemocompatibility evaluation of poly(glycerol-sebacate) in vitro for vascular tissue engineering, Biomaterials 27 (2006) 4315–4324, https://doi.org/10.1016/j.biomaterials.2006.04.010.

[7] Q.Z. Chen, A. Bismarck, U. Hansen, S. Junaid, M.Q. Tran, S.E. Harding, N.N. Ali, A.R. Boccaccini, Characterisation of a soft elastomer poly(glycerol sebacate) designed to match the mechanical properties of myocardial tissue, Biomaterials 29 (2008) 47–57 https://10.1016/j.biomaterials.2007.09.010.

[8] W.L. Neeley, S. Redenti, H. Klassen, S. Tao, T. Desai, M.J. Young, R. Langer, A microfabricated scaffold for retinal progenitor cell grafting, Biomaterials 29 (2008) 418–426, https://doi.org/10.1016/j.biomaterials.2007.10.007.

[9] C.J. Bettinger, B. Orrick, A. Misra, R. Langer, J.T. Borenstein, Microfabrication of poly(glycerol-sebacate) for contact guidance applications, Biomaterials 27 (2006) 2558–2565 https://10.1016/j.biomaterials.2005.11.029.

[10] C.A. Sundback, J.Y. Shyu, Y. Wang, W.C. Faquin, R.S. Langer, J.P. Vacanti, T.A. Hadlock, Biocompatibility analysis of poly(glycerol sebacate) as a nerve guide material, Biomaterials 26 (2005) 5454–5464 https://10.1016/j.biomaterials.2005.02.004.

[11] Z.J. Sun, C. Chen, M.Z. Sun, C.H. Ai, X.L. Lu, Y.F. Zheng, B.F. Yang, D.L. Dong, The application of poly (glycerol-sebacate) as biodegradable drug carrier, Biomaterials 30 (2009) 5209–5214 https://10.1016/j.biomaterials.2009.06.007.

[12] Z.Y. Ning, Q.S. Zhang, Q.P. Wu, Y.Z. Li, D.X. Ma, J.Z. Chen, Efficient synthesis of hydroxyl functioned polyesters from natural polyols and sebacic acid, Chin. Chem. Lett. 22 (2011) 635–638, https://doi.org/10.1016/j.cclet.2010.12.033.

[13] J.C. Paraji, H. Dominguez, J.M. Dominguez, Biotechnological production of xylitol. Part 1: interest of xylitol and fundamentals of its biosynthesis, Bioresour. Technol. 65 (1998) 191–201, https://doi.org/10.1016/S0960-8524(98)00038-8.

[14] J.P. Bruggeman, C.J. Bettinger, C.L.E. Nijst, D.S. Kohane, R. Langer, Biodegradable xylitol-based polymers, Adv. Mater. 20 (2008) 1922–1927, https://doi.org/10.1002/adma.200702377.

[15] J.P. Bruggeman, C.J. Bettinger, R. Langer, Biodegradable xylitol-based elastomers: in vivo behavior and biocompatibility, J. Biomed. Mater. Res. - Part A 95 (2010) 92–104, https://doi.org/10.1002/jbm.a.32733.

[16] J.P. Bruggeman, B.J. de Bruin, C.J. Bettinger, R. Langer, Biodegradable poly(polyol sebacate) polymers, Biomaterials 29 (2008) 4726–4735, https://doi.org/10.1016/j.biomaterials.2008.08.037.

[17] Q. Dasgupta, K. Chatterjee, G. Madras, Combinatorial approach to develop tailored biodegradable poly(xylitol dicarboxylate) polyesters, Biomacromolecules 15 (2014) 4302–4313, https://doi.org/10.1021/bm5013025.

# Synthesis and Selected Properties of Ester Elastomer Containing Sorbitol

**Marta Piątek-Hnat** [1],[*] , **Kuba Bomba** [1] **and Jakub Pęksiński** [2]

[1]   Faculty of Chemical Technology and Engineering Piastów Ave. 42, West Pomeranian University of Technology, 71-065 Szczecin, Poland; bk34688@zut.edu.pl
[2]   Faculty of Electrical Engineering, Sikorskiego Ave. 37, 71-313 Szczecin, Poland; jakub.peksinski@zut.edu.pl
[*]   Correspondence: marp@zut.edu.pl

**Abstract:** The aim of this work was synthesizing ester elastomers, using sorbitol as a monomer obtainable from renewable sources. Three polymers were synthesized, utilizing three different polycondensation times. Their mechanical and thermal properties were examined and compared. Poly(sorbitol sebacate-co-butylene sebacate) elastomers were synthesized as a result of polycondensation reaction, using sebacic acid, butylene glycol and sorbitol as monomers. Resulting materials had good mechanical properties and a cross-linked structure. Such elastomers are susceptible to hydrolytic degradation which has been confirmed in earlier studies. This paper shows that the material synthesized utilizing a 3.5 h polycondensation time has the most desirable mechanical and thermal properties, and the reaction is characterized by the highest degree of conversion of substrates.

**Keywords:** elastomers; polycondensation; sustainable sources; biodegradable material; material properties

## 1. Introduction

Due to environmental concerns, obtaining biodegradable polymers synthesized by utilizing monomers possible to acquire from renewable sources became a topic of interest among various researchers. One such group of materials is sugar alcohol-based polymers. The most researched materials of this type are glycerol-based. They have been proven to have many possible biomedical applications [1–10]. Various polymers obtained using sorbitol as monomers include sorbitol-based terpolyesters [11] and biocompatible polymers based on sebacic acid and different sugar alcohols, including sorbitol [12]. A biocompatible polymer based on sorbitol and sebacic acid was also obtained [13]. Copolymers with succinic acid, sorbitol and different diols were also obtained and tested [14]. A sorbitol-based polymer with citric and sebacic acid as monomers and its biodegradability was also described in earlier work [15]. Sorbitol can also be used as a chain extender in self-healing polyurethanes [16]. Biodegradable composites with hydroxyapatite in a poly(sorbitol sebacate malate) matrix can also be obtained [17].

Various examples of sugar alcohol-based polymers have been described in the literature. Polyesters were obtained using different xylitol–sebacic acid ratios. Their properties were tested, and the elastomers have been proven to be biocompatible in vitro [18]. Xylitol-based polymers synthesized using citric and sebacic acid were obtained. Poly(xylitol-co-citrate) was then copolymerized with methacrylic anhydride. The materials have been proven to be biocompatible in vivo [19]. Copolymers with two dicarboxylic acid segments were also synthesized and tested [20]. Sugar alcohol-based polymers have also been proven to be possible to synthesize using lipase as a catalyst [21]. Exact structure of non-cross-linked poly(xylitol sebacate) has also been

determined and proven to be a linear chain. The polymer contains mostly 1,5-diacyl and 1-acyl substitutions [22]. Other interesting materials obtained using sugar alcohols include: nanocomposites of poly(mannitol sebacate) with cellulose nanocrystals which display shape-memory properties [23], poly(xylitol-co-maleate-co-PEG) hydrogel, which can be used in order to encapsulate and inject cells [24], poly(xylitol sebacate), which can be electrospun by a core-shell method in order to obtain tissue-like material [25,26], biodegradable poly(xylitol-dodecanedioic acid) with possible future tissue-engineering applications [27], polymers able to reversibly solidify and liquefy, synthesized utilizing sugar alcohol and azo compounds [28], and conetworks based on poly(lactide) and sugar alcohols as core molecules [29].

In this work we focus on obtaining three-monomer-based copolyesters and analyze how changing the polycondensation time affects the mechanical and thermal properties of resulting material. The novelty in this work is that, to the best of our knowledge, material obtained using exactly those monomers has not yet been synthesized. It is also of importance that one of the monomers used—sorbitol—can be obtained from renewable sources.

## 2. Material and Methods

### 2.1. Synthesis of Poly(sorbitol Sebacate-Co-Butylene Sebacate) (PSBS)

Sigma-Aldrich (St. Louis, MO, USA) Corporation was the purveyor of the monomers used for the synthesis. Ti(BuO)$_4$ catalyst was purchased from Fluka. The monomer ratio of sebacic acid–sorbitol–butylene glycol was 2:1:1. Synthesis of sorbitol-based ester elastomers is comprised of three stages—esterification, polycondensation and post-polymerization. In the first stage, an esterification reaction catalyzed by Ti(OBu)$_4$ occurred between sebacic acid, sorbitol and butylene glycol at 150 °C. The second stage was a polycondensation reaction in a vacuum. Post-polymerization took place in a vacuum dryer; during this step, polymers cross-linked. Polycondensation was carried out utilizing three different reaction times: 1 h (PSBS 1 h); 2.5 h (PSBS 2.5 h) and 3.5 h (PSBS 3.5 h) in order to shorten the cross-linking stage of the synthesis and to determine which resulting material had the best thermal and mechanical properties. The reaction scheme is shown in Figure 1.

### 2.2. Methods

#### 2.2.1. Fourier-Transform Infrared Spectroscopy (FTIR)

In order to analyze the chemical structure of the materials, Fourier-transform infrared spectroscopy (FTIR) was used. The range of the transmission spectra recorded by the FTIR method was between 4000 and 400 cm$^{-1}$. The resolution used was 2 cm$^{-1}$. Software used to develop the test results was OMNIC 7.3 by the Thermo Electron Corporation.

#### 2.2.2. Differential Scanning Calorimetry (DSC)

Determination of the thermal properties was performed with a differential scanning calorimetry (DSC) (Q100, TA Instruments) apparatus. The temperature range of the heating cycle was −100 to 200 °C. The heating rate used was 10 °C/min. The samples were kept in a nitrogen atmosphere. Software used to develop the test results was TA Instruments Universal Analysis 2000, 3.9a.

#### 2.2.3. Dynamic Thermomechanical Analysis (DMTA)

In order to perform dynamic thermomechanical analysis, a DMA Q800 (TA Instruments) was used. The temperature range was −100 to 150 °C, with 1 Hz frequency. The heating rate was 2 °C/min. Software used to develop the test results was TA Instruments Universal Analysis 2000, 3.9a.
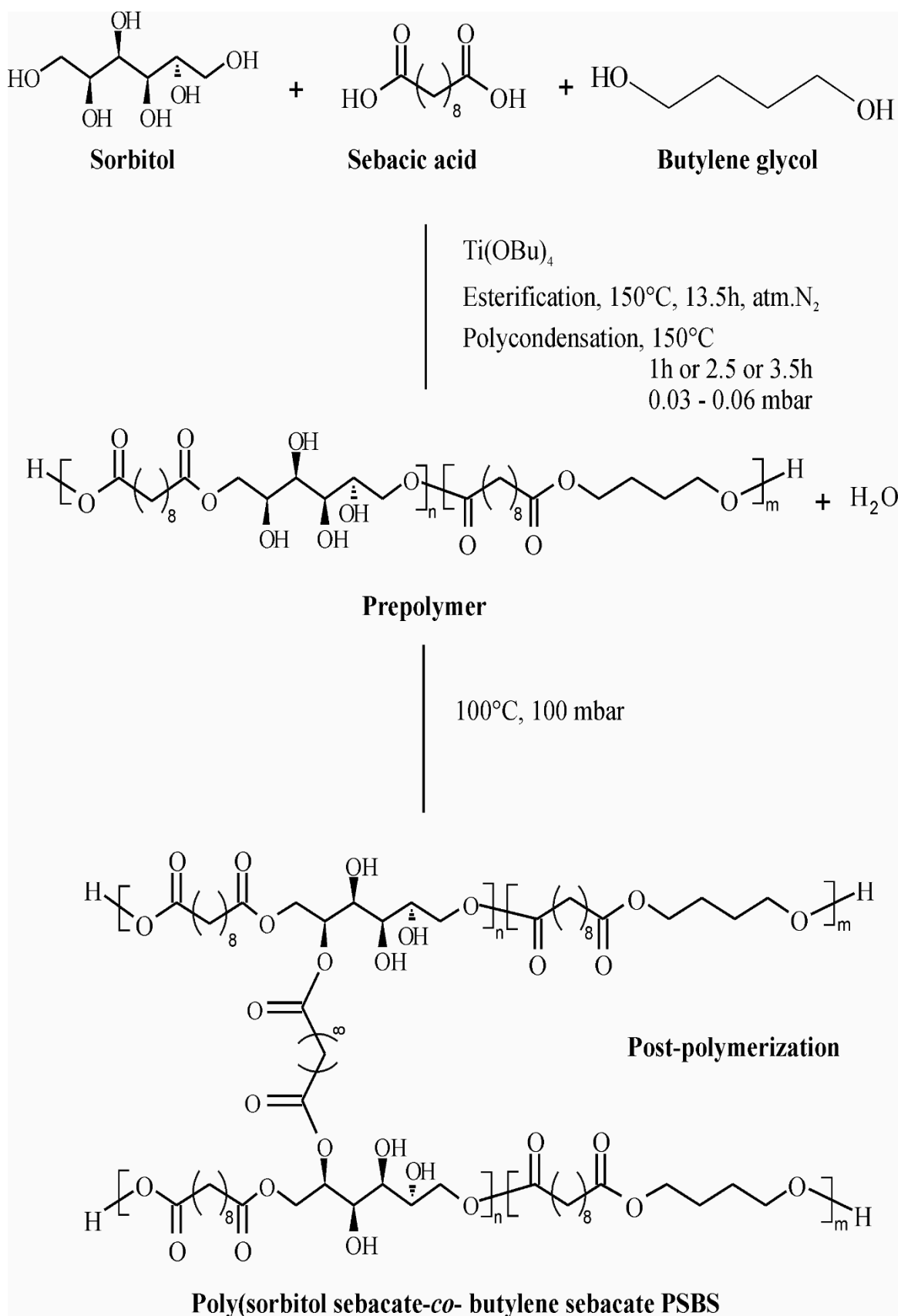
**Figure 1.** Scheme of poly(sorbitol sebacate-co-butylene sebacate) (PSBS) synthesis.

### 2.2.4. Mechanical Properties

In order to perform the mechanicals tests, an Instron 336 instrument was used. 500 N load cell was used. The tests were performed according to PN-EN-ISO 526/1:1996 standards. Crosshead speed was 100 mm/min. The temperature was 25 °C. Relative humidity was 50%.

### 2.2.5. Gel Fraction

In order to determine the gel fraction, the PN-EN-579:2001 extraction method was utilized. Samples of cross-linked material were used. The weight of each sample was about 1 g. A Schott crucible Type P2 was utilized. Samples were extracted with 100 cm$^3$ of boiling tetrahydrofuran. The extraction took 3 h. A vacuum oven was used to dry the samples. The drying process took 3 h and was performed in 25 °C. After that, the samples were dried in a desiccator. Formula (1) was used in order to calculate the gel fraction content. The mean of three measurements was used.

$$X = \frac{m_1}{m_0} \ 100\% \tag{1}$$

where $m_0$—mass of the sample before extraction, $m_1$—mass of the sample after extraction.

### 2.2.6. $^1$H Nuclear Magnetic Resonance Spectroscopy (NMR)

In order to analyze the chemical structure of PSBS, nuclear magnetic resonance spectroscopy (NMR) was performed. The instrument used to perform the analysis was a Bruker DPX 400 MHz. A sample of PSBS at 3.5 h was taken directly after the polycondensation. The polymer sample was dissolved in deuterated chloroform (CDCl$_3$). The results were developed with MestreNova software.

## 3. Results and Discussion

### 3.1. Fourier-Transform Infrared Spectroscopy (FTIR)

FTIR spectra (Figure 2) show four peak characteristics. The peak at about 3340 cm$^{-1}$ corresponds to intermolecularly-associated OH groups; the peak at 2900 cm$^{-1}$ s connected to alkyl groups; the peak at about 1720 cm$^{-1}$ can be assigned to C=O groups and the peak at about 1150 cm$^{-1}$ is due to C-O-C groups. Intensity of the peaks attributed to C-O-C groups is increasing with the increase of the polycondensation time, indicating a higher conversion rate of the monomers.
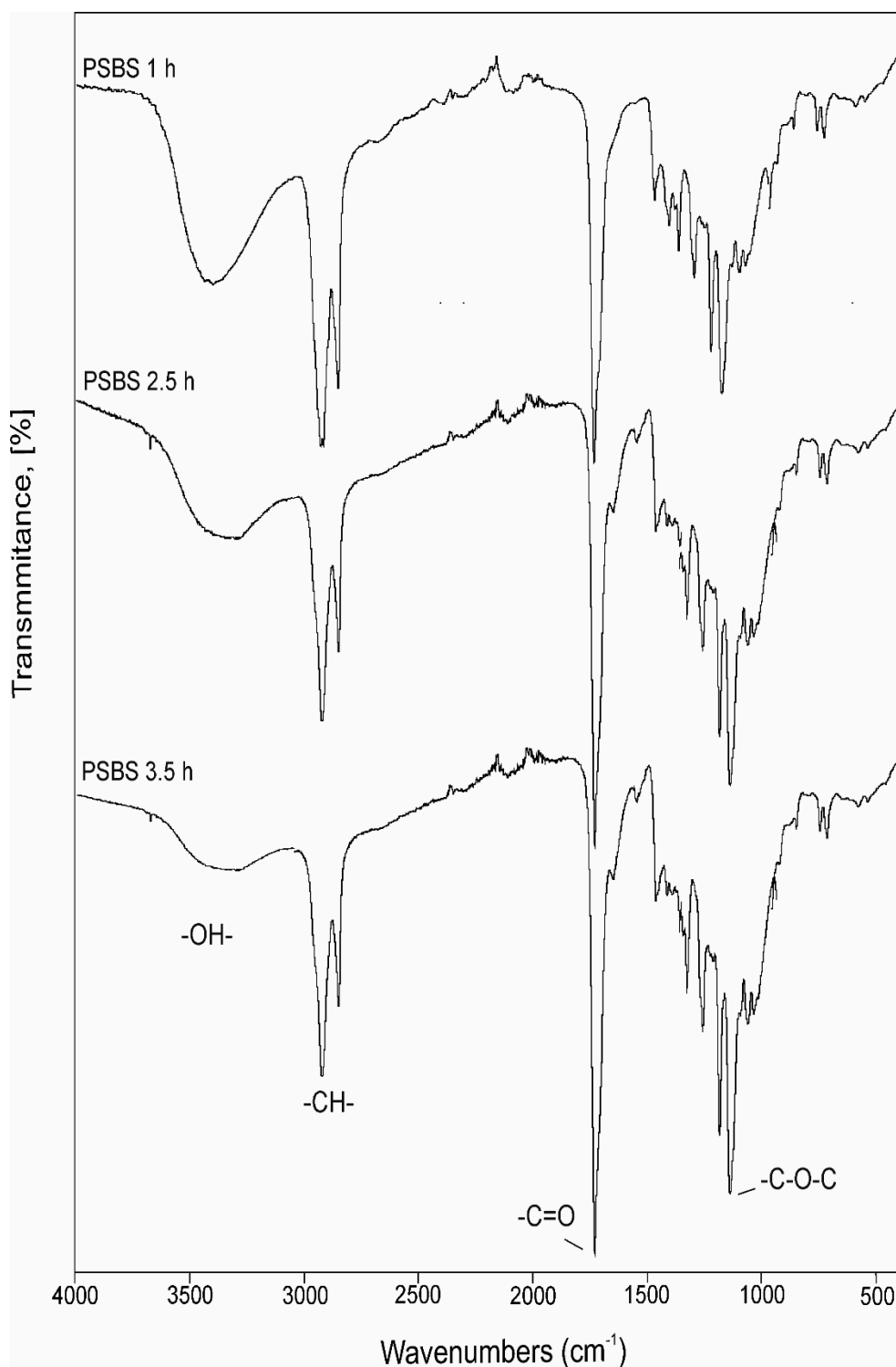
**Figure 2.** PSBS 1 h, PSBS 2.5 h and PSBS 3.5 h FTIR spectra.

*3.2. Differential Scanning Calorimetry (DSC)*

DSC was utilized in order to characterize thermal properties exhibited by PSBS elastomers obtained by utilizing three different polycondensation times (Figure 3).
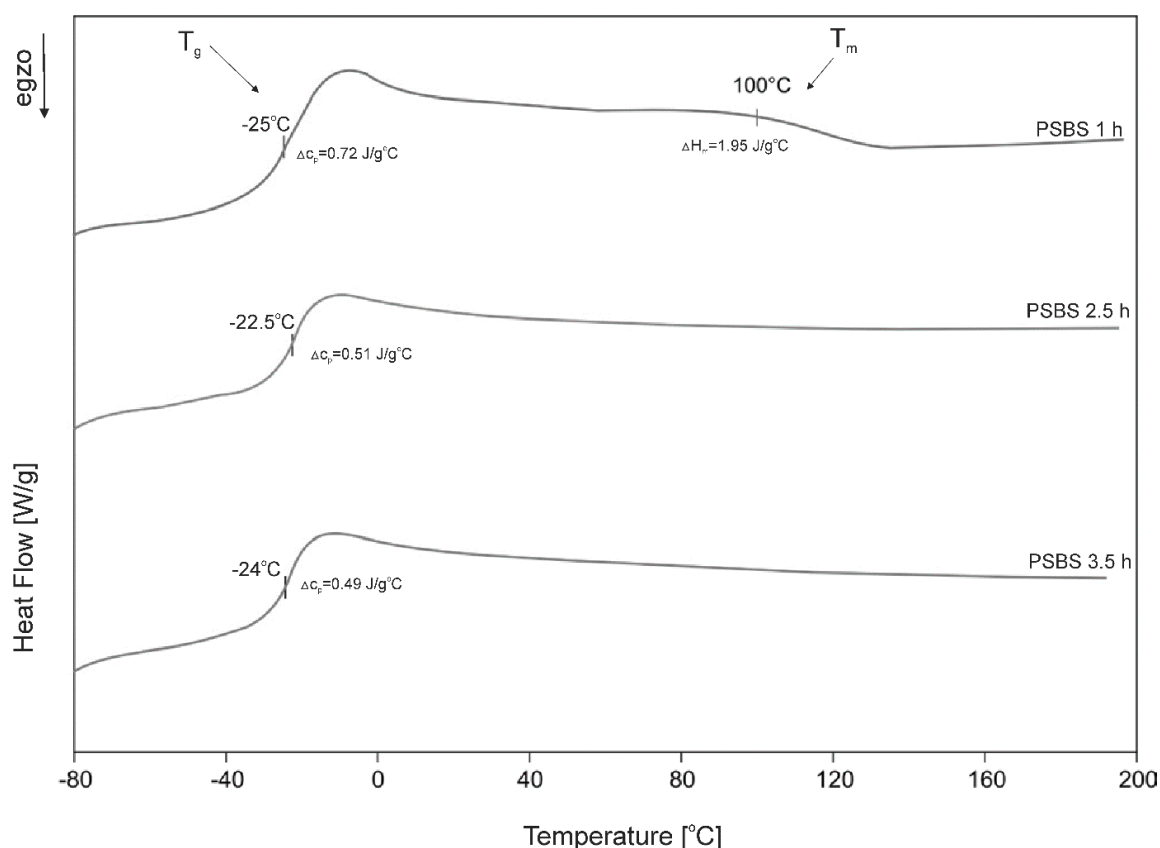
**Figure 3.** First-heating differential scanning calorimetry (DSC) thermograms of PSBS 1 h, PSBS 2.5 h and PSBS 3.5 h.

Glass-transition temperature ($T_g$) changes between materials, from −25 °C (PSBS 1 h) to −22.5 °C (PSBS 2.5 h). Change in heat-capacity during glass-transition decreases with the increase of the polycondensation time (from 0.72 J/g °C to 0.49 J/g °C). This behavior suggests an increase of cross-linking degrees and amorphous phase content and the loss of polymer-chains mobility associated with it. However, the lack of significant differences in glass-transition temperature indicates similar thermal properties of the elastomers. PSBS 1 h polymer also exhibits low-enthalpy melting, indicating small crystalline areas within amorphous polymer structures. This peak disappears with the increase of the polycondensation time due to the material being more cross-linked. The increase of cross-linking degrees and amorphous phase content, correlated with both the decrease in change in heat-capacity during glass-transition and the disappearing of the melting peak, is also confirmed by FTIR analysis. The amount of intermolecularly associated –OH groups decreases with the polycondensation time due to becoming a part of the cross-links, which causes the amount of ester groups to increase.

### 3.3. Dynamic Thermomechanical Analysis (DMTA)

DMTA results are shown in Figure 4. The relaxation behavior exhibited by PSBS 1 h, PSBS 2.5 h and PSBS 3.5 h was tested. Loss tangent (tan delta), loss modulus E″ and storage modulus E′ as a temperature function were measured.
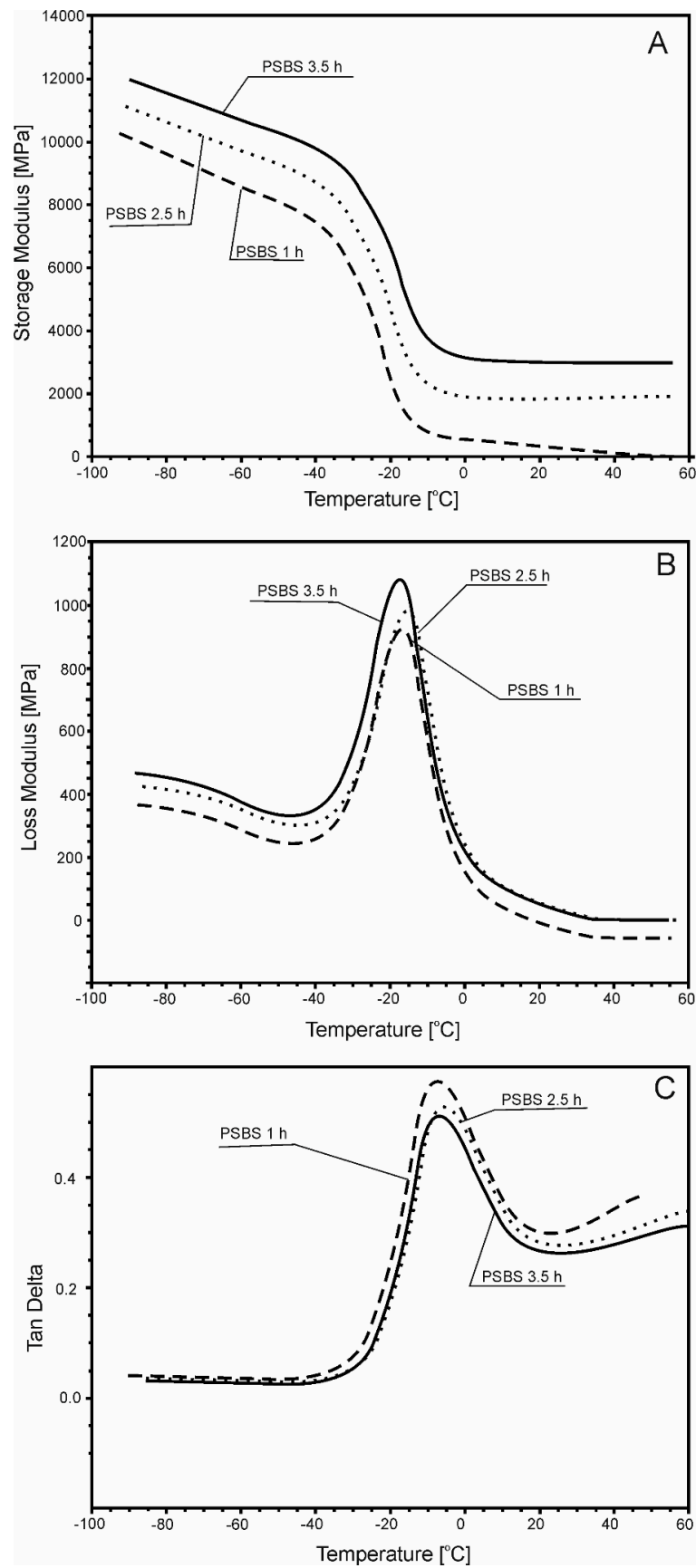
**Figure 4.** Storage modulus (E′) (**A**), loss modulus (E″) (**B**) and loss tangent (tan delta versus temperature) (**C**) for PSBS 1 h, PSBS 2.5 h and PSBS 3.5 h.

Three temperature ranges for the storage modulus can be observed. In the first temperature range (−100 °C to −40 °C), the storage modulus function does not show significant changes because polymers are in the glassy state. The initial value of the storage modulus for PSBS 3.5 h is significantly higher compared to its value for PSBS 2.5 h and PSBS 1 h. In the second temperature range (−40 °C to −10 °C), the value of the storage modulus decreases, which corresponds to a process of viscoelastic relaxation associated with the amorphous phase undergoing the glass-transition. In the third temperature range (0 °C to 50 °C), the storage modulus of PSBS 2.5 h and PSBS 3.5 h is constant, and a flexibility plateau can be observed. PSBS 1 h in the temperature range 0 °C to 50 °C exhibits the subservience of elastic to viscous properties and a rapid decline of the storage modulus. This phenomenon is not observed for PSBS 3.5 h and PSBS 2.5 h. The loss modulus $E'' = f(T)$ and loss tangent tan delta $= f(T)$ functions exhibit peak maximum corresponding to alpha relaxation. It is associated with the amorphous phase undergoing the glass-transition. The glass-transition temperature value measured by DMTA is 10 °C higher than the $T_g$ value measured by DSC. Such discrepancy in results is typical for those methods.

### 3.4. Mechanical Properties

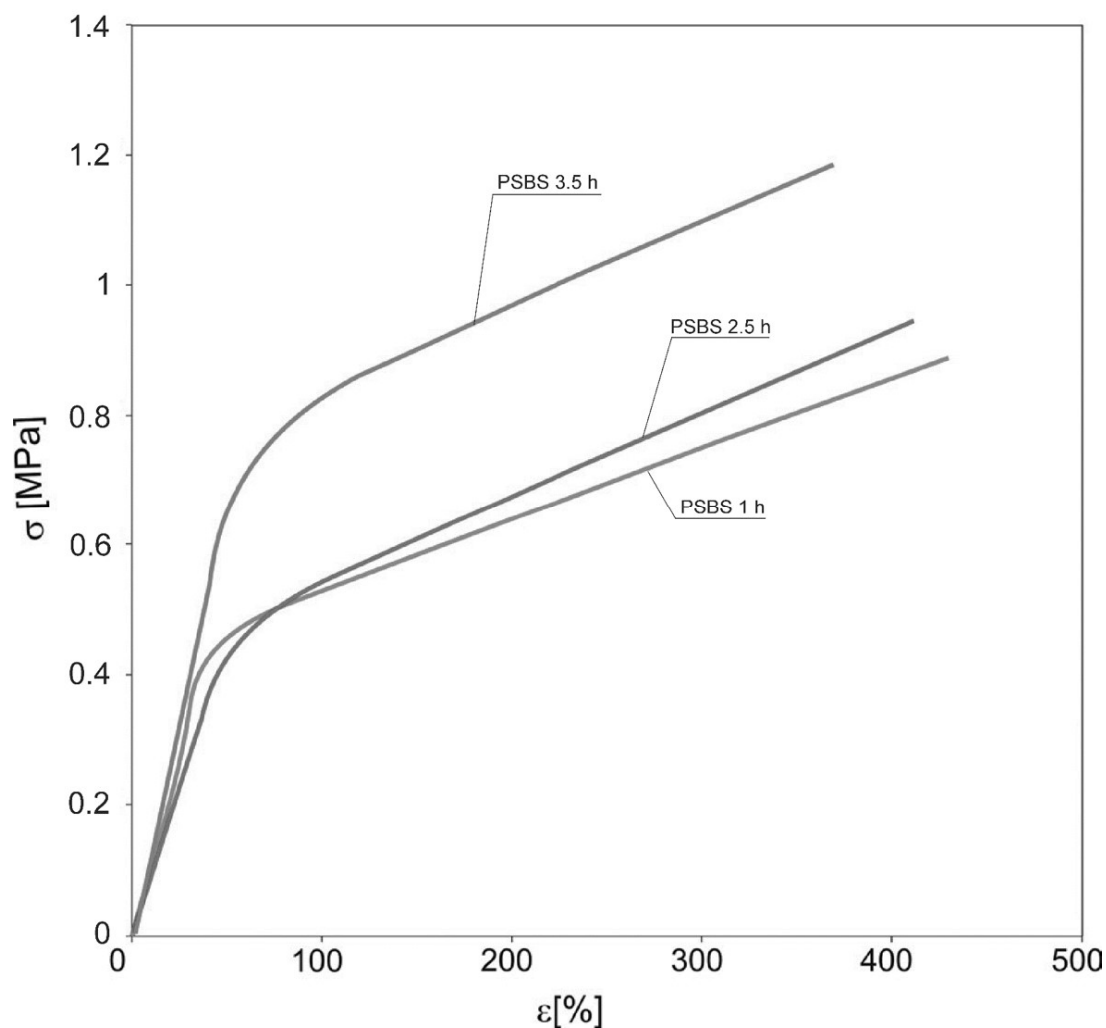Figure 5 presents the results of tensile tests for PSBS after 1, 2.5, and 3.5 h polycondensation time.



**Figure 5.** Mechanical properties of PSBS 1 h, PSBS 2.5 h and PSBS 3.5 h.

All obtained elastomers, regardless of polycondensation time, show the course of the stress–strain characteristic for elastomeric materials. It can be observed that the tensile stress increases with

increasing polycondensation time with a slight decrease in strain. PSBS 3.5 h shows a stress value of 1.2 MPa while maintaining a strain at 380%, which provides a good basis for qualifying this material as a competition for sorbitol-based materials described in the literature [11,12]. Higher tensile stress exhibited by PSBS 3.5 h correlates to DMTA results showing the highest storage modulus E' for this material.

*3.5. Gel Fraction*

The obtained elastomeric materials are characterized by a high degree of cross-linking, which can be observed in the gel fraction test. The results are presented in Figure 6.
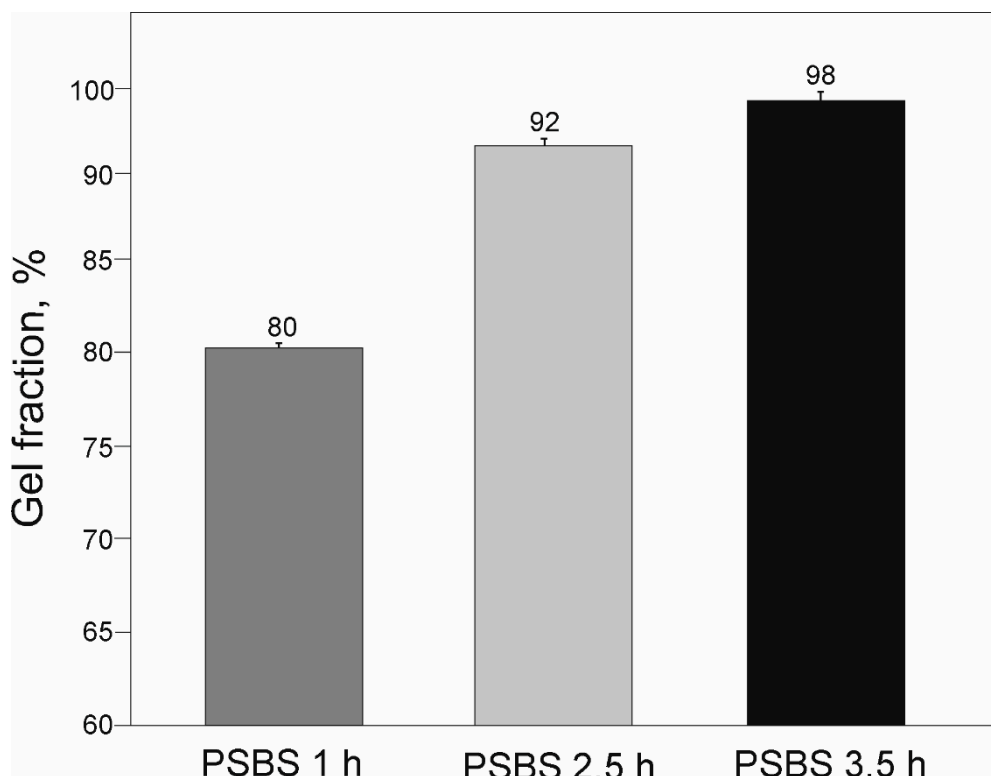


**Figure 6.** Gel fraction of PSBS 1 h, PSBS 2.5 h and PSBS 3.5 h.

The expected effect was the increase of gel fraction along with the polycondensation time. For PSBS 1 h, the value of the gel fraction is 80%, 92% for PSBS 2.5 h, and 98% for PSBS 3.5 h. These results correspond very well with thermal and mechanical results. The highest gel fraction of PSBS 3.5 h correlates with the best mechanical properties shown by mechanical tests and the highest content of the amorphous phase shown by both DSC and DMTA and confirms that 3.5 h of polycondensation time is the best option for synthesizing such materials.

*3.6. $^1$H Nuclear Magnetic Resonance Spectroscopy (NMR)*

In order to confirm the structure of the PSBS copolymer, $^1$H NMR analysis (Figure 7) was performed. The peak at about 1.30 ppm was due to a $CH_2(c)$ group doublet at 1.62, and the 1.71 ppm was connected to $CH_2(b)$ and $CH_2$ (g) groups; the peak at about 2.32 ppm was attributed to a $CH_2$ (a) group. The peak at about 4.09 ppm was assigned to the proton next to the oxygen atom, which is a part of the ester bond between sebacic acid and butylene glycol. The peak at about 4.23 ppm is due to the proton next to the oxygen atom, which is a part of the ester bond between sebacic acid and sorbitol. Peaks between about 4.02 ppm and 3.56 ppm are connected to $CH_2(d)$ groups in sorbitol.
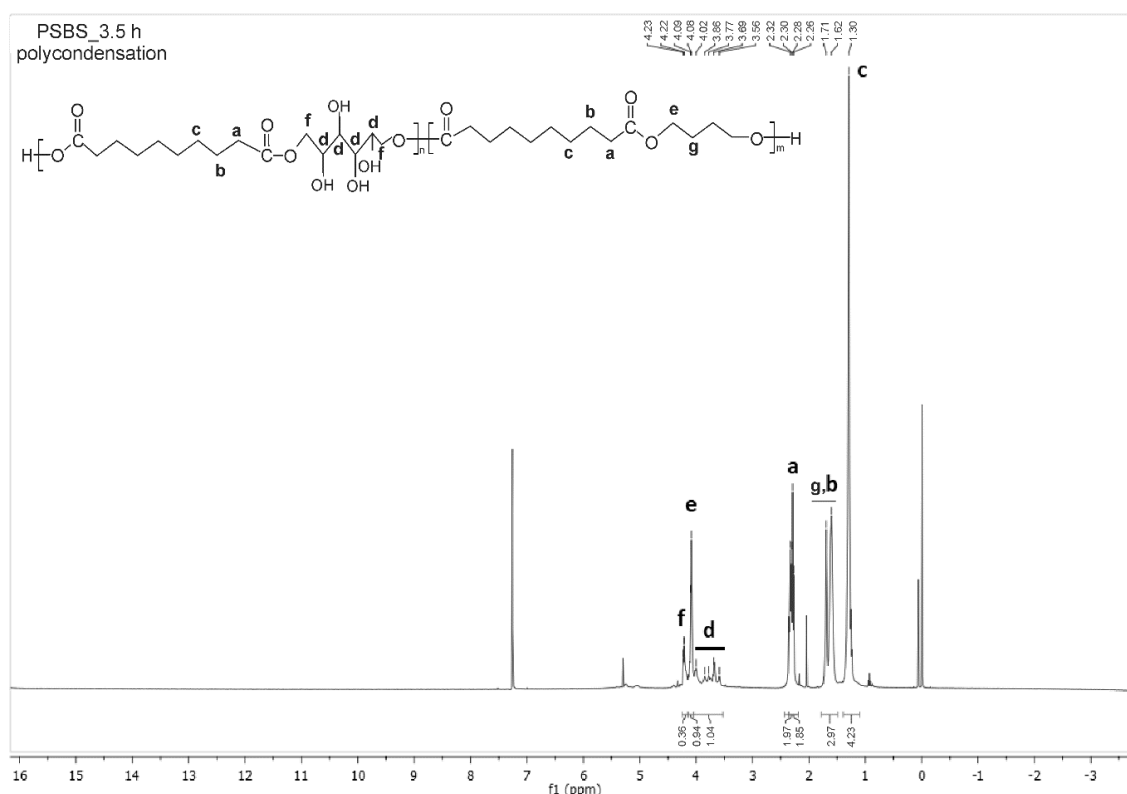
**Figure 7.** NMR analysis of PSBS 3.5 h.

## 4. Conclusions

Materials based on butylene glycol, sebacic acid and sorbitol monomers were obtained. Three different polycondensation times were used. Thermal and mechanical properties and gel fraction were tested. The results confirm that utilizing a 3.5 h polycondensation time leads to obtaining materials with the best properties, due to its highest cross-linking degree. Results obtained from different methods correlate well with each other. High gel fraction, thermal stability and good mechanical properties of PSBS elastomers suggest possible industrial applications.

## References

1.  Neeley, W.L.; Redenti, S.; Klassen, H.; Tao, S.; Desai, T.; Young, M.J.; Langer, R. A microfabricated scaffold for retinal progenitor cell grafting. *Biomaterials* **2008**, *29*, 418–426. [CrossRef] [PubMed]
2.  Sun, Z.J.; Chen, C.; Sun, M.Z.; Ai, C.H.; Lu, X.L.; Zheng, Y.F.; Yang, B.F.; Dong, D.L. The application of poly (glycerol-sebacate) as biodegradable drug carrier. *Biomaterials* **2009**, *30*, 5209–5214. [CrossRef] [PubMed]
3.  Zaky, S.H.; Lee, K.W.; Gao, J.; Jensen, A.; Verdelis, K.; Wang, Y.; Almarza, A.J.; Sfeir, C. Poly (glycerol sebacate) elastomer supports bone regeneration by its mechanical properties being closer to osteoid tissue rather than to mature bone. *Acta Biomater.* **2017**, *54*, 95–106. [CrossRef] [PubMed]
4.  Chen, Q.Z.; Bismarck, A.; Hansen, U.; Junaid, S.; Tran, M.Q.; Harding, S.E.; Ali, N.N.; Boccaccini, A.R. Characterisation of a soft elastomer poly(glycerol sebacate) designed to match the mechanical properties of myocardial tissue. *Biomaterials* **2008**, *29*, 47–57. [CrossRef]
5.  Motlagh, D.; Yang, J.; Lui, K.Y.; Webb, A.R.; Ameer, G.A. Hemocompatibility evaluation of poly(glycerol-sebacate) in vitro for vascular tissue engineering. *Biomaterials* **2006**, *27*, 4315–4324. [CrossRef]

6.  Bettinger, C.J.; Orrick, B.; Misra, A.; Langer, R.; Borenstein, J.T. Microfabrication of poly (glycerol-sebacate) for contact guidance applications. *Biomaterials* **2006**, *27*, 2558–2565. [CrossRef]

7.  Kemppainen, J.M.; Hollister, S.J. Tailoring the mechanical properties of 3D-designed poly(glycerol sebacate) scaffolds for cartilage applications. *J. Biomed. Mater. Res. Part A* **2010**, *94*, 9–18. [CrossRef]

8.  Rosenbalm, T.N.; Teruel, M.; Day, C.S.; Donati, G.L.; Morykwas, M.; Argenta, L.; Kuthirummal, N.; Levi-Polyachenko, N. Structural and mechanical characterization of bioresorbable, elastomeric nanocomposites from poly(glycerol sebacate)/nanohydroxyapatite for tissue transport applications. *J. Biomed. Mater. Res. Part B Appl. Biomater.* **2016**, *104*, 1366–1373. [CrossRef]

9.  Liang, S.L.; Cook, W.D.; Thouas, G.A.; Chen, Q.Z. The mechanical characteristics and in vitro biocompatibility of poly(glycerol sebacate)-Bioglass® elastomeric composites. *Biomaterials* **2010**, *31*, 8516–8529. [CrossRef]

10. Sundback, C.A.; Shyu, J.Y.; Wang, Y.; Faquin, W.C.; Langer, R.S.; Vacanti, J.P.; Hadlock, T.A. Biocompatibility analysis of poly(glycerol sebacate) as a nerve guide material. *Biomaterials* **2005**, *26*, 5454–5464. [CrossRef]

11. Kumar, A.; Kulshrestha, A.S.; Gao, W.; Gross, R.A. Versatile route to polyol polyesters by lipase catalysis. *Macromolecules* **2003**, *36*, 8219–8221. [CrossRef]

12. Bruggeman, J.P.; de Bruin, B.J.; Bettinger, C.J.; Langer, R. Biodegradable poly(polyol sebacate) polymers. *Biomaterials* **2008**, *29*, 4726–4735. [CrossRef] [PubMed]

13. Barrett, D.G.; Yousaf, M.N. Thermosets synthesized by thermal polyesterification for tissue engineering applications. *Soft Matter* **2010**, *6*, 5026–5036. [CrossRef]

14. Kavimani, V.; Jaisankar, V. Synthesis and Characterisation of Sorbitol Based Copolyesters for Biomedical Applications. *J. Phys. Sci. Appl.* **2014**, *4*, 507–515.

15. Piątek-hnat, M. Influence of the addition of citric acid on the physico-chemical properties of poly(sorbitol sebacate-co- butylene sebacate). *Int. J. Sci. Eng. Res.* **2018**, *9*, 1092–1094.

16. Lee, S.H.; Shin, S.R.; Lee, D.S. Sorbitol as a chain extender of polyurethane prepolymers to prepare self-healable and robust polyhydroxyurethane elastomers. *Molecules* **2018**, *23*, 2515. [CrossRef]

17. Tham, W.H.; Wahit, M.U.; Kadir, M.R.A.; Wong, T.W. Mechanical and thermal properties of biodegradable hydroxyapatite/poly(sorbitol sebacate malate) composites. *Songklanakarin J. Sci. Technol.* **2013**, *35*, 57–61.

18. Bruggeman, J.P.; Bettinger, C.J.; Langer, R. Biodegradable xylitol-based elastomers: In vivo behavior and biocompatibility. , *J. Biomed. Mater. Res. Part A* **2010**, *95*, 92–104. [CrossRef]

19. Bruggeman, J.P.; Bettinger, C.J.; Nijst, C.L.E.; Kohane, D.S.; Langer, R. Biodegradable xylitol-based polymers. *Adv. Mater.* **2008**, *20*, 1922–1927. [CrossRef]

20. Deepa, K.; Jaisankar, V. A Study on Xylitol Based Copolyester for In vitro Degradation Applications. *Int. J. Chem. Technol. Res.* **2018**, *11*, 69–76. [CrossRef]

21. Hu, J.; Gao, W.; Kulshrestha, A.; Gross, R.A. "Sweet polyesters": Lipase-catalyzed condensation-polymerizations of alditols. *ACS Symp. Ser.* **2008**, *999*, 275–284.

22. Moorhoff, C.; Li, Y.; Cook, W.D.; Braybrook, C.; Chen, Q.Z. Characterization of the prepolymer and gel of biocompatible poly(xylitol sebacate) in comparison with poly(glycerol sebacate) using a combination of mass spectrometry and nuclear magnetic resonance. *Polym. Int.* **2015**, *64*, 668–688. [CrossRef]

23. Sonseca, Á.; Camarero-Espinosa, S.; Peponi, L.; Weder, C.; Foster, E.J.; Kenny, J.M.; Giménez, E. Mechanical and shape-memory properties of poly(mannitol sebacate)/cellulose nanocrystal nanocomposites. *J. Polym. Sci. Part A Polym. Chem.* **2014**, *52*, 3123–3133. [CrossRef]

24. Selvam, S.; Pithapuram, M.V.; Victor, S.P.; Muthu, J. Injectable in situ forming xylitol-PEG-based hydrogels for cell encapsulation and delivery. *Colloids Surfaces B Biointerfaces* **2015**, *126*, 35–43. [CrossRef]

25. Li, Y.; Thouas, G.A.; Chen, Q. Novel elastomeric fibrous networks produced from poly(xylitol sebacate)2:5 by core/shell electrospinning: Fabrication and mechanical properties. *J. Mech. Behav. Biomed. Mater.* **2014**, *40*, 210–221. [CrossRef]

26. Li, Y.; Chen, Q.Z. Fabrication of mechanically tissue-like fibrous poly(xylitol sebacate) using core/shell electrospinning technique. *Adv. Eng. Mater.* **2015**, *17*, 324–329. [CrossRef]

27. Firoozi, N.; Kang, Y. A Highly Elastic and Autofluorescent Poly(xylitol-dodecanedioic Acid) for Tissue Engineering. *ACS Biomater. Sci. Eng.* **2019**, *5*, 1257–1267. [CrossRef]

28. Akiyama, H.; Yoshida, M. Photochemically reversible liquefaction and solidification of single compounds based on a sugar alcohol scaffold with multi azo-arms. *Adv. Mater.* **2012**, *24*, 2353–2356. [CrossRef]

29. Sugane, K.; Takahashi, H.; Shimasaki, T.; Teramoto, N.; Shibata, M. Stereocomplexation, Thermal and Mechanical Properties of Conetworks Composed of Star-Shaped L-Lactide, D-Lactide and $\varepsilon$-Caprolactone Oligomers Utilizing Sugar Alcohols as Core Molecules. *Polymers* **2017**, *9*, 582. [CrossRef]

# Structure and Properties of Biodegradable Poly (Xylitol Sebacate-Co-Butylene Sebacate) Copolyester

**Marta Piątek-Hnat [1,2,*]** , **Kuba Bomba [1,2]** and **Jakub Pęksiński [1,3]**

1    West Pomeranian University of Technology, Szczecin, Science, Piastów Ave. 17, 70-310 Szczecin, Poland; bk34688@zut.edu.pl (K.B.); jakub.peksinski@zut.edu.pl (J.P.)

2    Faculty of Chemical Technology and Engineering Piastów Ave. 42, 71-065 Szczecin, Poland

3    Faculty of Electrical Engineering, Sikorskiego Ave. 37, 71-313 Szczecin, Poland

*    Correspondence: marp@zut.edu.pl

**Abstract:** In this work, a bio-based copolyester with good mechanical properties was synthesized and characterized in terms of structure, main properties and biodegradability Determining the chemical structure of such materials is important to understand their behavior and properties. Performing an extraction of insoluble cross-linked polymer using different solvents allowed us to analyze how the polymer behaves when subjected to different chemical environments, and to obtain soluble samples suitable for more in-depth analysis. Chemical structure of poly (xylitol sebacate-co-butylene sebacate) was determined by a ^{1}H NMR and FTIR analysis of both prepolymer gel sample and samples obtained by extraction of cross-linked polymer using different solvents. Block structure of the copolymer was confirmed by both NMR and DSC. Gel fraction, swelling value, water contact angle, and mechanical properties were also analyzed. Biodegradability of this material was confirmed by performing enzymatic and hydrolytic degradation. Synthesizing sugar-alcohol based copolyester using three monomers leads to obtaining a material with interesting chemical structure and desirable mechanical properties comparable to conventional elastomers.

## 1. Introduction

Sugar alcohols as monomers for polymer synthesis have recently received an appreciable amount of attention from researchers, and have been used as substrates to synthesize a wide variety of materials with very different properties and possible applications. These materials include compounds with sugar alcohols scaffolds and azo-arms which can be reversibly photochemically liquefied and solidified [1], shape-memory poly (mannitol sebacate)/cellulose nanocrystal composites [2], hydroxyapatite composites with poly (sorbitol sebacate malate) matrix [3] polyurethanes with sorbitol as a chain extender for self-healing materials [4] and protective coatings [5]. Xylitol in particular has been used as a monomer for synthesis of multiple materials with different characteristics, which include: core-shell electrospinnable poly (xylitol sebacate) [6,7], elastomeric copolyester with two dicarboxylic acids used as other monomers [8], and autofluorescent poly (xylitol-dodecandioic acid) [9]. Xylitol was also used as a substrate to develop injectable poly (xylitol-co-maleate-co-PEG) hydrogels [10], and star-shaped lactide and $\varepsilon$-caprolactone oligomers with xylitol and other sugar alcohols as core molecules [11]. Xylitol has also been used to synthesize poly (xylitol sebacate) which was analyzed by ^{13}C NMR and determined to be a linear chain comprised mainly of 1-acyl and 1,5-diacyl substitutions. Secondary and tertiary hydroxyl groups have very low reactivity, which lead us to conclude that our polymer has a non-branching linear structure [12].

Possibility to fine-tune thermal and mechanical properties, and degradation times of sugar-alcohol based polyesters was investigated, by performing syntheses with different dicarboxylic acids [13,14], different sugar alcohols [15,16], or by changing the stoichiometric ratio of monomers [16–18]. Sugar alcohol based polyesters can also be synthesized using an additional monomer - with dicarboxylic acid, sugar alcohol and a diol as the third monomer. Properties of such copolymers can be modified by changing the chain length of diols used for the synthesis [19]. Such copolyesters can also be synthesized using enzymatic catalysis with Candida antarctica Lipase B as a catalyst [20]. Various biodegradable multiblock copolymers synthesized using dicarboxylic acid and butylene glycol have also been described in the literature [21–23].

Taking into account the considerable amount of interest received by sugar alcohols as monomers for polymer synthesis, and our earlier analysis of physiochemical properties of xylitol-containing polymer [24], and sorbitol-containing polymer [25] we have concluded that the next logical step in our research was an exact examination of chemical structure and properties of poly (xylitol sebacate-co-butylene sebacate) copolymer which is a good example of sugar-alcohol-based materials. In order to do so, an extraction on insoluble cross-linked polymer using many different solvents was performed. It allowed us to analyze how the polymer behaves after being subjected to different chemical environments, and to obtain soluble samples suitable for more in-depth analysis.

## 2. Results and Discussion

As a result of the synthesis described in 2.1 poly (xylitol sebacate-co-butylene sebacate) (PXBS) was obtained. Reaction scheme is shown in Figure 1. Polymer after cross-linking is characterized by mechanical properties typical for elastomer group (0.93 ± 0.25 MPa stress at break, 306 ± 64% elongation at break) and has hydrophilic (46° contact angle) surface properties.
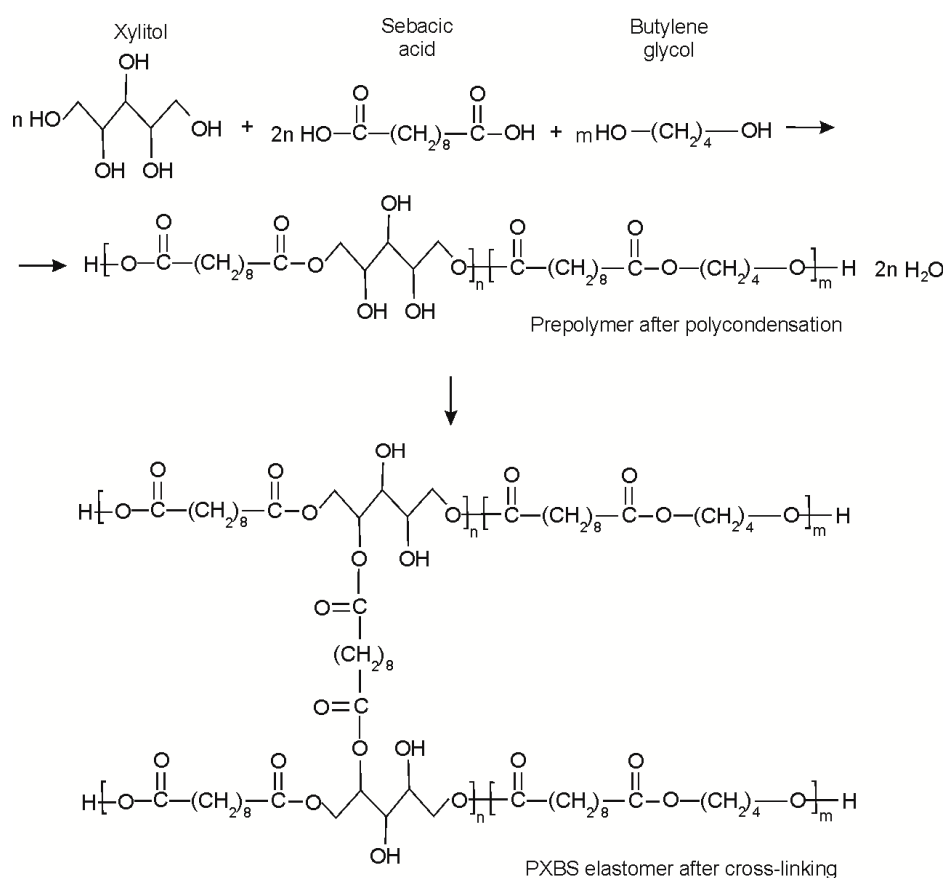


**Figure 1.** Reaction scheme of poly (xylitol sebacate-co-butylene sebacate) (PXBS) synthesis.

## 2.1. Swelling

Results of the swelling test are shown in the Figure 2. Swelling value in the range of 400–600% can be observed for samples which resided in THF, DMF, DMSO, and CHCl$_3$. Sample which resided in MeOH has the lowest swelling value. Highest swelling values are exhibited by samples which resided in HFIP (1280%) and TFA (1712%). Those fluorinated solvents penetrate the polymer network the most and cause its degradation. The degradation of polymer network was confirmed by DSC analysis which shows the lowest change in heat capacity during glass transition for polymer samples which resided in those solvents.
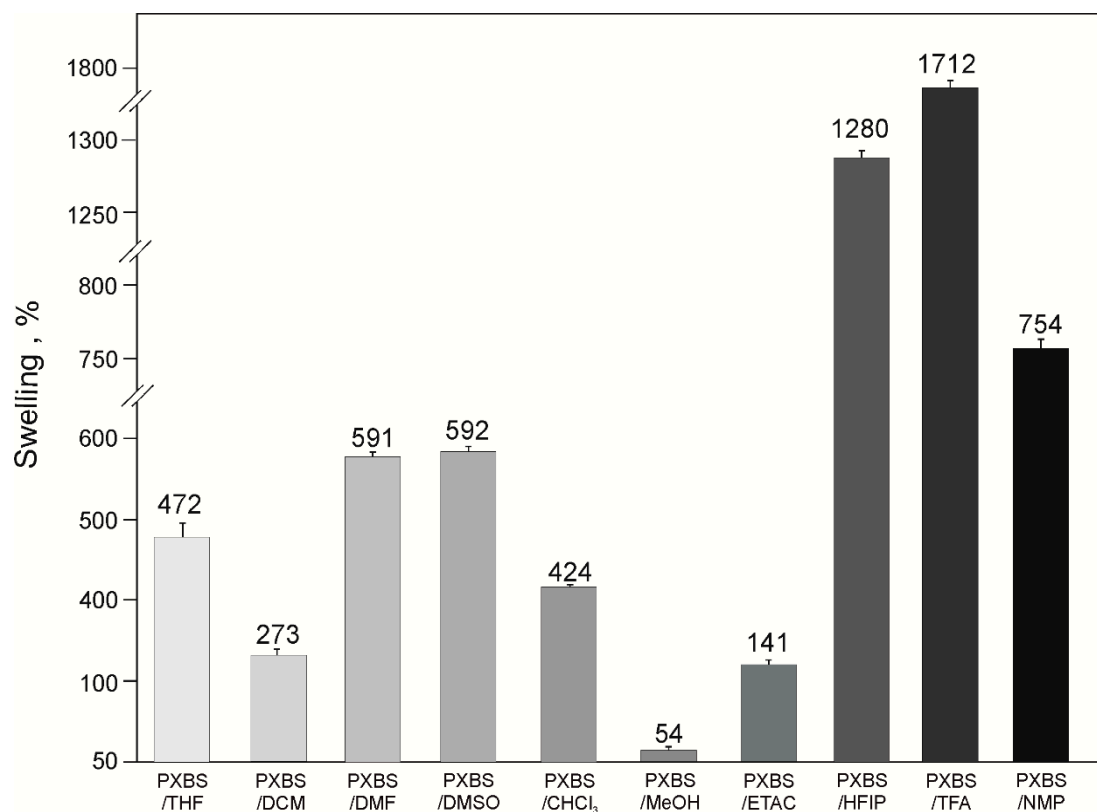


**Figure 2.** Swelling of PXBS.

## 2.2. Gel Fraction

Values of gel fraction (Figure 3) for all samples are in 65–90% range. Relatively high gel fraction in samples extracted using the most penetrating solvents (TFA and HFIP) is caused by solvent being confined deep within the polymer network which makes it impossible for it to completely evaporate. Solvent most suitable for purification of PXBS is DCM, because it has the least destructive effect on the polymer structure, as confirmed by the highest gel fraction value for the sample extracted by this solvent.
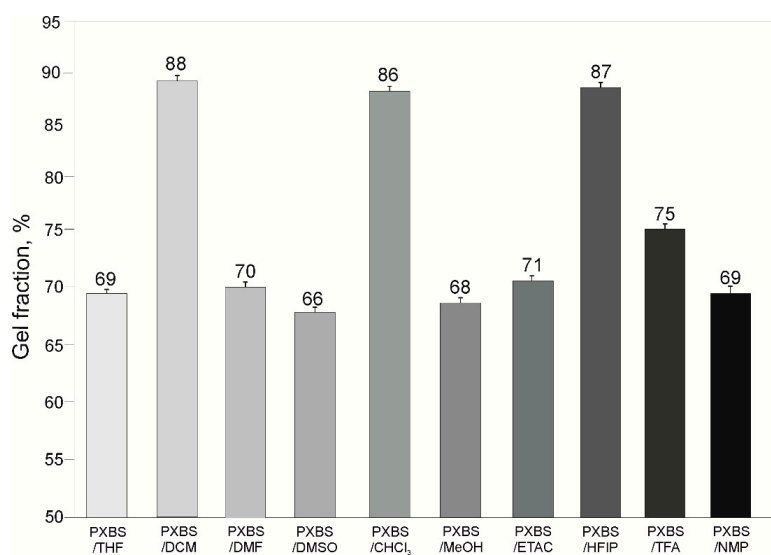
**Figure 3.** Gel fraction of PXBS.

### 2.3. Fourier Transform Infrared Spectroscopy (FTIR)

Figure 4 shows FTIR spectra of sample of cross-linked polymer, and samples of insoluble cross-linked polymer fraction left after extraction with various solvents (gel fraction). Figure 5 shows spectra of sample taken directly after polycondensation, and samples of soluble polymer fraction obtained by extraction (sol fraction). FTIR spectra show transmittance peaks typical for a polyester structure. Peak at about 1150 cm$^{-1}$ can be attributed to C-O-C groups, peak at about 1720 cm$^{-1}$ corresponds to C=O groups, peak at about 2900 cm$^{-1}$ can be assigned to alkyl groups, and peak at about 3440 cm$^{-1}$ can be attributed to intermolecularly associated OH groups. For samples after extraction, due to the C-O-C bonds breaking apart during the extraction process there is a slight separation in the peak at about 1700 cm$^{-1}$ because signals from dicarboxylic acid emerge. Another sign of the degradation process is increase in peak intensity in peaks assigned to -OH groups. For insoluble polymer sample after extraction by DCM there is an increase in intensity of non-intermolecularly-associated -OH groups due to the hydrogen bounds breaking apart.
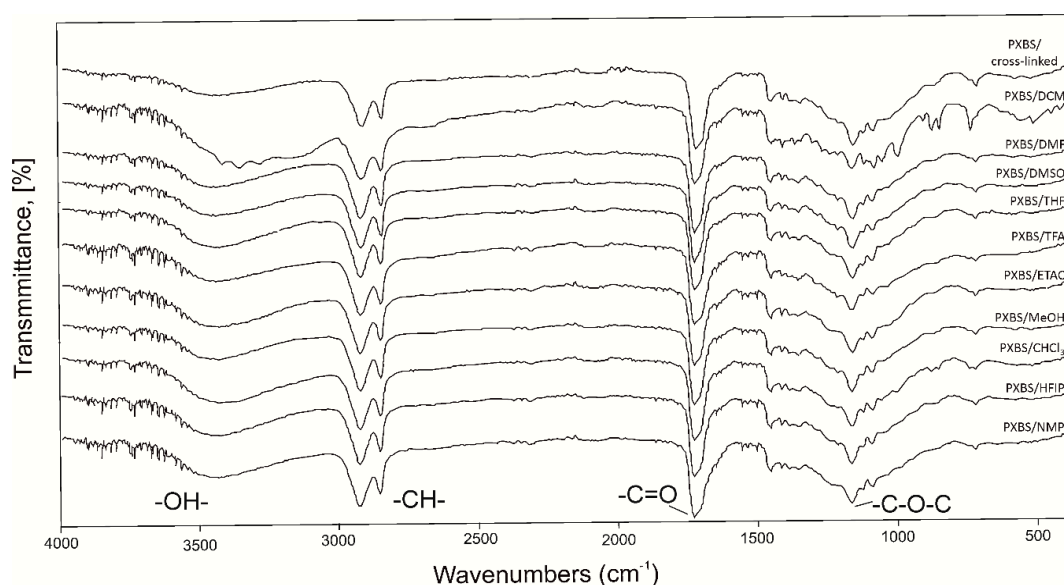


**Figure 4.** FTIR spectra of PXBS sample after cross-linking and samples of insoluble cross-linked polymer fraction left after extraction (gel fraction).
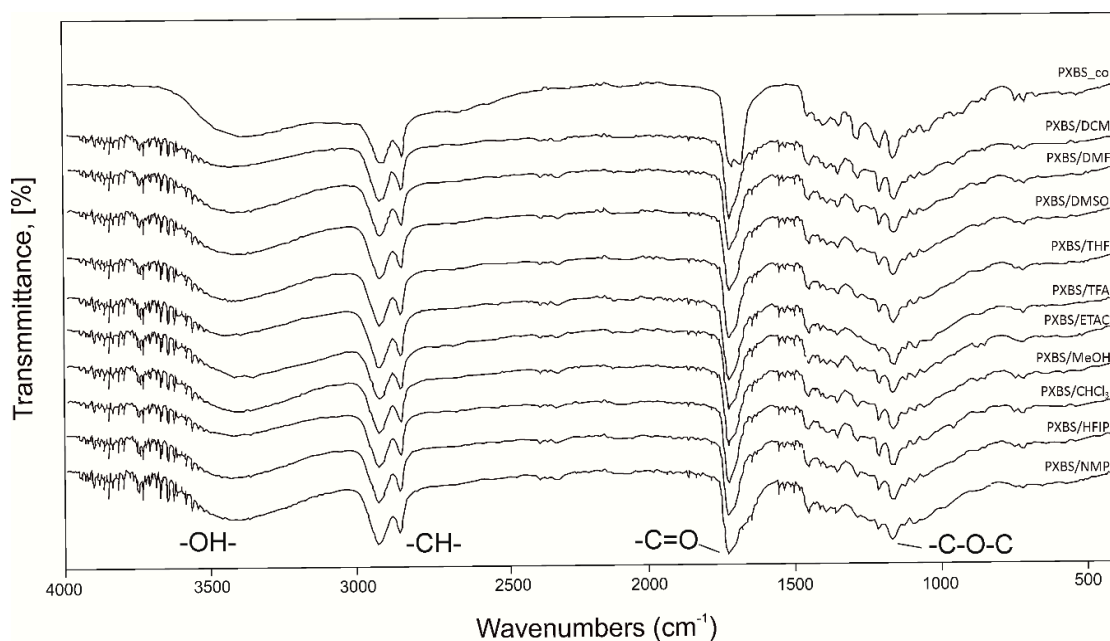
**Figure 5.** FTIR spectra of PXBS sample after polycondensation and samples of soluble polymer fraction obtained by extraction (sol fraction).

## 2.4. NMR Spectroscopy

^{1}H NMR analysis was performed in order to confirm if theoretically assumed structure of the PXBS copolymer was correct. Indeed, the ^{1}H NMR measurements (Figures 6–10) have proven that the copolymer structure is made up of xylitol-sebacic acid and butylene glycol-sebacic acid segments. Peak at about 4.21 ppm corresponds to the proton adjacent to the oxygen atom which is a part of the ester bond between xylitol and sebacic acid. Peak at about 4.08 ppm was attributed to the proton adjacent to the oxygen atom making up the ester bond between butylene glycol and sebacic acid. Following signals were assigned to alkyl groups in sebacic acid: peak at about 2.30 ppm corresponds to $CH_2$(a) group, doublet at 1.60 and 1.70 ppm was attributed to $CH_2$ (b), and $CH_2$ (g) group, and peak at about 1.30 was ascribed to $CH_2$(c) group. Peaks between about 4.00 and 3.58 ppm correspond to $CH_2$(d) groups in xylitol. Furthermore, it is worth noting that ^{1}H NMR spectrum of sample taken directly after polycondensation, and samples obtained by extraction of the cross-linked material are almost identical, which means that the extraction process completely destroyed the cross-links between polymer chains. The ratio of peak areas from peak at 4.08 ppm to the peak at 4.21 ppm is 2.42, which means that on average, for every xylitol-dicarboxylic acid ester bond there are 2.42 bonds between butylene glycol and dicarboxylic acid. This leads to a conclusion that xylitol is less reactive than butylene glycol in synthesis carried out using three monomers. Considering the fact that not every xylitol particle becomes a part of the linear, non-cross-linked polymer we assume that there are some unreacted xylitol left-overs confined within cross-linked polymer network.

Peak at about 5.4 is an average signal from protons from both carboxyl and hydroxyl groups. This signal averaging is caused by the rapid exchange of protons from both these groups [26]. Presence of this peak is a confirmation that there is some unreacted dicarboxylic acid in the sample taken directly after polycondensation.
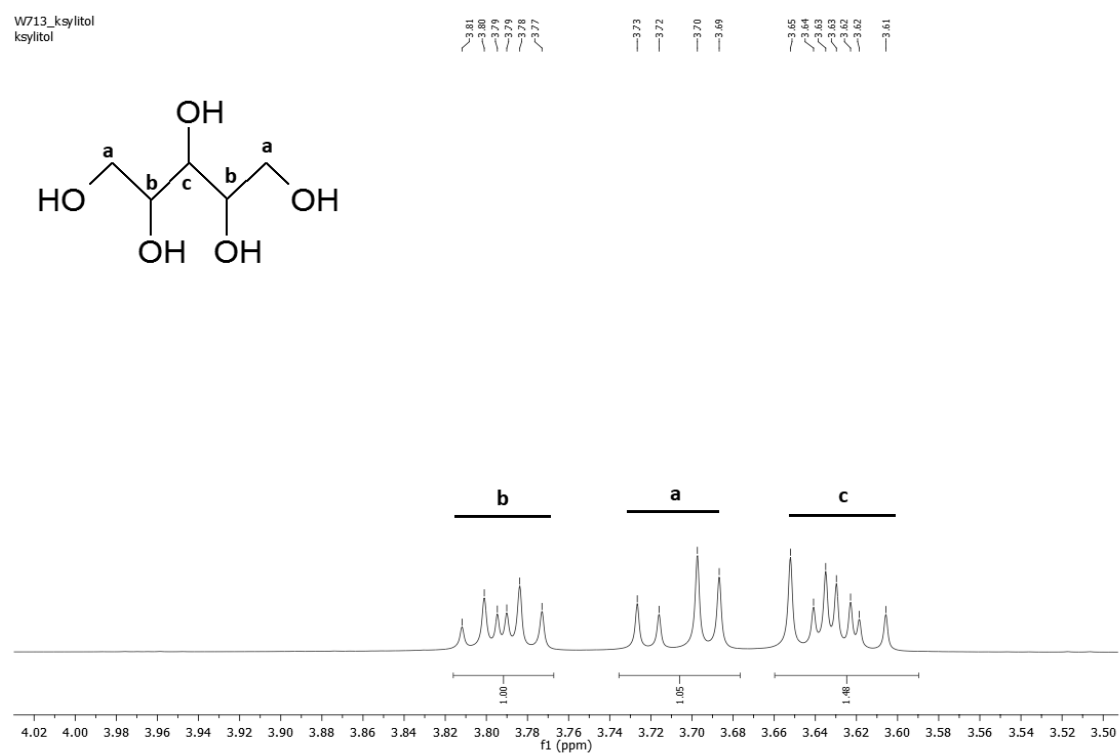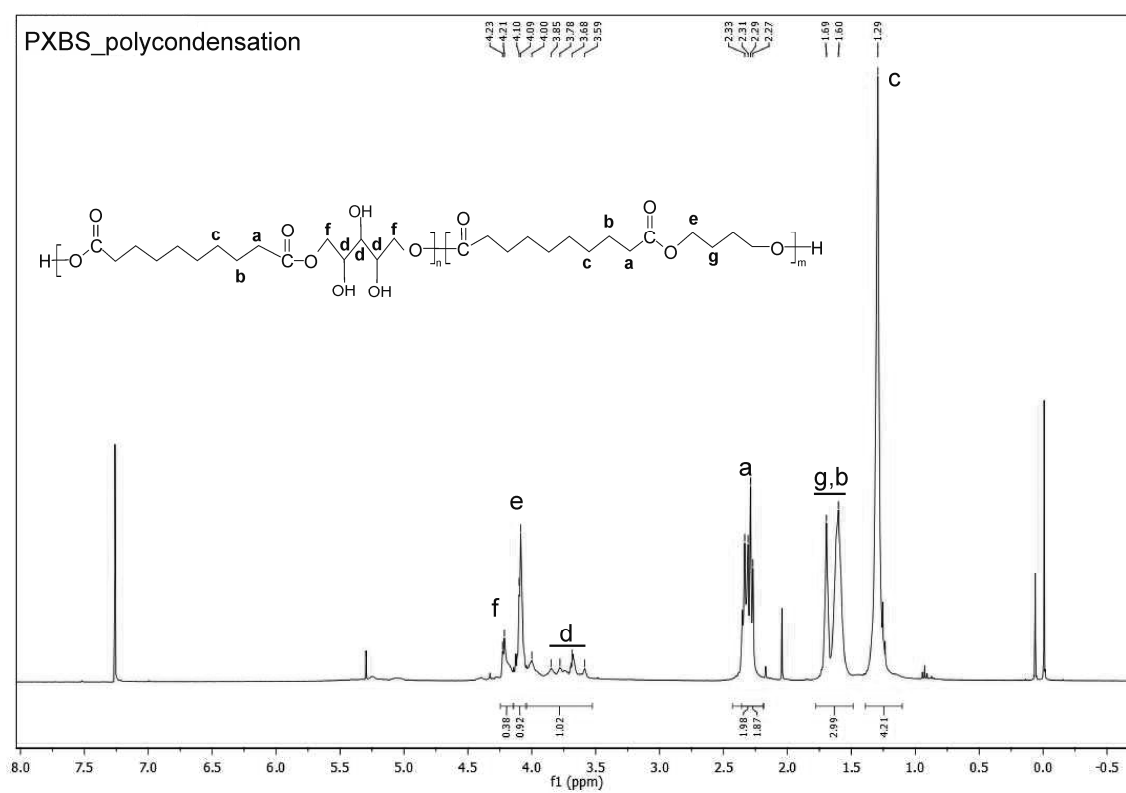
**Figure 6.** NMR spectrum of xylitol.



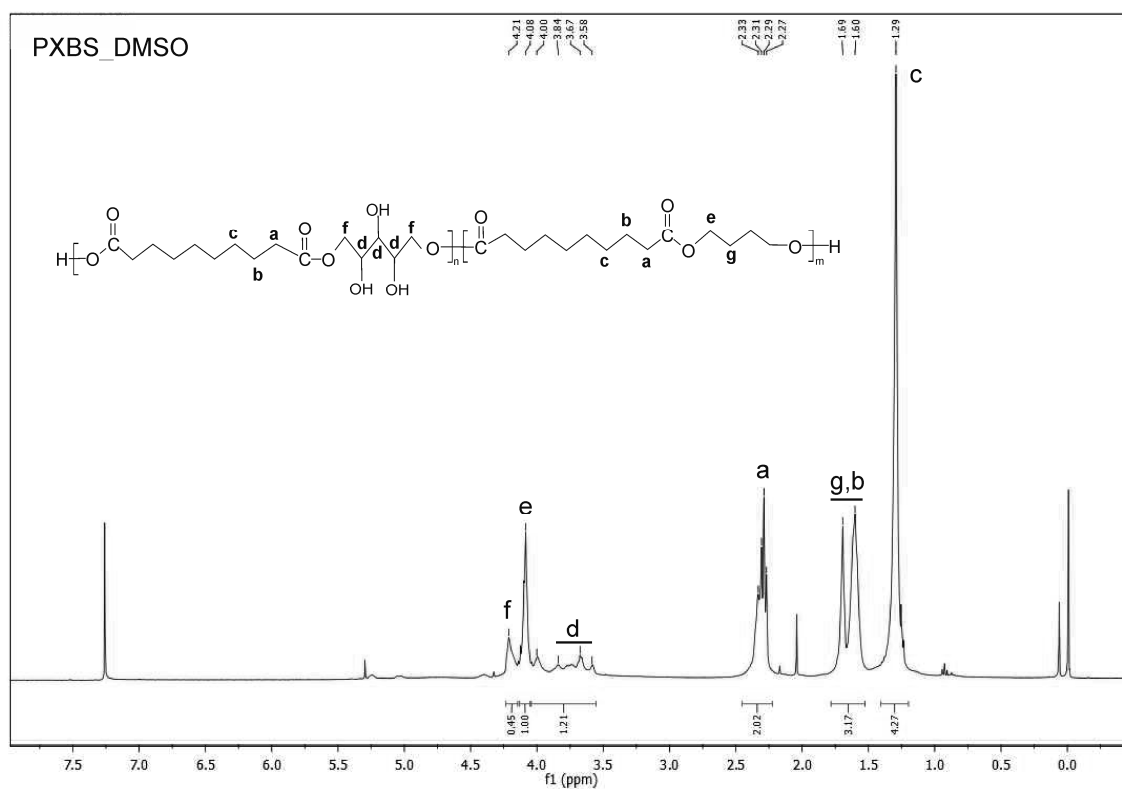**Figure 7.** *NMR spectrum of PXBS* after polycondensation.

**Figure 8.** NMR spectrum of sample of soluble PXBS fraction obtained by extraction in DMSO solvent.
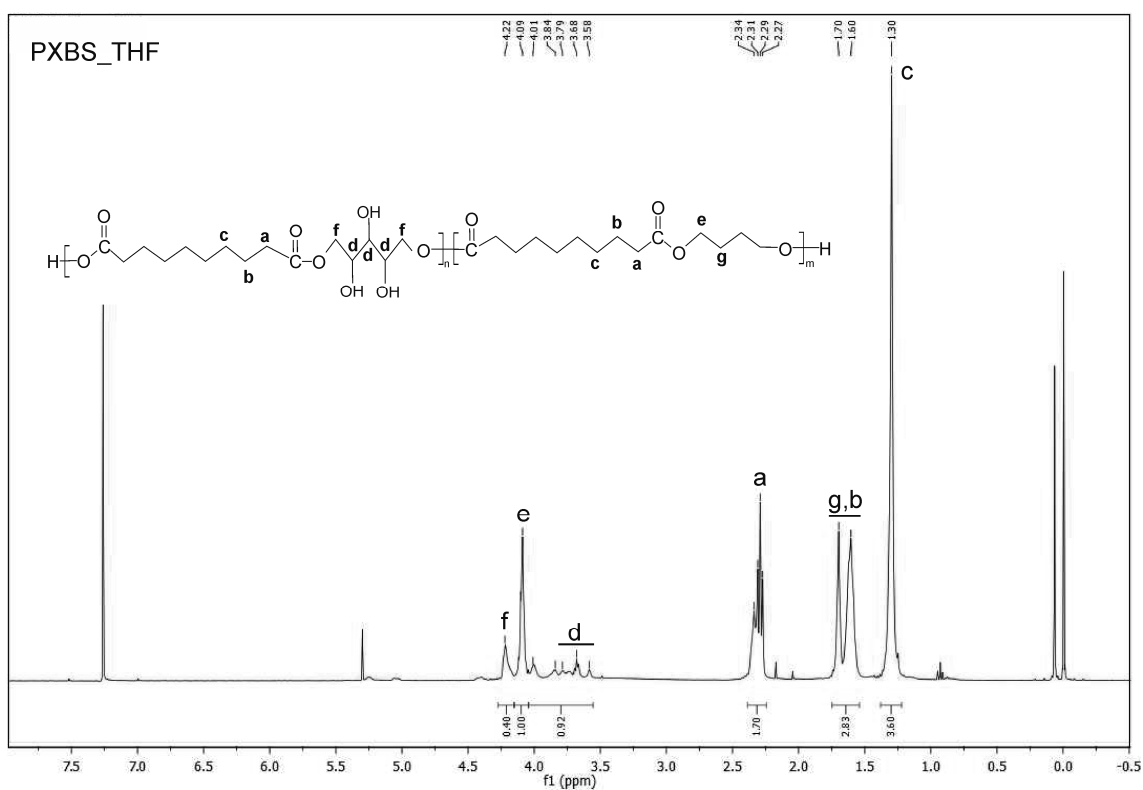


**Figure 9.** NMR spectrum of sample of soluble PXBS fraction obtained by extraction in THF solvent.
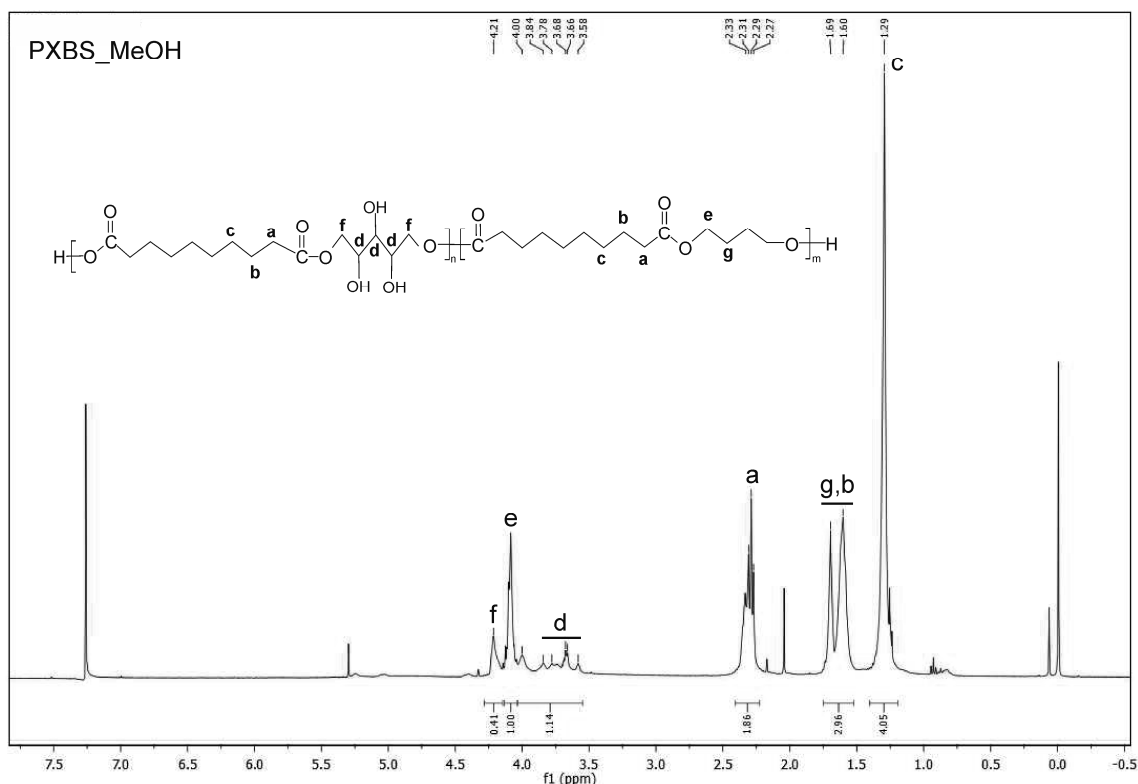
**Figure 10.** NMR spectrum of sample of soluble PXBS fraction obtained by extraction in MeOH solvent.

## 2.5. Differential Scanning Calorimetry (DSC).

In Table 1 (also available in Supplementary Materials) and Figure 11 results of DSC analysis are shown. For the sample of cross-linked material and samples of insoluble cross-linked polymer fraction left after extraction by different solvents (gel fraction) two transition temperatures can be seen. Presence of glass transition temperature ($T_{g1}$) and associated with it change in heat capacity ($\Delta c_p$) is a confirmation of cross-linked amorphous structure of the polymer. Melting transition ($T_{m1}$) is the result of the presence of crystalline areas confined within amorphous polymer network. Extracting the polymer with the most aggressive solvents (HFIP and TFA) leads to a disruption of the amorphous phase of the elastomers, and decrease of $\Delta c_p$.

**Table 1.** Thermal properties of PXBS sample after cross-linking and samples of insoluble cross-linked PXBS fraction left after extraction (PXBS_GEL) (**A**) and thermal properties of the PXBS sample taken after polycondensation (PXBS_co) and samples of soluble PXBS fraction obtained by extraction (PXBS_SOL) (**B**), first heating.

| Sample/Material | PXBS_GEL | | | | Sample/Material | PXBS_SOL | | | |
|---|---|---|---|---|---|---|---|---|---|
| | $T_{g1}$ [°C] | $\Delta c_p$ [J/g°C] | $T_{m1}$ [°C] | $\Delta H_{m1}$ [J/g] | | $T_{m2}$ [°C] | $\Delta H_{m2}$ [J/g] | $T_{m3}$ [°C] | $\Delta H_{m3}$ [J/g] |
| **PXBS_Cross-Linked** | −29.9 | 0.412 | 16.8 | 26.3 | PXBS_co | 19.1 | 26.4 | 44.8 | 50.9 |
| PXBS_THF | −28.3 | 0.550 | 11.1 | 9.1 | PXBS_THF | 16.5 | 44.2 | n.o | n.o |
| PXBS_DMSO | −31.7 | 0.439 | 14.7 | 28.2 | PXBS_DMSO | 20.4 | 33.3 | 47.9 | 18.6 |
| PXBS_HFIP | −25.8 | 0.342 | 18.4; 41.8 | 26.4; 1.6 | PXBS_HFIP | 20.1 | 29.8 | 41.2 | 14.8 |
| PXBS_TFA | −32.3 | 0.143 | 9.1; 20.8 | 40.3 | PXBS_TFA | 11.1; 25.2 | 19.8 | n.o | n.o. |

n.o.—not observed, where: $T_{g1}$-glass transition temperatures; $\Delta c_p$-change of the heat capacity at glass transition, $T_{m1}$, $T_{m2}$, $T_{m3}$-melting temperature; $\Delta H_{m1}$, $\Delta H_{m2}$, $\Delta H_{m3}$-enthalpy of melting at $T_{m1}$, $T_{m2}$, $T_{m3}$.
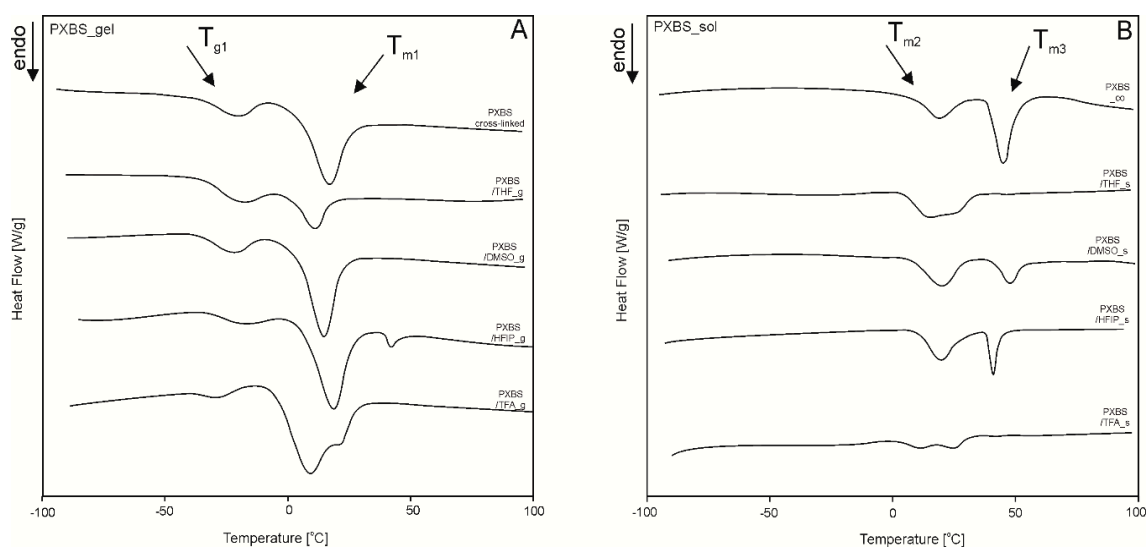
**Figure 11.** DSC thermograms of PXBS sample after cross-linking and samples of insoluble cross-linked PXBS fraction left after extraction (**A**) and thermograms of PXBS sample after polycondensation and samples of soluble PXBS fraction obtained by extraction (**B**).

For the sample taken directly after polycondensation, and samples of soluble polymer fraction obtained by extraction (sol fraction) melting transition observable for insoluble fraction ($T_{m1}$) splits into two, and two melting transitions can be observed. First melting transition ($T_{m2}$) is a result of melting of poly (xylitol sebacate) blocks, and second melting transition ($T_{m3}$) is a result of melting of poly (butylene sebacate) blocks. For samples after extraction, poly (butylene sebacate) blocks cannot crystalize properly when solvent evaporates, which leads to either decreased enthalpy ($\Delta H_{m3}$) (for DMSO and HFIP), or the transition not being observable at all (for THF and TFA).

### 2.6. Hydrolytic and Enzymatic Degradation

Results of hydrolytic and enzymatic degradation are shown in Figure 12.
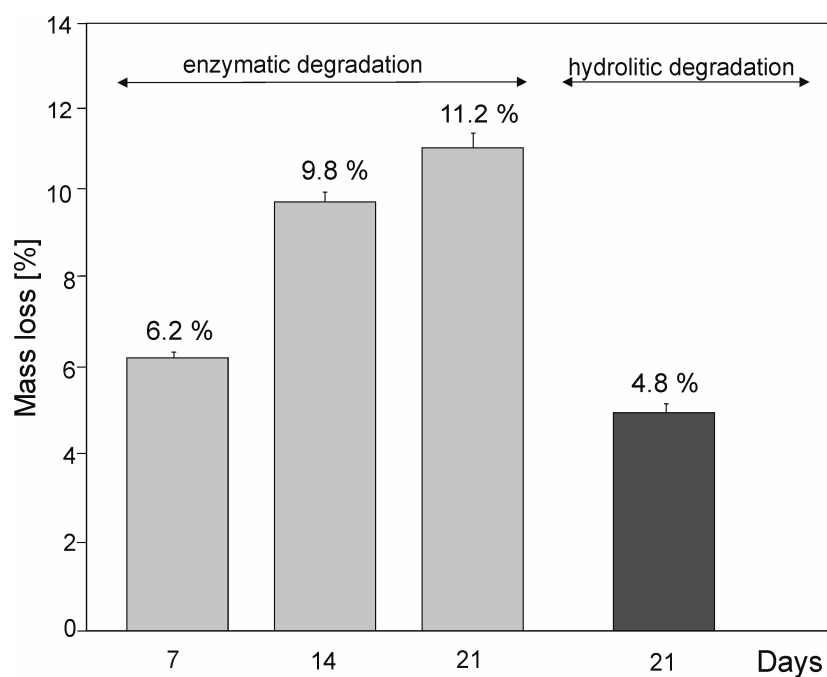


**Figure 12.** The enzymatic and hydrolytic degradation of PXBS.

Rate of enzymatic degradation is faster than the rate of hydrolytic degradation. After 7 days of enzymatic degradation, the mass loss (6.2%) is higher than the mass loss (4.8%) of the sample after 21 days of hydrolytic degradation. We have compared the results with degradation times of commercially available biodegradable polyesters: PLLA-co-PGA, PGA, and PDS and concluded that our material is biodegradable [27].

## 3. Materials and Methods

### 3.1. Synthesis of PXBS

All reagents were purchased from Sigma-Aldrich (St. Louis, MO, USA). Xylitol-containing copolymer:poly(xylitol sebacate-co-butylene sebacate) was synthesized with a sebacic acid:butylene glycol:xylitol ratio of 2:1:1 (PXBS). The monomers were melted in a flask at a temperature above 100 °C under a blanket of $N_2$. The esterification reaction was then carried out for 13.5 h at 150 °C in $N_2$ atmosphere, catalyzed by Ti (OBu)$_4$. The next step was a 3,5 h polycondensation reaction at 150 °C in a vacuum. The prepolymer was then cross-linked in a vacuum dryer at 100 °C in 100 mBar.

### 3.2. Extraction

Cross-linked polymer samples (10 g) were placed in a Soxhlet apparatus and subjected to extraction in boiling tetrahydrofuran (THF), dichloromethane (DCM), dimethylformamide (DMF), dimethyl sulfoxide (DMSO), trifluoroacetic acid (TFA), ethyl acetate (ETAC), methanol (MeOH), chloroform (CHCl$_3$), 1,1,1,3,3,3-hexafluoro-2-propanol (HFIP), n-methylpyrrolidone (NMP) (100 cm$^3$). Samples resided in the solvents for 3 h. After extraction, the samples were dried in a vacuum oven at 25 °C and then in a desiccator.

Two kinds of samples were acquired: samples of insoluble cross-linked polymer fraction left after extraction (gel fraction), and samples of soluble polymer fraction obtained by extraction (sol fraction).

### 3.3. Experimental Methods

#### 3.3.1. Swelling

Equilibrium swelling in tetrahydrofuran (THF), dichloromethane (DCM), dimethylformamide (DMF), dimethyl sulfoxide (DMSO), trifluoroacetic acid (TFA), ethyl acetate (ETAC), methanol (MeOH), chloroform (CHCl$_3$), 1,1,1,3,3,3- hexafluoro-2-propanol (HFIP), and n-methylpyrrolidone (NMP) was measured by calculating the relative percentage increase in the mass of the cross-linked samples residing in the solvents for 72 h at 20 °C, in accordance with PN-EN 579: 2001 method. Each sample subjected to swelling was 10 g. The content of swelling [%] was calculated from formula (1) as the mean of three measurements:

$$E = (l_t - l_0)/l_o \cdot 100\% \tag{1}$$

where: $l_t$—mass after time t = 72 h, $l_0$—mass at time t = 0.

#### 3.3.2. Gel Fraction

Determination of the gel fraction of elastomer after cross-linking was made by the extraction method PN-EN 579:2001. Samples of the material after cross-linking (about 10 g) were placed in Schott type P2 crucible and subjected to extraction in boiling tetrahydrofuran (THF), dichloromethane (DCM), dimethylformamide (DMF), dimethyl sulfoxide (DMSO), trifluoroacetic acid (TFA), ethyl acetate (ETAC), methanol (MeOH), chloroform (CHCl$_3$), 1,1,1,3,3,3- hexafluoro-2-propanol (HFIP), n-methylpyrrolidone (NMP) (100 cm$^3$) for 3 h. After extraction, the samples were dried in a vacuum oven at 25 °C and then in a desiccator. Three determinations were made for each sample. The content of gel fraction was calculated from formula (2) as the mean of three measurements:

$$X = m_1/m_0 \cdot 100\% \tag{2}$$

where: $m_1$—sample mass after extraction, $m_0$—sample mass before extraction

### 3.3.3. Fourier Transform Infrared Spectroscopy (FTIR)

Fourier transform infrared spectroscopy (ATR FTIR Alpha spectrometer, Bruker, Germany) was used to examine the chemical structure of the PXBS polymer. Sample of the polymer after cross-linking and samples of insoluble cross-linked polymer fraction left after extraction (gel fraction) were analyzed. Sample of polymer after polycondensation, and samples of soluble polymer fraction obtained by extraction (sol fraction) were also examined. FTIR transmittance spectra were recorded between 400 and 4000 $cm^{-1}$, with a resolution of 2 $cm^{-1}$, and 32 scans. Test results were developed using Omnic software.

### 3.3.4. NMR Spectroscopy

Nuclear magnetic resonance spectroscopy (NMR) was used to analyze the chemical structure of PXBS copolymer, and xylitol used for the synthesis. Analysis of the polymer was performed on four polymer samples. One sample was taken directly after polycondensation, and the next three samples were obtained by performing extraction of the cross-linked polymer, using three different solvents—dimethyl sulfoxide (DMSO), methanol (MeOH), and tetrahydrofuran (THF). All polymer samples were dissolved in deuterated chloroform ($CDCl_3$). Xylitol sample was dissolved in water. Measurements were performed on Bruker DPX 400 MHz. Results were analysed using MestReNova program.

### 3.3.5. Differential Scanning Calorimetry (DSC).

Thermal properties were analyzed using differential scanning calorimetry (DSC) (Q 2500, TA Instruments apparatus, New Castle, USA). The measurement was carried out in a heating cycle in temperature range from −100 to 100 °C, and 10 °C/min heating rate in nitrogen atmosphere. Sample of polymer after cross-linking and samples of insoluble cross-linked polymer fraction left after extraction (gel fraction) were analyzed. Sample of polymer after polycondensation, and samples of soluble polymer fraction obtained by extraction (sol fraction) were also examined. Weight of the samples was 10–15 mg. Results were analyzed with TA Instruments Universal Analysis program.

### 3.3.6. Mechanical Properties

Mechanical tests were carried out with an Instron 3366 instrument equipped with a 500 N load cell in accordance with standard PN-EN-ISO 527/1:1996 (crosshead speed of 100 mm/min, at 25 °C and 50% of relative humidity). Measurements were performed on a fully cross-linked polymer sample.

### 3.3.7. Water Contact Angle

Water contact angle was measured using a KRUSS DSA100 digital goniometer. Static contact angle measurements were performed on the surface of degreased material by placing a 2 μL droplet of deionized water using the automatic dispenser of the goniometer. Contact angle was calculated using Kruss drop shape analysis software (DSA4). Measurements were performed on a fully cross-linked polymer sample.

### 3.3.8. Hydrolytic Degradation

Hydrolytic degradation was carried out on previously sterilized 10 mm (0.5 g) polymer discs obtained from not-extracted, fully cross-linked material, for 21 days in phosphate-buffered saline (PBS) (Sigma Aldrich, Poznań, Poland) (pH range 7.1–7.2), in 37 °C. PBS solution was changed every 48 h. Sterilization was conducted in a laminar chamber for 15 min, using UV light. Samples were placed in a 24-well-plate. Each sample was covered with 1.5 mL of the solution. Samples after degradation were

dried in a vacuum dryer in 25 °C and then weighed. Mass loss after 21 days was calculated using formula (3)

$$D = (m_0 - m_1)/m_0 \cdot 100\% \tag{3}$$

where D—mass loss [%], $m_0$—sample mass before degradation [g], $m_1$—sample mass after degradation [g].

### 3.3.9. Enzymatic Degradation

Enzymatic degradation was carried out on previously sterilized 10 mm (0.5 g) polymer discs obtained from not-extracted, fully cross-linked material for 21 days in solution of lipase (*Pseudomonas Cepacia*) (Sigma Aldrich, Poznań, Poland) (25 units/mL) in phosphate-buffered saline (PBS) (Sigma Aldrich, Poznań, Poland) (pH range 7.1–7.2). Lipase solution was changed every 48 h. Sterilization was conducted in a laminar chamber for 15 min, using UV light. Samples were placed in a 24-well-plate. Each sample was covered with 1.5 mL of the solution. Samples after degradation were dried in vacuum dryer in 25 °C and then weighed. Mass loss after 7, 14, and 21 days was calculated using formula (4)

$$D = (m_0 - m_1)/m_0 \cdot 100\% \tag{4}$$

where D—mass loss [%], $m_0$—sample mass before degradation [g], $m_1$—sample mass after degradation [g].

## 4. Conclusions

In this paper we describe a biodegradable polymer which belongs to a recently developed group of xylitol-based materials.

It is characterized by good mechanical properties typical for the elastomer group. We have concluded that an exact determination of the polymer structure was necessary to better understand its behavior and properties. Because of the insolubility of cross-linked polymer, we have performed an extraction of this material using different solvents in order to obtain samples suitable for in-depth analysis. It has also allowed us to analyze how the polymer behaves after being subjected to different chemical environments.

NMR analysis has proven that this polymer has a structure consisting of poly (xylitol sebacate) and poly (butylene sebacate) blocks with dicarboxylic acid creating bonds between polymer chains during cross-linking process.

Furthermore, the structure was additionally confirmed by DSC analysis. Two characteristic melting temperatures from two different blocks were observed. Polymer biodegradability was also confirmed.

Additionally, it is worth noting that elastomers synthesized using butylene glycol as third monomer have better mechanical properties than materials synthesized using only sugar-alcohol and dicarboxylic acid, described in the literature.

## References

1. Akiyama, H.; Yoshida, M. Photochemically reversible liquefaction and solidification of single compounds based on a sugar alcohol scaffold with multi azo-arms. *Adv. Mater.* **2012**, *24*, 2353–2356. [CrossRef] [PubMed]
2. Sonseca, Á.; Camarero-Espinosa, S.; Peponi, L.; Weder, C.; Foster, E.J.; Kenny, J.M.; Giménez, E. Mechanical and shape-memory properties of poly (mannitol sebacate)/cellulose nanocrystal nanocomposites. *J. Polym. Sci. Part A Polym. Chem.* **2014**, *52*, 3123–3133. [CrossRef]
3. Tham, W.H.; Wahit, M.U.; Kadir, M.R.A.; Wong, T.W. Mechanical and thermal properties of biodegradable hydroxyapatite/poly (sorbitol sebacate malate) composites. *Songklanakarin J. Sci. Technol.* **2013**, *35*, 57–61.

4.  Lee, S.H.; Shin, S.R.; Lee, D.S. Sorbitol as a chain extender of polyurethane prepolymers to prepare self-healable and robust polyhydroxyurethane elastomers. *Molecules* **2018**, *23*, 2515. [CrossRef] [PubMed]

5.  Anand, A.; Kulkarni, R.D.; Patil, C.K.; Gite, V.V. Utilization of renewable bio-based resources, viz. sorbitol, diol, and diacid, in the preparation of two pack PU anticorrosive coatings. *RSC Adv.* **2016**, *6*, 9843–9850. [CrossRef]

6.  Li, Y.; Thouas, G.A.; Chen, Q. Novel elastomeric fibrous networks produced from poly (xylitol sebacate) 2:5 by core/shell electrospinning: Fabrication and mechanical properties. *J. Mech. Behav. Biomed. Mater.* **2014**, *40*, 210–221. [CrossRef]

7.  Li, Y.; Chen, Q.Z. Fabrication of mechanically tissue-like fibrous poly (xylitol sebacate) using core/shell electrospinning technique. *Adv. Eng. Mater.* **2015**, *17*, 324–329. [CrossRef]

8.  Deepa, K.; Jaisankar, V. A Study on Xylitol Based Copolyester for In vitro Degradation Applications. *Int. J. ChemTech Res.* **2018**, *11*, 69–76. [CrossRef]

9.  Firoozi, N.; Kang, Y. A Highly Elastic and Autofluorescent Poly (xylitol-dodecanedioic Acid) for Tissue Engineering. *ACS Biomater. Sci. Eng.* **2019**, *5*, 1257–1267. [CrossRef]

10. Selvam, S.; Pithapuram, M.V.; Victor, S.P.; Muthu, J. Injectable in situ forming xylitol-PEG-based hydrogels for cell encapsulation and delivery. *Colloids Surf. B Biointerfaces* **2015**, *126*, 35–43. [CrossRef]

11. Sugane, K.; Takahashi, H.; Shimasaki, T.; Teramoto, N.; Shibata, M. Stereocomplexation, thermal and mechanical properties of conetworks composed of star-shaped l-lactide, d-lactide and ε-caprolactone oligomers utilizing sugar alcohols as core molecules. *Polymers* **2017**, *9*, 582. [CrossRef] [PubMed]

12. Moorhoff, C.; Li, Y.; Cook, W.D.; Braybrook, C.; Chen, Q.Z. Characterization of the prepolymer and gel of biocompatible poly (xylitol sebacate) in comparison with poly (glycerol sebacate) using a combination of mass spectrometry and nuclear magnetic resonance. *Polym. Int.* **2015**, *64*, 668–688. [CrossRef]

13. Dasgupta, Q.; Chatterjee, K.; Madras, G. Combinatorial approach to develop tailored biodegradable poly (xylitol dicarboxylate) polyesters. *Biomacromolecules* **2014**, *15*, 4302–4313. [CrossRef] [PubMed]

14. Barrett, D.G.; Luo, W.; Yousaf, M.N. Aliphatic polyester elastomers derived from erythritol and α,ω-diacids. *Polym. Chem.* **2010**, *1*, 296–302. [CrossRef]

15. Ning, Z.Y.; Zhang, Q.S.; Wu, Q.P.; Li, Y.Z.; Ma, D.X.; Chen, J.Z. Efficient synthesis of hydroxyl functioned polyesters from natural polyols and sebacic acid. *Chinese Chem. Lett.* **2011**, *22*, 635–638. [CrossRef]

16. Bruggeman, J.P.; de Bruin, B.J.; Bettinger, C.J.; Langer, R. Biodegradable poly (polyol sebacate) polymers. *Biomaterials* **2008**, *29*, 4726–4735. [CrossRef]

17. Bruggeman, J.P.; Bettinger, C.J.; Nijst, C.L.E.; Kohane, D.S.; Langer, R. Biodegradable xylitol-based polymers. *Adv. Mater.* **2008**, *20*, 1922–1927. [CrossRef]

18. Bruggeman, J.P.; Bettinger, C.J.; Langer, R. Biodegradable xylitol-based elastomers: In vivo behavior and biocompatibility. *J. Biomed. Mater. Res. Part A* **2010**, *95*, 92–104. [CrossRef]

19. Kavimani, V.; Jaisankar, V. Synthesis and Characterisation of Sorbitol Based Copolyesters for Biomedical Applications. *J. Phys. Sci. Appl.* **2014**, *4*, 507–515.

20. Hu, J.; Gao, W.; Kulshrestha, A.; Gross, R.A. "Sweet polyesters": Lipase-catalyzed condensation-polymerizations of alditols. *ACS Symp. Ser.* **2008**, *999*, 275–284.

21. Zheng, L.; Wang, Z.; Wu, S.; Li, C.; Zhang, D.; Xiao, Y. Novel poly (butylene fumarate) and poly(butylene succinate) multiblock copolymers bearing reactive carbon-carbon double bonds: Synthesis, characterization, cocrystallization, and properties. *Ind. Eng. Chem. Res.* **2013**, *52*, 6147–6155. [CrossRef]

22. Zheng, L.; Li, C.; Wang, Z.; Wang, J.; Xiao, Y.; Zhang, D.; Guan, G. Novel biodegradable and double crystalline multiblock copolymers comprising of poly (butylene succinate) and poly(ε-caprolactone): Synthesis, characterization, and properties. *Ind. Eng. Chem. Res.* **2012**, *51*, 7264–7272. [CrossRef]

23. Zheng, L.; Li, C.; Huang, W.; Huang, X.; Zhang, D.; Guan, G.; Xiao, Y.; Wang, D. Synthesis of high-impact biodegradable multiblock copolymers comprising of poly (butylene succinate) and poly (1,2-propylene succinate) with hexamethylene diisocyanate as chain extender. *Polym. Adv. Technol.* **2011**, *22*, 279–285. [CrossRef]

24. Piątek-Hnat, M.; Bomba, K. The influence of of cross-linking process on the physicochemical properties of new copolyesters containing xylitol. *Mater. Today Commun.* **2020**, *20*, 100734. [CrossRef]

25. Piątek-Hnat, M.; Bomba, K.; Pęksiński, J. Synthesis and selected properties of ester elastomer containing sorbitol. *Appl. Sci.* **2020**, *10*, 1628. [CrossRef]

26.    Pretsch, E.; Bühlmann, P.; Badertscher, M. *Structure Determination of Organic Compounds*, 4th ed.; Springer-Verlag: Berlin/ Heidelberg, Germany, 2009.

27.    Amass, W.; Amass, A.; Tighe, B. A review of biodegradable polymers: Uses, current developments in the synthesis and characterization of biodegradable polyesters, blends of biodegradable polymers and recent advances in biodegradation studies. *Polym. Int.* **1998**, *47*, 89–144. [CrossRef]

**Sample Availability:** Samples of the compounds poly (xylitol-sebacate co butylene sebacate) are available from the authors.

*Article*

# Effect of E-Beam Irradiation on Thermal and Mechanical Properties of Ester Elastomers Containing Multifunctional Alcohols

**Marta Piątek-Hnat [1,*] , Kuba Bomba [1], Jakub Pęksiński [2] , Agnieszka Kozłowska [1], Jacek G. Sośnicki [3] and Tomasz J. Idzik [3]**

[1] Faculty of Chemical Technology and Engineering, West Pomeranian University of Technology, Piastów Ave. 42, 71-065 Szczecin, Poland; bk34688@zut.edu.pl (K.B.); agak@zut.edu.pl (A.K.)

[2] Faculty of Electrical Engineering, West Pomeranian University of Technology, Sikorskiego Ave. 37, 71-313 Szczecin, Poland; jakub.peksinski@zut.edu.pl

[3] Department of Organic and Physical Chemistry, Faculty of Chemical Technology and Engineering, West Pomeranian University of Technology, Piastów Ave. 42, 71-065 Szczecin, Poland; jacek.sosnicki@zut.edu.pl (J.G.S.); tomasz.idzik@zut.edu.pl (T.J.I.)

\* Correspondence: marp@zut.edu.pl

check for updates

**Abstract:** The aim of this work was to investigate the thermal and mechanical properties of novel, electron beam-modified ester elastomers containing multifunctional alcohols. Polymers tested in this work consist of two blocks: sebacic acid–butylene glycol block and sebacic acid–sugar alcohol block. Different sugar alcohols were utilized in the polymer synthesis: glycerol, sorbitol, xylitol, erythritol, and mannitol. The polymers have undergone an irradiation procedure. The materials were irradiated with doses of 50 kGy, 100 kGy, and 150 kGy. The expected effect of using ionizing radiation was crosslinking process and improvement of the mechanical properties. Additionally, a beneficial side effect of the irradiation process is sterilization of the affected materials. It is also worth noting that the materials described in this paper do not require either sensitizers or cross-linking agent in order to perform radiation modification. Radiation-modified poly(polyol sebacate-co-butylene sebacate) elastomers have been characterized in respect to the mechanical properties (quasi-static tensile tests), cross-link density, thermal properties (Differential Scanning Calorimetry (DSC)), chemical properties: Fourier transform infrared spectroscopy (FTIR), and wettability (water contact angle). Poly(polyol sebacate-co-butylene sebacate) preopolymers were characterized with nuclear magnetic resonance spectroscopy ($^1$H NMR and $^{13}$C NMR) and gel permeation chromatography (GPC). Thermal stability of cross-linked materials (directly after synthesis process) was tested with thermogravimetric analysis (TGA).

**Keywords:** ester elastomers; sugar alcohols; e-beam irradiation; mechanical and thermal properties

## 1. Introduction

Radiation modification is a method of cross-linking polymer materials that allows not only to save energy compared to a chemical cross-linking, but also provides a higher degree of control over the cross-link density. Some materials such as polyethylene are susceptible to radiation modification on their own; others, like polyisobutylene, require addition of a cross-linking agent. On the industrial scale, radiation cross-linking is used mostly in the production of poly(vinyl chloride) (PVC) and polyethylene (PE) wires and cables [1,2]. Other applications include modification of polyurethanes [3,4], polyamide 6 [5,6] and polyamide 12 [7], and rubber vulcanization [8,9].

Radiation cross-linking of polyesters in particular has attracted a noticeable amount of attention from researchers. Examples of aromatic polyesters cross-linked by radiation are poly(butylene terephthalate) (PBT) [10] and pol(ethylene terephthalate) (PET), though due to its properties it requires addition of a sensitizer [11,12]. Polyester-based thermoplastic elastomers can also be modified by radiation [13]

In case of biodegradable aliphatic polyesters, polylactide (PLA) have been most extensively tested. It has been radiation-modified with the use of triallyl isocyanurate as cross-linking agent [14–16]. Using pentaerythritol tetraacrylate as a cross-linking agent in order to modify both PLA and its copolymer, PLGA has also been reported [17]. It has also been reported that PLA cross-linking is possible without any crosslinking agents [18]. Other aliphatic polyesters cross-linked with radiation include polycaprolactone (PCl) cross-linked both with [19] and without [20] any cross-linking agents, and poly(butylene succinate) (PBS) in the presence of trimethallyl isocyanurate [21]

Electron-beam irradiation of sugar alcohol-based polyester elastomers has so far only been conducted in order to sterilize poly(glycerol sebacate) [22], even though this group of materials has been widely described in the literature.

Poly(glycerol sebacate) is the most notable example of sugar alcohol-based polyesters, and has been extensively investigated in respect of possible medical uses [23–29].

In general, sugar alcohol-based elastomers have been determined to be biocompatible and biodegradable [30,31]. A great advantage of those elastomers is the possibility of tailoring their properties by utilizing different sugar alcohols [32,33], or different dicarboxylic acids [34]. Third monomer, a diol can also be introduced into the synthesis, which leads to obtaining a material with better mechanical properties which can be fine-tuned by utilizing different diols [35]. Sugar alcohol-based copolyesters obtained using three monomers have also been described in our previous work [36–38].

Considering the many advantages of such polyesters we have concluded that the possibility of improving their properties even further by utilizing electron-beam radiation was a subject worth investigating. It is worth noting that utilizing radiation not only improves their properties, but also sterilizes the materials. The novelty in this work is that such modification of sugar alcohol-based elastomers synthesized using three monomers has never been described in the literature.

## 2. Materials and Methods

### 2.1. Synthesis of Elastomers

All reagents were purchased from Sigma-Aldrich (St. Louis, MO, USA). Five polymers were synthesized utilizing sebacic acid, butanediol, and 5 different sugar alcohols (glycerol, erythritol, xylitol, sorbitol and mannitol). The monomer ratio of sebacic acid:sugar alcohol:butylene glycol was 2:1:1. Following materials were obtained: poly(glycerol sebacate-co-butylene sebacate) (PGBS), poly(erythritol sebacate-co-butylene sebacate) (PEBS), poly(xylitol sebacate-co-butylene sebacate) (PXBS), poly(sorbitol sebacate-co-butylene sebacate) (PSBS), and poly(mannitol sebacate-co-butylene sebacate) (PMBS).

The first step of each synthesis was esterification of sebacic acid, butylene glycol, and polyol in $N_2$ atmosphere in 150 °C for 13.5 h. A flask with reaction mixture was heated in an oil bath until the substrates melted. Then, 3 mL of $Ti(BuO)_4$ catalyst was added. The second step was polycondensation. Another portion of the catalyst, 2 mL of $Ti(BuO)_4$, was added at the beginning of the polycondensation, which was conducted in a vacuum atmosphere in 150 °C for 3.5 h. The materials were then casted into silicone forms and were cross-linked in a vacuum dryer in 100 °C in 100 mb.

### 2.2. Irradiation

Materials after cross-linking were e-beam irradiated in the Institute of Nuclear Chemistry and Technology (Warsaw) A linear electron accelerator Elektronika 10/10 (NPO Torij, Russia) was used to

generate a 10 MeV beam of different dosages, namely, 50, 100, and 150 kGy. Radiation was split into 25 kGy doses. Average set current was 360 mA; samples were moved with 0.368 m/min speed. The process was carried out in adherence to PN-ISO 11137-2007 standard.

### 2.3. Experimental Methods

#### 2.3.1. Nuclear Magnetic Resonance Spectroscopy (NMR)

$^1$H and $^{13}$C NMR spectroscopic measurements were performed on a Bruker DPX 400 AVANCE III HD spectrometer (Bruker, Rheinstetten, Germany) operating at 400.1 and 100.6 MHz, respectively. Approximately 50 mg of each sample was dissolved in 0.7 mL of deuterated chloroform ($CDCl_3$). TMS was used as internal reference and spectra were acquired in 5 mm probes. For NMR analyses, MestReNova (version 12.0.3, Mestrelab, Santiago de Compostela, Spain) program was used.

#### 2.3.2. Fourier Transform Infrared Spectroscopy (FTIR)

Analysis of the chemical structure of the polymers was conducted with Fourier transform infrared spectroscopy (FTIR). An Alpha Spectrometer Bruker (Bruker, Germany) was used. Recorded transmission spectra were in the range between 4000 cm$^{-1}$ and 400 cm$^{-1}$ with resolution of 2 cm$^{-1}$. In order to develop the results, Omnic 7.3 software by the Thermo Electron Corporation (Waltham, MA, USA) was used. Analyses were performed on elastomers before and after irradiation.

#### 2.3.3. Differential Scanning Calorimetry (DSC)

In order to determine the thermal properties of the materials, differential scanning calorimetry (DSC) was utilized. TA Instruments apparatus Q2500 (New Castle, DE, USA) was used. Parameters of the analysis were $-100$ °C to 200 °C heating cycle and 10 °C/min heating rate. Tests were performed in a nitrogen atmosphere. In order to develop the results, TA Instruments Universal Analysis 2000, 3.9a software (New Castle, DE, USA) was used. Tests were performed on elastomers before and after irradiation.

#### 2.3.4. Thermogravimetric Analysis (TGA)

TGA analysis was performed in order to analyze the thermal stability of the elastomers. Q500 TGA instrument (TA Instruments, New Castle, DE, USA) equipped with platinum crucibles was used. A heating rate of 2 °C was utilized. The temperature range was 25 °C to 600 °C. Weight of the samples was ~15 mg. The test was conducted in dry air atmosphere.

Analysis was performed for non-irradiated, cross-linked elastomer samples, taken directly after synthesis.

#### 2.3.5. Mechanical Properties

Testing of the mechanical properties was performed using Instron 36 instrument (Norwood, MA, USA). Parameters of the tests were 25 °C, 50% of relative humidity, 100 mm/min crosshead speed, and 500 N load cell. Tests were performed in keeping with PN-EN-ISO 526/1:1996 standard. Tests were performed on elastomers before and after irradiation

#### 2.3.6. Water Contact Angle

Measurement of the water contact angle was carried out with KRUSS DSA100 digital goniometer (Hamburg, Germany). In order to perform static contact angle tests, 2 μL droplet of deionized water was placed on the surface of degreased materials. Automatic dispenser was used. Calculation of the contact angle was carried out with drop shape analysis software (DSA4) by Kruss (Hamburg, Germany). Tests were performed on elastomers before and after irradiation.

### 2.3.7. Cross-Link Density

Two grams of polymer samples of each material before and after irradiation was prepared. Three samples of each material were prepared. Each sample was immersed in 20 mL of Tetrahydrofuran (THF) in 20 °C for 5 days. After that, polymer samples were separated from the solvent and weighed (wet fraction). Next, polymer samples were dried for 8 days in a vacuum dryer in 20 °C and weighed again (dry fraction).

The Flory–Rehner equation [39] was used to calculate the cross-link density,

$$v = \frac{\ln(1 - v_2) + v_2 + \chi v_2^2}{v_1\left(\left(\frac{v_2}{2}\right) - v_2^{\frac{1}{3}}\right)} \tag{1}$$

$$v_2 = \left[1 + \left(\frac{m_1 - m_2}{m_2}\right)\left(\frac{\rho_s}{\rho_p}\right)\right]^{-1} \tag{2}$$

where $v$ is the strand density (half of the cross-link density), $v_2$ is the polymer volume fraction at equilibrium swelling, $\chi$ is the polymer–solvent interaction parameter ($\chi = 0.42$), $\rho_s$ is the solvent density, $\rho_p$ is the polymer density, $v_1$ is the solvent molar volume, $v_2$ is the polymer volume fraction at equilibrium swelling, $m_1$ is the wet fraction weight, and $m_2$ is the dry fraction weight

### 2.3.8. Gel Permeation Chromatography (GPC)

Determination of the molecular weights of the PGBS, PEBS, PXBS, PSBS, and PMBS prepolymers was conducted using gel permeation chromatography (GPC). Styragel column (Waters, Milford, MA, USA) was utilized. Samples were dissolved (1 mg/mL) in tetrahydrofuran (THF).

## 3. Results and Discussion

The composition and properties of elastomers are summarized in Tables 1 and 2, and a scheme of the structure is shown in Figure 1.

**Table 1.** Composition and molecular weight distributions of pre-polymers. Poly(glycerol sebacate-co-butylene sebacate) (PGBS), poly(erythritol sebacate-co-butylene sebacate) (PEBS), poly(xylitol sebacate-co-butylene sebacate) (PXBS), poly(sorbitol sebacate-co-butylene sebacate) (PSBS), and poly(mannitol sebacate-co-butylene sebacate) (PMBS).

| Pre-Polymer | Molar Composition [mol] | | | $M_w$ [g/mol] | PDI | Composition (PBS to PPS Segments) by ^{1}H NMR |
|---|---|---|---|---|---|---|
| PGBS | SA 2 | GL 1 | BG 1 | 40,000 | 2.1 | 1.84:1 |
| PEBS | SA 2 | ER 1 | BG 1 | 42,000 | 1.7 | 1.64:1 |
| PXBS | SA 2 | XL 1 | BG 1 | 38,000 | 1.8 | 1.86:0.67 |
| PSBS | SA 2 | SB 1 | BG 1 | 20,000 | 1.4 | 4.24:1 |
| PMBS | SA 2 | MN 1 | BG 1 | 29,000 | 2.5 | 2.51:1 |

where $M_w$: weight average molecular weight, PDI: polydispersity index, SA: sebacic acid, BG: butylene glycol, XL: xylitol, SB: sorbitol, ER: erythrytol, GL: glycerol, Mn: mannitol, PBS: poly(butylene sebacate) segment, PPS: poly(polyol sebacate) segment.

**Table 2.** Composition and selected properties of poly(glycerol sebacate-co-butylene sebacate) (PGBS), poly(erythritol sebacate-co-butylene sebacate) (PEBS), poly(xylitol sebacate-co-butylene sebacate) PXBS, poly(sorbitol sebacate-co-butylene sebacate) (PSBS),poly(mannitol sebacate-co-butylene sebacate) (PMBS) before and after irradiation.

| Material/Dose | Molar Composition [mol] | | | E_50% [MPa] | E_100% [MPa] | $\sigma_r$ [MPa] | $\varepsilon_r$ [%] | $n$ [mol/m$^3$] |
|---|---|---|---|---|---|---|---|---|
| - | SA | GL | BG | | | - | | |
| PGBS_0 kGy | | | | 1.34 +/−0.09 | 0.910 +/−0.04 | 1.34 +/−0.35 | 230 +/−92.66 | 120.45 +/−52.66 |
| PGBS_50 kGy | 2 | 1 | 1 | 2.77 +/−0.69 | 1.50 +/−0.35 | 1.62 +/−0.37 | 156 +/−47.44 | 142.31 +/−43.32 |
| PGBS_100 kGy | | | | 2.44 +/−0.36 | 1.34 +/−0.15 | 1.55 +/−0.26 | 186 +/−59.41 | 139.20 +/−57.21 |
| PGBS_150 kGy | | | | 1.95 +/−0.38 | 1.13 +/−0.16 | 1.22 +/−0.21 | 143 +/−30.86 | 110.42 +/−28.81 |
| - | SA | ER | BG | | | - | | |
| PEBS_0 kGy | | | | 0.799 +/−0.16 | 0.632 +/−0.09 | 1.06 +/−0.35 | 219 +/−85.12 | 189.58 +/−75.22 |
| PEBS _50 kGy | 2 | 1 | 1 | 2.84 +/−0.76 | 1.60 +/−0.33 | 1.75 +/−0.36 | 163 +/−40.65 | 249.23 +/−53.71 |
| PEBS_100 kGy | | | | 2.06 +/−0.45 | 1.36 +/−0.15 | 1.38 +/−0.33 | 139 +/−47.89 | 215.32 +/−43.59 |
| PEBS_150 kGy | | | | 2.33 +/−0.58 | 1.38 +/−0.20 | 1.56 +/−0.23 | 172 +/−43.60 | 231.42 +/−46.88 |
| - | SA | XL | BG | | | - | | |
| PXBS_0 kGy | | | | 0.345 +/−0.04 | 0.296 +/−0.04 | 0.931 +/−0.46 | 362 +/−68.8 | 287.42 +/−57.32 |
| PXBS_50 kGy | 2 | 1 | 1 | 0.492 +/−0.08 | 0.424 +/−0.07 | 1.41 +/−0.35 | 372 +/−52.3 | 310.58 +/−45.24 |
| PXBS_100 kGy | | | | 0.456 +/−0.14 | 0.395 +/−0.11 | 1.47 +/−0.47 | 431 +/−81,13 | 321.44 +/−41.54 |
| PXBS_150 kGy | | | | 0.345 +/−0.03 | 0.298 +/−0.03 | 1.29 +/−0.22 | 409 +/−32.91 | 299.32 +/−38.87 |
| - | SA | SB | BG | | | - | | |
| PSBS_0 kGy | | | | 0.536 +/−0.11 | 0.455 +/−0.03 | 1.32 +/−0.41 | 395 +/−37.08 | 430.15 +/−45.13 |
| PSBS_50 kGy | 2 | 1 | 1 | 0.826 +/−0.13 | 0.624 +/−0.07 | 1.49 +/−0.18 | 400 +/−17.50 | 437.11 +/−38.63 |
| PSBS_100 kGy | | | | 0.234 +/−0.04 | 0.216 +/−0.03 | 0.77 +/−0.14 | 440 +/−57.21 | 425.38 +/−47.28 |
| PSBS _150 kGy | | | | 0.311 +/−0.12 | 0.269 +/−0.09 | 0.89 +/−0.25 | 403 +/−33.90 | 387.31 +/−43.76 |
| - | SA | MN | BG | | | - | | |
| PMBS_0 kGy | | | | 0.329 +/−0.13 | 0.264 +/−0.08 | 0.593 +/−0.17 | 275 +/−44.70 | 221.32 +/−42.85 |
| PMBS_50 kGy | 2 | 1 | 1 | 0.394 +/−0.10 | 0.316 +/−0.06 | 0.557 +/−0.10 | 221 +/−23.87 | 241.48 +/−45.31 |
| PMBS_100 kGy | | | | 0.384 +/−0.09 | 0.302 +/−0.06 | 0.629 +/−0.11 | 281 +/−30.51 | 254.32 +/−49.28 |
| PMBS_150 kGy | | | | 0.347 +/−0.14 | 0.275 +/−0.08 | 0.489 +/−0.12 | 237 +/−29.77 | 189.41 +/−39.87 |

where: $\sigma_r$: Stress in break, $\varepsilon$: Elongation, E_50%: Modulus at 50% elongation, E_100%: Modulus at 100% elongation, $n$: Cross-linking density, SA: sebacic acid, BG: butylene glycol, XL: xylitol, SB: sorbitol, ER: erythrytol, GL: glycerol, Mn: mannitol.
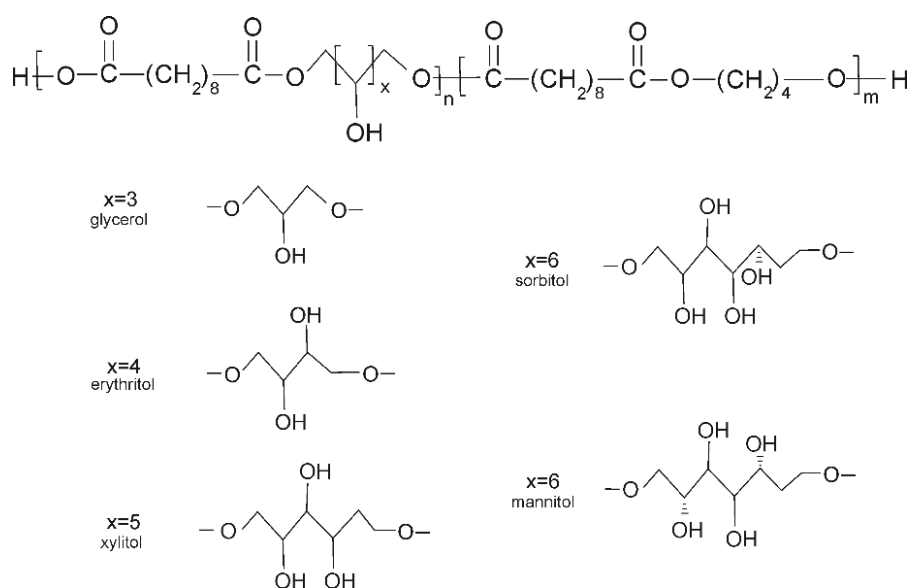
$$H-[O-\overset{O}{\overset{\|}{C}}-(CH_2)_8-\overset{O}{\overset{\|}{C}}-O\diagup\diagdown\diagup\diagdown_x O]_n[\overset{O}{\overset{\|}{C}}-(CH_2)_8-\overset{O}{\overset{\|}{C}}-O-(CH_2)_4-O]_m H$$

OH

x=3
glycerol

x=4
erythritol

x=5
xylitol

x=6
sorbitol

x=6
mannitol

**Figure 1.** Scheme of of poly(polyol sebacate-co-butylene sebacate) structure.

### 3.1. Nuclear Magnetic Resonance Spectroscopy (NMR)

In order to confirm the success of the performed syntheses and establish the chemical structure of the obtained polymers, both $^{13}$C NMR and $^{1}$H NMR were performed.

In $^{1}$H NMR (Figure 2) two peaks assigned to a proton next to an ester bond can be seen: the peak at ~4.25 ppm corresponds to a proton next to an ester bond between sugar alcohol and sebacic acid, and the peak at ~4.1 ppm corresponds to an ester bond between butylene glycol and sebacic acid.

The ratio of the area of the peak at 4.25 ppm to the area of the peak at 4.1 ppm tells us the reactivity of sugar alcohols as compared to butylene glycol. Erythritol is the most reactive, with the ratio of sebacic acid–butylene glycol ester bonds to sebacic acid–sugar alcohol ester bonds being 1.64, while sorbitol is the least reactive, with a 4.24 ratio. Those results correspond well to the $M_w$ of the polymers, determined by GPC.

The peak at 1.30 ppm is connected to $CH_2$ (c) and $CH_2$ (d) groups in sebacic acid, and the doublet at about 1.61 and 1.70 ppm is linked to $CH_2$ (b) group in sebacic acid and $CH_2$ (e) group in butylene glycol. The peak at 2.30 ppm is linked to $CH_2$ (a) groups in sebacic acid. The peaks between 3.60 and 3.85 ppm are connected to hydroxyl groups in sugar alcohols.

In $^{13}$C NMR (Figure 3), two peaks assigned to carbons next to an ester bond: the peak at ~63.8 ppm corresponds to a C(h) carbon next to an ester bond between butylene glycol and sebacic acid, and the peak at ~65.3 ppm corresponds to a C(g) carbon next to an ester bond between sugar alcohol and sebacic acid. Peaks in the 70 to 72 ppm range are due to carbon atoms in $CH_2OH$ groups in sugar alcohols. The peak at 174 ppm is connected to C(i) carbon atoms in C=O groups. The peak at 178 ppm is due to –COOH groups in leftover unreacted carboxylic acid.
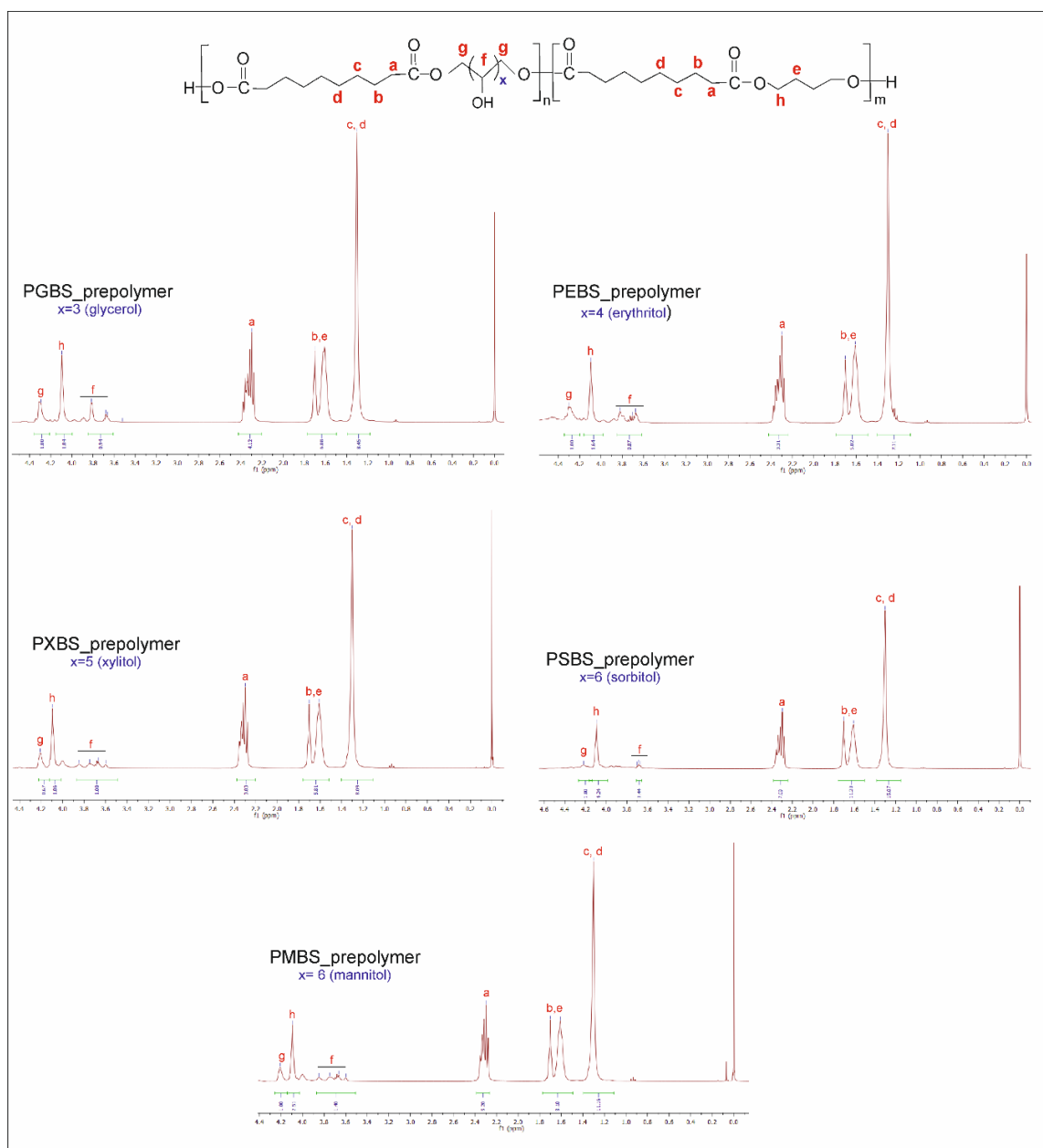
**Figure 2.** Nuclear magnetic resonance spectroscopy ($^1$H NMR) of poly(glycerol sebacate-co-butylene sebacate) (PGBS), poly(erythritol sebacate-co-butylene sebacate) (PEBS), poly(xylitol sebacate-co-butylene sebacate) (PXBS), poly(sorbitol sebacate-co-butylene sebacate) (PSBS), and poly(mannitol sebacate-co-butylene sebacate) (PMBS) prepolymers.
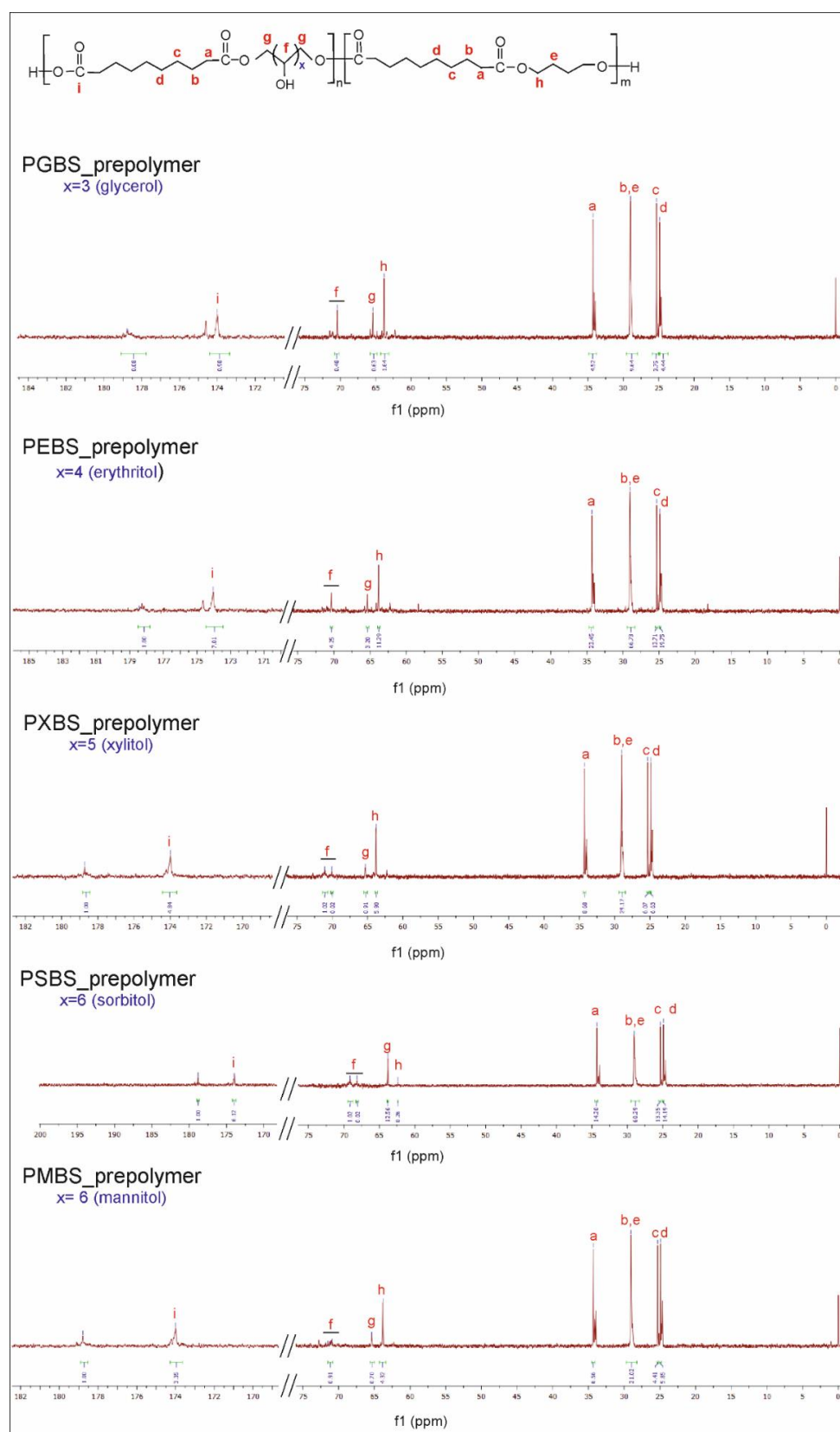
**Figure 3.** $^{13}$C NMR of PGBS, PEBS, PXBS, PSBS, and PMBS prepolymers.

The peak at ~24.9 ppm is linked to CH$_2$ (d) group, peak at about 25.3 ppm is connected to CH$_2$ (c) group, and the peak at about 29.00 ppm was assigned to both the CH$_2$ (b) group in sebacic acid and CH$_2$ (e) group in butylene glycol. Peak at about 34.3 ppm was ascribed to CH$_2$ (a) group in sebacic acid.

### 3.2. Fourier Transform Infrared Spectroscopy (FTIR)

Four transmittance peaks characteristic for sugar alcohol-based polyesters can be seen on the FTIR spectra (Figure S1–S5).

The peak at 1170 cm$^{-1}$ is related to –C–O–C groups, the peak at 2930 cm$^{-1}$ is linked to –CH groups, the peak at 3450 cm$^{-1}$ is associated with –OH groups, and the peak at 1730 cm$^{-1}$ was assigned to –C=O groups. Radiation modification did not cause any significant changes in the intensity of peaks connected to –CH- and –C=O groups, but a slight increase in the intensity of peaks assigned to –C–O–C groups can be seen, due to the cross-linking process taking place. In the spectra of PEBS, PGBS, and PMBS, peak associated with –OH groups split into two. Peak emerging at about 3200 cm$^{-1}$ is ascribed to –OH groups that are not hydrogen-bound. It is a result of hydrogen bonds between –OH groups in neighboring polymer chains breaking apart due to irradiation. This process is most strongly visible in case of PEBS material. It leads to elongation at break being lower in the irradiated material than in the not irradiated material.

### 3.3. Thermal Properties: Differential Scanning Calorimetry (DSC) and Thermogravimetric Analysis (TGA)

The DSC 1nd heating thermograms for PXBS, PSBS, PEBS, PGBS, and PMBS are shown in Figure 4, and the thermal properties of the elastomers before and after irradiation are given in Table 3.

All materials expect PMBS exhibit two melting transitions. $T_{m1}$ is attributed to the melting of the sebacic acid−polyol blocks, and $T_{m2}$ is a result of melting of the sebacic acid−butanediol blocks.

In the first heating, all the materials affected by e-beam radiation exhibit some changes in their transition temperatures and enthalpies. Temperature values associated with glass transition exhibit only small alterations between non-irradiated materials and irradiated materials However, a noticeable change in $\Delta C_p$, can be observed. It is linked to the changes in the amorphous phase and rearrangement of the cross-linked structure caused by irradiation process. Those changes are connected with the alteration of the mechanical properties and cross-link density of the materials shown by the mechanical tests, and cross-link density results

A noticeable decrease in $T_{m1}$ of PEBS after radiation modification of the material is linked to the breaking apart of the hydrogen bonds between erythritol particles in adjacent polymer chains which was confirmed by the FTIR analysis. TGA results for cross-linked samples taken directly after synthesis are shown in Figure 5. All materials show similar slopes of the function curve, and have thermal stability up to 220 °C.
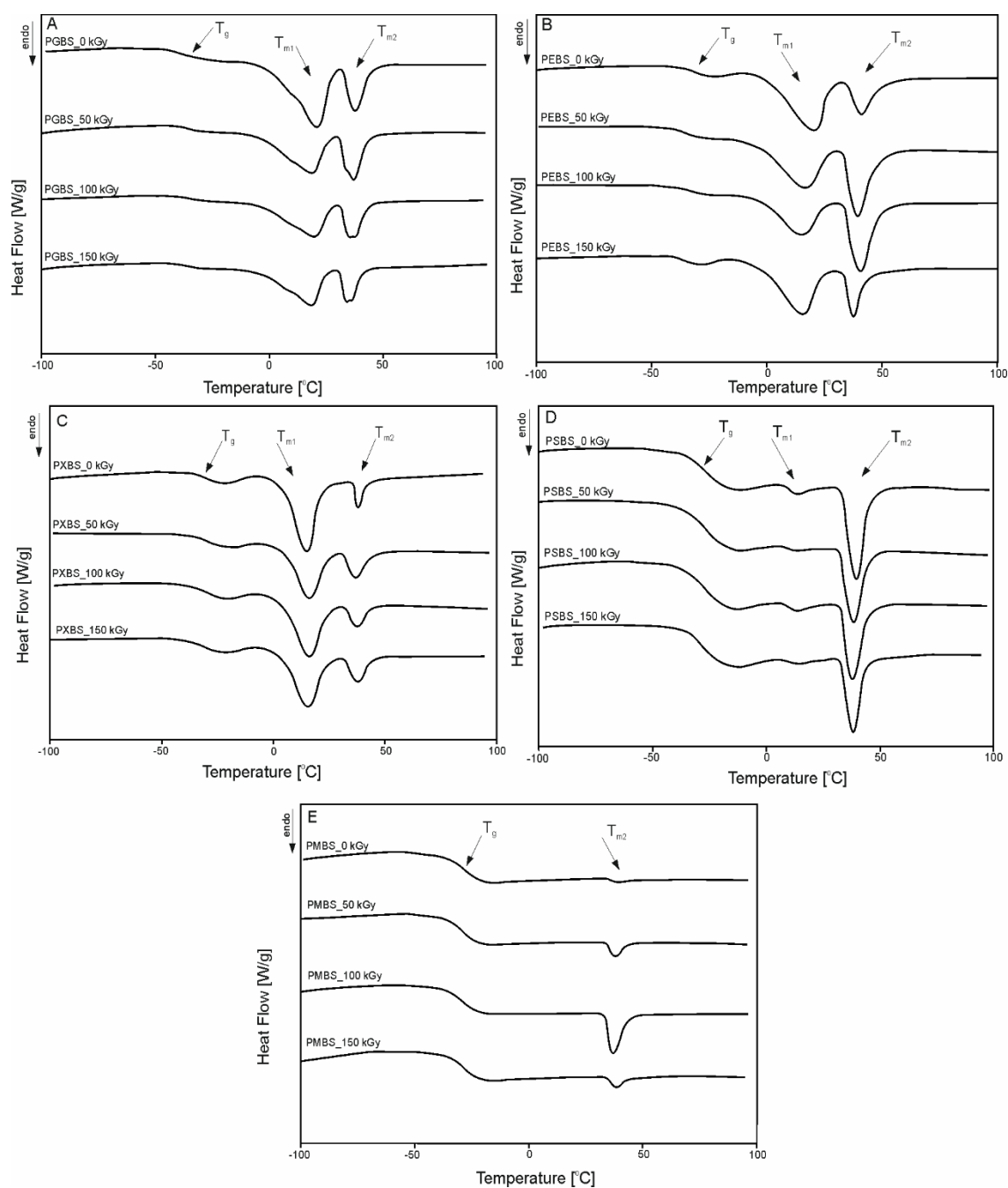
**Figure 4.** First-heating differential scanning calorimetry (DSC) thermograms of (**A**) PGBS, (**B**) PEBS, (**C**) PXBS, (**D**) PSBS, and (**E**) PMBS before and after irradiation.

**Table 3.** DSC termograms of poly(glycerol sebacate-co-butylene sebacate) (PGBS), poly(erythrytol sebacate-co-butylene sebacate) (PEBS), poly(xylitol sebacate-co-butylene sebacate) PXBS, poly(sorbitol sebacate-co-butylene sebacate) (PSBS), poly(mannitol sebacate-co-butylene sebacate) (PMBS) before and after irradiation.

| Material/Dose | I HEATING | | | | | |
|---|---|---|---|---|---|---|
| | $T_g$ | $\Delta C_p$ | $T_{m1}$ | $\Delta H_{m1}$ | $T_{m2}$ | $\Delta H_{m2}$ |
| | [°C] | [J/g°C] | [°C] | [J/g] | [°C] | [J/g] |
| PGBS | | | | - | | |
| PGBS_0 kGy | −39.4 | 0.508 | 21.1 | 48.9 | 38.2 | 17.1 |
| PGBS_50 kGy | −36.1 | 0.319 | 18.9 | 35 | 37.2 | 18.7 |
| PGBS _100 kGy | −36.4 | 0.276 | 19.9 | 30.5 | 37.9 | 14.4 |
| PGBS _150 kGy | −37.5 | 0.216 | 18.6 | 31.2 | 34.2 | 12.1 |
| PEBS | | | | - | | |
| PEBS_0 kGy | −36.5 | 0.248 | 20.2 | 28.8 | 41.6 | 10.6 |
| PEBS_50 kGy | −35.9 | 0.341 | 16.4 | 24.6 | 39.6 | 22.2 |
| PEBS_100 kGy | −33.4 | 0.259 | 14.4 | 19.9 | 40.9 | 24.4 |
| PEBS_150 kGy | −37.4 | 0.267 | 14.9 | 26.9 | 37.4 | 10.5 |
| PXBS | | | | - | | |
| PXBS_0 kGy | −31.6 | 0.368 | 15.3 | 30.6 | 38.4 | 3.8 |
| PXBS_50 kGy | −30.9 | 0.387 | 16.6 | 21.5 | 37.4 | 6.7 |
| PXBS_100 kGy | −34.1 | 0.423 | 16.2 | 24.9 | 38.3 | 5.1 |
| PXBS_150 kGy | −33.5 | 0.39 | 15.6 | 23.9 | 38.3 | 6.5 |
| PSBS | | | | - | | |
| PSBS_0 kGy | −29.2 | 0.562 | 14.4 | 1.2 | 39.7 | 12.7 |
| PSBS_50 kGy | −29.7 | 0.646 | 13.9 | 0.485 | 38.6 | 10.6 |
| PSBS_100 kGy | −29.7 | 0.633 | 13.9 | 1.1 | 38.3 | 10.5 |
| PSBS_150 kGy | −29.2 | 0.6 | 14.3 | 0.543 | 38.7 | 9.5 |
| PMBS | | | | - | | |
| PMBS_0 kGy | −30.1 | 0.69 | – | – | 39.8 | 0.56 |
| PMBS_50 kGy | −30.9 | 0.726 | – | – | 38.4 | 2.3 |
| PMBS _100 kGy | −30.2 | 0.627 | – | – | 37 | 6,8 |
| PMBS_150 kGy | −29.7 | 0.64 | – | – | 38.7 | 1.5 |

where $\Delta C_p$: change of the heat capacity,, $T_g$: glass transition temperature, $T_{m1}$ and $T_{m2}$: melting temperature, $\Delta H_{m1}$ and $\Delta H_{m2}$: heat of melting.
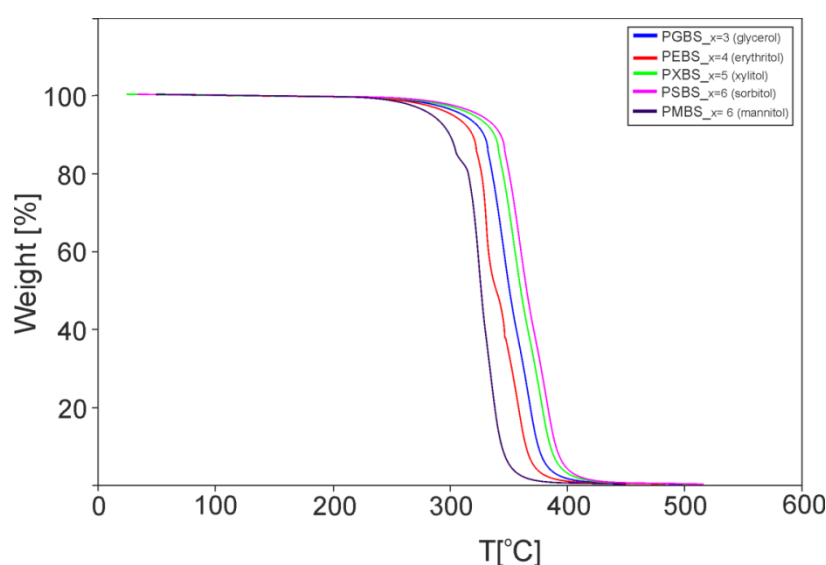


**Figure 5.** Thermogravimetric analysis (TGA) of the cross-linked samples taken directly after synthesis.

## 3.4. Mechanical Properties

Figure 6 shows the results of the mechanical tests of the elastomers before and after radiation modification. For all the non-irradiated samples except PSBS, values of the moduli at 100% and 50% elongation (Table 1) decrease with the increase of hydroxyl group content.

In general, a noticeable change of the mechanical properties of radiation-modified materials can be observed. PGBS and PEBS seem to be most receptive to the procedure, with all of their mechanical properties improving. PMBS material is the least receptive to the radiation modification, and should not be modified in such way. The 50 kGy dose leads to the greatest improvement of mechanical properties, whereas the effects caused by the 150 kGy dose are the least desirable. Therefore, modifying such materials with 50 kGy radiation can be considered the best choice.
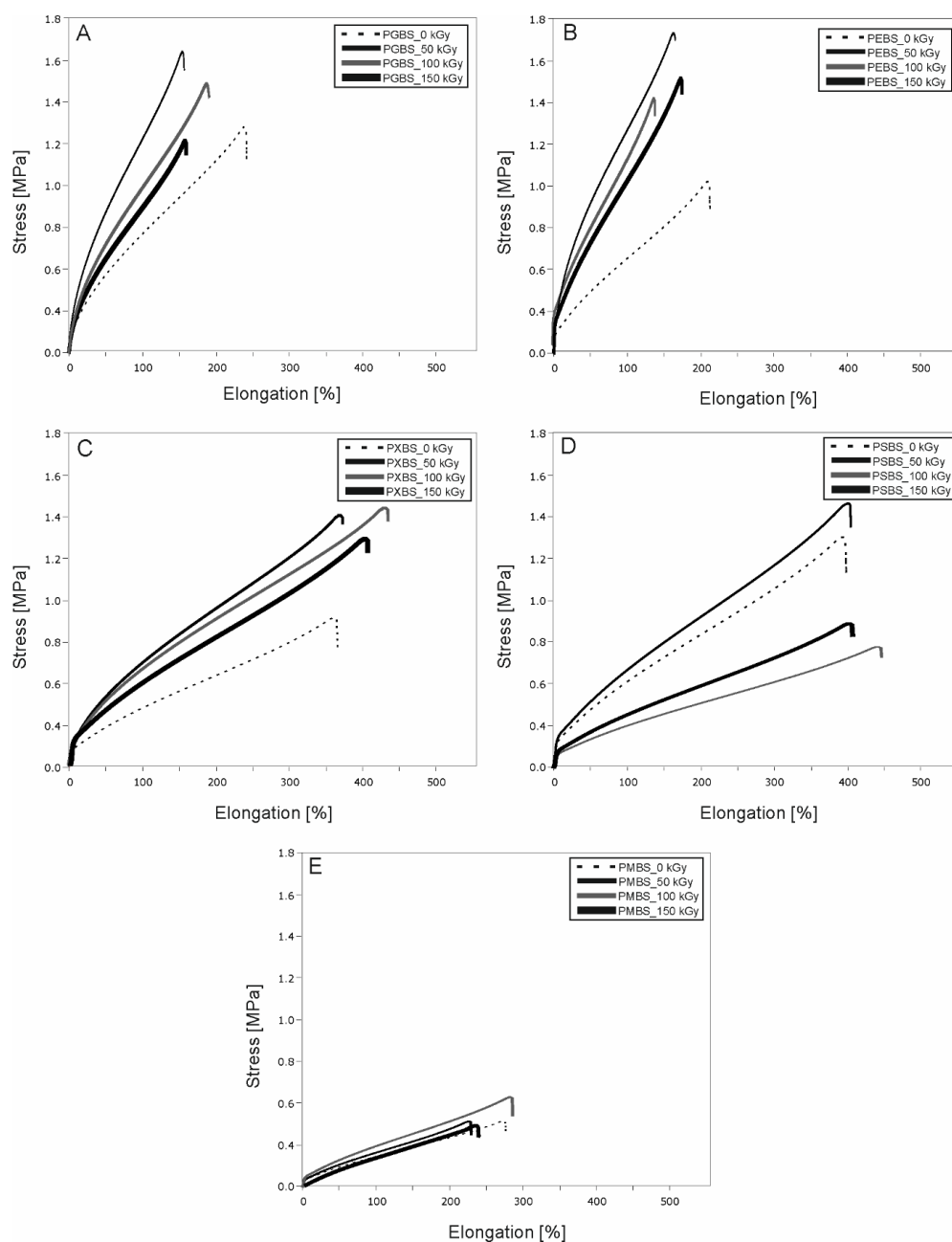


**Figure 6.** Mechanical properties of (**A**) PGBS, (**B**) PEBS, (**C**) PXBS, (**D**) PSBS, and (**E**) PMBS before and after irradiation.

### 3.5. Cross-Link Density

Cross-link density (Figure 7) of materials before irradiation depends on the sugar alcohol used for the synthesis. It can be observed that the cross-link density increases with increasing amount of hydroxyl groups in sugar−alcohols, except for mannitol, in which not all hydroxyl groups take part in the cross-linking reaction due to its stereochemical structure. In all cases, the 50 kGy dose seems to be the most optimal and leads to increase of cross-link density, which directly correlates with improved mechanical properties. 150 kGy dose leads to the least desirable results and should not be used to modify those materials.
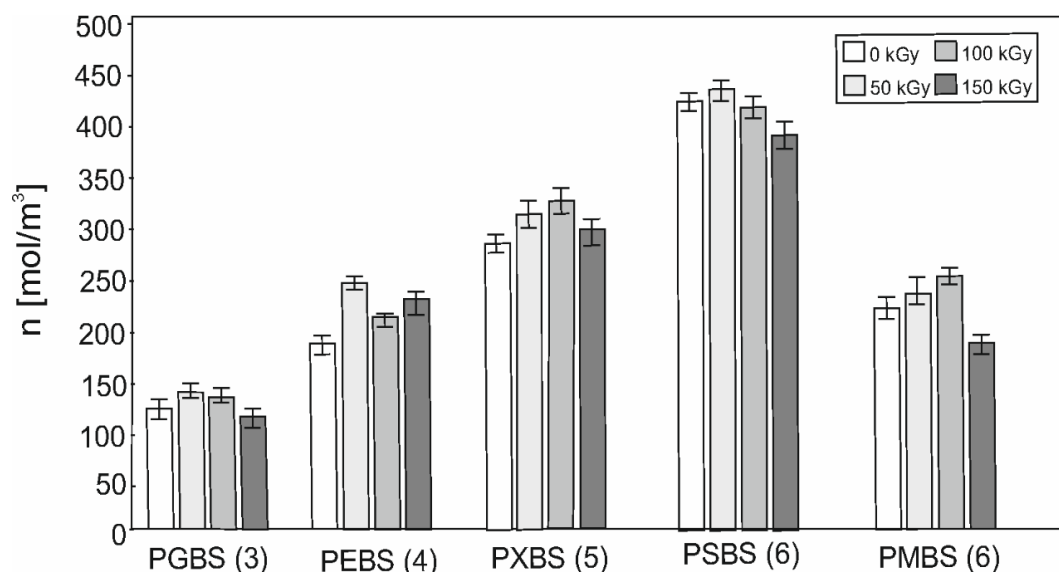


**Figure 7.** Crosslinking density of PGBS, PEBS, PXBS, PSBS, and PMBS before and after irradiation. Numbers in the brackets indicate the amount of hydroxyl groups in the sugar alcohols.

### 3.6. Water Contact Angle

Irradiation of the elastomers leads to a change in the contact angle for all materials. It can be observed that the improvement of mechanical properties does not correlate to the enhancement of their hydrophilic characteristics (Figure 8).

While in the case of PXBS and PSBS a 50 kGy dose shows the best results, which is a similar tendency to that observed in the mechanical properties section of the paper, in the case of the PEBS elastomer, 150 kGy leads to the most noteworthy improvement. This may be linked to the increase of non-hydrogen-bonded –OH groups being present, which is confirmed by the FTIR analysis. For PGBS and PMBS elastomers, radiation modification actually worsens their hydrophilic properties, with the decline being most apparent for PMBS material, which reinforces our conclusion that it should not be modified in such a way. Improved wettability leads to better cell adhesion, which is important for eventual future biomedical uses.
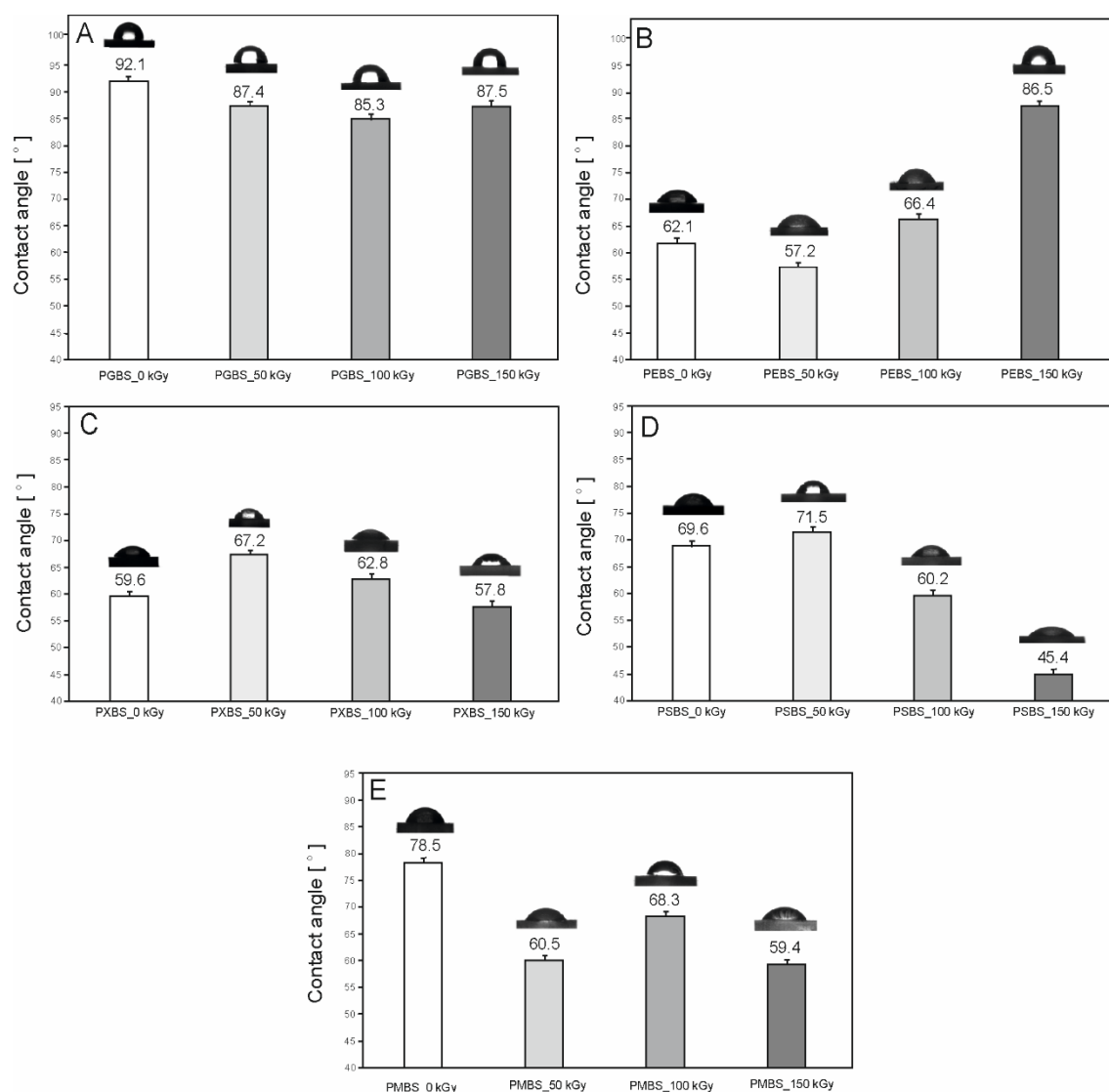
**Figure 8.** Contact angle of (**A**) PGBS, (**B**) PEBS, (**C**) PXBS, (**D**) PSBS, and (**E**) PMBS before and after irradiation.

## 4. Conclusions

The effects of radiation modification of sugar−alcohol-based polyesters were studied. Chemical, thermal, and mechanicals properties were all affected. Materials affected by 50 kGy dose showed the greatest improvement, whereas treatment with a 150 kGy dose leads to least desirable properties. Selection of the right dose of radiation is important for possible future industrial applications. A change in the amorphous structure confirmed by DSC was also apparent. All materials except PMBS were concluded to be susceptible and well suited for such modification, as confirmed by the improvement of mechanical properties and the increase of cross-link density. Radiation modification has the advantage not only because of the improvement of the mechanical properties, but also because affected materials are sterilized. Simplicity of modification of such materials is worth noting: no cross-linking agents or sensitizers are required, and the materials can be modified directly after synthesis, without any additional processing.

FTIR spectra of poly(sorbitol sebacate-co-butylene sebacate) (PSBS) before and after irradiation, Figure S5: FTIR spectra of poly(mannitol sebacate-co-butylene sebacate) (PMBS) before and after irradiation.

**Conflicts of Interest:** The authors declare no conflict of interest.

## References

1. Drobny, J.G. *Ionizing Radiation and Polymers: Principles, Technology, and Applications*; William Andrew: Norwich, NY, USA, 2012.

2. Rouif, S. Radiation cross−linked polymers: Recent developments and new applications. *Nucl. Instrum. Methods Phys. Res. Sect. B Beam Interact. Mater. At.* **2005**, *236*, 68–72. [CrossRef]

3. Zhang, C.; Jiang, X.; Zhao, Z.; Mao, L.; Zhang, L.; Coates, P. Effects of wide−range γ−irradiation doses on the structures and properties of 4,4−dicyclohexyl methane diisocyanate based poly(carbonate urethane)s. *J. Appl. Polym. Sci.* **2014**, *131*, 1–10. [CrossRef]

4. Murray, K.A.; Kennedy, J.E.; McEvoy, B.; Vrain, O.; Ryan, D.; Cowman, R.; Higginbotham, C.L. The influence of electron beam irradiation conducted in air on the thermal, chemical, structural and surface properties of medical grade polyurethane. *Eur. Polym. J.* **2013**, *49*, 1782–1795. [CrossRef]

5. Pinto, C.; Andrade e Silva, L.G. Study of ionizing radiation on the properties of polyamide 6 with fiberglass reinforcement. *Radiat. Phys. Chem.* **2007**, *76*, 1708–1710. [CrossRef]

6. Mizera, A.; Manas, M.; Holik, Z.; Manas, D.; Stanek, M.; Cerny, J.; Bednarik, M.; Ovsik, M. Properties of selected polymers after radiation cross−linking. *Int. J. Math. Comput. Simul.* **2012**, *6*, 592–599.

7. Seefried, A.; Fuchs, M.; Drummer, D. Radiation crosslinking of semicrystalline thermoplastics: A novel approach to modifying a material's thermoformability. *Plast. Eng.* **2012**, *68*, 14–22. [CrossRef]

8. Marinović-Cincović, M.; Marković, G.; Samaržija-Jovanović, S.; Budinski-Simendić, J.; Jovanović, V. The influence of γ radiation on the properties of elastomers based on ethylene propylene diene terpolymer and chlorosulfonated polyethylene rubber. *J. Thermoplast. Compos. Mater.* **2015**, *28*, 1361–1372. [CrossRef]

9. Bik, J.; Głuszewski, W.; Rzymski, W.M.; Zagórski, Z.P. EB radiation crosslinking of elastomers. *Radiat. Phys. Chem.* **2003**, *67*, 421–423. [CrossRef]

10. Mizera, A.; Manas, M.; Manas, D.; Holik, Z.; Stanek, M.; Navratil, J.; Bednarik, M. Temperature stability of modified PBT by radiation cross−linking. *Adv. Mater. Res.* **2014**, *1025–1026*, 256–260.

11. Zhu, S.; Shi, M.; Tian, M.; Qu, L.; Chen, G. Effects of irradiation on polyethyleneterephthalate(PET) fibers impregnated with sensitizer. *J. Text. Inst.* **2018**, *109*, 294–299. [CrossRef]

12. Zhu, S.; Shi, M.; Tian, M. Burning behavior of irradiated PET flame−retardant fabrics impregnated with sensitizer. *Mater. Lett.* **2015**, *160*, 58–60. [CrossRef]

13. Manas, D.; Mizera, A.; Navratil, M.; Manas, M.; Ovsik, M.; Sehnalek, S.; Stoklasek, P. The electrical, mechanical and surface properties of thermoplastic polyester elastomer modified by electron beta radiation. *Polymers* **2018**, *10*, 1057. [CrossRef] [PubMed]

14. Quynh, T.M.; Mai, H.H.; Lan, P.N. Properties of radiation−induced crosslinking stereocomplexes derived from poly(L−Lactide) and different poly(D−Lactide). *Radiat. Phys. Chem.* **2013**, *83*, 105–110. [CrossRef]

15. Nagasawa, N.; Kasai, N.; Yagi, T.; Yoshii, F.; Tamada, M. Radiation−induced crosslinking and post−processing of poly(L−lactic acid) composite. *Radiat. Phys. Chem.* **2011**, *80*, 145–148. [CrossRef]

16. Sugane, K.; Takahashi, H.; Shimasaki, T.; Teramoto, N.; Shibata, M. Stereocomplexation, thermal and mechanical properties of conetworks composed of star−shaped L−lactide, D−lactide and ε−caprolactone oligomers utilizing sugar alcohols as core molecules. *Polymers* **2017**, *9*, 582. [CrossRef]

17. Phong, L.; Han, E.S.C.; Xiong, S.; Pan, J.; Loo, S.C.J. Properties and hydrolysis of PLGA and PLLA cross−linked with electron beam radiation. *Polym. Degrad. Stab.* **2010**, *95*, 771–777. [CrossRef]

18. Huang, Y.; Gohs, U.; Müller, M.T.; Zschech, C.; Wiessner, S. Electron beam treatment of polylactide at elevated temperature in nitrogen atmosphere. *Radiat. Phys. Chem.* **2019**, *159*, 166–173. [CrossRef]

19. Zhu, G.; Xu, Q.; Qin, R.; Yan, H.; Liang, G. Effect of γ−radiation on crystallization of polycaprolactone. *Radiat. Phys. Chem.* **2005**, *74*, 42–50. [CrossRef]

20. Zhu, G.; Liang, G.; Xu, Q.; Yu, Q. Shape−memory effects of radiation crosslinked Poly($\varepsilon$−caprolactone). *J. Appl. Polym. Sci.* **2003**, *90*, 1589–1595. [CrossRef]

21. Suhartini, M.; Mitomo, H.; Nagasawa, N.; Yoshii, F.; Kume, T. Radiation crosslinking of poly(butylene succinate) in the presence of low concentrations of trimethallyl isocyanurate and its properties. *J. Appl. Polym. Sci.* **2003**, *88*, 2238–2246. [CrossRef]

22. Rai, R.; Tallawi, M.; Roether, J.A.; Detsch, R.; Barbani, N.; Rosellini, E.; Kaschta, J.; Schubert, D.W.; Boccaccini, A.R. Sterilization effects on the physical properties and cytotoxicity of poly(glycerol sebacate). *Mater. Lett.* **2013**, *105*, 32–35. [CrossRef]

23. Sun, Z.J.; Chen, C.; Sun, M.Z.; Ai, C.H.; Lu, X.L.; Zheng, Y.F.; Yang, B.F.; Dong, D.L. The application of poly (glycerol−sebacate) as biodegradable drug carrier. *Biomaterials* **2009**, *30*, 5209–5214. [CrossRef] [PubMed]

24. Zaky, S.H.; Lee, K.W.; Gao, J.; Jensen, A.; Verdelis, K.; Wang, Y.; Almarza, A.J.; Sfeir, C. Poly (glycerol sebacate) elastomer supports bone regeneration by its mechanical properties being closer to osteoid tissue rather than to mature bone. *Acta Biomater.* **2017**, *54*, 95–106. [CrossRef] [PubMed]

25. Kemppainen, J.M.; Hollister, S.J. Tailoring the mechanical properties of 3D−designed poly(glycerol sebacate) scaffolds for cartilage applications. *J. Biomed. Mater. Res.-Part A* **2010**, *94*, 9–18. [CrossRef]

26. Sundback, C.A.; Shyu, J.Y.; Wang, Y.; Faquin, W.C.; Langer, R.S.; Vacanti, J.P.; Hadlock, T.A. Biocompatibility analysis of poly(glycerol sebacate) as a nerve guide material. *Biomaterials* **2005**, *26*, 5454–5464. [CrossRef]

27. Motlagh, D.; Yang, J.; Lui, K.Y.; Webb, A.R.; Ameer, G.A. Hemocompatibility evaluation of poly(glycerol−sebacate) in vitro for vascular tissue engineering. *Biomaterials* **2006**, *27*, 4315–4324. [CrossRef]

28. Chen, Q.Z.; Bismarck, A.; Hansen, U.; Junaid, S.; Tran, M.Q.; Harding, S.E.; Ali, N.N.; Boccaccini, A.R. Characterisation of a soft elastomer poly(glycerol sebacate) designed to match the mechanical properties of myocardial tissue. *Biomaterials* **2008**, *29*, 47–57. [CrossRef]

29. Neeley, W.L.; Redenti, S.; Klassen, H.; Tao, S.; Desai, T.; Young, M.J.; Langer, R. A microfabricated scaffold for retinal progenitor cell grafting. *Biomaterials* **2008**, *29*, 418–426. [CrossRef]

30. Bruggeman, J.P.; Bettinger, C.J.; Langer, R. Biodegradable xylitol−based elastomers: In vivo behavior and biocompatibility. *J. Biomed. Mater. Res.-Part A* **2010**, *95*, 92–104. [CrossRef]

31. Bruggeman, J.P.; Bettinger, C.J.; Nijst, C.L.E.; Kohane, D.S.; Langer, R. Biodegradable xylitol−based polymers. *Adv. Mater.* **2008**, *20*, 1922–1927. [CrossRef]

32. Bruggeman, J.P.; de Bruin, B.J.; Bettinger, C.J.; Langer, R. Biodegradable poly(polyol sebacate) polymers. *Biomaterials* **2008**, *29*, 4726–4735. [CrossRef] [PubMed]

33. Ning, Z.Y.; Zhang, Q.S.; Wu, Q.P.; Li, Y.Z.; Ma, D.X.; Chen, J.Z. Efficient synthesis of hydroxyl functioned polyesters from natural polyols and sebacic acid. *Chin. Chem. Lett.* **2011**, *22*, 635–638. [CrossRef]

34. Dasgupta, Q.; Chatterjee, K.; Madras, G. Combinatorial approach to develop tailored biodegradable poly(xylitol dicarboxylate) polyesters. *Biomacromolecules* **2014**, *15*, 4302–4313. [CrossRef] [PubMed]

35. Kavimani, V.; Jaisankar, V. Synthesis and characterisation of sorbitol based copolyesters for biomedical applications. *J. Phys. Sci. Appl.* **2014**, *4*, 507–515.

36. Piątek-Hnat, M.; Bomba, K. The influence of of cross−linking process on the physicochemical properties of new copolyesters containing xylitol. *Mater. Today Commun.* **2020**, *20*, 100734. [CrossRef]

37. Piątek-Hnat, M.; Bomba, K.; Pęksiński, J. Synthesis and selected properties of ester elastomer containing sorbitol. *Appl. Sci.* **2020**, *10*, 1628. [CrossRef]

38. Piatek-Hnat, M.; Bomba, K.; Pęksiński, J. Structure and properties of biodegradable poly (Xylitol Sebacate−Co−Butylene Sebacate) copolyester. *Molecules* **2020**, *25*, 1541. [CrossRef]

39. Flory, P.J. *Principles of Polymer Chemistry*; Cornell University Press: Ithaca, NY, USA, 1953.

# Influence of e-Beam Irradiation on the Physicochemical Properties of Poly(polyol Succinate-co-Butylene Succinate) Ester Elastomers

**Marta Piątek-Hnat [1],\* , Kuba Bomba [1], Jakub Pęksiński [2] , Agnieszka Kozłowska [1] , Jacek G. Sośnicki [3], Tomasz J. Idzik [3] , Danuta Piwowarska [4] and Jolanta Janik [1]**

[1] Department of Polymer and Biomaterials Science, Faculty of Chemical Technology and Engineering, West Pomeranian University of Technology, Piastów Ave. 42, 71-065 Szczecin, Poland; bk34688@zut.edu.pl (K.B.); agak@zut.edu.pl (A.K.); jolanta.janik@zut.edu.pl (J.J.)

[2] Faculty of Electrical Engineering, West Pomeranian University of Technology, Sikorskiego Ave. 37, 71-313 Szczecin, Poland; jakub.peksinski@zut.edu.pl

[3] Department of Organic and Physical Chemistry, Faculty of Chemical Technology and Engineering, West Pomeranian University of Technology, Piastów Ave. 42, 71-065 Szczecin, Poland; jacek.sosnicki@zut.edu.pl (J.G.S.); tomasz.idzik@zut.edu.pl (T.J.I.)

[4] Department of Technical Physics, Faculty of Mechanical Engineering and Mechatronics, West Pomeranian University of Technology, Al. Piastów 48, 70-310 Szczecin, Poland; danuta.piwowarska@zut.edu.pl

\* Correspondence: marp@zut.edu.pl

**Abstract:** The purpose of this research was synthesis and electron beam modification of novel ester elastomers consisting of sugar alcohol–succinic acid block and butylene glycol–succinic acid block. Four different alditols were used in the synthesis—sorbitol, erythritol, xylitol, and glycerol. The materials were irradiated with doses of 50, 100, and 150 kGy in order to determine which dose is the most beneficial. As expected, irradiation of the materials has led to the cross-link density becoming higher and improvement of the mechanical properties. Additionally, the materials were also sterilized in the process. The great advantage of elastomers described in the paper is the fact that they do not need chemical cross-linking agents or sensitizers in order to undergo radiation modification. The following tests were performed on cross-linked poly(polyol succinate-co-butylene succinate) elastomers: quasi-static tensile test, determination of cross-link density, differential scanning calorimetry (DSC), dynamic thermomechanical analysis (DMTA), wettability (water contact angle), and Fourier transform infrared spectroscopy (FTIR). In order to confirm successful synthesis, prepolymers were analyzed by nuclear magnetic resonance spectroscopy ($^1$H NMR and $^{13}$C NMR).

**Keywords:** e-beam modification; mechanical and thermal properties; sugar alcohols; ester elastomers

## 1. Introduction

Increasing demand for engineering plastics with very good mechanical properties has made it necessary to find a way to greatly enhance properties of common polymers in a cost-efficient manner that allowed mass production. Radiation modification is such a method. In addition to being economical in terms of saving energy, space, and time, it also allows for a high degree of control over the cross-linking process and eliminates the risk of microvoids being present in the material. In addition to mechanical properties, chemical and thermal characteristics are also improved in the process. Radiation modification has many commercial applications, such as cross-linking polyethylene (PE), polypropylene (PP), and poly(vinyl chloride) (PVC) for wire insulation, curing rubber compounds for tires, production of cross-linked PE pipes, and heat-shrinkable polyolefine tubing [1,2].

In case of polymers with possible medical uses, radiation modification serves a double role—in addition to improving the properties, it also sterilizes the material. Most researched polyesters belonging to this group are polycaprolactone (PCL) and polylactide (PLA). Radiation modification of PCL with chemical cross-linkers, including polyester acrylate [3], triallyl isocyanurate (TAIC) [4], and without any cross-linking agents [5], was reported. PLA was successfully radiation cross-linked both without any cross-linking agents [6] and with addition of TAIC [7–9].

Radiation modification of other polyesters was also reported, such as poly(butylene succinate) (PBS) with addition of trimethallyl isocyanurate (TMAIC) [10], various thermoplastic elastomers with and without cross-linking agents [11,12], poly(ethylene terephthalate) impregnated with radiation sensitizer—trimethylopropane triacrylate (TMPTA) [13,14], poly(butylene adipate-co-terephthalate) (PBAT) with TAIC [15], poly(butylene terephthalate) (PBT) with triallyl cyanurate [16], and without any cross-linking agents [17]. Bacterial polyesters were also radiation cross-linked without requiring any cross-linking agents [18,19].

In case of polyesters based on sugar alcohols, as far as we know, the only reported use of radiation by other authors was conducted in very low doses in order to only sterilize the material and not modify its properties [20].

In general, materials synthesized utilizing sugar alcohols as monomers have desirable properties, making them a perfect candidate for further research. They are not only biodegradable, but also biocompatible [21,22]. While retaining this core characteristic, their properties can be fine-tuned by changing the monomer chain length and monomer ratio [23], by using different sugar alcohols [24,25], or by introducing a diol to the synthesis [26–28]. In our previous work, we have synthesized and tested various sugar alcohol-based polyesters [29–31]. We have also used radiation to modify different poly(polyol succinate-co-butylene succinate) elastomers [32]. Based on our previous paper, we have deemed it scientifically valuable to radiation-modify a group of sugar alcohol-based polyester based on a dicarboxylic acid with a much shorter chain length—succinic acid. It is of note that our polyesters do not require addition of chemical cross-linking agents or sensitizers. It is very important since such substances could leave potentially harmful residuals in the material after cross-linking, which makes them much less desirable in potential food packaging or medical uses.

## 2. Materials and Methods

### 2.1. Synthesis of Elastomers and Sample Preparation

Four alditols (erythritol, sorbitol, glycerol, and xylitol), succinic acid, and butanediol (Sigma-Aldrich, St. Louis, MO, USA) were used to synthesize four polymers—poly(glycerol succinate-co-butylene succinate) (PGBSu), poly(erythritol succinate-co-butylene succinate) (PEBSu), poly(xylitol succinate-co-butylene succinate) (PXBSu), and poly(sorbitol succinate-co-butylene succinate) (PSBSu).

The succinic acid:alditol:butylene glycol monomer ratio used was 2:1:1. Synthesis was carried out according to the procedure described in previous papers [29–32]. Esterification of succinic acid, alditol, and butylene glycol for 13.5 h in 150 °C and $N_2$ atmosphere was the first step of the synthesis. Next, 3.5 h of polycondensation reaction in vacuum in 150 °C took place. The materials obtained directly after polycondensation are called "prepolymers" further in the text. Following polycondensation, prepolymers were cast into forms made of silicon. After that, cross-linking in a vacuum dryer in 100 °C and 100 mBar atmosphere was carried out. Samples for further tests were cut from the cross-linked sheets of the material using a punching die.

### 2.2. Irradiation

E-beam irradiation was performed on the cross-linked samples. The procedure was carried out in the Institute of Nuclear Chemistry and Technology (Warsaw, Poland). Elektronika 10/10 (NPO Torij, Moscow, Russia) linear electron accelerator was utilized. The parameters of the process were as follows:

360 mA average set current, 10 MeV beam, and 0.368 m/min sample moving speed. Standard [33] was adhered to, and 50, 100, and 150 kGy radiation doses were used.

*2.3. Experimental Methods*

2.3.1. Nuclear Magnetic Resonance Spectroscopy (NMR)

Bruker DPX 400 AVANCE III HD spectrometer (Bruker, Rheinstetten, Germany) was used to carry out the $^{13}$C and $^1$H NMR analyses. The parameters of the process were as follows: 400.1 MHz for $^1$H analysis and 100.6 mHz for $^{13}$C analysis. Five-millimeter probes were used to obtain the spectra. Deuterated chloroform ($CDCl_3$) was used as solvent. The weight of each sample was approximately 50 mg, and the volume of the solvent was 0.7 mL. The internal reference used was tetramethylsilan (TMS). Development of the results was done with the following software: MestReNova 12.03 (Mestrelab, Santiago de Compostela, Spain).

2.3.2. Fourier Transform Infrared Spectroscopy (FTIR)

Bruker Alpha Spectrometer (Bruker, Rheinstetten, Germany) was utilized to perform Fourier transform infrared spectroscopy (Attenuated Total Reflection (ATR) FTIR). The parameters of the procedure were as follows: 4000 to 400 cm$^{-1}$ range, 2 cm$^{-1}$ resolution, 32 scans. Development of the results was done with following software: Omnic 7.3 (Thermo Electron Corporation, Waltham, MA, USA). Both non-irradiated and radiation-modified materials were analyzed.

2.3.3. Differential Scanning Calorimetry (DSC)

Q2500 DSC instrument (TA instruments, New Castle, DE, USA) was utilized to perform differential scanning calorimetry. The following parameters were used: nitrogen atmosphere, heating rate of 10 °C/min, heating cycle from −100 to 100 °C. Both non-irradiated and radiation-modified materials were analyzed. Development of the results was done with the following software: 3.9a TA Instruments Universal Analysis 2000 (New Castle, DE, USA).

2.3.4. Dynamic Thermomechanical Analysis (DMTA)

DMA Q800 (TA Instruments, New Castle, DE, USA) was utilized to carry out dynamic thermomechanical analysis (DMTA). The following parameters were used: −100 to 100 °C temperature range, heating rate of 2 °C/min, 1 Hz frequency. Development of the results was done with the following software: 3.9a TA Instruments Universal Analysis 2000 (New Castle, DE, USA). Both non-irradiated and radiation-modified materials were analyzed.

2.3.5. Mechanical Properties

Instron 36 (Norwood, MA, USA) was utilized to carry out the tensile tests. The following parameters were used: relative humidity of 50%, 100 mm/min speed of the crosshead, 25 °C, 500N load cell. Standard [34] was adhered to. Both non-irradiated and radiation-modified materials were tested.

2.3.6. Water Contact Angle

Digital goniometer KRUSS DSA100 (Hamburg, Germany) was utilized to carry out the water contact angle test. An automatic dispenser was utilized to place 2 μL of deionized water on the material surface, which was previously degreased. Development of the results was done with the following software: DSA4 drop shape analysis (Kruss, Hamburg, Germany). Both non-irradiated and radiation-modified materials were tested.

### 2.3.7. Cross-Linking Density

Three samples (each weighing about 2 g) of all materials, both before and after irradiation, were prepared. Tetrahydrofuran (THF) was used to submerge every sample. The volume of THF used for each sample was 20 mL. The temperature was 20 °C, and the time of immersion was 5 days. Next, separation of each sample from the solvent was carried out, and the samples were weighed in order to measure the wet fraction. After that, 8 days of drying in 20 °C in a vacuum dryer was carried out. The dried samples were weighed in order to measure the dry fraction.

Calculation of cross-link density was done using the Flory-Rehner Equation [35]

$$v = \frac{\ln(1 - v_2) + v_2 + \chi v_2^2}{v_1\left(\left(\frac{v_2}{2}\right) - v_2^{\frac{1}{3}}\right)} \tag{1}$$

$$v_2 = \left[1 + \left(\frac{m_1 - m_2}{m_2}\right)\left(\frac{\rho_s}{\rho_\rho}\right)\right]^{-1} \tag{2}$$

The meaning of the symbol is as follows: $v$—$\frac{1}{2}$ of the number of active network chain segments per unit volume (cross-link density, $n$), $\chi$—polymer–solvent interaction parameter ($\chi = 0.42$, as determined for sugar alcohol-based materials [36]), $v_2$—polymer volume fraction at equilibrium swelling, $\rho_p$—polymer density, $\rho_s$—solvent density, $v_2$—the polymer volume fraction, $v_1$—solvent molar volume at equilibrium swelling, $m_1$—wet fraction weight, and $m_2$—dry fraction weight.

### 2.3.8. Hardness

Hardness (H) for materials before and after irradiation was measured using a Zwick/Material Testing 3100 Shore A hardness tester (ZwickRoell, Kennesaw, GA, USA)

### 2.3.9. Gel Permeation Chromatography

Gel Permeation Chromatography (GPC) was utilized in order to determine the molecular weights of PGBSu, PEBSu, PXBSu, and PSBSu. Tests were conducted using Styragel column (Waters, Milford, CT, USA), with tetrahydrofuran (THF) as solvent in which samples (1 mg/mL) were dissolved.

## 3. Results and Discussion

Tables 1 and 2 contain the polymer composition and properties; Figure 1 presents the polymer structure scheme and suspected scheme of radiation-induced crosslinking.

### 3.1. Nuclear Magnetic Resonance Spectroscopy (NMR)

The success of the synthesis was confirmed, and the polymer structure was analyzed by ^{13}C NMR and ^{1}H NMR.

In ^{13}C NMR (Figure 2), two peaks linked to the $CH_2$ groups can be seen—peak at 25 ppm corresponding to the $CH_2$(e) groups and peak at 30 ppm connected to the $CH_2$(a) group. Two peaks at approximately 65 ppm are present—the first one was ascribed to a carbon atom C(h) adjacent to an ester bond between dicarboxylic acid and butylene glycol, and the second one was attributed to a carbon atom C(g) next to an ester bond between dicarboxylic acid and sugar alcohol. The peak at approximately 170 ppm is linked to a carbon atom C(i) in a carbonyl group in dicarboxylic acid.

In ^{1}H NMR (Figure 3), two peaks connected to the $CH_2$ groups are observed—the signal at 1.7 ppm linked to the $CH_2$(e) groups, and the signal at 2.7 ppm corresponding to the $CH_2$(a) group. Two peaks linked to hydrogen atoms adjacent to ester bonds are present—one at 4.1 ppm linked to the hydrogen atom (h) in butylene glycol and one at 4.3 ppm connected to the hydrogen atom (g) in sugar alcohol. The peaks in the range of 3.6–3.8 ppm were connected to the $CH_2$ (f) groups in sugar alcohol. By comparing the signal integration of peaks linked to the $CH_2$(h) and $CH_2$(g)

groups, we have calculated the molar composition of the polymers. The difference between the molar composition in the feed and the actual molar composition calculated by $^1$H NMR is due to the alditols having lower reactivity as compared with butylene glycol. This reactivity also varies between different sugar alcohols.
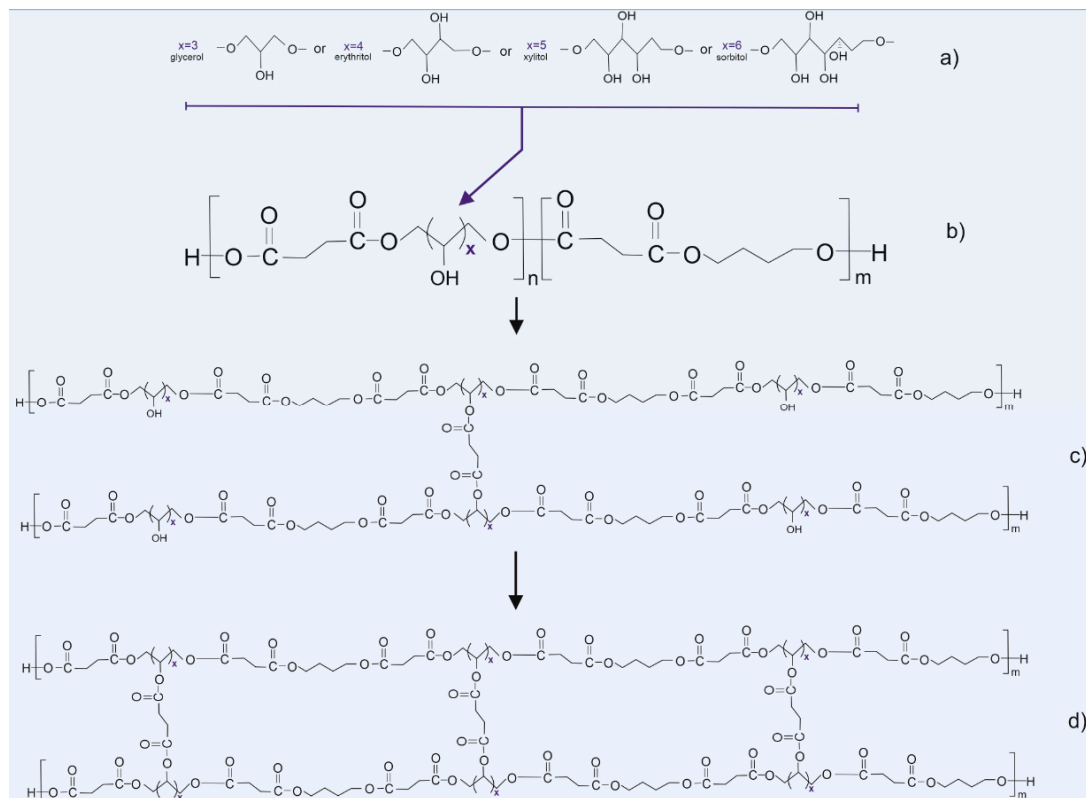


**Figure 1.** Scheme of synthesis and modification of the polymers: (**a**) sugar alcohols used in the synthesis, (**b**) prepolymer structure, (**c**) thermally cross-linked polymer, and (**d**) radiation cross-linked polymer.

**Table 1.** Selected properties and composition of poly(glycerol succinate-co-butylene succinate) (PGBSu), poly(erythritol succinate-co-butylene succinate) (PEBSu), poly(xylitol succinate-co-butylene succinate) (PXBSu), poly(sorbitol succinate-co-butylene succinate). Data for both non-irradiated and radiation-modified materials is presented.

| Material/Dose | Molar Composition (mol) | | | H ShA | CA | Prepolymer | Molar Composition by $^1$H NMR (mol) | | $M_w$ (g/mol) | PDI |
|---|---|---|---|---|---|---|---|---|---|---|
| - | SuA | GL | BG | - | | - | GL | BG | - | |
| PGBSu_0 kGy | | | | 38.8 +/− 4.95 | 68.1 +/− 2.04 | | | | | |
| PGBSu_50 kGy | | | | 45.8 +/− 4.84 | 74.1 +/− 1.35 | PGBSu | 0.32 | 1.00 | 35,000 | 1.3 |
| PGBSu_100 kGy | 2 | 1 | 1 | 37.7 +/− 3.34 | 84.6 +/− 1.15 | | | | | |
| PGBSu_150 kGy | | | | 38.9 +/− 2.50 | 111.3 +/− 1.16 | | | | | |
| - | SuA | ER | BG | | | | ER | BG | - | |
| PEBSu_0 kGy | | | | 32.7 +/− 2.77 | 64 +/− 10.15 | | | | | |
| PEBSu _50 kGy | | | | 43.08 +/− 4.01 | 76.7 +/− 8.33 | PEBSu | 0.20 | 1.00 | 32,000 | 1.6 |
| PEBSu_100 kGy | 2 | 1 | 1 | 42.8 +/− 5.27 | 86.4 +/− 9.15 | | | | | |
| PEBSu_150 kGy | | | | 37.08 +/− 3.45 | 100.8 +/− 4.20 | | | | | |
| - | SuA | XL | BG | - | | | XL | BG | - | |
| PXBSu_0 kGy | | | | 30.2 +/− 6.77 | 49.9 +/− 3.05 | | | | | |
| PXBSu_50 kGy | | | | 41.33 +/− 3.73 | 88.8 +/− 2.05 | PXBSu | 0.25 | 1.00 | 28,000 | 2.0 |
| PXBSu_100 kGy | 2 | 1 | 1 | 48.25 +/− 2.42 | 96.8 +/− 2.14 | | | | | |
| PXBSu_150 kGy | | | | 41.25 +/− 3.08 | 112.9 +/− 5.12 | | | | | |
| - | SuA | SB | BG | - | | - | SB | BG | - | |
| PSBSu_0 kGy | | | | 66.8 +/− 2.25 | 48.7 +/− 2.43 | | | | | |
| PSBSu_50 kGy | | | | 59.27 +/− 6.38 | 71.1 +/− 3.24 | PSBSu | 0.22 | 1.00 | 24,000 | 2.3 |
| PSBSu_100 kGy | 2 | 1 | 1 | 71.08 +/− 6.10 | 89.7 +/− 5.11 | | | | | |
| PSBSu _150 kGy | | | | 65.83 +/− 1.34 | 105.4 +/− 4.23 | | | | | |

where SuA: succinic acid, BG: butylene glycol, GL: glycerol, ER: erythritol XL: xylitol, SB: sorbitol, PBS: poly(butylene succinate) segment, PPS: poly(polyol succinate) segment, H: hardness, CA: contact angle.

**Table 2.** Mechanical properties and cross-linking density of poly(glycerol succinate-co-butylene succinate) (PGBSu), poly(erythritol succinate-co-butylene succinate) (PEBSu), poly(xylitol succinate-co-butylene succinate) (PXBSu), poly(sorbitol succinate-co-butylene succinate). Data for both non-irradiated and radiation-modified materials is presented.

| Material/Dose | Molar Composition (mol) | | | E_50% (MPa) | E_100% (MPa) | $\sigma_r$ (MPa) | $\varepsilon_r$ (%) | $n$ (mol/m³) |
|---|---|---|---|---|---|---|---|---|
| - | SuA | GL | BG | | | - | | |
| PGBSu_0 kGy | | | | 0.07 +/− 0.01 | 0.06 +/− 0.02 | 0.40 +/− 0.03 | 501 +/− 35.09 | 19.36 +/− 8.66 |
| PGBSu_50 kGy | | | | 0.12 +/− 0.1 | 0.10 +/− 0.01 | 0.21+/− 0.03 | 414 +/− 12.01 | 16.20 +/− 12.32 |
| PGBSu_100 kGy | 2 | 1 | 1 | 0.18 +/− 0.03 | 0.16 +/− 0.03 | 0.31 +/− 0.05 | 357 +/− 33.09 | 12.34 +/− 17.21 |
| PGBSu_150 kGy | | | | 0.19 +/− 0.02 | 0.17 +/− 0.12 | 0.38 +/− 0.06 | 312 +/− 32.58 | 13.20 +/− 21.81 |
| - | SuA | ER | BG | | | - | | |
| PEBSu_0 kGy | | | | 0.204 +/−0.04 | 0.190+/−0.04 | 0.509+/−0.12 | 239 +/− 55.44 | 66.34 +/−25.22 |
| PEBSu_50 kGy | | | | 0.272 +/− 0.11 | 0.278 +/− 0.11 | 0.733 +/− 0.19 | 324 +/− 17.81 | 165.21 +/− 53.71 |
| PEBSu_100 kGy | 2 | 1 | 1 | 0.267 +/− 0.06 | 0.279 +/− 0.06 | 0.663 +/− 0.09 | 215 +/− 68.17 | 124.93 +/− 33.59 |
| PEBSu_150 kGy | | | | 0.248 +/− 0.05 | 0.261 +/− 0.06 | 0.669 +/− 0.07 | 234 +/− 79.12 | 71.29 +/− 16.88 |
| - | SuA | XL | BG | | | - | | |
| PXBSu_0 kGy | | | | 0.215 +/− 0.06 | 0.175 +/− 0.05 | 0.545+/− 0.06 | 259 +/− 31.64 | 251.78 +/− 37.32 |
| PXBSu_50 kGy | | | | 0.220 +/− 0.05 | 0.184 +/− 0.05 | 0.66+/− 0.10 | 263 +/− 27.75 | 254.83 +/− 35.24 |
| PXBSu_100 kGy | 2 | 1 | 1 | 0.212 +/− 0.03 | 0.177 +/− 0.03 | 0.641 +/− 0.06 | 275 +/− 21.91 | 287.44 +/− 31.54 |
| PXBSu_150 kGy | | | | 0.196 +/− 0.07 | 0.155 +/− 0.07 | 0.694 +/− 0.12 | 301 +/− 66.80 | 287.51 +/− 36.77 |
| - | SuA | SB | BG | | | - | | |
| PSBSu_0 kGy | | | | 0.503 +/− 0.06 | 0.396 +/− 0.05 | 0.93 +/− 0.41 | 205 +/− 13.03 | 450.04 +/− 42.19 |
| PSBSu_50 kGy | | | | 0.428 +/− 0.11 | 0.357 +/− 0.10 | 0.90 +/− 0.09 | 208 +/− 30.34 | 414.22 +/− 36.68 |
| PSBSu_100 kGy | 2 | 1 | 1 | 0.385 +/− 0.05 | 0.322 +/− 0.05 | 0.88 +/− 0.10 | 215 +/− 13.22 | 432.16 +/− 47.28 |
| PSBSu _150 kGy | | | | 0.426 +/− 0.07 | 0.355 +/− 0.05 | 0.95 +/− 0.12 | 209 +/− 13.70 | 399.48 +/− 40.82 |

where: $\sigma_r$: stress at break, $\varepsilon_r$: elongation at break, E_50%: modulus at 50% elongation, E_100%: modulus at 100% elongation, n: cross-linking density, SuA: succinic acid, BG: butylene glycol, GL: glycerol, ER: erythritol, XL: xylitol, SB: sorbitol.
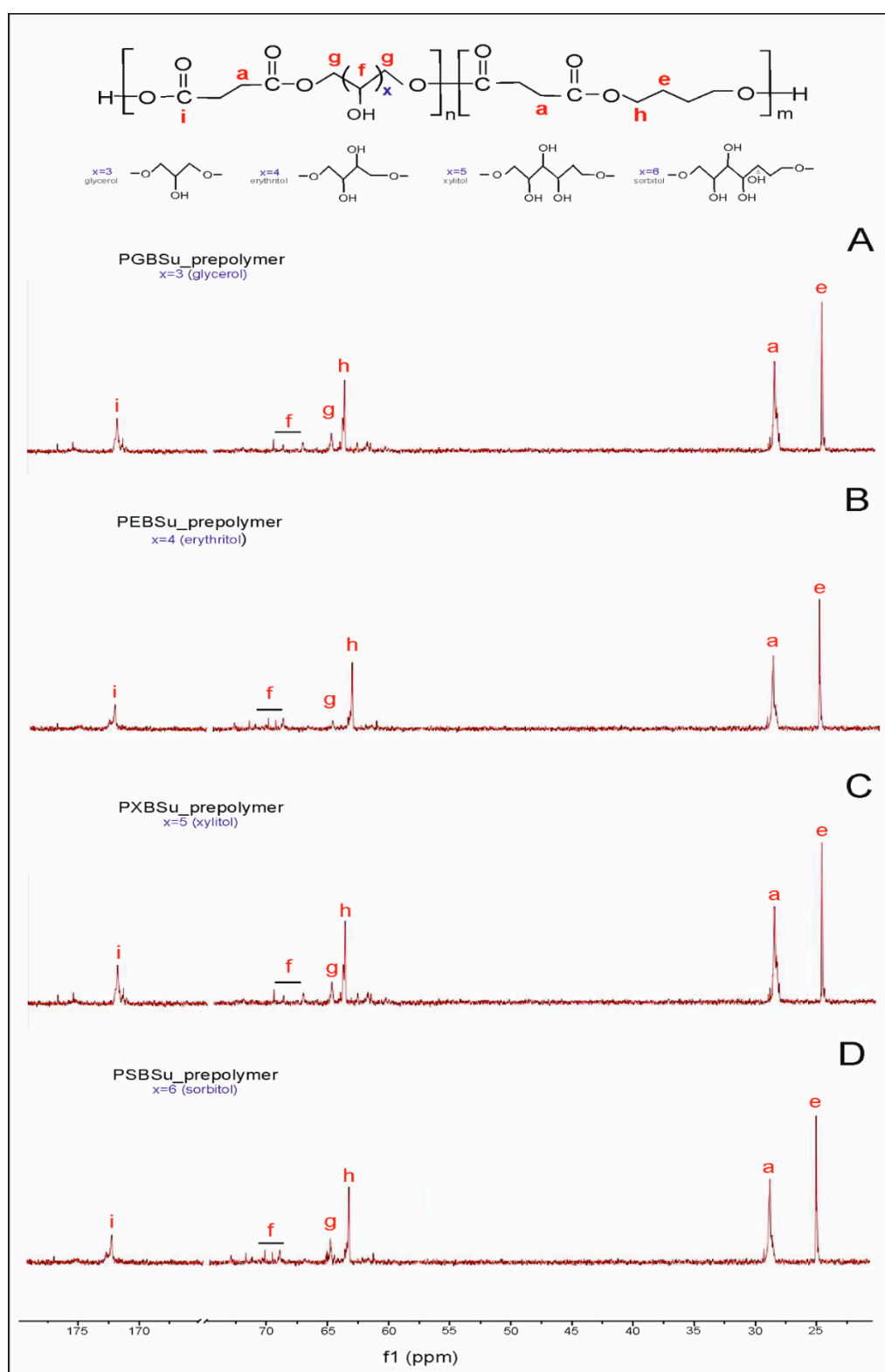
**Figure 2.** $^{13}$C NMR of PGBSu (**A**), PEBSu (**B**), PXBSu (**C**), and PSBSu (**D**) prepolymers.
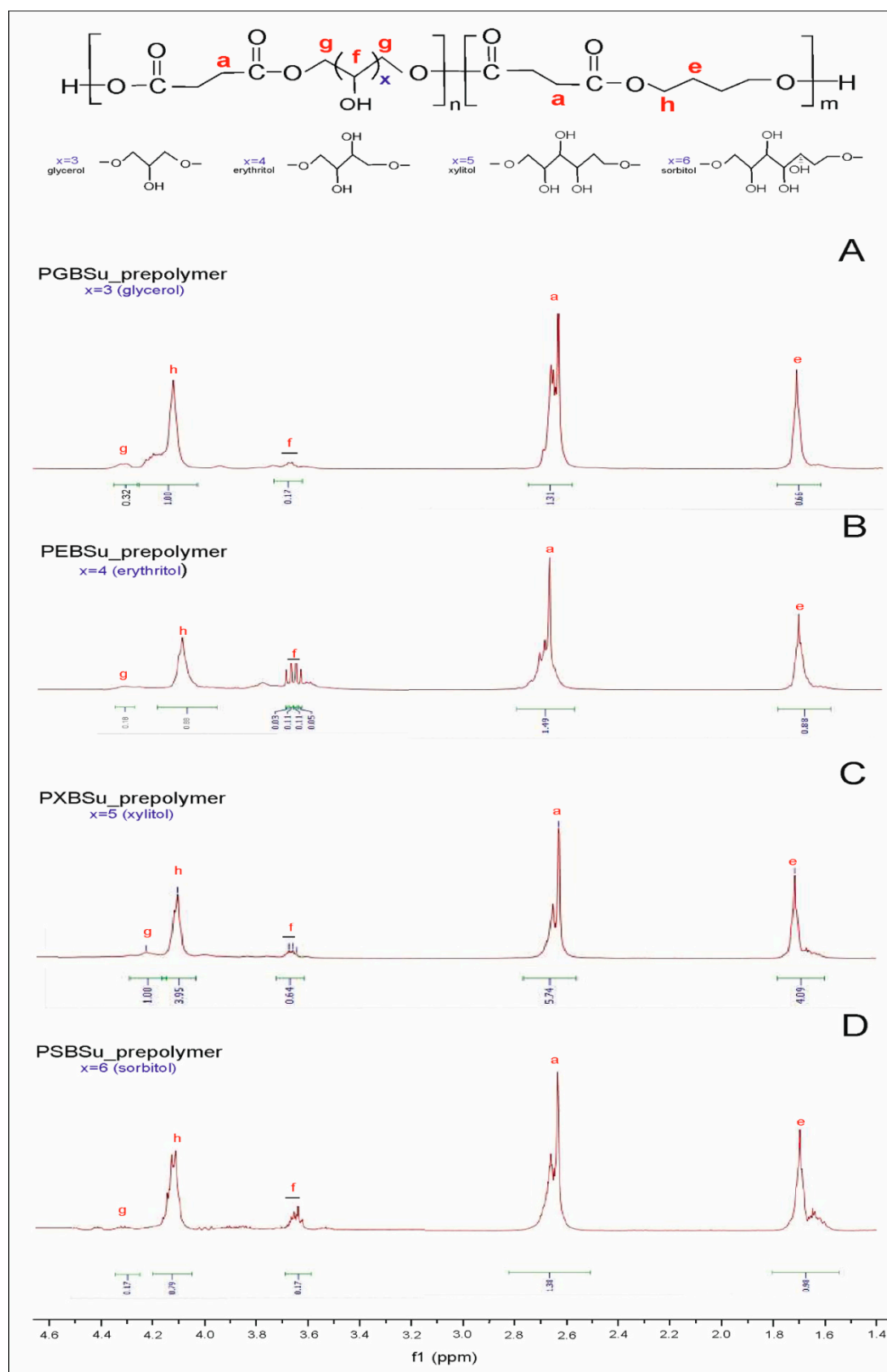
**Figure 3.** $^1$H NMR of PGBSu (**A**), PEBSu (**B**), PXBSu (**C**), and PSBSu(**D**) prepolymers.

## 3.2. Fourier Transform Infrared Spectroscopy (FTIR)

In the FTIR (Figure 4), four peaks linked to groups typical for poly(polyol succinate-co-butylene succinate) elastomers are present: -OH groups at 3450 cm$^{-1}$, -CH groups at 2930 cm$^{-1}$, C=O groups at 1725 cm$^{-1}$, and –C–O–C groups at 1170 cm$^{-1}$, which confirms a successful synthesis. A small change in the intensity of signals connected to the hydroxyl groups was observed when comparing the spectra for the material before and after irradiation—it decreases for PEBSu and PXBSu and increases for PSBSu. It is connected to the cross-link density results—the cross-link density increases for PEBSu and PXBSu and decreases for PSBSu. It is caused by ester bond formation between chains in case of all materials except for PSBSu, in case of which, those bonds undergo scission.

Lack of significant changes in the spectra of materials after modification confirms that the ester structure is retained after applying radiation treatment.
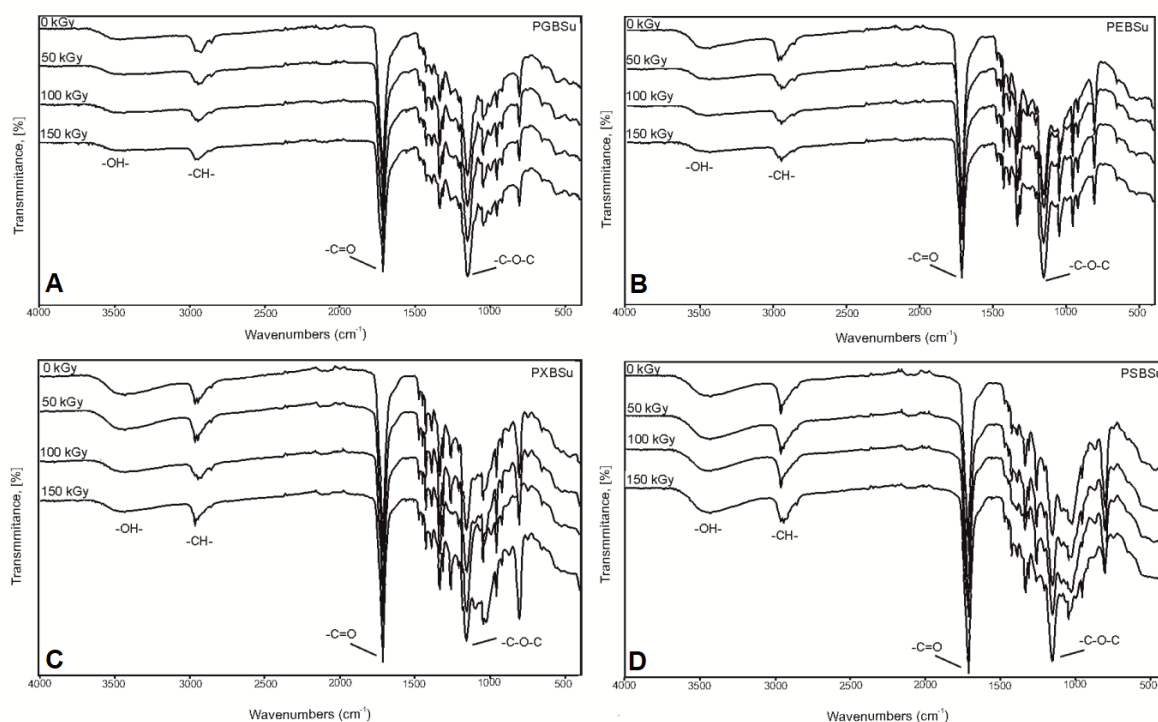


**Figure 4.** FTIR spectra of PGBSu (**A**), PEBSu (**B**), PXBSu (**C**), and PSBSu (**D**) polymers before and after radiation treatment.

## 3.3. Thermal Properties: Differential Scanning Calorimetry (DSC)

DSC analysis (Table 3 and Figure 5) was conducted in order to see how radiation modification affects the thermal properties of poly(polyol succinate-co-butylene succinate) elastomers. The value of change in heat capacity does not differ much between polymers based on various sugar alcohols and between different radiation doses due to the amount of amorphous phase being at a similar level in all cases. However, glass transition temperature shows an upward tendency linked to increase in the amount of –OH groups, which is linked to a lower chain mobility and corresponds to a higher value in cross-link density as shown in Section 3.5 of this paper. Glass transition temperature also increases due to radiation treatment and further cross-linking taking place, and corresponds with higher cross-link density.

Values of the melting enthalpy show a downward tendency corresponding with the increase of the amount of –OH groups and the increase of cross-link density (for materials before modification). Radiation treatment leads to the melting temperature and enthalpy due to crystalline structure becoming more ordered.

**Table 3.** First-heating data for differential scanning calorimetry (DSC) analysis of non-irradiated and radiation-modified poly(glycerol succinate-co-butylene succinate) (PGBSu), poly(erythritol succinate-co-butylene succinate) (PEBSu), poly(xylitol succinate-co-butylene succinate) (PXBSu), and poly(sorbitol succinate-co-butylene succinate) (PSBSu).

| Material/Dose | $T_g$ (°C) | $\Delta C_p$ (J/g°C) | $T_m$ (°C) | $\Delta H_m$ (J/g) |
|---|---|---|---|---|
| PGBSu | | | | |
| PGBSu_0 kGy | −25.5 | 0.749 | 48.9 | 2.83 |
| PGBSu_50 kGy | −21.9 | 0.626 | 51.3 | 12.14 |
| PGBSu_100 kGy | −22.1 | 0.635 | 51.2 | 11.79 |
| PGBSu_150 kGy | −22.9 | 0.719 | 50.9 | 12.85 |
| PEBSu | | | | |
| PEBSu_0 kGy | −18.9 | 0.731 | 53.8 | 3.19 |
| PEBSu_50 kGy | −14.7 | 0.708 | 55.4 | 5.24 |
| PEBSu_100 kGy | −14.8 | 0.701 | 55.8 | 4.87 |
| PEBSu_150 kGy | −15.1 | 0.734 | 55.1 | 5.52 |
| PXBSu | | | | |
| PXBSu_0 kGy | −13.7 | 0.763 | - | - |
| PXBSu_50 kGy | −8.2 | 0.799 | - | - |
| PXBSu_100 kGy | −7.4 | 0.759 | - | - |
| PXBSu_150 kGy | −4.5 | 0.729 | - | - |
| PSBSu | | | | |
| PSBSu_0 kGy | −2.6 | 0.686 | - | - |
| PSBSu_50 kGy | −0.4 | 0.764 | - | - |
| PSBSu_100 kGy | 1.9 | 0.729 | - | - |
| PSBSu_150 kGy | −0.3 | 0.769 | - | - |

where: $T_g$: glass transition temperature, $\Delta C_p$: change of the heat capacity, $T_m$: melting temperature, $\Delta H_m$: melting enthalpy.

### 3.4. Dynamic Thermomechanical Analysis (DMTA)

DMTA (Figure 6) was used to test the relaxation behavior displayed by PGBSu, PEBSu, PXBSu, and PSBSu (before and after radiation modification with 100 kGy) and measure the loss tangent (tan delta), loss modulus E″, and storage modulus E′ as a temperature function.

The values of storage moduli, loss moduli, and tan delta increase after radiation treatment for all materials, except sorbitol, which corresponds to the change of the values of the moduli at 50% and 100% strain as determined by mechanical tests (Section 3.4.). In the temperatures between −100 and −20 °C, the materials are in a glassy state. In the temperatures between −20 and 0 °C, a significant decrease of storage modulus can be observed. It is linked to a viscoelastic relaxation process associated with the glass transition process. A flexibility plateau can be seen in the temperatures between 0 and 50 °C. In case of PGBSu and PEBSu, the storage modulus values decrease almost to 0, which corresponds to the melting transition shown by DSC analysis. The peak maxima of the loss modulus and loss tangent functions associated with α relaxation correspond well with the glass transition temperature determined by DSC. The peak area of the loss modulus and loss tangent functions is similar for all materials due to the amorphous phase content being comparable for all materials, which is also confirmed by the DSC results. Overall, all of the DMTA results complement well with the results of the DSC analysis.
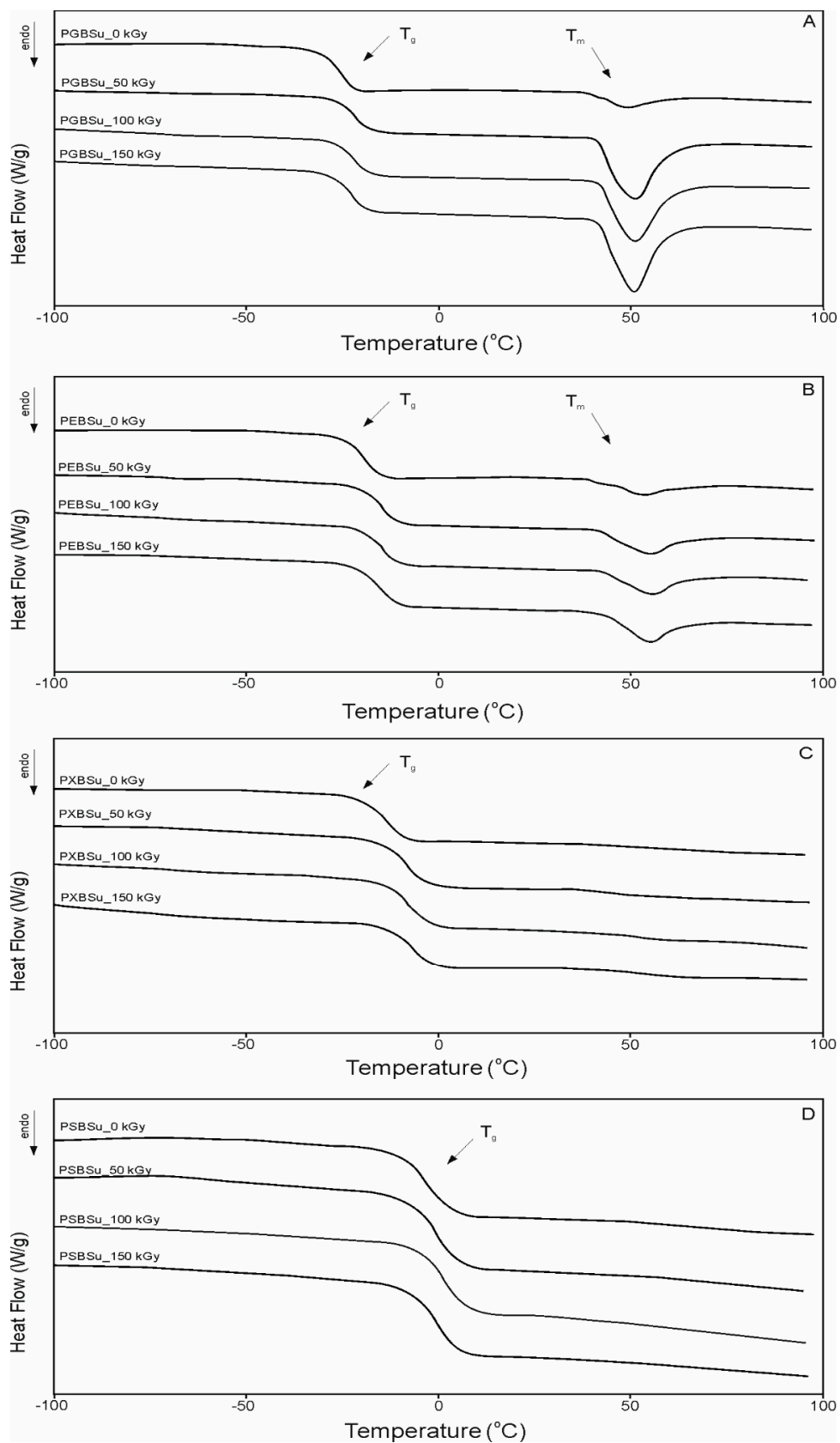
**Figure 5.** Differential scanning calorimetry (DSC) thermograms for first heating. (**A**) PGBSu, (**B**) PEBSu, (**C**) PXBSu, and (**D**) PSBSu before and after irradiation.
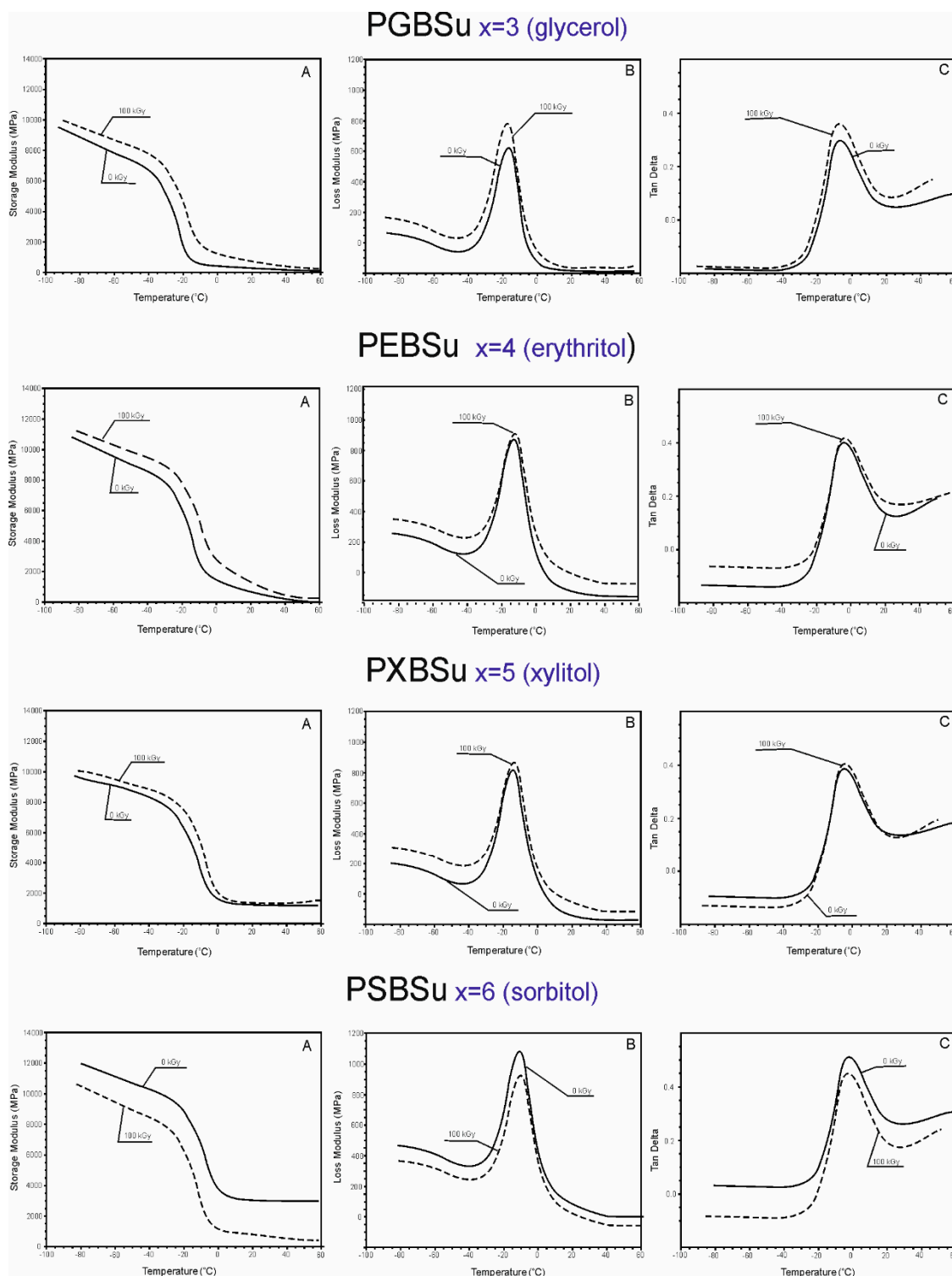
**Figure 6.** Dynamic thermomechanical analysis (DMTA). (**A**) Storage modulus (E'), (**B**) loss modulus (E''), and (**C**) loss tangent (tan delta versus temperature) for PGBSu, PEBSu, PXBSu, and PSBSu.

## 3.5. Mechanical Properties

In order to examine the radiation treatment effects on the elastomers, mechanical tests (Table 2, Figure 7) were performed. Four materials with different hydroxyl group contents per repeating unit were tested. The materials were as follows: PGBSu (3 hydroxyl groups), PEBSu (4 hydroxyl groups), PXBSu (5 hydroxyl groups), and PSBSu (6 hydroxyl groups). Both non-irradiated materials and

materials after modification with 50, 100, and 150 kGy doses were tested. With the increase of hydroxyl group content, an increase of stress at break value and value of moduli at 50% strain can be observed. It is due to higher cross-link density (for PGBSu, PEBSu, PXBSu, and PSBSu).

Radiation modification leads to an increase in stress at break for PEBSu and PXBSu. The values of the moduli at 50% and 100% show an increase for all the irradiation doses for PGBSu, and for 50 and 100 kGy doses for PEBSu.

The dose of 150 kGy is the most beneficial for PGBSu, the dose of 50 kGy is the most beneficial for PEBSu, and the dose of 100 kGy is the most beneficial for PXBSu. Sorbitol has a very high hydroxyl group content per repeating unit, which leads to the highest cross-link density and highest values of the moduli at 50% and 100% and stress at break. Radiation modification of this material leads only to worsening of those properties.
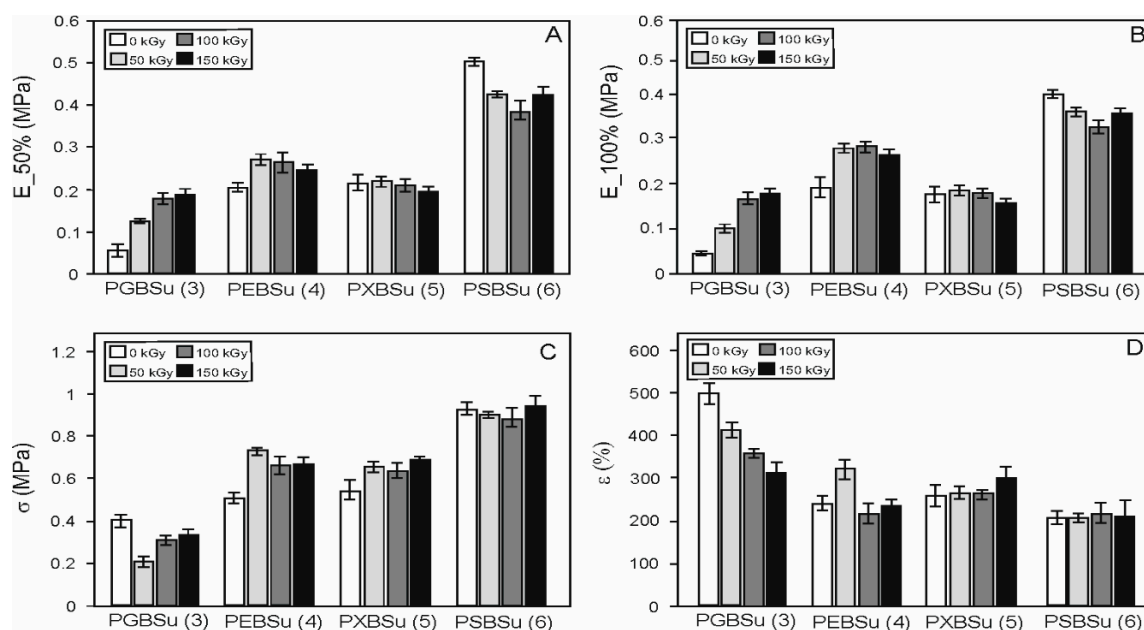


**Figure 7.** Mechanical properties of PGBSu, PEBSu, PXBSu, and PSBSu before and after irradiation. Tangent modulus at 50% elongation (**A**), tangent modulus at 100% elongation (**B**), stress at break (**C**), and elongation at break (**D**).

*3.6. Cross-Linking Density*

Cross-link density results are shown in Table 2 and Figure 8. Increasing content of the hydroxyl groups is followed by the cross-link density increase (for non-irradiated materials). Radiation treatment leads to decline of the cross-link density for all the doses in case of PGBSu and PSBSu. For PEBSu, the dose of 50 kGy leads to the biggest improvement of cross-link density. The dose of 100 kGy leads to the biggest improvement of cross-link density for PXBSu.

PEBSu seems to be the best suited for radiation modification because when modified with 50 kGy dose, the cross-link density increases more (as compared with the initial value) than in the case of PXBSu. It is also followed by the most noticeable improvement of mechanical properties exhibited by this material.
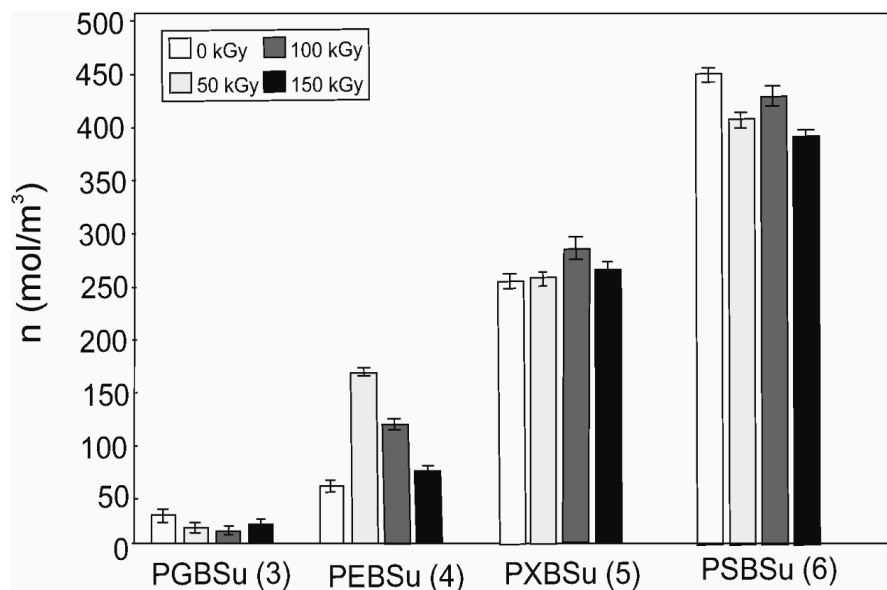
**Figure 8.** Cross-linking density of non-irradiated and radiation-modified PGBSu, PEBSu, PXBSu, and PSBSu. Hydroxyl group amount is indicated by the numbers in the brackets.

### 3.7. Water Contact Angle

Results of water contact angle tests are shown in Figure 9 and Table 1. Increasing hydroxyl group content leads to a decrease of water contact angle and increase in hydrophilicity. Applying radiation treatment leads to an increase of hydrophobicity. Higher doses of radiation result in higher hydrophobicity of the affected materials.
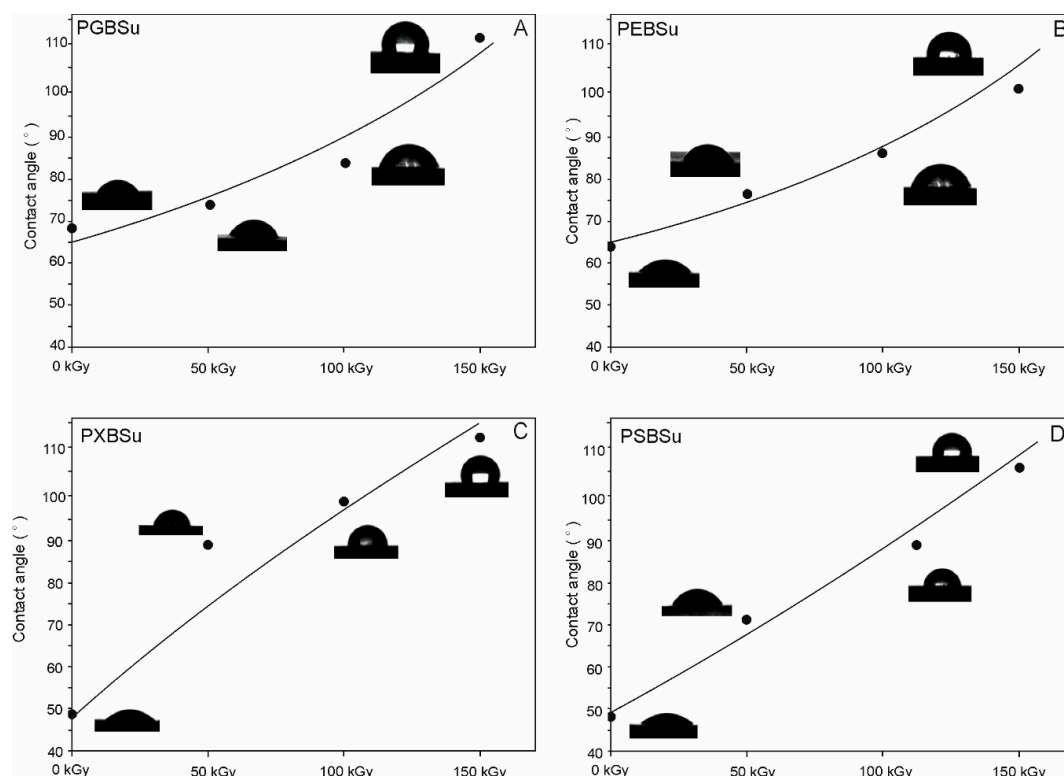


**Figure 9.** (**A**) PGBSu, (**B**) PEBSu, (**C**) PXBSu, and (**D**) PSBSu water contact angle before and after irradiation.

## 4. Conclusions

In order to improve the properties of different poly(polyol succinate-co-butylene succinate) elastomers, radiation modification was carried out. Such modification has proven to be simple and effective, materials directly after synthesis were utilized, and no cross-linking agents were necessary. A valuable side effect of this treatment was the sterilization of the materials.

It has been established that polymers have a semi-crystalline structure with the amorphous phase being dominant. The increasing hydroxyl group content leads to the amorphous phase becoming more prominent, and the cross-link density increasing, which is followed by better mechanical properties.

The influence of various doses of radiation on thermal, mechanical, and chemical properties was analyzed in order to select the dose that is most optimal.

Radiation treatment has proven useful for PEBSu and PXBSu materials, as seen in the increase of cross-link density and improvement of the mechanical properties. PSBSu and PGBSu turned out to be not well suited for such modification, with its properties worsening.

**Conflicts of Interest:** The authors declare no conflict of interest.

## References

1. Rouif, S. Radiation cross-linked polymers: Recent developments and new applications. *Nucl. Instrum. Methods Phys. Res. Sect. B Beam Interact. Mater. Atoms* **2005**, *236*, 68–72. [CrossRef]

2. Drobny, J.G. *Ionizing Radiation and Polymers: Principles, Technology, and Applications*; William Andrew: Norwich, NY, USA, 2012.

3. Zhu, G.; Xu, Q.; Qin, R.; Yan, H.; Liang, G. Effect of γ-radiation on crystallization of polycaprolactone. *Radiat. Phys. Chem.* **2005**, *74*, 42–50. [CrossRef]

4. Changyu, H.; Xianghai, R.; Kunyu, Z.; Yugang, Z.; Lisong, D. Thermal and Mechanical Properties of Poly(e-caprolactone) Crosslinked with g Radiation in the Presence of Triallyl Isocyanurate. *J. Appl. Polym. Sci.* **2006**, *103*, 2676–2681.

5. Zhu, G.; Liang, G.; Xu, Q.; Yu, Q. Shape-memory effects of radiation crosslinked Poly(ε-caprolactone). *J. Appl. Polym. Sci.* **2003**, *90*, 1589–1595. [CrossRef]

6. Huang, Y.; Gohs, U.; Müller, M.T.; Zschech, C.; Wiessner, S. Electron beam treatment of polylactide at elevated temperature in nitrogen atmosphere. *Radiat. Phys. Chem.* **2019**, *159*, 166–173. [CrossRef]

7. Quynh, T.M.; Mai, H.H.; Lan, P.N. Properties of Radiation-Induced Crosslinking Stereocomplexes Derived From Poly(L-Lactide) and Different Poly(D-Lactide). *Radiat. Phys. Chem.* **2013**, *83*, 105–110. [CrossRef]

8. Nagasawa, N.; Kasai, N.; Yagi, T.; Yoshii, F.; Tamada, M. Radiation-induced crosslinking and post-processing of poly(l-lactic acid) composite. *Radiat. Phys. Chem.* **2011**, *80*, 145–148. [CrossRef]

9. Jung, C.H.; Hwang, I.T.; Jung, C.H.; Choi, J.H. Preparation of flexible PLA/PEG-POSS nanocomposites by melt blending and radiation crosslinking. *Radiat. Phys. Chem.* **2014**, *102*, 23–28. [CrossRef]

10. Suhartini, M.; Mitomo, H.; Nagasawa, N.; Yoshii, F.; Kume, T. Radiation crosslinking of poly(butylene succinate) in the presence of low concentrations of trimethallyl isocyanurate and its properties. *J. Appl. Polym. Sci.* **2003**, *88*, 2238–2246. [CrossRef]

11. Manas, D.; Mizera, A.; Navratil, M.; Manas, M.; Ovsik, M.; Sehnalek, S.; Stoklasek, P. The electrical, mechanical and surface properties of thermoplastic polyester elastomer modified by electron beta radiation. *Polymers* **2018**, *10*, 1057. [CrossRef]

12. Mizera, A.; Manas, M.; Manas, D.; Stoklasek, P.; Bednarik, M.; Hylova, L. Mechanical properties change of thermoplastic elastomer after using of different dosage of irradiation by beta rays. *MATEC Web Conf.* **2016**, *76*, 8–11. [CrossRef]

13. Zhu, S.; Shi, M.; Tian, M.; Qu, L.; Chen, G. Effects of irradiation on polyethyleneterephthalate(PET) fibers impregnated with sensitizer. *J. Text. Inst.* **2018**, *109*, 294–299. [CrossRef]

14. Zhu, S.; Shi, M.; Tian, M.; Xiaoqingguo, L. Burning behavior of irradiated PET flame-retardant fabrics impregnated with sensitizer. *Mater. Lett.* **2015**, *160*, 58–60. [CrossRef]

15. Malinowski, R. Application of the electron radiation and triallyl isocyanurate for production of aliphatic-aromatic co-polyester of modified properties. *Int. J. Adv. Manuf. Technol.* **2016**, *87*, 3307–3314. [CrossRef]

16. Hooshangi, Z.; Feghhi, S.A.H.; Sheikh, N. The effect of electron-beam irradiation and halogen-free flame retardants on properties of poly butylene terephthalate. *Radiat. Phys. Chem.* **2015**, *108*, 54–59. [CrossRef]

17. Mizera, A.; Manas, M.; Manas, D.; Holik, Z.; Stanek, M.; Navratil, J.; Bednarik, M. Temperature stability of Modified PBT by Radiation Cross-Linking. In *Advanced Materials Research*; Trans Tech Publications Ltd: Stafa-Zurich, Switzerland, 2014; Volume 1025, pp. 256–260.

18. Ashby, R.D.; Cromwick, A.M.; Foglia, T.A. Radiation crosslinking of a bacterial medium-chain-length poly(hydroxyalkanoate) elastomer from tallow. *Int. J. Biol. Macromol.* **1998**, *23*, 61–72. [CrossRef]

19. Bergmann, A.; Teßmar, J.; Owen, A. Influence of electron irradiation on the crystallisation, molecular weight and mechanical properties of poly-(R)-3-hydroxybutyrate. *J. Mater. Sci.* **2007**, *42*, 3732–3738. [CrossRef]

20. Rai, R.; Tallawi, M.; Roether, J.A.; Detsch, R.; Barbani, N.; Rosellini, E.; Kaschta, J.; Schubert, D.W.; Boccaccini, A.R. Sterilization effects on the physical properties and cytotoxicity of poly(glycerol sebacate). *Mater. Lett.* **2013**, *105*, 32–35. [CrossRef]

21. Bruggeman, J.P.; Bettinger, C.J.; Nijst, C.L.E.; Kohane, D.S.; Langer, R. Biodegradable xylitol-based polymers. *Adv. Mater.* **2008**, *20*, 1922–1927. [CrossRef]

22. Bruggeman, J.P.; Bettinger, C.J.; Langer, R. Biodegradable xylitol-based elastomers: In vivo behavior and biocompatibility. *J. Biomed. Mater. Res. Part A* **2010**, *95*, 92–104. [CrossRef]

23. Dasgupta, Q.; Chatterjee, K.; Madras, G. Combinatorial approach to develop tailored biodegradable poly(xylitol dicarboxylate) polyesters. *Biomacromolecules* **2014**, *15*, 4302–4313. [CrossRef] [PubMed]

24. Bruggeman, J.P.; De Bruin, B.J.; Bettinger, C.J.; Langer, R. Biodegradable poly(polyol sebacate) polymers. *Biomaterials* **2008**, *29*, 4726–4735. [CrossRef] [PubMed]

25. Ning, Z.Y.; Zhang, Q.S.; Wu, Q.P.; Li, Y.Z.; Ma, D.X.; Chen, J.Z. Efficient synthesis of hydroxyl functioned polyesters from natural polyols and sebacic acid. *Chinese Chem. Lett.* **2011**, *22*, 635–638. [CrossRef]

26. Kavimani, V.; Jaisankar, V. Synthesis and Characterisation of Sorbitol Based Copolyesters for Biomedical Applications. *J. Phys. Sci. Appl.* **2014**, *4*, 507–515.

27. Hu, J.; Gao, W.; Kulshrestha, A.; Gross, R.A. "Sweet polyesters": Lipase-catalyzed condensation-polymerizations of alditols. *ACS Symp. Ser.* **2006**, *999*, 275–284.

28. Kumar, A.; Kulshrestha, A.S.; Gao, W.; Gross, R.A. Versatile route to polyol polyesters by lipase catalysis. *Macromolecules* **2003**, *36*, 8219–8221. [CrossRef]

29. Piątek-Hnat, M.; Bomba, K.; Pęksiński, J. Synthesis and selected properties of ester elastomer containing sorbitol. *Appl. Sci.* **2020**, *10*, 1628. [CrossRef]

30. Piątek-Hnat, M.; Bomba, K. The influence of of cross-linking process on the physicochemical properties of new copolyesters containing xylitol. *Mater. Today Commun.* **2020**, *22*, 100734. [CrossRef]

31. Piatek-Hnat, M.; Bomba, K.; Pęksiński, J. Structure and Properties of Biodegradable Poly (Xylitol Sebacate-Co-Butylene Sebacate) Copolyester. *Molecules* **2020**, *25*, 1541. [CrossRef]

32. Piątek-Hnat, M.; Bomba, K.; Pęksiński, J.; Kozłowska, A.; Sośnicki, J.G.; Idzik, T.J. Effect of E-Beam Irradiation on Thermal and Mechanical Properties of Ester Elastomers Containing Multifunctional Alcohols. *Polymers* **2020**, *12*, 1043. [CrossRef]

33. *ISO 111 37 1:2006 Sterilization of health care products—Radiation—Part 1: Requirements for development, validation and routine control of a sterilization process for medical devices*; American National Standards Institute (ANSI): Washington, DC, USA, 2007.

34. *PN EN ISO 527:2019 Plastics—Determination of tensile properties*; Polish Committee for Standardization: Warsaw, Poland, 2019.

35. Flory, P.J. *Principles of Polymer Chemistry*; Cornell University Press: Ithaca, NY, USA, 1953.

36. Chen, Q.Z.; Bismarck, A.; Hansen, U.; Junaid, S.; Tran, M.Q.; Harding, S.E.; Ali, N.N.; Boccaccini, A.R. Characterisation of a soft elastomer poly(glycerol sebacate) designed to match the mechanical properties of myocardial tissue. *Biomaterials* **2008**, *29*, 47–57. [CrossRef] [PubMed]

# Tailoring the Physico-Chemical Properties of Poly(xylitol-dicarboxylate-*co*-butylene dicarboxylate) Polyesters by Adjusting the Cross-Linking Time

**Marta Piątek-Hnat [1],\* [iD], Paulina Sładkiewicz [1], Kuba Bomba [1] [iD], Jakub Pęksiński [2] [iD], Agnieszka Kozłowska [1] [iD], Jacek G. Sośnicki [3] and Tomasz J. Idzik [3] [iD]**

[1] Department of Polymer and Biomaterials Science, Faculty of Chemical Technology and Engineering, West Pomeranian University of Technology, Piastów Ave. 42, 71-065 Szczecin, Poland; paulina.sladkiewicz@gmail.com (P.S.); bk34688@zut.edu.pl (K.B.); agak@zut.edu.pl (A.K.)

[2] Faculty of Electrical Engineering, West Pomeranian University of Technology, Sikorskiego Ave. 37, 71-313 Szczecin, Poland; jakub.peksinski@zut.edu.pl

[3] Department of Organic and Physical Chemistry, Faculty of Chemical Technology and Engineering, West Pomeranian University of Technology, Piastów Ave. 42, 71-065 Szczecin, Poland; jacek.sosnicki@zut.edu.pl (J.G.S.); tomasz.idzik@zut.edu.pl (T.J.I.)

\* Correspondence: marp@zut.edu.pl

**Abstract:** Determining the cross-linking time resulting in the best achievable properties in elastomers is a very important factor when considering their mass production. In this paper, five biodegradable polymers were synthesized—poly(xylitol-dicarboxylate-co-butylene dicarboxylate) polymers, based on xylitol obtained from renewable sources. Five different dicarboxylic acids with even numbers of carbon atoms in the aliphatic chain were used: succinic acid, adipic acid, suberic acid, sebacic acid, and dodecanedioic acid. Samples were taken directly after polycondensation (prepolymer samples) and at different stages of the cross-linking process. Physiochemical properties were determined by a gel fraction test, differential scanning calorimetry (DSC), Fourier-transform infrared spectroscopy (FTIR), quasi-static tensile tests, nuclear magnetic resonance spectroscopy ($^1$H NMR and $^{13}$C NMR), and an in vitro biodegradation test. The best cross-linking time was determined to be 288h. Properties and degradation time can be tailored for specific applications by adjusting the dicarboxylic acid chain length.

**Keywords:** ester elastomers; renewable sources; crosslinking; mechanical properties; biodegradation

## 1. Introduction

Due to environmental concerns and declines in world oil reserves, it is of great importance to find monomers for polymer synthesis that are obtainable from renewable sources. One such group of compounds is sugar alcohols. These multifunctional alcohols exhibit a great deal of flexibility in terms of their possible applications as monomers for polymer synthesis, with the most researched group of sugar alcohol-based polymers being poly(polyol dicarboxylate). In general, polymers belonging to this polyester family have been proven to be biocompatible both in vitro and in vivo [1–3]. While retaining a core property of biodegradability, and eco-friendliness, a wide variety of sugar alcohol-based elastomers with different physico-chemical properties suitable for specific uses can be obtained by using different dicarboxylic acids and a specific sugar alcohol, like erythritol [4] or xylitol [5]. Another way to fine tune the characteristics is to choose a specific dicarboxylic acid and perform the synthesis using different sugar alcohols [3,6] Further tailoring of their properties can be performed by copolymerization with various diol-dicarboxylates [7–9].

Research into specific possible applications of poly(polyol dicarboxylate) polyesters has been reported in the literature. Poly(glycerol sebacate) has attracted the largest amount of attention, with a wide range of potential uses including scaffolds for the regeneration of bone tissue [10,11], myocardial tissue [12], retinal cells [13], blood vessels [14], nerves [15], cartilage [16], and as drug carriers [17].

Potential medical uses of xylitol-based polymers have also been reported. They include poly(xylitol-co-maleate-co-PEG) hydrogels for cell encapsulation [18], and fibrous networks of poly(xylitol sebacate) electrospun using the core–shell method for potential tissue engineering applications [19,20].

In our previous work various elastomers were synthesized and tested: poly(sorbitol sebacate-co-butylene sebacate) [21] and poly(xylitol sebacate-co-butylene sebacate) [22]. Poly(polyol sebacate-co-butylene sebacate) elastomers were also proven to be suitable for radiation modification. [23] The influence of the cross-linking time on the physiochemical properties of elastomers synthesized using succinic and sebacic acid was also tested [24] The novelty of this work is performing a successful synthesis of sugar alcohol-based polyesters without the use of a catalyst and using a much wider range of dicarboxylic acids (consisting of two, four, six, eight and 10 carbon atoms in the aliphatic chain) as monomers.

## 2. Materials and Methods

### 2.1. Synthesis of Elastomers

All reagents were purchased from Sigma-Aldrich (St. Louis, MO, USA). All the reagents were of over 99% purity. Synthesis of five polymers was carried out. The monomers used were: butanediol, xylitol and five different dicarboxylic acids with even-numbered chain lengths—succinic acid (poly(xylitol succinate-co-butylene succinate) (PXBSu), adipic acid (poly(xylitol adipicate-co-butylene adipicate)) (PXBA), suberic acid (poly(xylitol suberate-co-butylene suberate)) (PXBSb), sebacic acid (poly(xylitol sebacate-co-butylene sebacate)) (PXBS), and dodecanedioic acid (poly(xylitol dodecanedioate-co-butylene dodecanedioate)) (PXBD). A monomer ratio of 2:1:1 (dicarboxylic acid: xylitol:butylene glycol) was used. Esterification of the dicarboxylic acid, xylitol and butylene glycol in $N_2$ atmosphere at 150 °C for 13.5h was the first step of each synthesis. The second step was polycondensation in a vacuum atmosphere at 150 °C. After the synthesis materials were cast into silicone forms and cross-linked at 100 °C in 100 mb in a vacuum dryer. Materials were considered fully cross-linked after 288h because the value of the gel fraction did not increase for the materials cross-linked for a longer period of time.

### 2.2. Experimental Methods

#### 2.2.1. Nuclear Magnetic Resonance Spectroscopy (NMR)

$^1$H and $^{13}$C NMR spectroscopic measurements were performed on a Bruker DPX 400 AVANCE III HD spectrometer (Bruker, Rheinstetten, Germany) operating at 400.1 and 100.6 MHz, respectively. Approximately 50 mg of each sample was dissolved in 0.7mL of deuterated chloroform (CDCl$_3$). TMS was used as an internal reference and spectra were acquired in 5-mm probes. For NMR analyses, the MestReNova (version 12.0.3, Mestrelab, Santiago de Compostela, Spain) program was used.

#### 2.2.2. Fourier Transform Infrared Spectroscopy (FTIR)

An analysis of the chemical structure of the polymers was conducted with Fourier transform infrared spectroscopy (FTIR). An Alpha Spectrometer Bruker (Bruker, Germany) was used. Recorded transmission spectra were in the range between 4000 cm$^{-1}$ and 400 cm$^{-1}$ with resolution of 2 cm$^{-1}$. In order to develop the results, Omnic 7.3 software by the Thermo Electron Corporation (Waltham, MA, USA) was used.

### 2.2.3. Differential Scanning Calorimetry (DSC)

In order to determine the thermal properties of the materials, differential scanning calorimetry (DSC) was utilized. TA Instruments apparatus Q2500 (New Castle, DE, USA) was used. The parameters of the analysis were −90 °C to 150 °C heating cycle and 10 °C/min heating rate. Tests were performed in a nitrogen atmosphere. In order to develop the results, TA Instruments Universal Analysis 2000, 3.9a software (New Castle, DE, USA), was used.

### 2.2.4. Mechanical Properties

The testing of the mechanical properties was performed using an Instron 36 instrument (Norwood, MA, USA). The parameters of the tests were 25 °C, 50% relative humidity, 100 mm/min crosshead speed, and 500 N load cell. Tests were performed in keeping with PN-EN-ISO 526/1:1996 standard. In total, 12 samples were used for each test.

### 2.2.5. Hardness

Hardness (H) for materials after 288 h was measured using a Zwick/Material Testing 3100 Shore A hardness tester.

### 2.2.6. Gel Fraction

In order to determine the gel fraction, the PN-EN-579:2001 extraction method was utilized. Samples of material after 48 h, 192 h and 288 h (fully cross-linked material) were used. The weight of each sample was about 1 g. A Schott crucible Type P2 was utilized. Samples were extracted with 100 cm$^3$ of boiling tetrahydrofuran. The extraction took 3 h. A vacuum oven was used to dry the samples. The drying process took 3 h and was performed at 25 °C. After that, the samples were dried in a desiccator. Three samples for each cross-linking time were used. Formula (1) was used in order to calculate the gel fraction content. The mean of three measurements was used.

$$X = \frac{m_1}{m_0} \times 100\% \tag{1}$$

where $m_0$—mass of the sample before extraction, $m_1$—mass of the sample after extraction.

### 2.2.7. Hydrolytic Degradation

Hydrolytic degradation was carried out on previously sterilized 10 mm polymer discs for 21 days in phosphate-buffered saline (PBS) (Sigma Aldrich, Poznań, Poland) (pH range 7.1–7.2), in 37 °C. Three samples were used. PBS solution was changed every 48 h. Sterilization was conducted in a laminar chamber for 15 min, using UV light. Samples were placed in a 24-well plate. Each sample was covered with 1.5 mL of the solution. Samples after degradation were dried in a vacuum dryer in 25 °C, and then weighed. Mass loss after 21 days was calculated using formula (2)

$$D = (m_0 - m_1)/m_0 \times 100\% \tag{2}$$

where D—mass loss [%], $m_0$—sample mass before degradation [g], $m_1$—sample mass after degradation [g].

### 2.2.8. Enzymatic Degradation

Enzymatic degradation was carried out on previously sterilized 10-mm polymer discs for 21 days in solution of lipase (*Pseudomonas Cepacia*) (Sigma Aldrich, Poznań, Poland) (25 units/mL) in phosphate-buffered saline (PBS) (Sigma Aldrich, Poznań, Poland) (pH range 7.1–7.2). The lipase solution was changed every 48 h. Sterilization was conducted in a laminar chamber for 15 min, using UV light. Samples were placed in a 24-well plate. Each sample was covered with 1.5 mL of the solution.

Three samples were used for each degradation period. Samples after degradation were dried in a vacuum dryer in 25 °C and then weighed. Mass loss after 4, 8, 12, 16, and 21 days was calculated using formula (3)

$$D = (m_0 - m_1)/m_0 \times 100\%$$ (3)

where D—mass loss [%], $m_0$—sample mass before degradation [g], $m_1$—sample mass after degradation [g].

## 3. Results and Discussion

The composition and properties of elastomers are summarized in Table 1, and a scheme of the structure is shown in Figure 1.

**Table 1.** Composition and selected properties of poly(xylitol succinate-*co*-butylene succinate) (PXBSu), poly(xylitol adipicate-*co*-butylene adipicate) (PXBA), poly(xylitol suberate-*co*-butylene suberate) (PXBSb), poly(xylitol sebacate-*co*-butylene sebacate) (PXBS), poly(xylitol dodecanedioate -*co*-butylene dodecanedioate) (PXBD).

| Polymer Sample | Molar Composition [mol] | | | Molar Composition Determined by $^1$H NMR [mol] | | E_50% [MPa] | E_100% [MPa] | $\sigma_r$ [MPa] | $\varepsilon_r$ [%] | H *ShA* |
|---|---|---|---|---|---|---|---|---|---|---|
| | SuA | XL | BG | XL | BG | | | | | |
| PXBSu (succinic acid) | 2 | 1 | 1 | 1.0 | 3.95 | 0.469 +/−0.04 | 0.403 +/−0.03 | 0.991 +/−0.13 | 214 +/15.51 | 46.4 +/−0.42 |
| | AA | XL | BG | XL | BG | | | | | |
| PXBA (adipic acid) | 2 | 1 | 1 | 1.0 | 4.10 | 0.165 +/−0.04 | 0.148 +/−0.04 | 0.408 +/−0.09 | 248 +/67.55 | 36.8 +/−0.38 |
| | SbA | XL | BG | XL | BG | | | | | |
| PXBSb (suberic acid) | 2 | 1 | 1 | 1.0 | 3.41 | 0.212 ± 0.082 | 0.188 ± 0.07 | 0.328 ± 0.05 | 196 +/51.73 | 44.9 +/−0.34 |
| | SA | XL | BG | XL | BG | | | | | |
| PXBS (sebacic acid) | 2 | 1 | 1 | 1.0 | 2.33 | 0.756 ± 0.04 | 0.605 ± 0.03 | 1.632 ± 0.28 | 339 +/59.18 | 35.3 +/−0.45 |
| | DA | XL | BG | XL | BG | | | | | |
| PXBD (dodecanedioic acid) | 2 | 1 | 1 | 1.0 | 2:14 | 1.945 ± 0.08 | 1.876 ± 0.05 | 2.995 ± 0.35 | 42 +/24.16 | 28.6 +/−0.31 |

Stress at break ($\sigma_r$), elongation at break ($\varepsilon_r$), modulus at 50% elongation (E_50%), modulus at 100% elongation (E_100%), hardness (H), succinic acid (SuA), adipic acid (AA), suberic acid (SbA), sebacic acid (SA), dodecanedioic acid (DA), butylene glycol (BG), xylitol (XL).
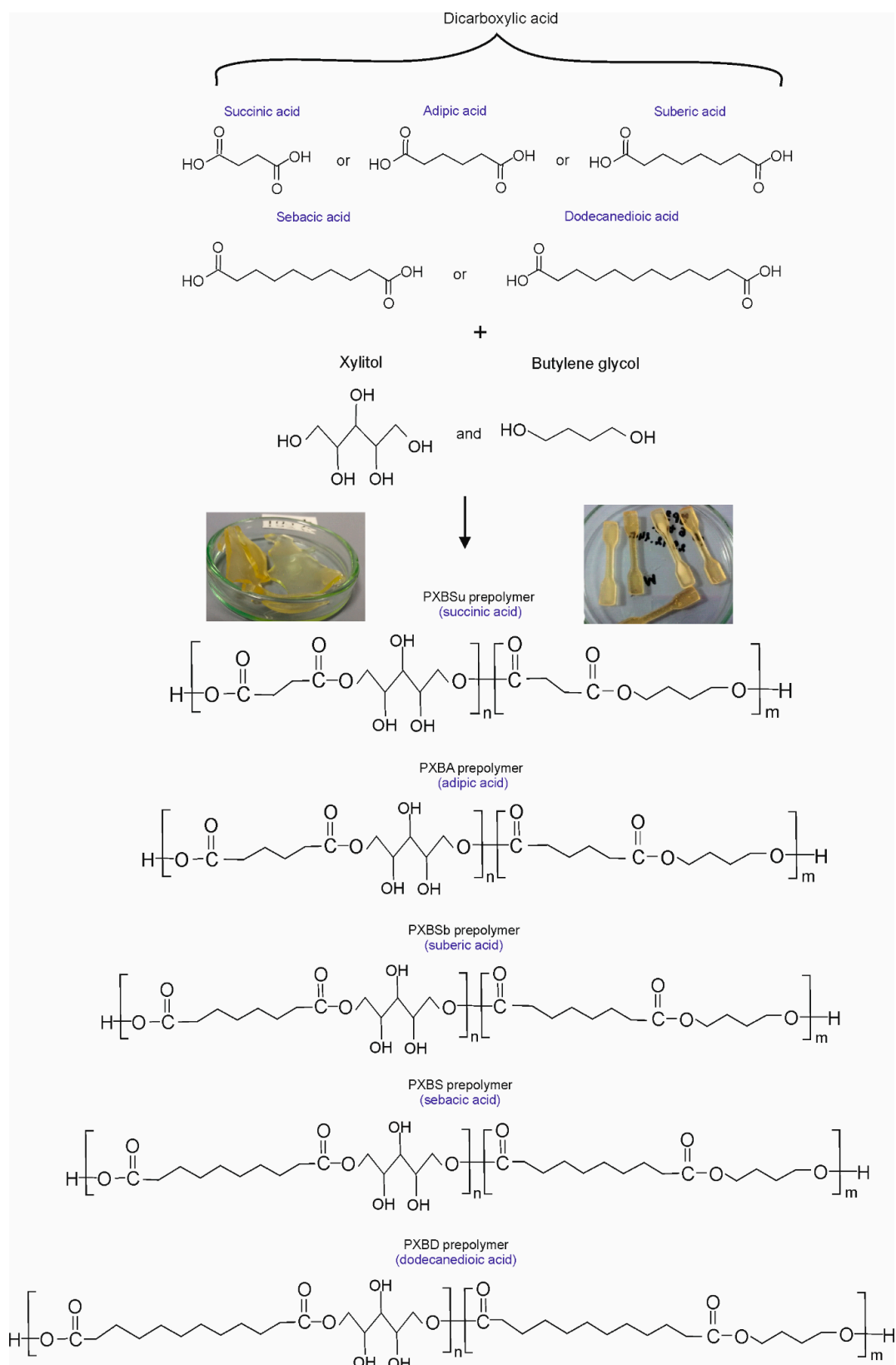
**Figure 1.** Scheme of poly(xylitol-dicarboxylate-co-butylene dicarboxylate) synthesis and structure.

## 3.1. Nuclear Magnetic Resonance Spectroscopy (NMR)

In order to analyze the chemical structure of the obtained polymers, and to confirm that the synthesis was successful, $^{1}$H NMR (Figure 2) and $^{13}$C NMR (Figure 3) analyses were performed. In $^{1}$H NMR peaks in the range of 1.2 to 2.8 ppm are due to CH$_2$ groups in dicarboxylic acids and butylene glycol. Signals in the range of 3.6 to 4.0 ppm are due to CH$_2$ groups in xylitol.
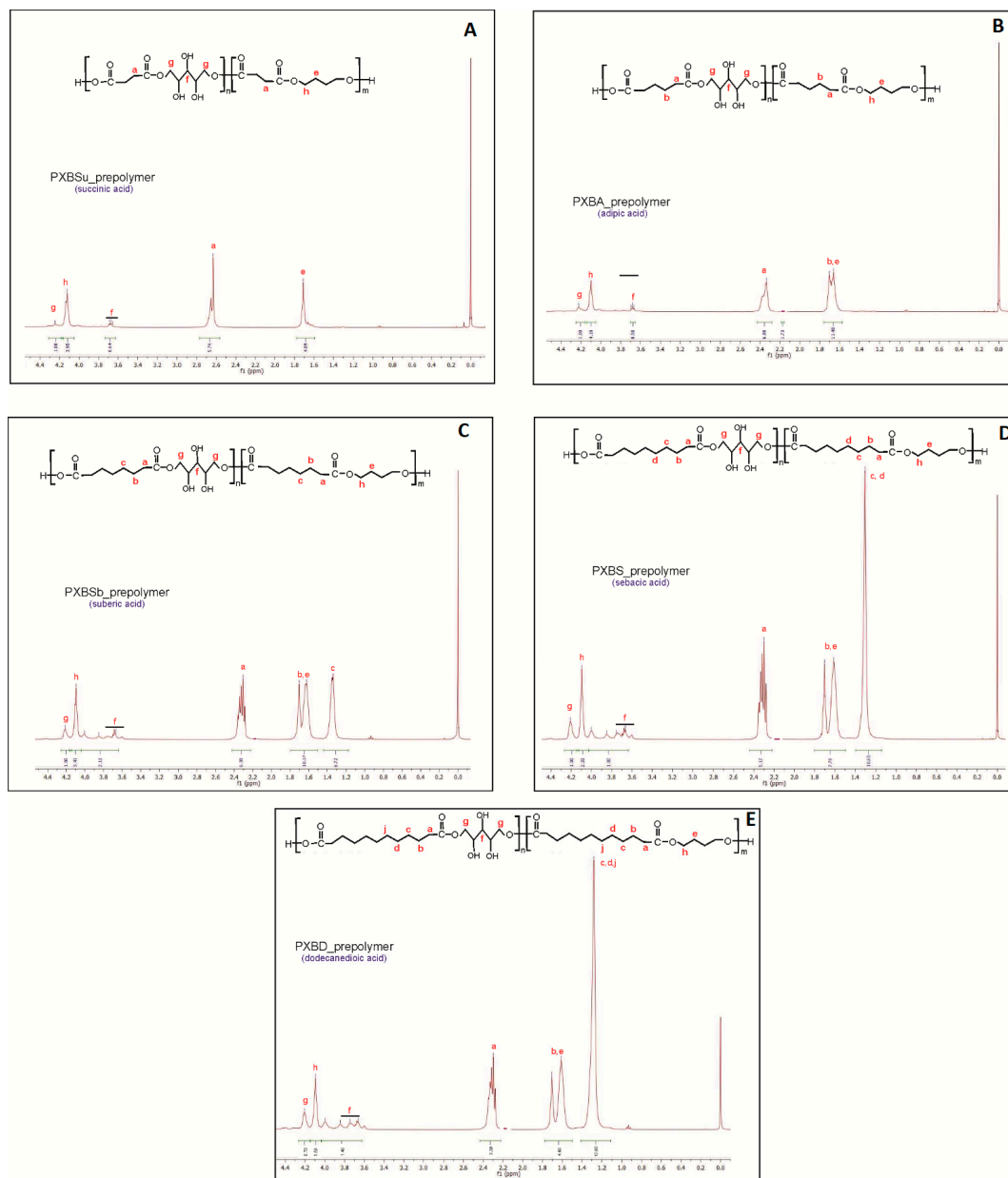


**Figure 2.** $^{1}$H NMR of PXBSu(**A**), PXBA(**B**), PXBSb(**C**), PXBS(**D**), PXBD(**E**) prepolymers.
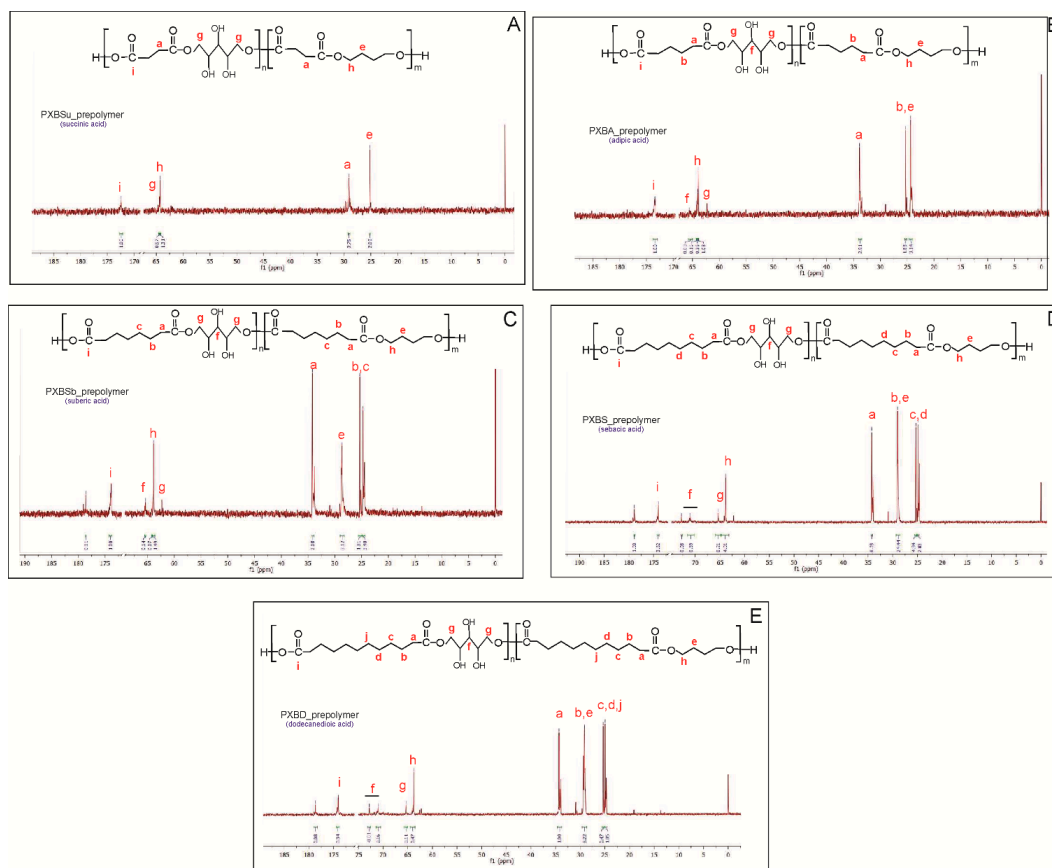
**Figure 3.** $^{13}$C NMR of PXBSu(**A**), PXBA(**B**), PXBSb(**C**), PXBS(**D**), PXBD(**E**) prepolymers.

The peak at about 4.1 ppm was attributed to the proton adjacent to the ester bond between dicarboxylic acid and butylene glycol, and the peak at about 4.2 ppm was ascribed to the proton adjacent to an ester bond between xylitol and dicarboxylic acid.

In $^{13}$C NMR, peaks in the range of 25 to 35 ppm are connected to carbon atoms in CH$_2$ groups in dicarboxylic acids and butylene glycol. The peak at about 175 ppm was ascribed to carbon atoms in carbonyl groups. Two peaks at about 65 ppm are present—one is connected to carbon atoms next to an ester bond between dicarboxylic acid and butylene glycol, and the other is linked to a carbon atom adjacent to an ester bond between dicarboxylic acid and xylitol.

### 3.2. Fourier Transform Infrared Spectroscopy (FTIR)

The FTIR spectra (Figure 4) show four peaks typical for sugar alcohol-based polyesters. The peak at 3450 cm$^{-1}$ is connected to –OH groups (stretching), the peak at 2930 cm$^{-1}$ is linked to –CH groups (asymmetrical, stretching vibration), the peak at 1730 cm$^{-1}$ is associated with –C=O groups (asymmetrical, stretching), and the peak at 1170 cm$^{-1}$ is related to –C–O–C groups (asymmetrical stretching). Due to –OH groups creating ester bonds during the cross-linking process, the intensity of the peaks at 3450 cm$^{-1}$ is decreasing, and the intensity of the peaks at 1170 cm$^{-1}$ is increasing with the progress of the cross-linking.
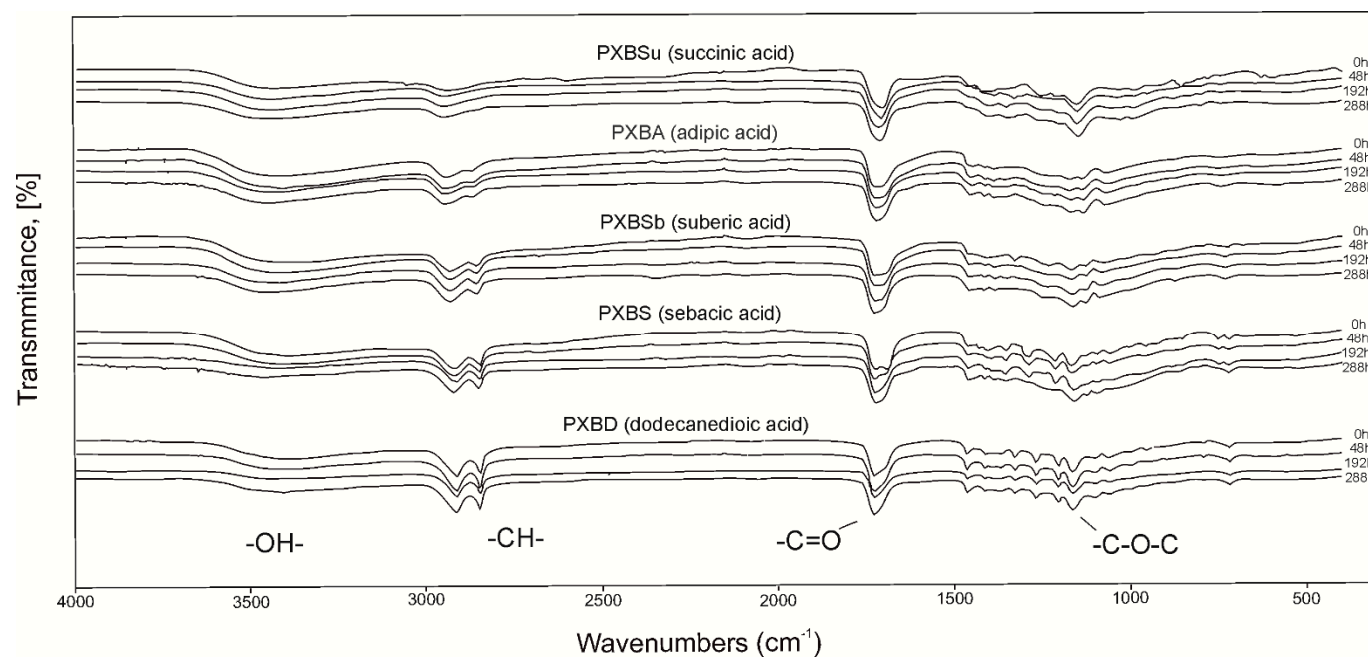
**Figure 4.** FTIR spectra of PXBSu, PXBA, PXBSb, PXBS, and PXBD prepolymers (0 h) and polymers at consecutive stages of cross-linking process (48 h, 144 h, 192 h and 288 h).

### 3.3. Thermal Properties: Differential Scanning Calorimetry (DSC)

The DSC thermograms for PXBSu, PXBA, PXBSb, PXBS, and PXBD are shown in Figures 5–9 and the thermal properties of the elastomers are given in Table 2.
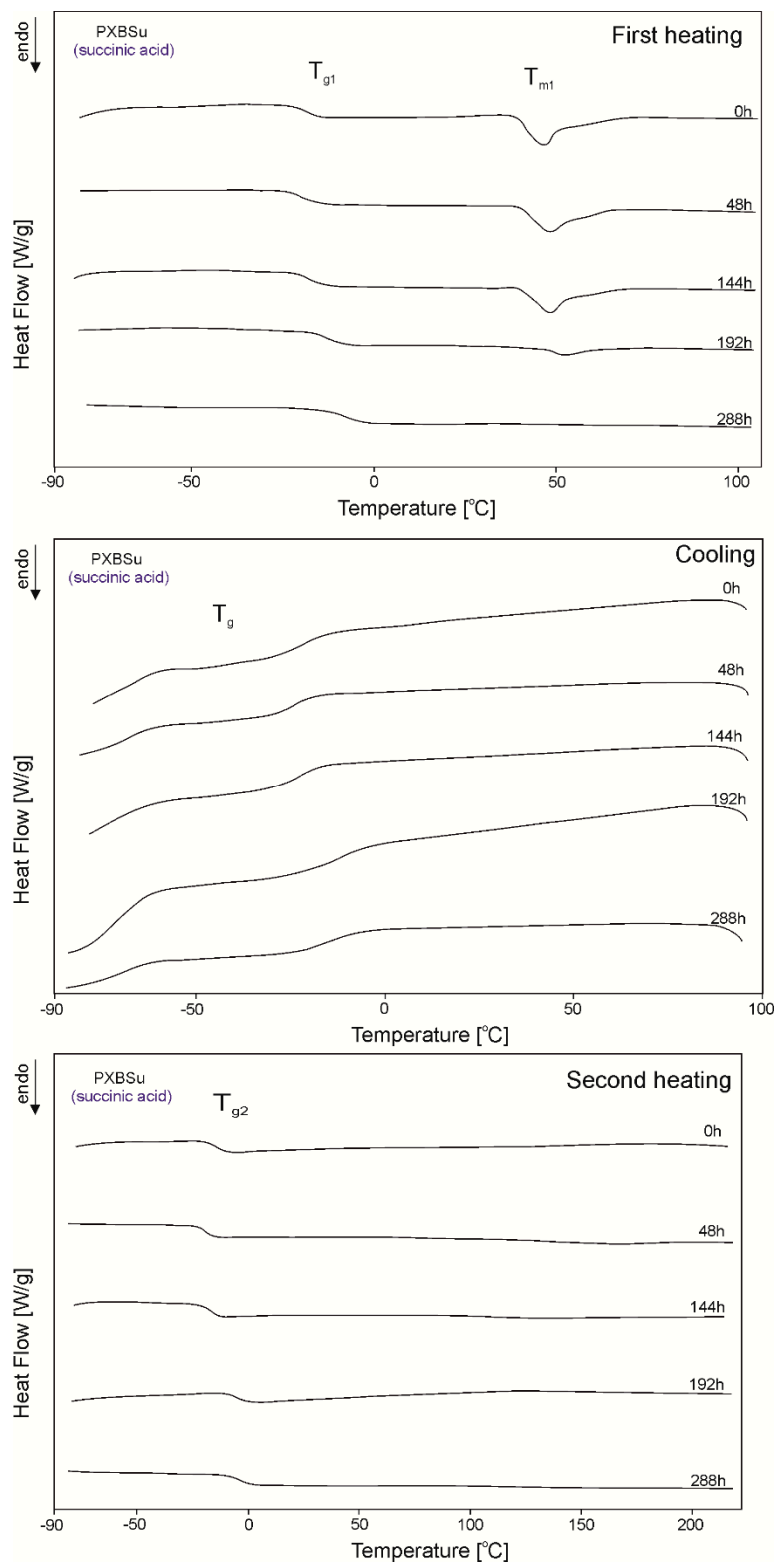


**Figure 5.** Differential scanning calorimetry (DSC) thermograms of PXBSu at the crosslinking stages subjected to first heating, second heating and cooling.
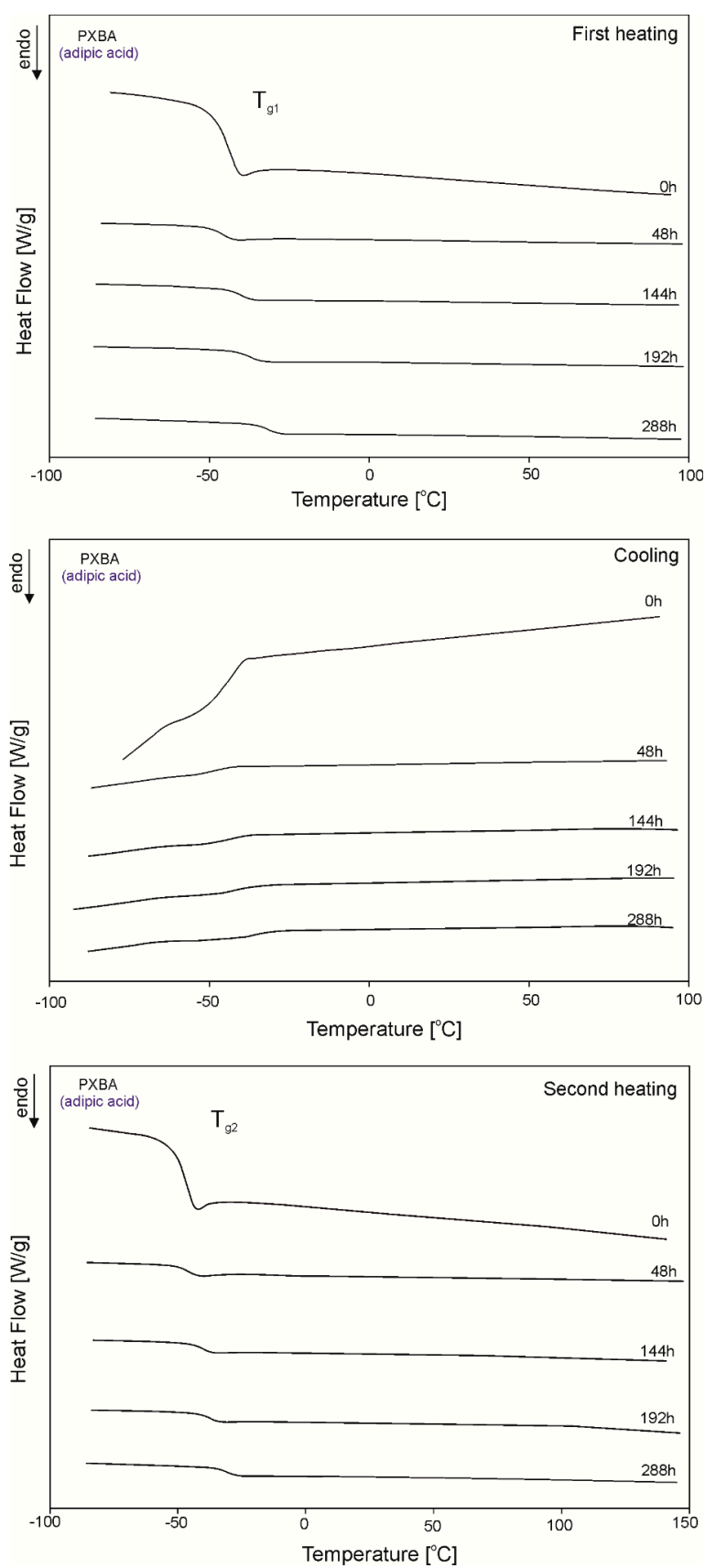
**Figure 6.** DSC thermograms of PXBA at the crosslinking stages subjected to first heating, second heating and cooling.
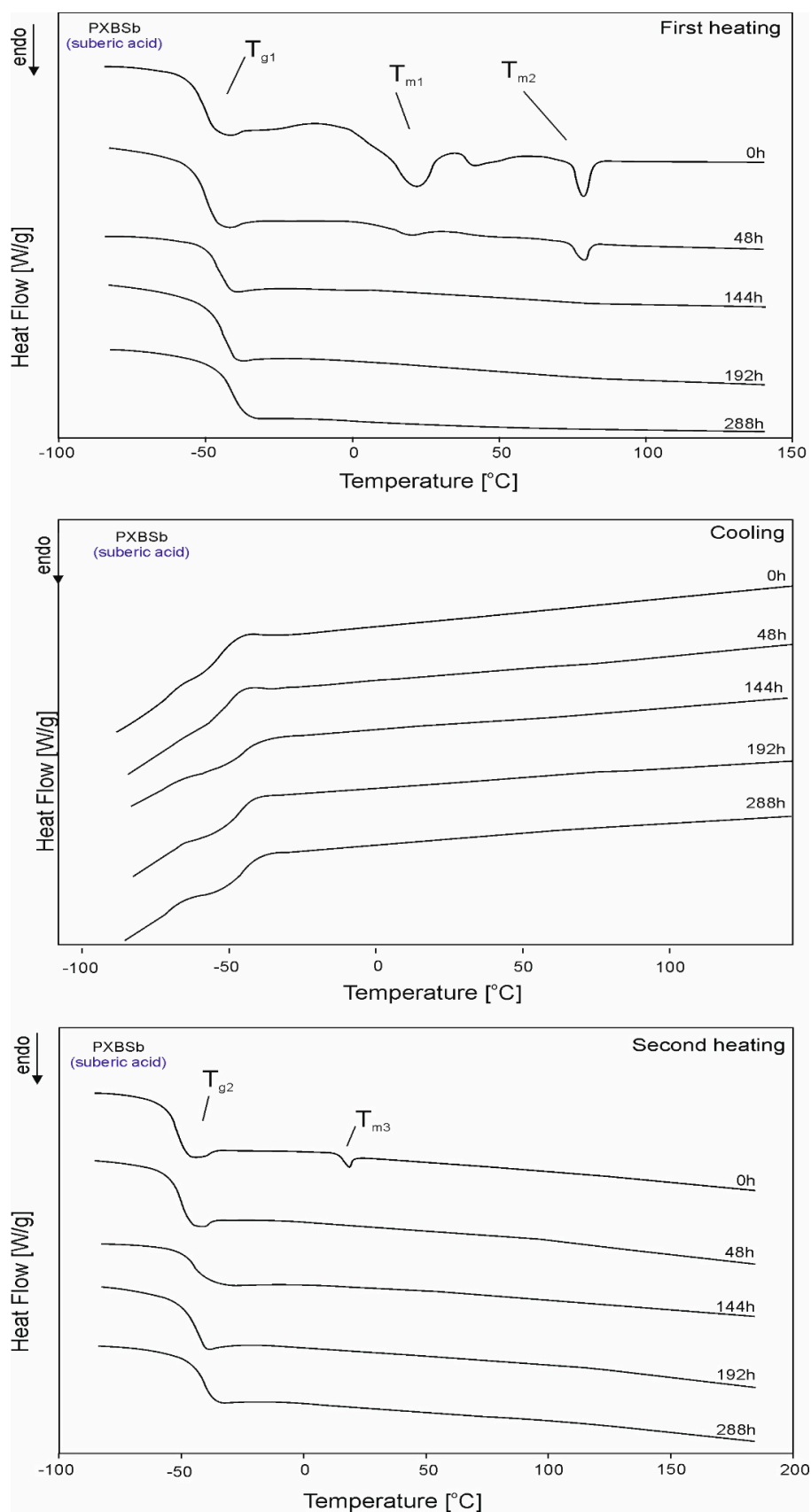
**Figure 7.** DSC thermograms of PXBSb at the crosslinking stages subjected to first heating, second heating and cooling.
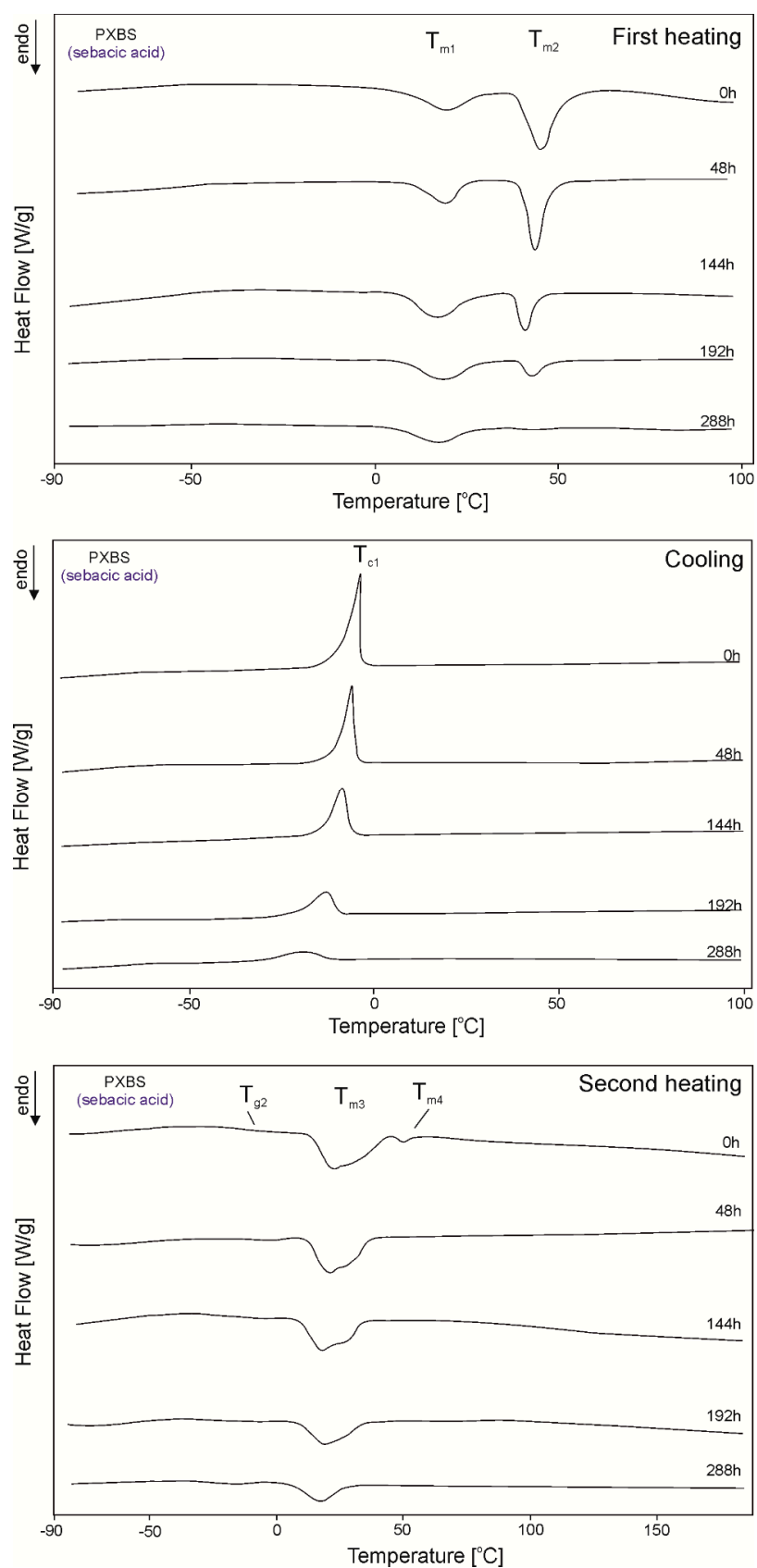
**Figure 8.** DSC thermograms of PXBS at the crosslinking stages subjected to first heating, second heating and cooling.
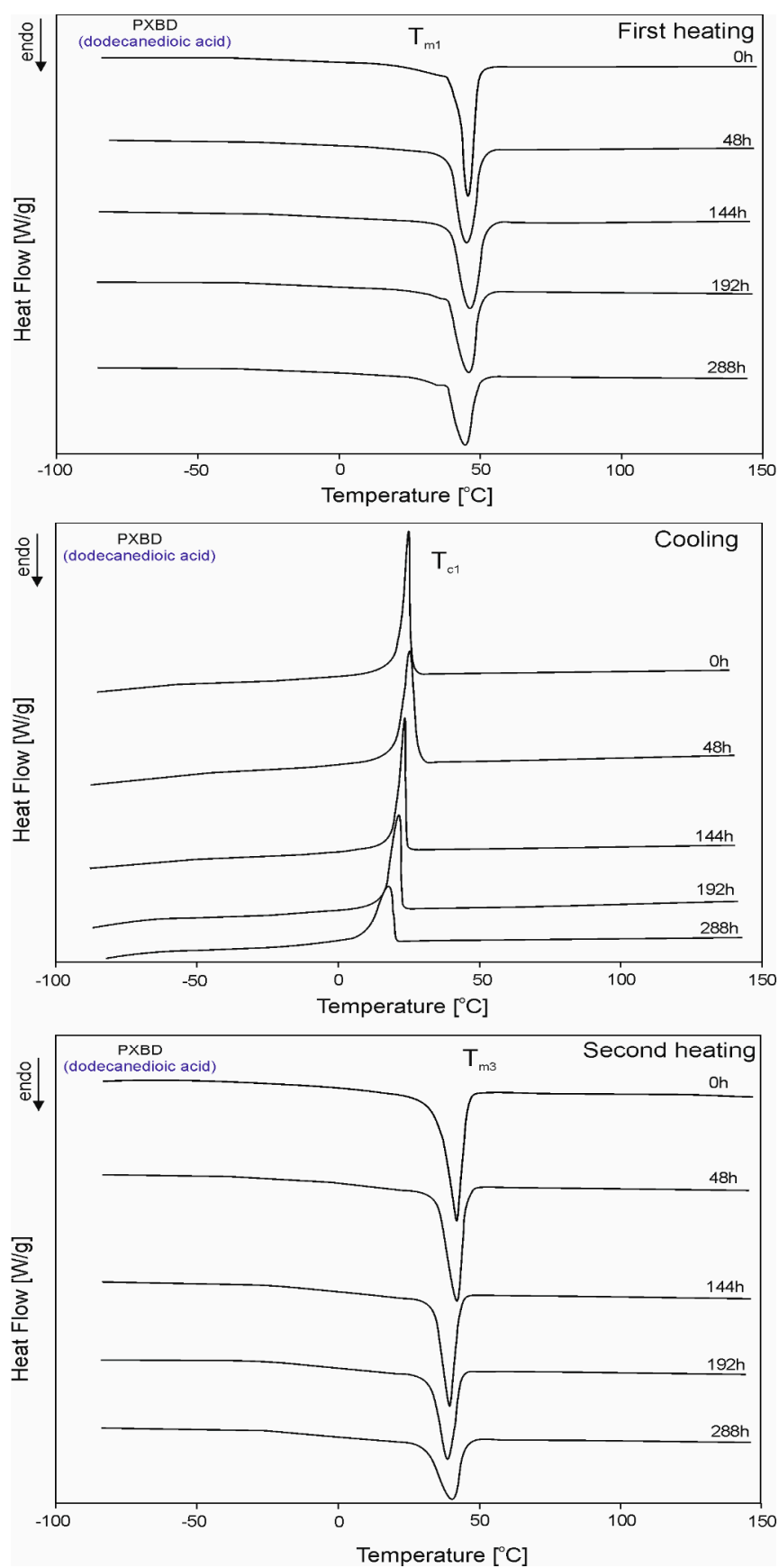
**Figure 9.** DSC thermograms of PXBD at the crosslinking stages subjected to first heating, second heating and cooling.

**Table 2.** Thermal properties of the PXBSu, PXBA, PXBSb, PXBS, PXBD.

| Cross–Linking Time | First Heating | | | | | | Cooling | | Second Heating | | | | | |
| | $T_{g1}$ [°C] | $\Delta c_p$ [J/g°C] | $T_{m1}$ [°C] | $\Delta H_{m1}$ [J/g] | $T_{m2}$ [°C] | $\Delta H_{m2}$ [J/g] | $T_{c1}$ [°C] | $\Delta H_{c1}$ [J/g] | $T_{g2}$ [°C] | $\Delta c_p$ [J/g°C] | $T_{m3}$ [°C] | $\Delta H_{m3}$ [J/g] | $T_{m4}$ [°C] | $\Delta H_{m4}$ [J/g] |
|---|---|---|---|---|---|---|---|---|---|---|---|---|---|---|
| *PXBSu (succinic acid)* | | | | | | | | | | | | | | |
| 0 h | −19.9 | 0.522 | 46.8 | 15.41 | - | - | −26.4 | 0.84 | −15.7 | 0.57 | - | - | - | - |
| 48 h | −18.6 | 0.533 | 48.4 | 13.92 | -. | - | −24.8 | 0.542 | −18.8 | 0.651 | - | - | - | - |
| 144 h | −17.6 | 0.596 | 48.5 | 12.32 | - | -. | −22.5 | 0.668 | −17.5 | 0.719 | - | - | - | - |
| 192 h | −12.2 | 0.449 | 50.9 | 7.77 | -. | - | −18.9 | 0.897 | −5.2 | 0.475 | - | - | - | - |
| 288 h | −7 | 0.572 | n.o. | n.o. | - | - | −18.6 | 0.624 | −2.8 | 0.543 | - | - | - | - |
| *PXBA (adipic acid)* | | | | | | | | | | | | | | |
| 0 h | −46.3 | 0.983 | - | - | - | - | - | - | −44.6 | 0.975 | - | - | - | - |
| 48 h | −45.6 | 0.705 | - | - | - | - | - | - | −44.9 | 0.709 | - | - | - | - |
| 144 h | −40.3 | 0.677 | - | - | - | - | - | - | −40.4 | 0.690 | - | - | - | - |
| 192 h | −37.5 | 0.652 | - | - | - | - | - | - | −37.6 | 0.648 | - | - | - | - |
| 288 h | −30.9 | 0.592 | - | - | - | - | - | - | −30.6 | 0.557 | - | - | - | - |
| *PXBSb (suberic acid)* | | | | | | | | | | | | | | |
| 0 h | −50.8 | 0.676 | 20.4 | 7.32 | 78.8 | 2.41 | - | - | −52.7 | 0.738 | 18.7 | 0.65 | - | - |
| 48 h | −50.1 | 0.740 | 19.3 | 0.95 | 78.9 | 1.13 | - | - | −50.4 | 0.757 | - | - | - | - |
| 144 h | −45.9 | 0.553 | - | - | - | - | - | - | −44.2 | 0.526 | - | - | - | - |
| 192 h | −44.6 | 0.670 | - | - | - | - | - | - | −46.1 | 0.642 | - | - | - | - |
| 288 h | −41.6 | 0.624 | - | - | - | - | - | - | −41.4 | 0.656 | - | - | - | - |
| *PXBS (sebacic acid)* | | | | | | | | | | | | | | |
| 0 h | - | - | 19 | 24.17 | 44.9 | 50.89 | −3.9 | 65.87 | −13.1 | 0.558 | 22.6 | 61.3 | 50.7 | 3.17 |
| 48 h | - | - | 19.5 | 23.28 | 43.5 | 41.56 | −6.3 | 47.16 | −12.8 | 0.128 | 21.1 | 53.15 | - | - |
| 144 h | - | - | 17.2 | 34.1 | 41 | 18.18 | −8.8 | 42.77 | −19.3 | 0.426 | 18.3 | 48.41 | - | - |
| 192 h | - | - | 18.9 | 28.67 | 42.9 | 9.76 | −13.3 | 30.3 | −20.5 | 0.264 | 19.9 | 35.52 | - | - |
| 288 h | - | - | 17.5 | 24.01 | 41.2 | 0.66 | −19 | 15.87 | −28 | 0.248 | 17.6 | 23.18 | - | - |
| *PXBD (dodecanedioic acid)* | | | | | | | | | | | | | | |
| 0 h | - | - | 45.6 | 83.43 | - | - | 24.8 | 65.43 | - | - | 41.8 | 74.92 | - | - |
| 48 h | - | - | 44.2 | 80.80 | - | - | 25.3 | 72.71 | - | - | 41.9 | 65.60 | - | - |
| 144 h | - | - | 46.3 | 75.23 | - | - | 23.5 | 55.16 | - | - | 38.2 | 54.83 | - | - |
| 192 h | - | - | 45.6 | 67.79 | - | - | 21.5 | 52.23 | - | - | 38.7 | 51.73 | - | - |
| 288 h | - | - | 44.7 | 57.92 | - | - | 17.6 | 44.35 | - | - | 40.4 | 40.92 | - | - |

$T_{g1}$ and $T_{g2}$—glass transition temperatures; $\Delta c_p$—change in the heat capacity during glass transition at $T_{g1}$ and $T_{g2}$; $T_{m1}$, $T_{m2}$, $T_{m3}$ and $T_{m4}$—melting temperature; $T_{c1}$—crystallization temperatures; $\Delta H_{m1}$, $\Delta H_{m2}$, $\Delta H_{m3}$ and $\Delta H_{m4}$—heat of melting at $T_{m1}$, $T_{m2}$, $T_{m3}$ and $T_{m4}$; $\Delta H_{c1}$—crystallization heat in $T_{c1}$.

A glass transition is observed for all polymers except PXBD. With cross-linking progress, the glass transition temperature ($T_g$) increases, and the value of the change in heat capacity ($\Delta C_p$) during the glass transition decreases with the progress of the cross-linking process due to lower chain mobility, which confirms that cross-linking is indeed taking place. A melting transition is observed for all polymers except for PXBA, and its enthalpy decreases with the progress of the cross-linking process and the transition of the polymer structure into an amorphous system. Polymers with longer dicarboxylic acid chains have increased crystallinity, which is confirmed by the presence of two melting transitions with higher melting enthalpy (PXBSb and PXBS), and the much higher melting enthalpy exhibited by the PXBD polymer. Those results showing an increase in crystallinity also correlate with gel fraction test results. Two melting transitions displayed by PXBA and PXBSb are due to the melting of the poly(xylitol-dicarboxylate) block ($T_{m1}$) and poly(butylene-dicarboxylate) block ($T_{m2}$). A crystallization transition is only observable for two polymers with the longest dicarboxylic acid chains, and the highest crystallinity—PXBS and PXBD. The melting and crystallization transition being observable only for polymers based on dicarboxylic acids with the highest chain lengths is due to the crystalline structure becoming more ordered. PXBD is highly crystalline and it was not possible to determine the glass transition.

### 3.4. Gel Fraction

Gel fraction (Figure 10) decreases with the length of the dicarboxylic acid chains due to the higher polymer crystallinity. The highest value is observed for the PXBSu polymer, and the lowest value is exhibited by the PXBD polymer. The gel fraction value increases at consecutive stages of the cross-linking process and the results correspond well to FTIR and DSC results.
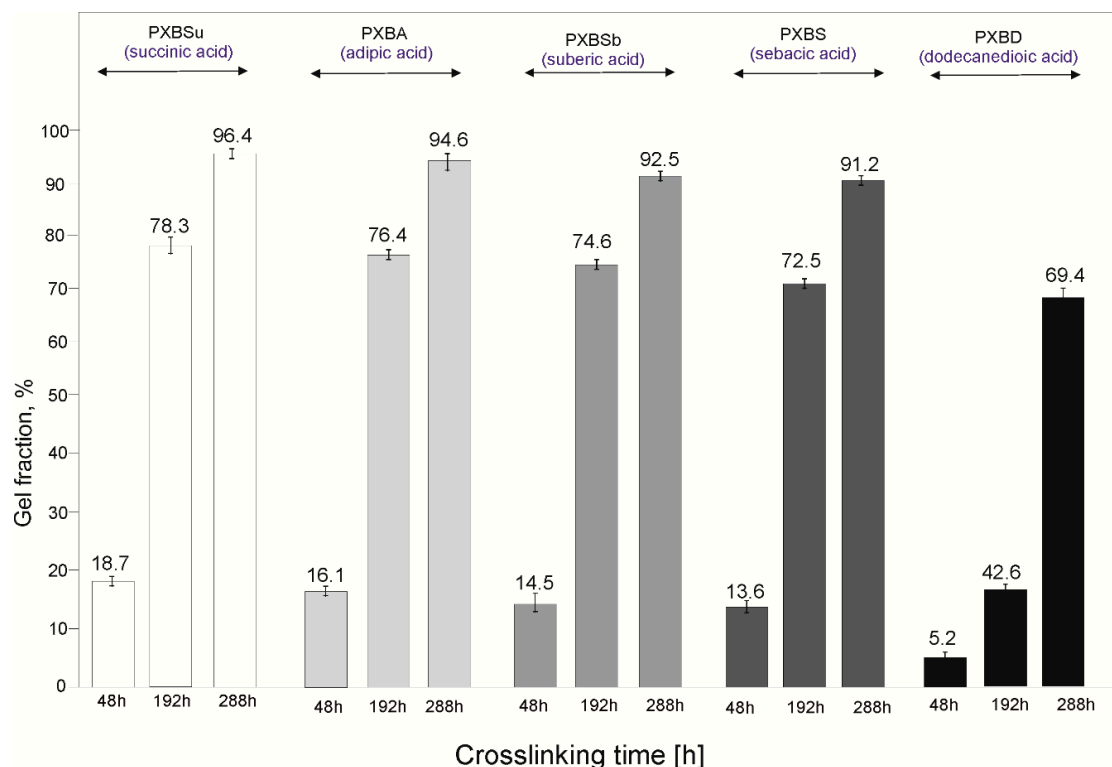


**Figure 10.** Gel fraction results for PXBSu, PXBA, PXBSb, PXBS and PXBD polymers.

### 3.5. Mechanical Properties

Fully cross-linked materials (after 288h of cross-linking), before and after 8 days of degradation, were tested (Figure 11). The highest stress at break was exhibited by materials based on the longest dicarboxylic acids. The lowest stress at break was exhibited by PXBA and PXBSb materials. An interesting characteristic of all polymers is the increase in the value of elongation at break and stress at break for materials after 8 days of degradation, which is speculated to be due to the stabilization of the amorphous structure. PXBD is characterized by the highest stress at break and lowest elongation at break, due to its very high crystallinity, confirmed by both DSC and gel fraction analysis. Such a material no longer exhibits properties characteristic of elastomers.
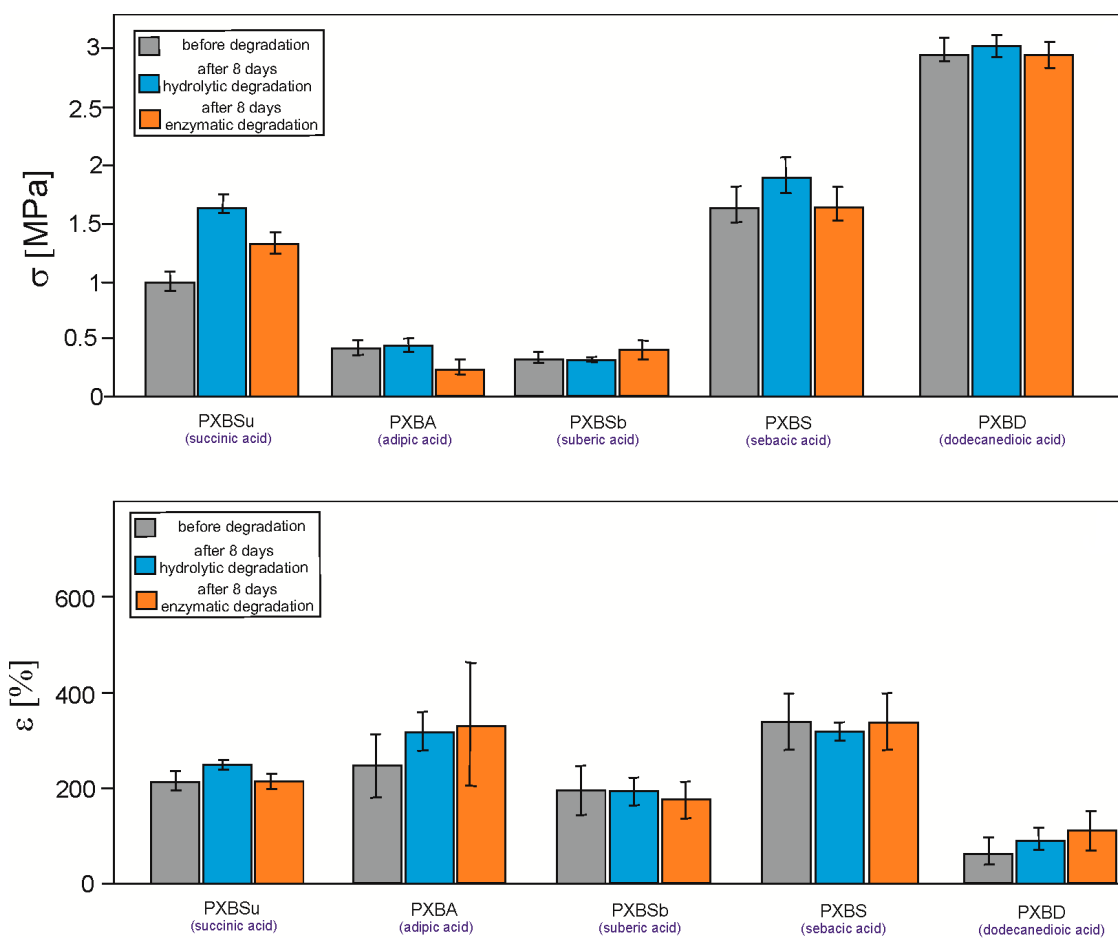
**Figure 11.** Mechanical properties of PXBSu, PXBA, PXBSb, PXBS and PXBD polymers.

## 3.6. Hydrolytic and Enzymatic Degradation

All the materials are biodegradable both enzymatically and hydrolytically (Figure 12). With the increase in the dicarboxylic chain length, the susceptibility to degradation decreases due to the higher crystallinity of the polymers. Higher crystallinity was confirmed by the DSC and gel fraction analysis. The polymers are more susceptible to enzymatic than hydrolytic degradation.
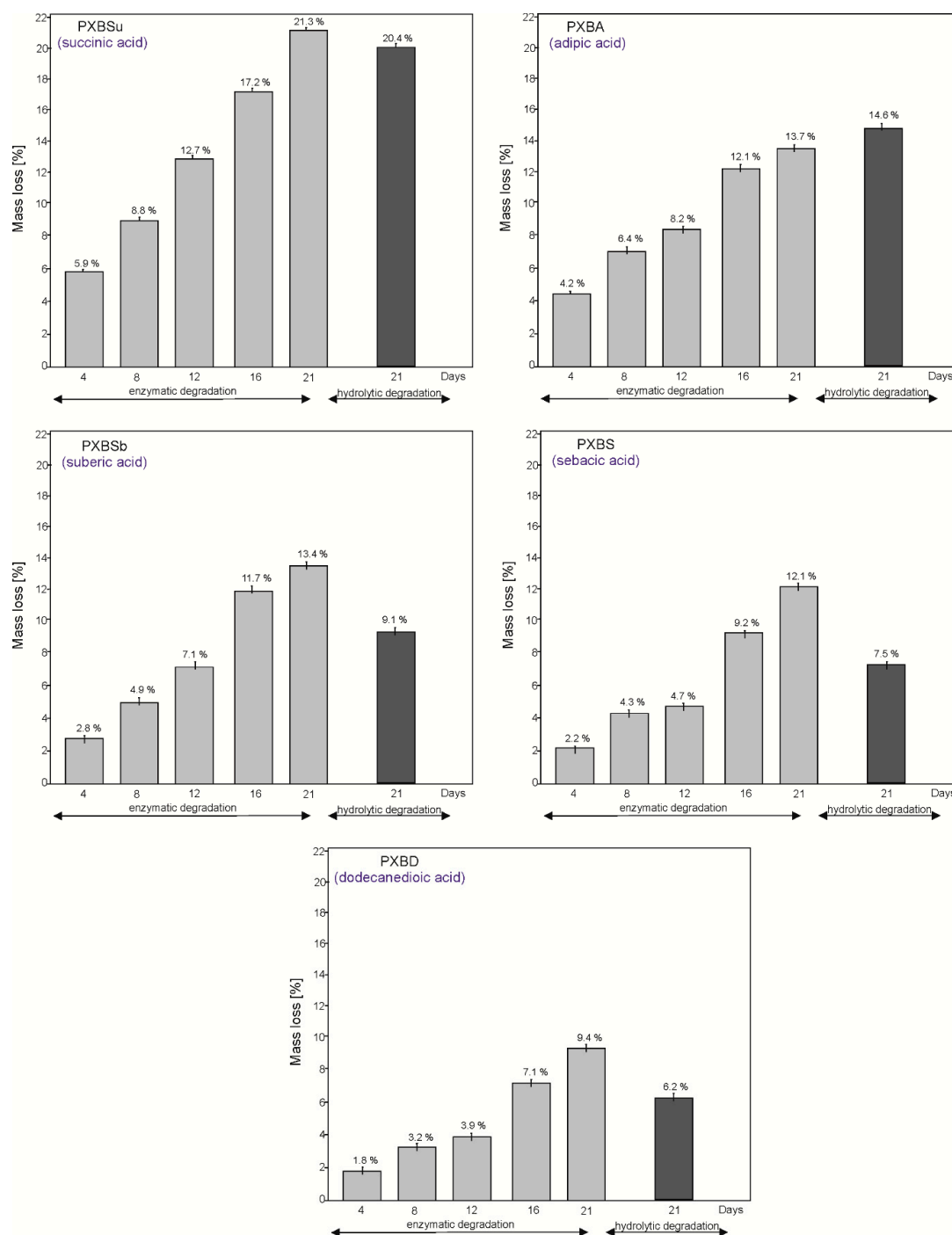
**Figure 12.** Hydrolytic and enzymatic degradation of PXBSu, PXBA, PXBSb, PXBS and PXBD polymers.

## 4. Conclusions

In this paper, poly(xylitol dicarboxylate-co-butylene dicarboxylate) materials based on dicarboxylic acids with different, even-numbered chain lengths are described. All the materials except PXBD have properties typical for elastomers. Successful synthesis was confirmed by both ^{1}H NMR, ^{13}C NMR and FTIR analyses. By performing gel fraction tests and DSC analysis, the best cross-linking time was determined to be 288h. The progress of cross-linking at different stages was confirmed by the increase in the gel fraction value, the decrease in melting enthalpies and the decrease in peak intensities related to –OH groups, as well as the increase in peak intensities linked to –C–O–C groups as determined by FTIR. Degradation times and mechanical properties can be tailored for specific applications by using

different dicarboxylic acids. With respect to tailoring the properties, it is better to change the acid chain length than the hydroxyl group content [23], since a change in properties obtained by changing the acid chain length is much more predictable. Possible future research could include the synthesis of an even wider variety of alditol-based polyesters with either different glycols or odd-numbered dicarboxylic acids.

**Author Contributions:** Conceptualization, K.B.; Formal analysis, M.P.-H. and T.J.I.; Investigation, J.G.S.; Methodology, M.P.-H., P.S., K.B., J.P., A.K., J.G.S. and T.J.I.; Project administration, M.P.-H.; Writing – original draft, M.P.-H., K.B., J.P., A.K. and T.J.I. All authors have read and agreed to the published version of the manuscript.

**Conflicts of Interest:** The authors declare no conflicts of interest.

## References

1. Bruggeman, J.P.; Bettinger, C.J.; Nijst, C.L.E.; Kohane, D.S.; Langer, R. Biodegradable xylitol-based polymers. *Adv. Mater.* **2008**, *20*, 1922–1927. [CrossRef]

2. Bruggeman, J.P.; Bettinger, C.J.; Langer, R. Biodegradable xylitol-based elastomers: In vivo behavior and biocompatibility. *J. Biomed. Mater. Res. Part A* **2010**, *95*, 92–104. [CrossRef] [PubMed]

3. Bruggeman, J.P.; de Bruin, B.J.; Bettinger, C.J.; Langer, R. Biodegradable poly(polyol sebacate) polymers. *Biomaterials* **2008**, *29*, 4726–4735. [CrossRef] [PubMed]

4. Barrett, D.G.; Luo, W.; Yousaf, M.N. Aliphatic polyester elastomers derived from erythritol and $\alpha,\omega$-diacids. *Polym. Chem.* **2010**, *1*, 296–302. [CrossRef]

5. Dasgupta, Q.; Chatterjee, K.; Madras, G. Combinatorial approach to develop tailored biodegradable poly(xylitol dicarboxylate) polyesters. *Biomacromolecules* **2014**, *15*, 4302–4313. [CrossRef]

6. Ning, Z.Y.; Zhang, Q.S.; Wu, Q.P.; Li, Y.Z.; Ma, D.X.; Chen, J.Z. Efficient synthesis of hydroxyl functioned polyesters from natural polyols and sebacic acid. *Chin. Chem. Lett.* **2011**, *22*, 635–638. [CrossRef]

7. Kavimani, V.; Jaisankar, V. Synthesis and Characterisation of Sorbitol Based Copolyesters for Biomedical Applications. *J. Phys. Sci. Appl.* **2014**, *4*, 507–515.

8. Hu, J.; Gao, W.; Kulshrestha, A.; Gross, R.A. "Sweet polyesters": Lipase-catalyzed condensation-polymerizations of alditols. *ACS Symp. Ser.* **2006**, *999*, 275–284.

9. Kumar, A.; Kulshrestha, A.S.; Gao, W.; Gross, R.A. Versatile route to polyol polyesters by lipase catalysis. *Macromolecules* **2003**, *36*, 8219–8221. [CrossRef]

10. Zaky, S.H.; Lee, K.W.; Gao, J.; Jensen, A.; Verdelis, K.; Wang, Y.; Almarza, A.J.; Sfeir, C. Poly (glycerol sebacate) elastomer supports bone regeneration by its mechanical properties being closer to osteoid tissue rather than to mature bone. *Acta Biomater.* **2017**, *54*, 95–106. [CrossRef]

11. Zaky, S.H.; Lee, K.W.; Gao, J.; Jensen, A.; Close, J.; Wang, Y.; Almarza, A.J.; Sfeir, C. Poly(Glycerol Sebacate) elastomer: A novel material for mechanically loaded bone regeneration. *Tissue Eng. Part A* **2014**, *20*, 45–53. [CrossRef] [PubMed]

12. Chen, Q.Z.; Bismarck, A.; Hansen, U.; Junaid, S.; Tran, M.Q.; Harding, S.E.; Ali, N.N.; Boccaccini, A.R. Characterisation of a soft elastomer poly(glycerol sebacate) designed to match the mechanical properties of myocardial tissue. *Biomaterials* **2008**, *29*, 47–57. [CrossRef] [PubMed]

13. Neeley, W.L.; Redenti, S.; Klassen, H.; Tao, S.; Desai, T.; Young, M.J.; Langer, R. A microfabricated scaffold for retinal progenitor cell grafting. *Biomaterials* **2008**, *29*, 418–426. [CrossRef] [PubMed]

14. Motlagh, D.; Yang, J.; Lui, K.Y.; Webb, A.R.; Ameer, G.A. Hemocompatibility evaluation of poly(glycerol-sebacate) in vitro for vascular tissue engineering. *Biomaterials* **2006**, *27*, 4315–4324. [CrossRef]

15. Sundback, C.A.; Shyu, J.Y.; Wang, Y.; Faquin, W.C.; Langer, R.S.; Vacanti, J.P.; Hadlock, T.A. Biocompatibility analysis of poly(glycerol sebacate) as a nerve guide material. *Biomaterials* **2005**, *26*, 5454–5464. [CrossRef]

16. Kemppainen, J.M.; Hollister, S.J. Tailoring the mechanical properties of 3D-designed poly(glycerol sebacate) scaffolds for cartilage applications. *J. Biomed. Mater. Res. Part A* **2010**, *94*, 9–18. [CrossRef] [PubMed]

17. Sun, Z.J.; Chen, C.; Sun, M.Z.; Ai, C.H.; Lu, X.L.; Zheng, Y.F.; Yang, B.F.; Dong, D.L. The application of poly (glycerol-sebacate) as biodegradable drug carrier. *Biomaterials* **2009**, *30*, 5209–5214. [CrossRef] [PubMed]

18. Selvam, S.; Pithapuram, M.V.; Victor, S.P.; Muthu, J. Injectable in situ forming xylitol-PEG-based hydrogels for cell encapsulation and delivery. *Colloids Surfaces B Biointerfaces* **2015**, *126*, 35–43. [CrossRef] [PubMed]

19. Li, Y.; Thouas, G.A.; Chen, Q. Novel elastomeric fibrous networks produced from poly(xylitol sebacate)2:5 by core/shell electrospinning: Fabrication and mechanical properties. *J. Mech. Behav. Biomed. Mater.* **2014**, *40*, 210–221. [CrossRef]

20. Li, Y.; Chen, Q.Z. Fabrication of mechanically tissue-like fibrous poly(xylitol sebacate) using core/shell electrospinning technique. *Adv. Eng. Mater.* **2015**, *17*, 324–329. [CrossRef]

21. Piątek-Hnat, M.; Bomba, K.; Pęksiński, J. Synthesis and selected properties of ester elastomer containing sorbitol. *Appl. Sci.* **2020**, *10*, 1628. [CrossRef]

22. Piatek-Hnat, M.; Bomba, K.; Pęksiński, J. Structure and Properties of Biodegradable Poly (Xylitol Sebacate-Co-Butylene Sebacate) Copolyester. *Molecules* **2020**, *25*, 1541. [CrossRef] [PubMed]

23. Piątek-Hnat, M.; Bomba, K.; Pęksiński, J.; Kozłowska, A.; Sośnicki, J.G.; Idzik, T.J. Effect of E-Beam Irradiation on Thermal and Mechanical Properties of Ester Elastomers Containing Multifunctional Alcohols. *Polymers* **2020**, *12*, 1043. [CrossRef] [PubMed]

24. Piątek-Hnat, M.; Bomba, K. The influence of of cross-linking process on the physicochemical properties of new copolyesters containing xylitol. *Mater. Today Commun.* **2020**, *25*, 1541. [CrossRef]

# Physical Effects of Radiation Modification of Biodegradable Xylitol-Based Materials Synthesized Using a Combination of Different Monomers

**Marta Piątek-Hnat [1,*]**, **Kuba Bomba [1]**, **Janusz P. Kowalski-Stankiewicz [2]**, **Jakub Pęksiński [3]**, **Agnieszka Kozłowska [1]**, **Jacek G. Sośnicki [4]**, **Tomasz J. Idzik [4]**, **Beata Schmidt [5]**, **Krzysztof Kowalczyk [5]**, **Marta Walo [6]** and **Agnieszka Kochmańska [7]**

1    Faculty of Chemical Technology and Engineering, West Pomeranian University of Technology, 71-065 Szczecin, Poland; bk34688@zut.edu.pl (K.B.); agak@zut.edu.pl (A.K.)
2    Department of Computer Sciences in Medicine & Education Quality Evaluation, Pomeranian Medical University in Szczecin, 70-204 Szczecin, Poland; janus@pum.edu.pl
3    Faculty of Electrical Engineering, West Pomeranian University of Technology, 71-313 Szczecin, Poland; jakub.peksinski@zut.edu.pl
4    Department of Organic and Physical Chemistry, Faculty of Chemical Technology and Engineering, West Pomeranian University of Technology, 71-065 Szczecin, Poland; jacek.sosnicki@zut.edu.pl (J.G.S.); tomasz.idzik@zut.edu.pl (T.J.I.)
5    Department of Chemical Organic Technology and Polymeric Materials, Faculty of Chemical Technology and Engineering, West Pomeranian University of Technology, 71-065 Szczecin, Poland; Beata.Schmidt@zut.edu.pl (B.S.); Krzysztof.Kowalczyk@zut.edu.pl (K.K.)
6    Laboratory for Measurements of Technological Doses, Institute of Nuclear Chemistry and Technology, 03-195 Warszawa, Poland; M.Walo@ichtj.waw.pl
7    Department of Materials Technology, West Pomeranian University of Technology, 70-310 Szczecin, Poland; akochmanska@zut.edu.pl
*    Correspondence: marp@zut.edu.pl

**Abstract:** There is a possibility of obtaining xylitol-based elastomers sharing common characteristics of biodegradability, thermal stability, and elastomeric behavior by using monomers with different chain-lengths. Therefore, we have synthesized eight elastomers using a combination of four different diols (ethanediol, 1.3-propanediol, 1.4-buanediol, and 1.5-pentanediol) and two different dicarboxylic acids (succinic acid and adipic acid). The obtained materials were further modified by performing e-beam treatment with a dose of 100 kGy. Materials both before and after radiation modification were tested by DSC, DMTA, TGA, tensile tests, gel fraction determination, hydrolytic and enzymatic degradation tests, $^1$H NMR and $^{13}$C NMR and FTIR.

**Keywords:** radiation modification; e-beam; xylitol; biodegradable elastomers; mechanical and thermal properties

## 1. Introduction

Recent trends in commodity elastomers have focused on obtaining biodegradable materials and, at least partially, monomers from renewable sources. An example of one of these monomers is sugar alcohols.

Elastomers based on sugar alcohols can be divided into two main groups: (1) poly (polyol dicarboxylates) [1–3], with the most notable examples being poly(glycerol sebacate) (PGS) [4–8] and poly (xylitol sebacate) [9–12]; and (2) poly (polyol dicarboxylates-co-diol-dicarboxylates) [13–20].

An important advantage of sugar-alcohol-based polyesters is the possibility to tailor their properties (such as degradation time, glass transition temperature, elongation, and stress at break) for a specific application while retaining their core characteristics of biodegradability, thermal stability, and elastomeric behavior. A number of approaches

can be utilized to do so. There are five options regarding poly (polyol dicarboxylates): (1) carrying out the synthesis using the same dicarboxylic acids but different polyols [1,2]; (2) performing the synthesis using the same polyol but different dicarboxylic acids [3,21]; (3) conducting the synthesis using the same monomers but with different stoichiometric ratios [1,12]; (4) copolymerization of those homopolymers [22]; and (5) finally performing the syntheses with different reaction temperatures [4].

In the case of poly (polyol dicarboxylate-co-diol-dicarboxylates), fine-tuning the characteristics can be done by changing the polyol used in the synthesis [13,15,16], utilizing different dicarboxylic acids [18] or different diols [14], and by changing the polycondensation duration [19]. The range of attainable properties widens even further when taking into consideration the possibility of modifying those elastomers with different doses of e-beam radiation [15,16].

Research into e-beam radiation modification of biodegradable polyesters is fairly limited, with poly (lactic acid) [23–25] and polycaprolactone [26,27] being the most intensely investigated materials, and other research including poly(butylene succinate) [28], bacterial polyesters-poly (hydroxyalkanoate) [29], and poly-(R)-3-hydroxybutyrate [30].

Regarding the lack of scientific data on radiation modification of biodegradable polyesters, continued research in this field is important. Due to the fact that sugar-alcohol-based elastomers are well-suited for such modification, we decided to study a range of those materials, most of which, to the best of our knowledge, have never been synthesized and radiation modified before. We obtained eight elastomers based on xylitol, two different dicarboxylic acids, and four different diols. Compared to our previous papers [15–20], the synthesis method was modified as compared to our previous papers [15–20], allowing us to apply a crosslinking time from 12 days to 48 h on average. Moreover, a 100 kGy dose of radiation was chosen based on our previous research [15,16].

## 2. Materials and Methods

### 2.1. Synthesis of Elastomers

All chemicals were purchased from Sigma-Aldrich (St. Louis, MO, USA). In this study, eight poly (xylitol dicarboxylate-diol dicarboxylate) elastomers were synthesized.

Poly (xylitol succinate-co ethylene succinate) (PXESu) was synthesized using xylitol, succinic acid, and ethanediol. Poly (xylitol succinate-co-propylene succinate) (PXPSu) was synthesized using xylitol, succinic acid, and 1.3-propanediol. Poly (xylitol succinate-co-butylene succinate) (PXBSu) was synthesized using xylitol, succinic acid, and 1.4-butanediol. Poly (xylitol succinate-co-pentylene succinate) (PXPeSu) was synthesized using xylitol, succinic acid, and 1.5-pentanediol.

Poly (xylitol adipate-co-ethylene adipate) (PXEA) was synthesized using xylitol, adipic acid, and ethanodiol. Poly (xylitol adipate-co-propylene adipate) (PXPA) was synthesized using xylitol, adipic acid, and 1.3-propanediol. Poly (xylitol adipate-co-butylene adipate) (PXBA) was synthesized using xylitol, adipic acid, and 1.4-butanediol. Poly (xylitol adipate-co-pentylene adipate) (PXPeA) was synthesized using xylitol, adipic acid, and 1.5-pentanediol.

The synthesis process consists of three steps: (1) 9 h esterification reaction in 150 °C in nitrogen atmosphere in a vacuum evaporator; (2) 3 h polycondensation reaction in 150 °C in low-pressure-atmosphere in a vacuum evaporator; and (3) crosslinking reaction of materials cast into silicone forms at 150 °C in a low-pressure-atmosphere in a vacuum dryer.

Samples obtained after polycondensation are called prepolymers which are then cured and crosslinked elastomers are obtained. Then, crosslinked elastomers are modified with e-beam.

The molar ratio of dicarboxylic acid:xylitol:diol was 2:1:1. No catalyst was used for the synthesis. The value of the vacuum applied was 100 mBar during both polycondensation and crosslinking.

## 2.2. Irradiation

After crosslinking, materials were e-beam irradiated in the Institute of Nuclear Chemistry and Technology (Warsaw). A linear electron accelerator Elektronika 10/10 (NPO Torij, Russia) was used to generate a 10 MeV at a 100 kGy dose. Radiation was split into 25 kGy doses. The average set current was 360 mA, and samples were moved with 0.368 m/min speed.

## 3. Experimental Methods

### 3.1. Nuclear Magnetic Resonance Spectroscopy (NMR)

$^1$H and $^{13}$C NMR spectroscopic measurements were performed on a Bruker DPX 400 AVANCE III HD spectrometer (Bruker, Rheinstetten, Germany), operating at 400.1 and 100.6 MHz, respectively. Approximately 50 mg of each sample was dissolved in 0.7 mL of deuterated chloroform ($CDCl_3$). TMS was used as an internal reference, and spectra were acquired in 5 mm probes. For NMR analyses, the MestReNova program (version 12.0.3, Mestrelab, Santiago de Compostela, Spain) was used.

### 3.2. Fourier Transform Infrared Spectroscopy (FTIR)

Analyses of the chemical structures of the polymers were conducted with Fourier transform infrared spectroscopy (FTIR). An Alpha Spectrometer Bruker (Bruker, Germany) was used. Recorded transmission spectra were in the range between 4000 cm$^{-1}$ and 400 cm$^{-1}$ with a resolution of 2 cm$^{-1}$. In order to develop the results, the Omnic 7.3 software by the Thermo Electron Corporation (Waltham, MA, USA) was used. Analyses were performed on the elastomers before and after irradiation.

### 3.3. Differential Scanning Calorimetry (DSC)

In order to determine the thermal properties of the materials, differential scanning calorimetry (DSC) was utilized. TA Instruments apparatus Q2500 (New Castle, DE, USA) was used. Parameters of the analysis were −100 to 100 °C heating cycle and 10 °C/min heating rate. Tests were performed in a nitrogen atmosphere. In order to develop the results, TA Instruments Universal Analysis 2000, 3.9a software (New Castle, DE, USA) was used. Tests were performed on elastomers before and after irradiation.

### 3.4. Dynamic Thermomechanical Analysis (DMTA)

In order to perform dynamic thermomechanical analysis, a DMA Q800 (TA Instruments, New Castle, DE, USA) was used. The temperature range was −100 to 100 °C with 1 Hz frequency. The heating rate was 2 °C/min. Analysis was carried out on nonmodified samples, and samples modified using 100 kGy. The TA Instruments Universal Analysis 2000, 3.9a software used to develop the test results.

### 3.5. Mechanical Properties

Testing of the mechanical properties was performed using Instron 36 instrument (Norwood, MA, USA). Parameters of the tests were 25 °C, 50% of relative humidity, 100 mm/min crosshead speed, and 500 N load cell. Tests were performed in keeping with PN-EN-ISO 526/1:1996 standard. Tests were performed on elastomers before and after irradiation.

### 3.6. Gel Fraction

Each crosslinked polymer sample (about 0.5g) was placed in a container and immersed in tetrahydrofuran for 5 days. Samples were then dried in a desiccator at lowered pressure for 14 days at 25 °C. The following formula was used to calculate the gel fraction content:

$$X = \frac{m_0}{m_1} \times 100\% \tag{1}$$

where $m_1$-mass of the sample after extraction and $m_0$-mass of the sample before extraction

### 3.7. Hydrolytic Degradation

In order to perform the hydrolytic degradation, 10 mm polymer discs were prepared. Samples were placed in a 48-well plate and sterilized with UV light for 20 min in a laminar chamber. After sterilization, each sample was covered with 1.5 mL of phosphate-buffered saline (PBS) (Sigma Aldrich, St. Louis, MO, USA) solution with a pH range of 7.1 to 7.2. The samples were kept at 37 °C for 21 days. Every two days, the samples were sterilized again, and the PBS solution was changed. The following formula was used to calculate mass loss after 21 days:

$$D = (m_0 - m_1)/m_0 \times 100\% \tag{2}$$

where $m_0$ is the mass of the sample before degradation, $m_1$ is the mass of the sample after degradation, and D is the mass loss.

### 3.8. Enzymatic Degradation

In order to perform the enzymatic degradation, 10 mm polymer discs were prepared. Samples were placed in a 48-well plate and sterilized with UV light for 20 min in a laminar chamber. After sterilization, each sample was covered with 1.5 mL of a solution of porcine lipase in PBS (Sigma Aldrich, Poznań, Poland) solution with pH range of 7.1 to 7.2. The samples were kept at 37 °C for 21 days. Every two days, the samples were sterilized again, and the lipase solution was changed. The following formula was used to calculate mass loss after 21 days:

$$D = (m_0 - m_1)/m_0 \times 100\% \tag{3}$$

where $m_0$ is the mass of the sample before degradation, $m_1$ is the mass of the sample after degradation, and D is the mass loss.

### 3.9. Thermogravimetric Analysis (TGA)

TGA analysis was performed to analyze the thermal stability of the elastomers. A Q500 TGA instrument (TA Instruments, New Castle, DE, USA), equipped with platinum crucibles, was used. A heating rate of 10 °C was utilized. The temperature range was 25 °C to 600 °C. The weight of the samples was ~15 mg. The test was conducted in dry air atmosphere.

Analyses were performed for nonirradiated, crosslinked elastomer samples which were taken directly after synthesis.

### 3.10. Gel Permeation Chromatography (GPC)

Determination of the molecular weights of the PGBS, PEBS, PXBS, PSBS, and PMBS prepolymers was conducted using gel permeation chromatography (GPC). Styragel column (Waters, Milford, MA, USA) was utilized. Samples were dissolved (1 mg/mL) in tetrahydrofuran (THF).

### 3.11. Scanning Electron Microscopy (SEM)

Field emission scanning electron microscopy (FE-SEM) analysis was carried out using the Hitachi SU-70 microscope (Tokyo, Japan). The samples were coated with palladium-gold alloy thin film using thermal evaporation the physical vapor deposition (PVD) method to provide electric conductivity using JEOL JEE 4x (Tokyo, Japan). SEM analyses were performed at an accelerating voltage of 1 kV, and secondary electron images were acquired.

## 4. Results and Discussion

The composition and properties of the elastomers are summarized in Table 1, and a synthesis scheme is shown in Figure 1.

**Table 1.** Composition and selected properties of poly (xylitol dicarboxylate-co-diol dicarboxylate) before and after irradiation.

| Material | MC | Stress at Break $\sigma_r$ [MPa] | Elongation at Break $\varepsilon$ [%] | Modulus at 50% Elongation E_50% [MPa] | $M_w$ (g/mol) | PDI |
|---|---|---|---|---|---|---|
| PXESu (x = 2, y = 2) | 1.21 | 6.60 +/− 0.88 | 283.2 +/− 17.23 | 0.97 +/− 0.20 | 34,000 | 2.5 |
| PXESu (radiation-modified) | - | 3.49 +/− 0.29 | 182.3 +/− 3.4 | 0.67 +/− 0.08 | | |
| PXPSu (x = 2, y = 3) | 0.28 | 2.72 +/− 0.36 | 233.7 +/− 11.01 | 0.44 +/− 0.05 | 20,000 | 1.6 |
| PXPSu (radiation-modified) | - | 1.99 +/− 0.13 | 213 +/− 14.4 | 1.37 +/− 0.5 | | |
| PXBSu (x = 2, y = 4) | 0.28 | 2.15 +/− 0.22 | 200.30 +/− 17.85 | 0.41 +/− 0.09 | 21,000 | 1.5 |
| PXBSu (radiation-modified) | - | 2.02 +/− 0.19 | 192 +/− 14.7 | 0.4 +/− 0.06 | | |
| PXPeSu (x = 2, y = 5) | 0.37 | 1.08 +/− 0.12 | 196.88 +/− 23.68 | 0.25 +/− 0.05 | 24,000 | 2.1 |
| PXPeSu (radiation-modified) | - | 1.57 +/− 0.39 | 218 +/− 11.25 | 0.278 +/− 0.09 | | |
| PXEA (x = 4, y = 2) | 1.21 | 0.98 +/− 0.18 | 84.41 +/− 7.05 | 0.72 +/− 0.18 | 36,000 | 2.4 |
| PXEA (radiation-modified) | - | 1.19 +/− 0.255 | 76.7 +/− 10.25 | 0.95 +/− 0.035 | | |
| PXPA (x = 4, y = 3) | 0.4 | 0.59 +/− 0.16 | 85.32 +/− 20.56 | 0.44 +/− 0.08 | 27,000 | 1.9 |
| PXPA (radiation-modified) | - | 0.96 +/− 0.14 | 103 +/− 10.7 | 0.54 +/− 0.05 | | |
| PXBA (x = 4, y = 4) | 0.2 | 0.59 +/− 0.08 | 82.08 +/− 4.48 | 0.47 +/− 0.03 | 22,000 | 1.4 |
| PXBA (radiation-modified) | - | 0.7 +/− 0.09 | 81.1 +/− 11 | 0.54 +/− 0.05 | | |
| PXPeA (x = 4, y = 5) | 0.26 | 0.67 +/− 0.6 | 85.74 +/− 10.46 | 0.50 +/− 0.06 | 21,000 | 1.5 |
| PXPeA (radiation-modified) | - | 0.67 +/− 0.17 | 73.21 +/− 7.12 | 0.61 +/− 0.05 | | |

Where $\sigma_r$: Stress at break; $\varepsilon$: Elongation at break, E_50%: Modulus at 50% elongation, E_100%; Modulus at 100% elongation; MC-Molar composition (ratio of poly(xylitol dicarboxylate) blocks to poly(diol dicarboxylate) blocks) determined by ^{1}H NMR for prepolymers, $M_w$-weight average molecular weight, and PDI-polydispersity index.
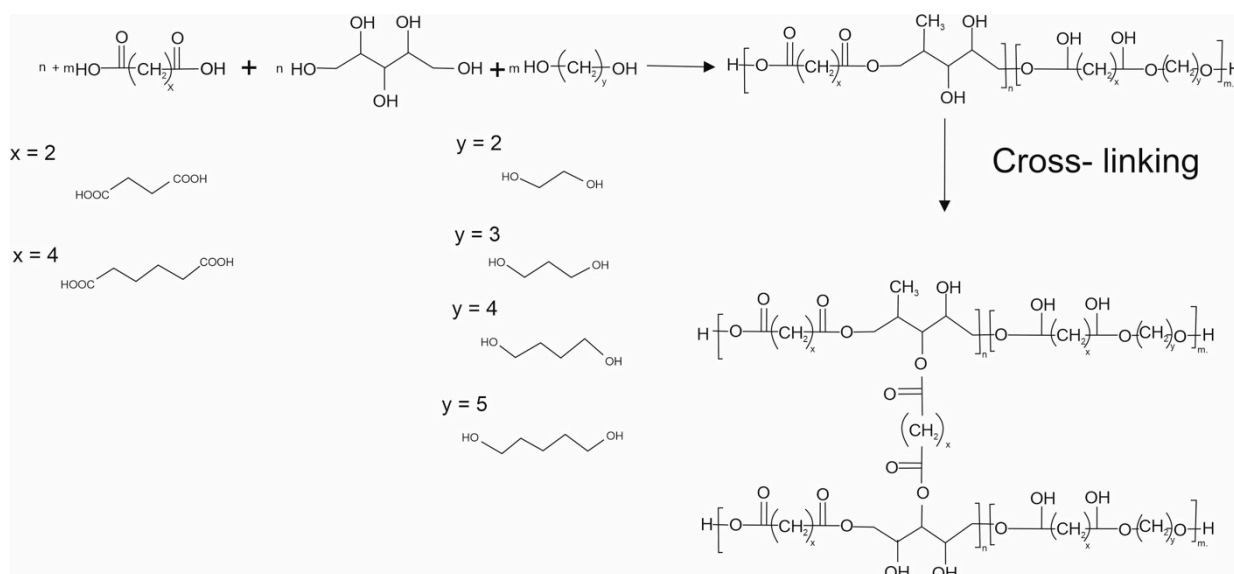


**Figure 1.** Scheme of the poly (xylitol dicarboxylate-co-diol dicarboxylate) synthesis.

*4.1. Nuclear Magnetic Resonance Spectroscopy (NMR)*

To determine the chemical structure of the obtained magnetic nuclear resonance spectroscopy, ^{1}H NMR and ^{13}C was carried out. The results are presented in Figures 2–5.
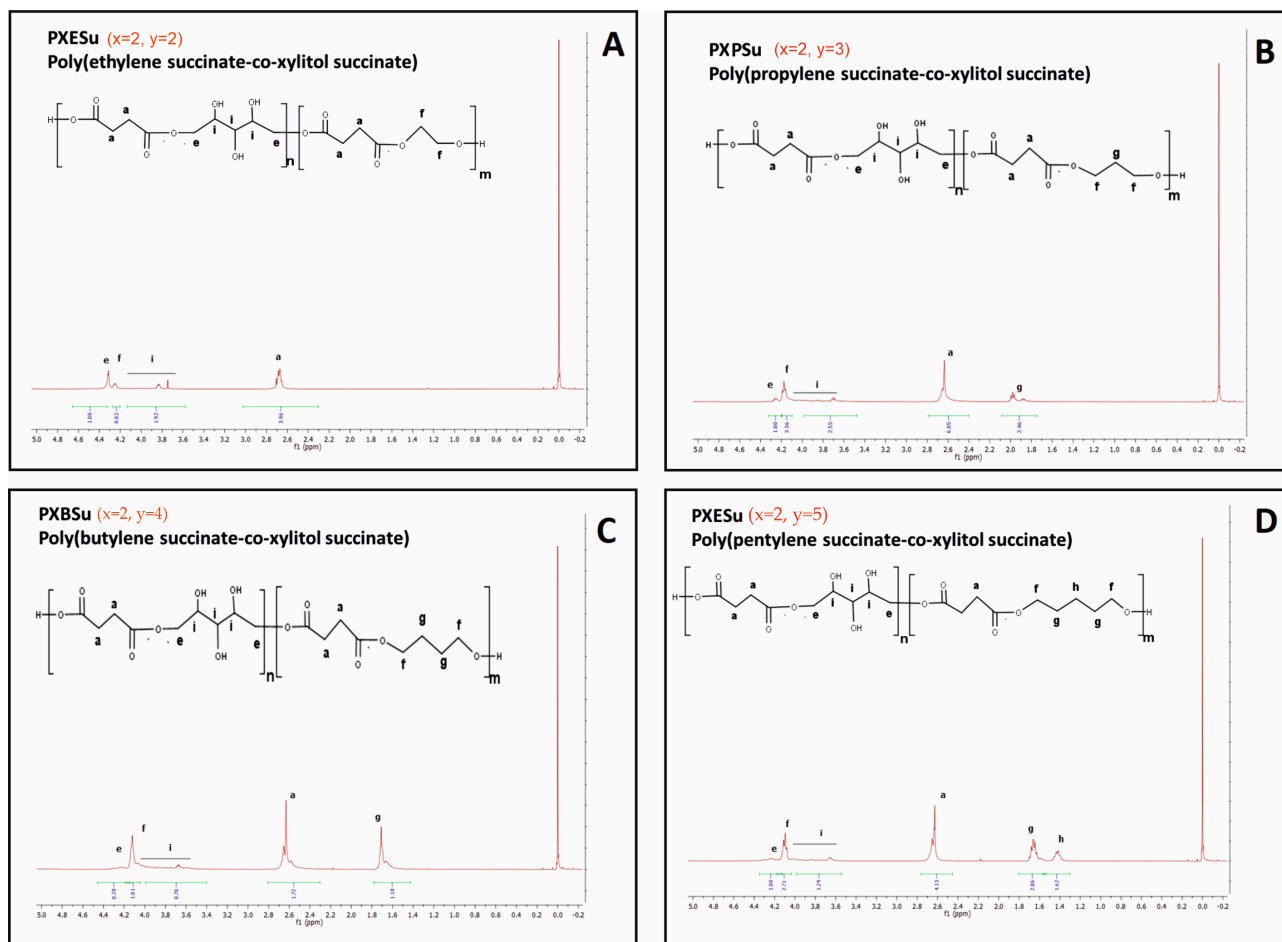


**Figure 2.** 1H NMR of PXESu (**A**), PXPSu (**B**), PXBSu (**C**), and PXPeSu (**D**) prepolymers.

In ^{1}H NMR, peaks ranging from about 2.6 ppm to 1.2 ppm were attributed to –CH2 groups in both diols and dicarboxylic acid peaks at about 1.4 ppm. This association was due to the CH2 (h) group in diol with a peak at about 1.6–1.8 ppm, linked to the CH2 (b) group in dicarboxylic acid and CH2 (g) group in diol. The peak at about 2.4–2.6 ppm was associated with the CH2 (a) group in the dicarboxylic acids. Peaks in the range of 3.6–4.6 ppm were associated with secondary –OH groups in xylitol. The peak at about 4.2 ppm was linked to the ester bond between diol and dicarboxylic acid, and the peak at about 4.4 ppm was due to the ester bond between xylitol and dicarboxylic acid.

By dividing the area of the peak at 4.4 ppm by the area of that at 4.2 ppm, the molar composition of obtained prepolymers was calculated and presented in Table 1.

In ^{13}C NMR, the following peaks could be assigned to –CH$_2$ groups in aliphatic chains: (1) the peak at about 34 ppm was linked to CH$_2$ (a) groups in dicarboxylic acid; (2) the peak at about 28 ppm was connected to CH$_2$ (g) group in diol; (3) the peak at about 24 ppm was due to the CH$_2$ (b) groups in dicarboxylic acid and; (4) the peak at about 22 ppm was associated with the CH$_2$ (h) group in diol. The peak at about 65 ppm was linked to CH$_2$OH (i) groups in xylitol. The peak at about 64 ppm was connected to the carbon atom next to the ester bond between xylitol and dicarboxylic acid, and that at about 62 ppm was linked to the carbon atom next to the ester bond between diol and dicarboxylic acid. The peak at about 172 ppm was linked to the carbonyl group.
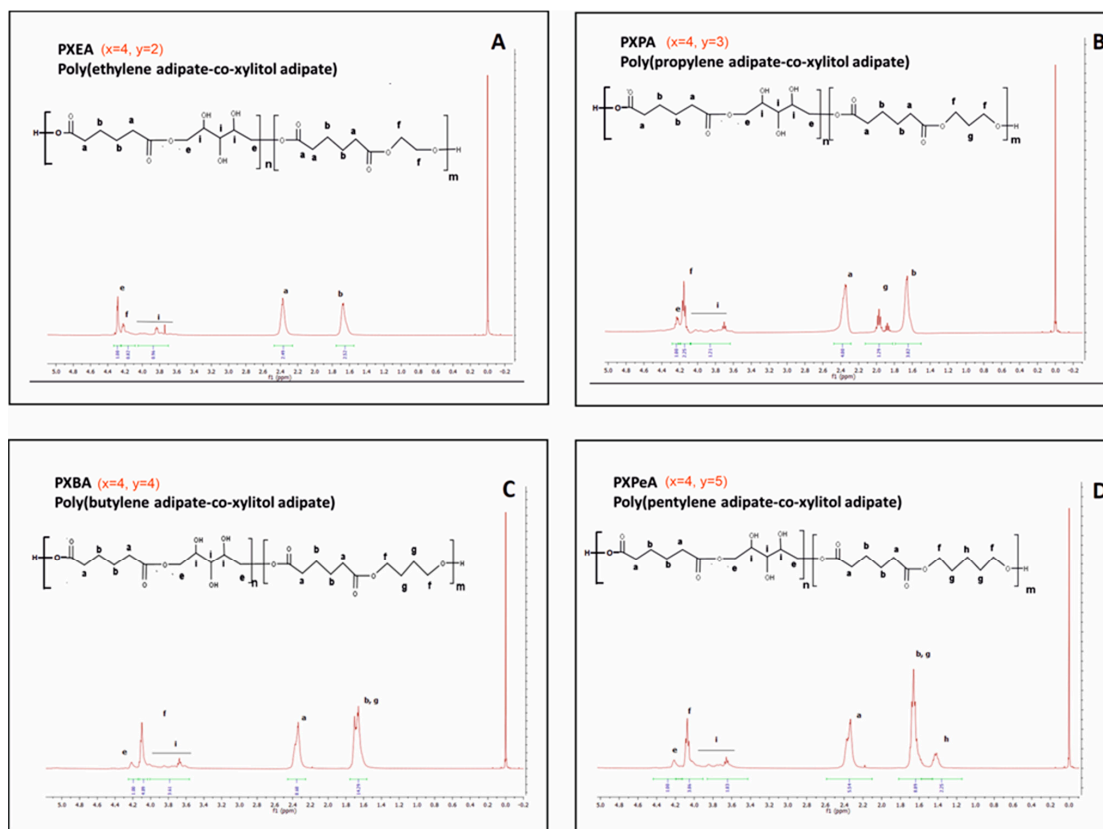
**Figure 3.** 1H NMR of PXEA (**A**), PXPA (**B**), PXBA (**C**), and PXPeA (**D**) prepolymers.
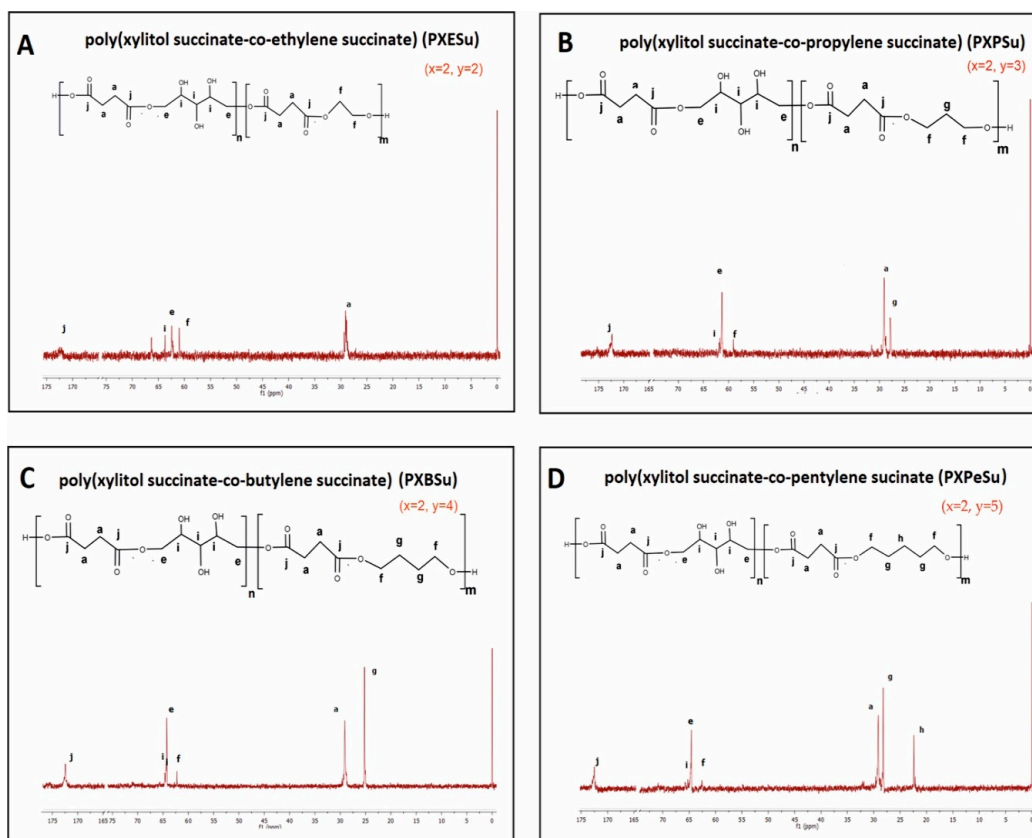


**Figure 4.** $^{13}$C NMR of PXESu (**A**), PXPSu (**B**), PXBSu (**C**), and PXPeSu (**D**).

### 4.2. Fourier Transform Infrared Spectroscopy (FTIR)

Figures 6 and 7 show the FTIR spectra of poly (xylitol dicarboxylate-co-diol dicarboxylate) elastomers. Four signals that are typical for sugar-alcohol-based polyesters can be observed. The signal at 1170 cm$^{-1}$ was linked to $-$C-O-C groups, that at 1725 cm$^{-1}$ was due to the C = O groups, that at 2930 cm$^{-1}$ was connected to $-$CH2$^-$ groups, and that at 3450 cm$^{-1}$ was linked to nonmolecularly associated –OH groups. The lack of significant changes in the spectra of polymers after radiation-modification showed that the polymers do not degrade as a result of e-beam treatment.

A small decrease in the signal intensities was linked to free $-$OH groups, and an increase was linked to $-$C-O-C$-$ groups was seen when comparing the spectra of prepolymers and crosslinked polymers. This occurred due to the creation of crosslinks between polymer chains, which, in turn, resulted from the reaction of hydroxyl groups and left-over unreacted dicarboxylic acid molecules. This change in signal intensities was a confirmation that the crosslinking process had taken place.
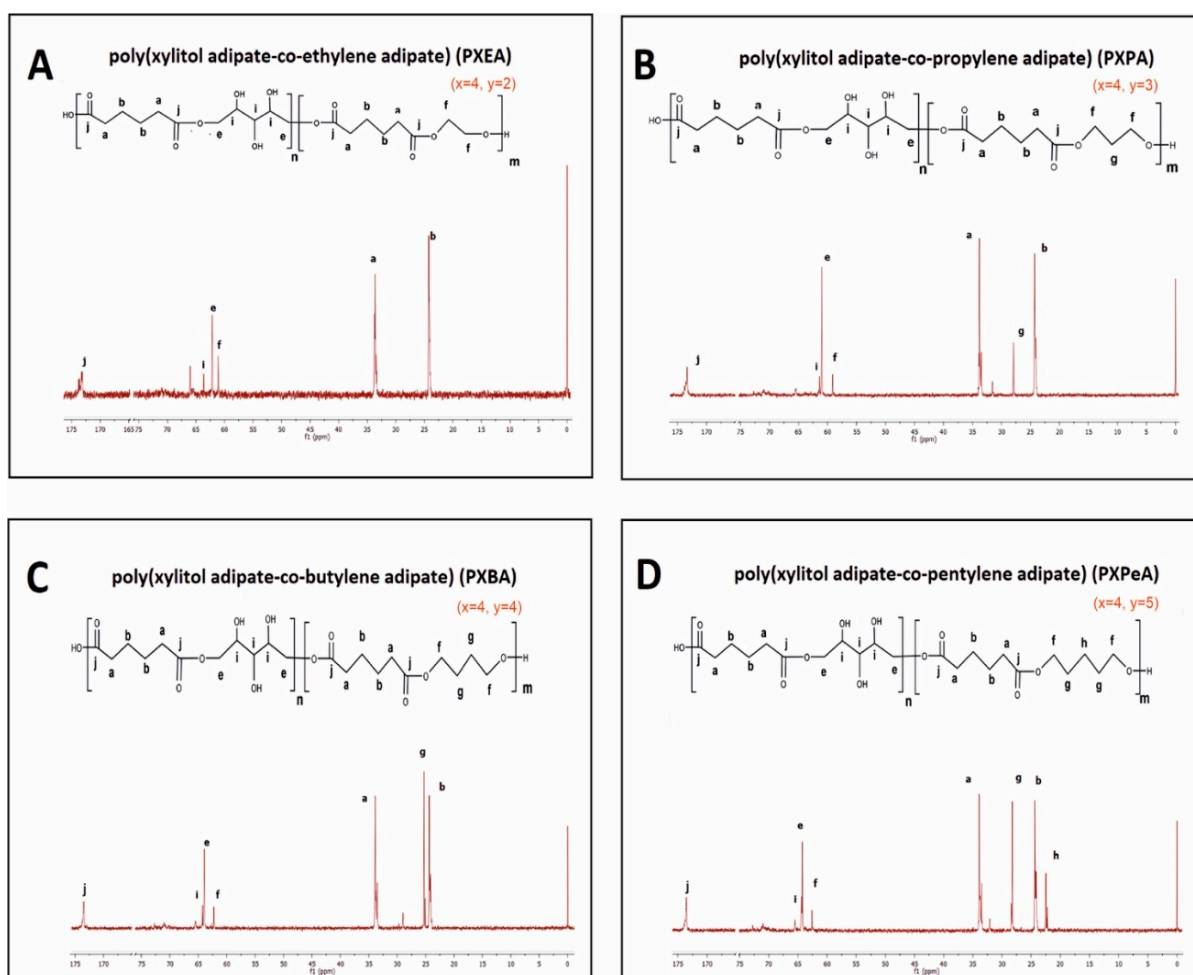


**Figure 5.** $^{13}$C NMR of PXEA (**A**), PXPA (**B**), PXBA (**C**), and PXPeA (**D**) prepolymers.
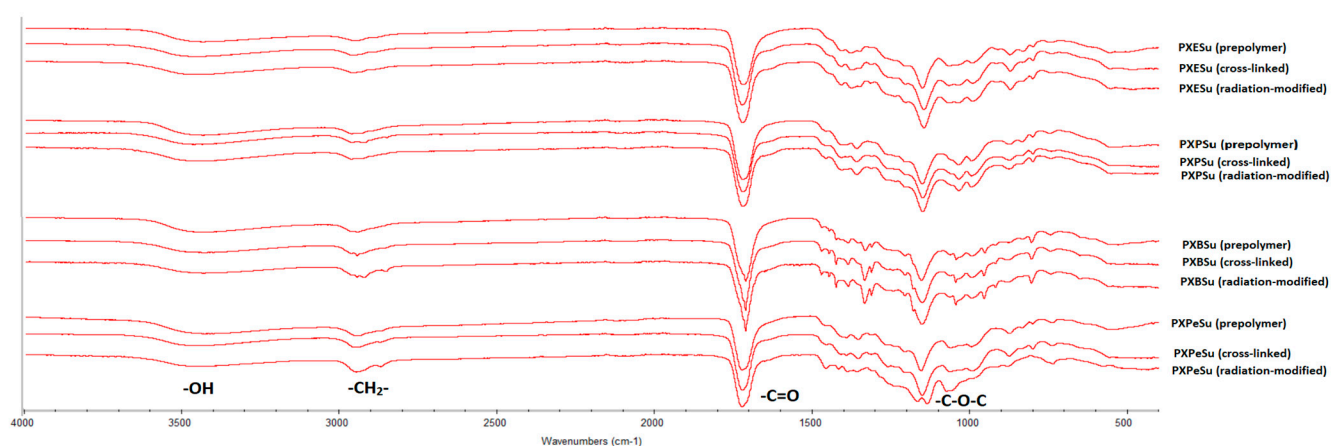
**Figure 6.** FTIR spectra of PXESu, PXPSu, PXBSu, and PXPeSu prepolymers and polymer crosslinked and polymer after radiation modified.
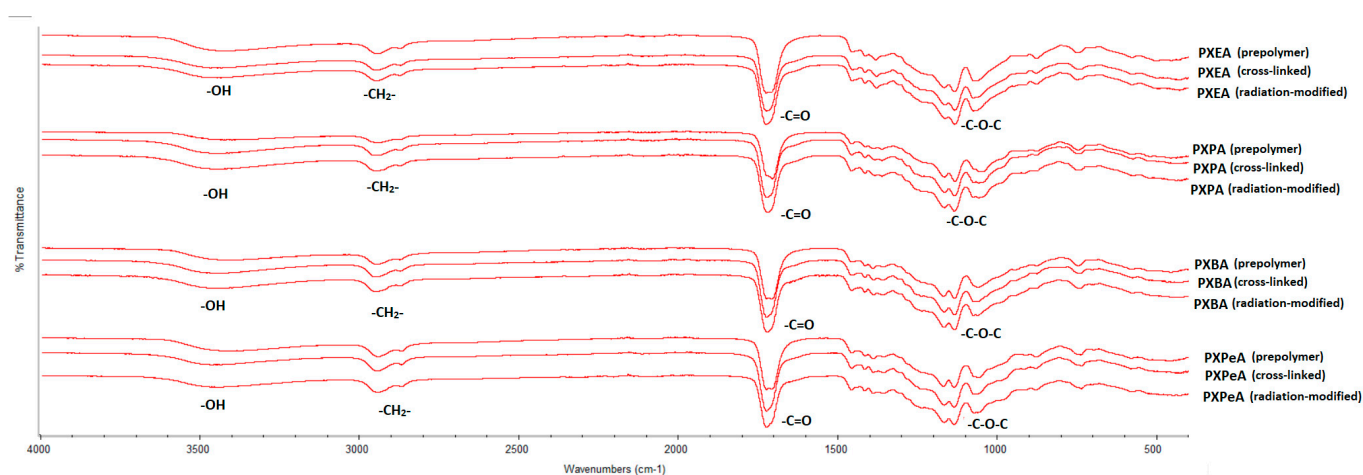


**Figure 7.** FTIR spectra of PXEA, PXPA, PXBA, and PXPeA prepolymers, polymer crosslinked, and polymer after radiation modified.

### 4.3. Thermal Properties: Differential Scanning Calorimetry (DSC)

Differential scanning calorimetry was carried out to determine how the thermal properties of the obtained elastomers were affected by syntheses with different combinations of dicarboxylic acids and diols. The results are presented in Figures 8 and 9 and Table 2.

PXBSu was the only material that exhibited a melting transition. This transition was not present for crosslinked material. All prepolymers, crosslinked polymers, and radiation-modified polymers exhibited glass transition temperatures. Glass transition temperatures exhibited a decrease when both the diol chain length and dicarboxylic acid chain length increased. This was due to the lower mobility of macromolecules when synthesized using longer-chained monomers.

Glass transition temperature also decreased due to the crosslinking process and increased again as a result of radiation-modification.

Changes in heat capacity ($\Delta C_p$) were linked to the grass transition remaining within a similar range for both nonmodified and radiation-modified polyesters. This relationship was due to the lack of change in the content of materials in the amorphous phase. This finding proved that the materials did not degrade as a result of e-beam treatment. This correlates well with the FTIR result, which showed a lack of change in the chemical structure due to radiation-modification, and also proved that the elastomers did not degrade as a result of e-beam treatment.
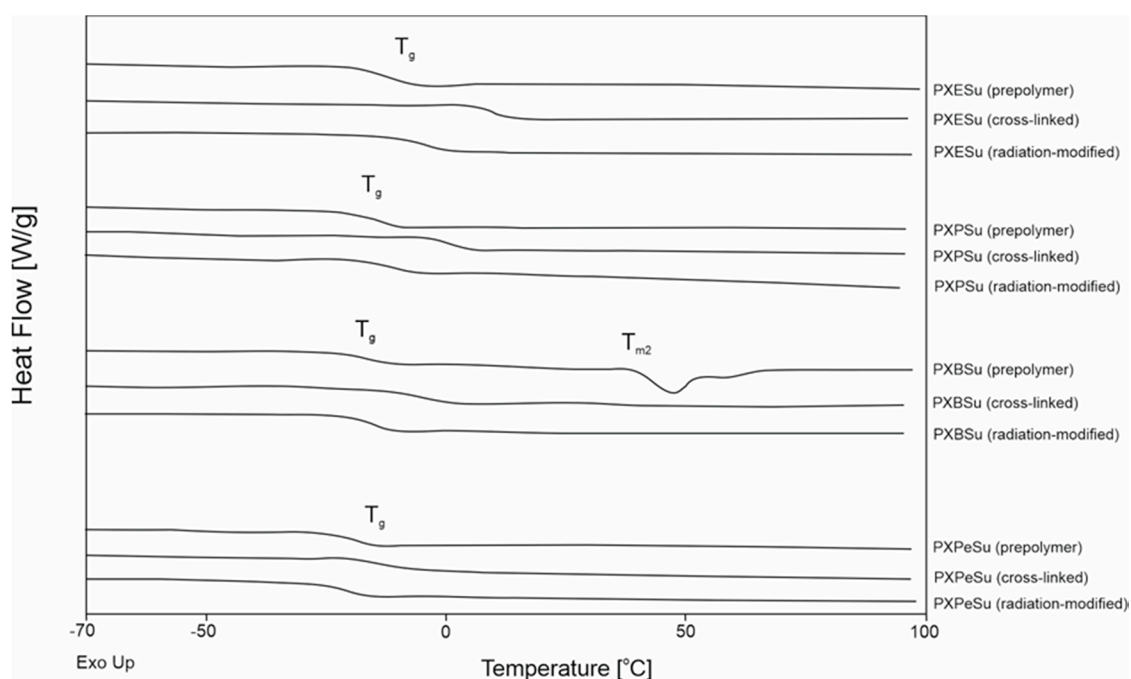
**Figure 8.** Differential scanning calorimetry (DSC) thermograms for first-heating of PXESu, PXPSu, PXBSu, PXPeSu prepolymers and polymer crosslinked and polymer after radiation modified.
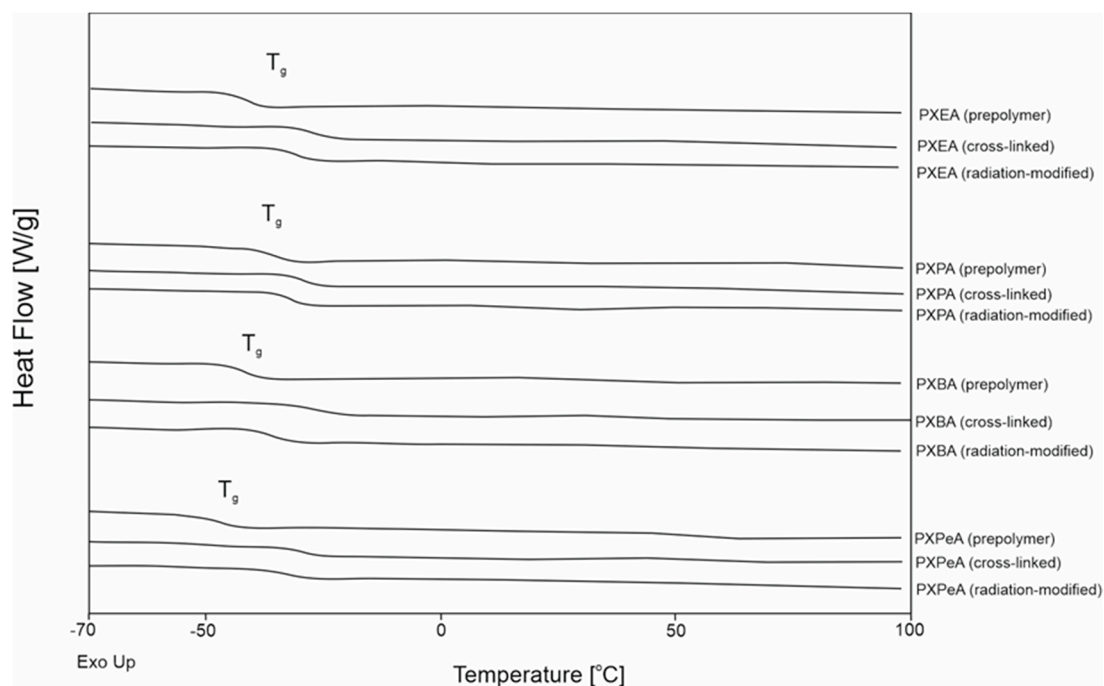


**Figure 9.** Differential scanning calorimetry (DSC) thermograms for first-heating of PXEA, PXPA, PXBA, and PXPeA prepolymers and polymer crosslinked and polymer after radiation modified.

**Table 2.** DSC termograms of poly (xylitol dicarboxylate-co-diol dicarboxylate) before and after irradiation.

| Material | Glass Transition Temperature $T_g$ [°C] | Change in Heat Capacity $\Delta C_P$ [J/g °C] | Melting Temperature $T_{m2}$ [°C] | Melting Enthalphy $H_{m2}$ [J/g] | Degradation Onset Temperature $T_d$ [°C] |
|---|---|---|---|---|---|
| PXESu prepolymer | −10.21 | 0.63 | – | – | |
| *PXESu crosslinked* | 10.22 | 0.61 | – | – | 231 |
| **PXESu (radiation-modified)** | −2.11 | 0.6050 | | | |
| PXPSu prepolymer | −14.36 | 0.6701 | – | – | |
| *PXPSu crosslinked* | 1.62 | 0.55 | – | – | 220.6 |
| **PXPSu (radiation-modified)** | −9.69 | 0.6326 | | | |
| PXBSu prepolymer | −15.35 | 0.56 | 47.27 | 12.59 | |
| *PXBSu crosslinked* | −6.07 | 0.58 | – | – | 224.5 |
| **PXBSu (radiation-modified)** | −14.92 | 0.5953 | | | |
| PXPeSu prepolymer | −18.11 | 0.60 | – | – | |
| *PXPeSu crosslinked* | −12.63 | 0.61 | – | – | 227 |
| **PXPeSu (radiation-modified)** | −20.23 | 0.6186 | | | |
| PXEA prepolymer | −33.29 | 0.62 | – | – | |
| *PXEA crosslinked* | −16.79 | 0.53 | – | – | 213.5 |
| **PXEA (radiation-modified)** | −26.67 | 0.56 | | | |
| PXPA prepolymer | −34.86 | 0.61 | – | – | |
| *PXPA crosslinked* | −28.37 | 0.58 | – | – | 209.5 |
| **PXPA (radiation-modified)** | −31.21 | 0.5580 | | | |
| PXBA prepolymer | −40.52 | 0.64 | – | – | |
| *PXBA crosslinked* | −25.73 | 0.4758 | – | – | 215.8 |
| **PXBA (radiation-modified)** | −34.99 | 0.5807 | | | |
| PXPeA prepolymer | −46.33 | 0.61 | – | – | |
| *PXPeA crosslinked* | −28.63 | 0.51 | – | – | 207.9 |
| **PXPeA (radiation-modified)** | −33.31 | 0.55 | | | |

Where $\Delta C_p$: change of the heat capacity; $T_g$: glass transition temperature; $T_{m1}$: melting temperature, $\Delta H_{m1}$: melting enthalphy.

### 4.4. Dynamic Thermomechanical Analysis (DMTA)

DMTA was used to test the relaxation behavior displayed by PXESu, PXPSu, PXBSu, and PXPeSu (Figure 10) and PXEA, PXPA, PXBA, and PXPeA (Figure 11) before and after radiation modification with 100 kGy. Modulus E′, loss modulus E″, and loss tangent (tan delta) were measured as a temperature function. The materials were in a glassy state in the temperature range between −90 and −20 °C. A viscoelastic relaxation process, associated with the glass transition, was related to a significant decrease of storage modulus which was observed in the temperature range between 20 and 0 °C. The peak maxima of the loss modulus and loss tangent functions associated with α relaxation correspond well with the glass transition temperature determined by DSC. The peak maxima of the loss tangent shift in the direction of lower temperatures was a result of radiation modification. This finding corresponded well with the glass transition temperatures decreasing as a result of radiation modification as confirmed by DSC.
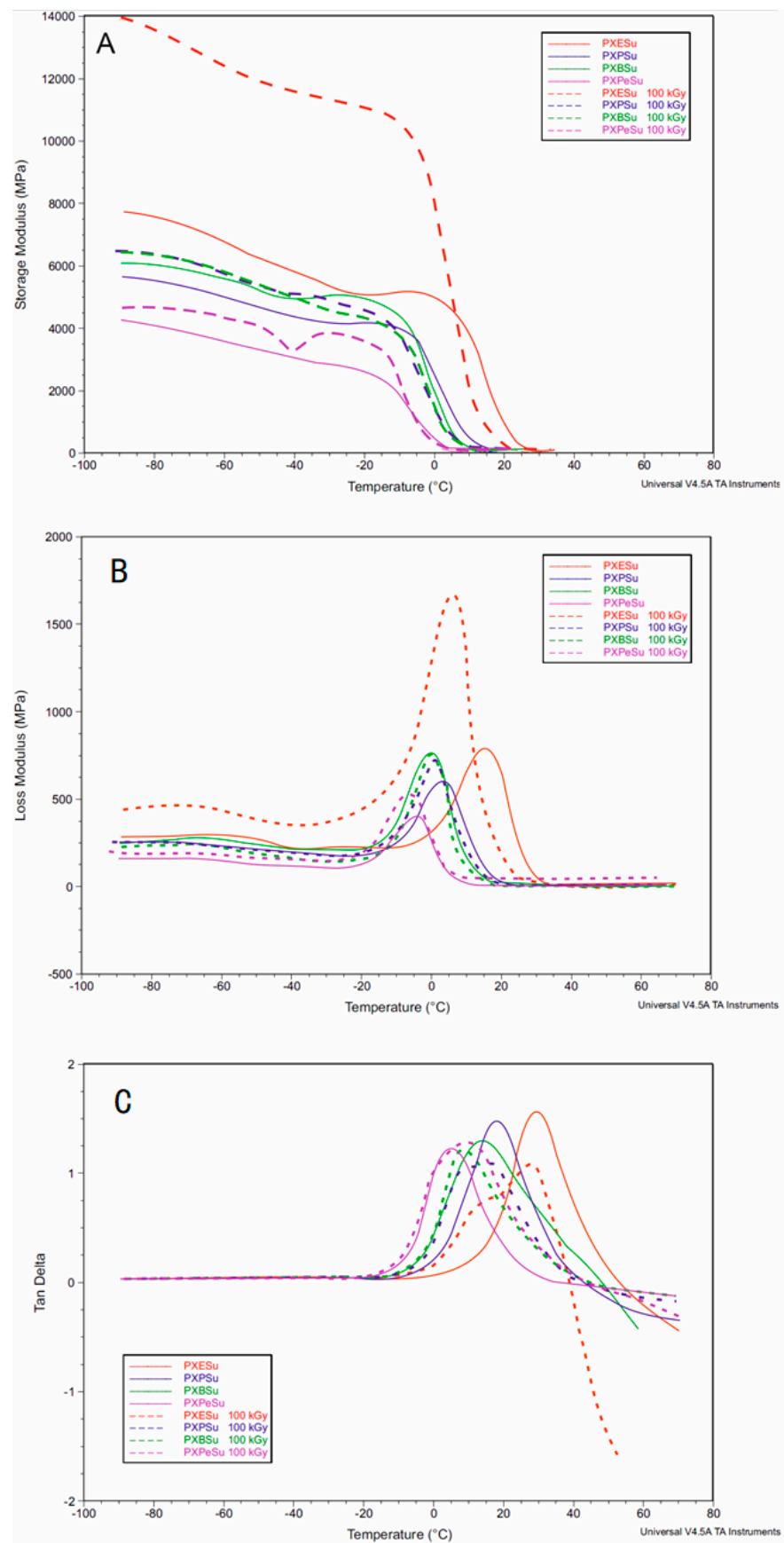
**Figure 10.** DMTA (**A**) Storage modulus (E′), (**B**) loss modulus (E″), (**C**) loss tangent (tan delta versus temperature) for PXESu, PXPSu, PXBSu, and PXPeSu.
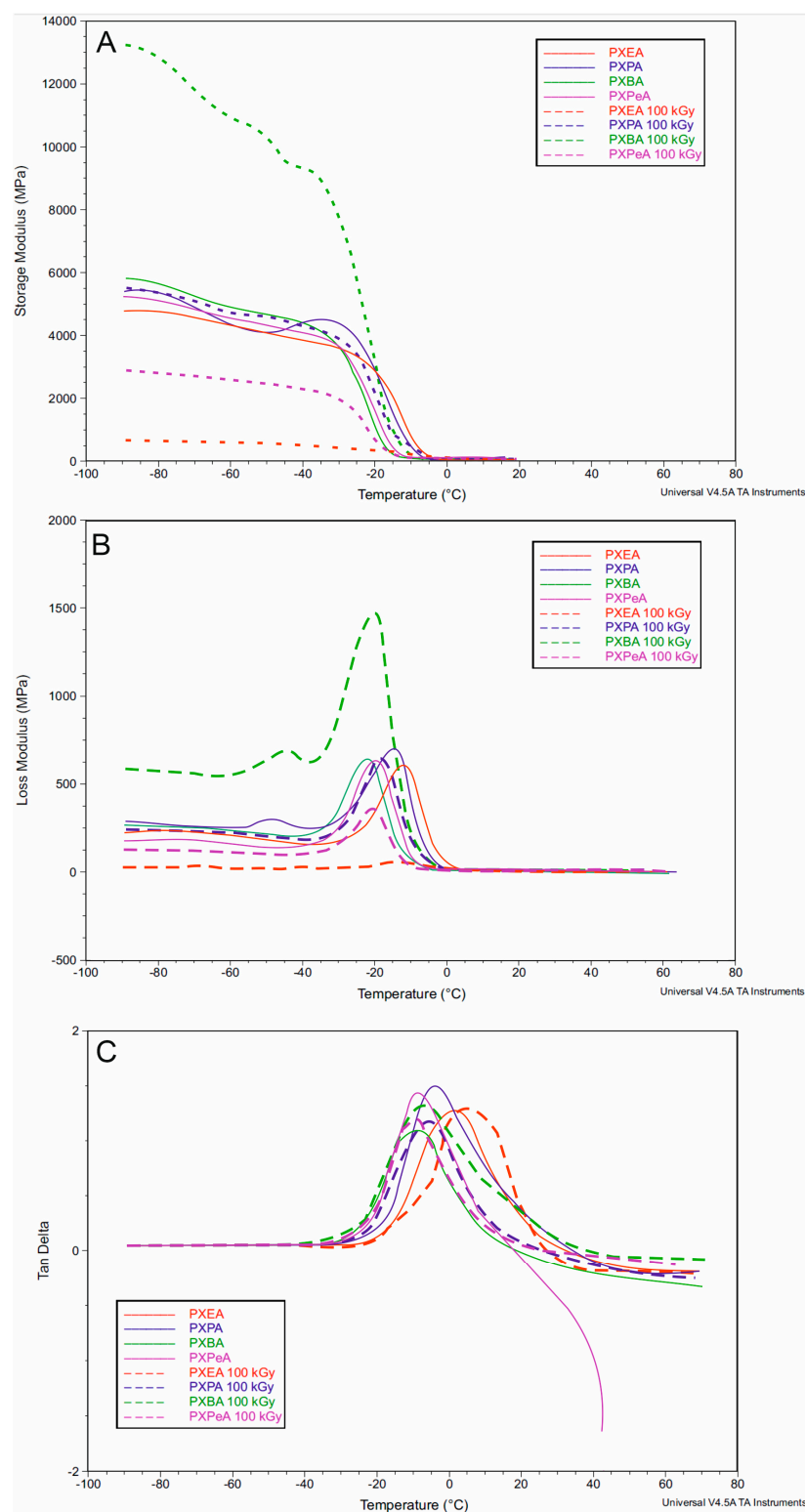
**Figure 11.** DMTA (**A**) Storage modulus (E′), (**B**) loss modulus (E″), (**C**) loss tangent (tan delta versus temperature) for PXEA, PXPA, PXBA, and PXPeA.

The peak area of the loss modulus and value of storage modulus significantly increased for PXESu and PXBA while decreasing for PXEA materials due to radiation modification. However, radiation-modification did not correlate with a change in mechanical properties, thermal stability, or degradation susceptibility. Overall, all of the DMTA results complemented the results of the DSC analysis.

### 4.5. Mechanical Properties

Tensile tests determined the influence of monomer chain length on the mechanical properties of the obtained elastomers. The results are presented in Figure 12 and Table 1. The elastomer based on monomers with the shortest chain (PXESu) exhibited the best mechanical properties. Both the elongation at break and stress at break were significantly higher than those of the rest of the materials. Radiation-modification led to an increase of stress at break of PXPeSu, PXEA, PXPA, and PXBA elastomers. The modulus at 50% elongation improved for all materials except for PXESu. PXESu was the only elastomer that did not show any beneficial changes due to the e-beam treatment. Adipic acid-based materials were better suited for radiation modification, but succinic-acid-based elastomers had overall better mechanical properties.
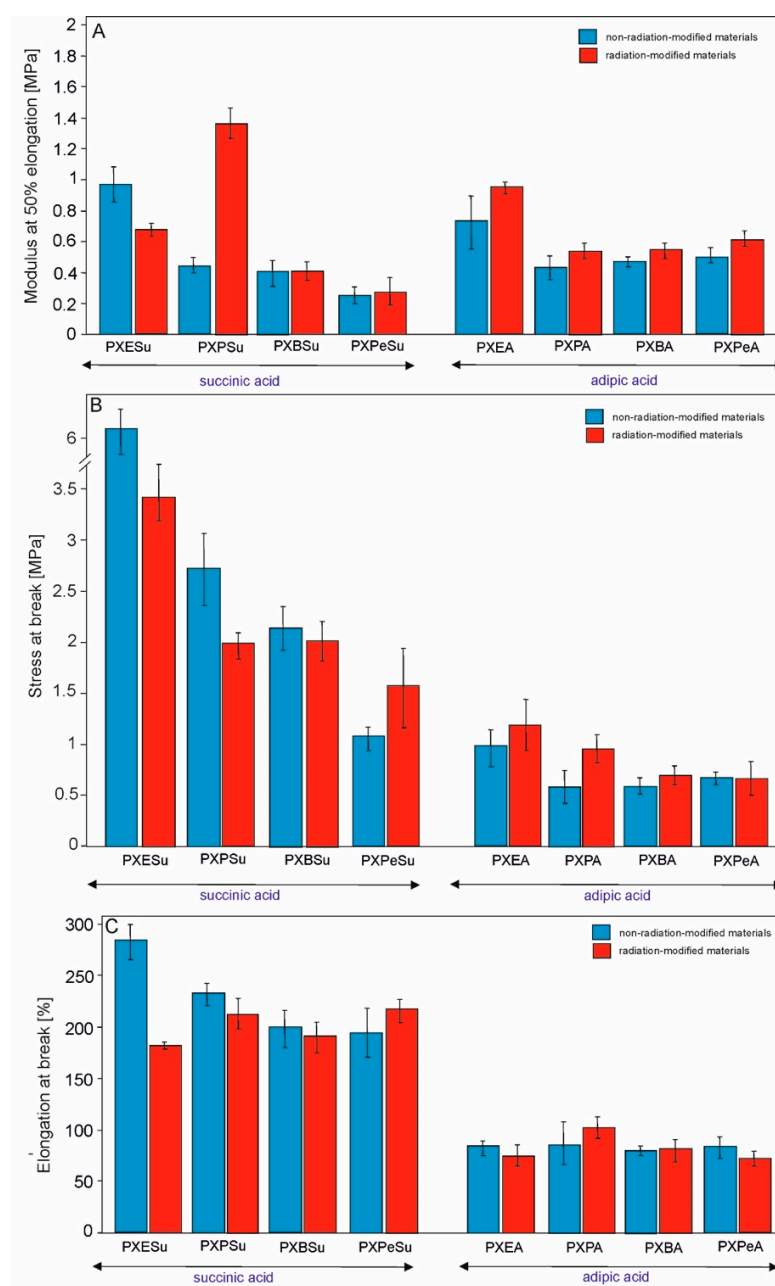


**Figure 12.** Mechanical properties of PXESu, PXPSu, PXBSu, PXPeSu and PXEA, PXPA, PXBA, and PXPeA nonradiation-modified materials (blue) and radiation-modified materials (red). Tangent modulus at 50% elongation (**A**), stress at break (**B**), and elongation at break (**C**).

### 4.6. Gel Fraction

The results of gel fraction determination are provided in Figure 13. The gel fraction content of all the materials was within the range of about 71–87%. In all the elastomers except for PXEA, radiation modification led to a decrease of gel fraction content. However, there was no correlation between the value of gel fraction content and its change due to e-beam treatment and the mechanical properties of the elastomers. There was, however, a connection between the decrease of gel fraction content as a result of e-beam treatment and a better susceptibility of the materials to biodegradation.
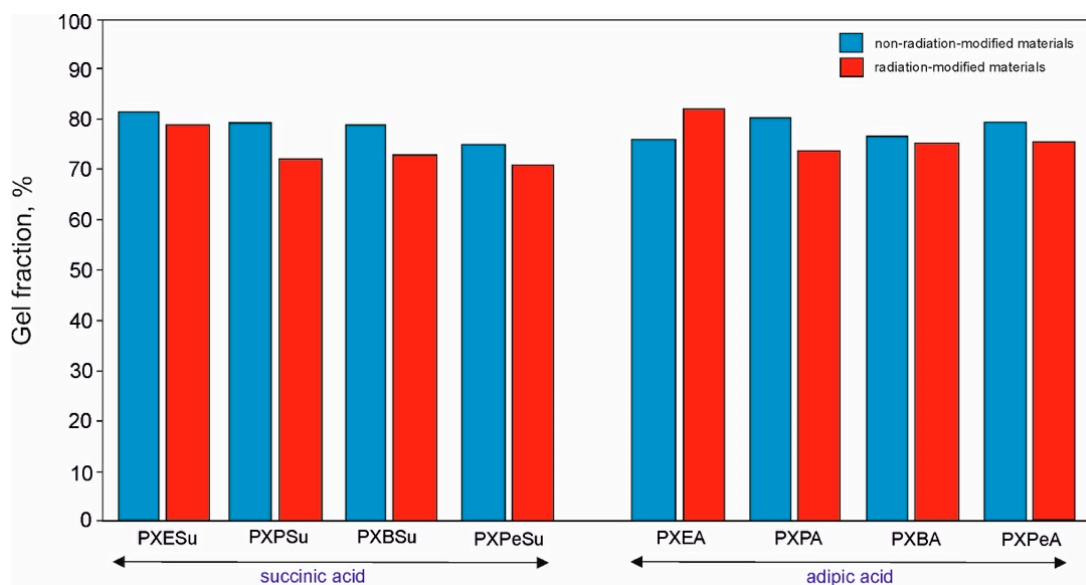


**Figure 13.** Gel fraction results for PXESu, PXPSu, PXBSu, PXPeSu and PXEA, PXPA, PXBA, and PXPeA nonradiation-modified materials (blue) and radiation-modified materials (red).

### 4.7. Biodegradation

To determine whether the obtained elastomers were biodegradable, and to see how the monomer chain-length affected their susceptibility to degradation, materials were subjected to hydrolytic and enzymatic degradation. Tests were conducted on crosslinked elastomers before and after radiation-modification. The results are provided in Figure 14.

UPTOHERE For hydrolytic degradation, the mass loss after 21 days decreased with the increase of monomer chain length. Mass loss due to the enzymatic degradation, however, showed no correlation with the chain length of the monomers used for the synthesis. It was highest for PXESu and PXPSu and stayed within a similar range for the rest of the materials. The radiation-modification increased the degradation susceptibility of the elastomers. Mass loss due to the enzymatic degradation is higher than in case of the hydrolytic degradation.
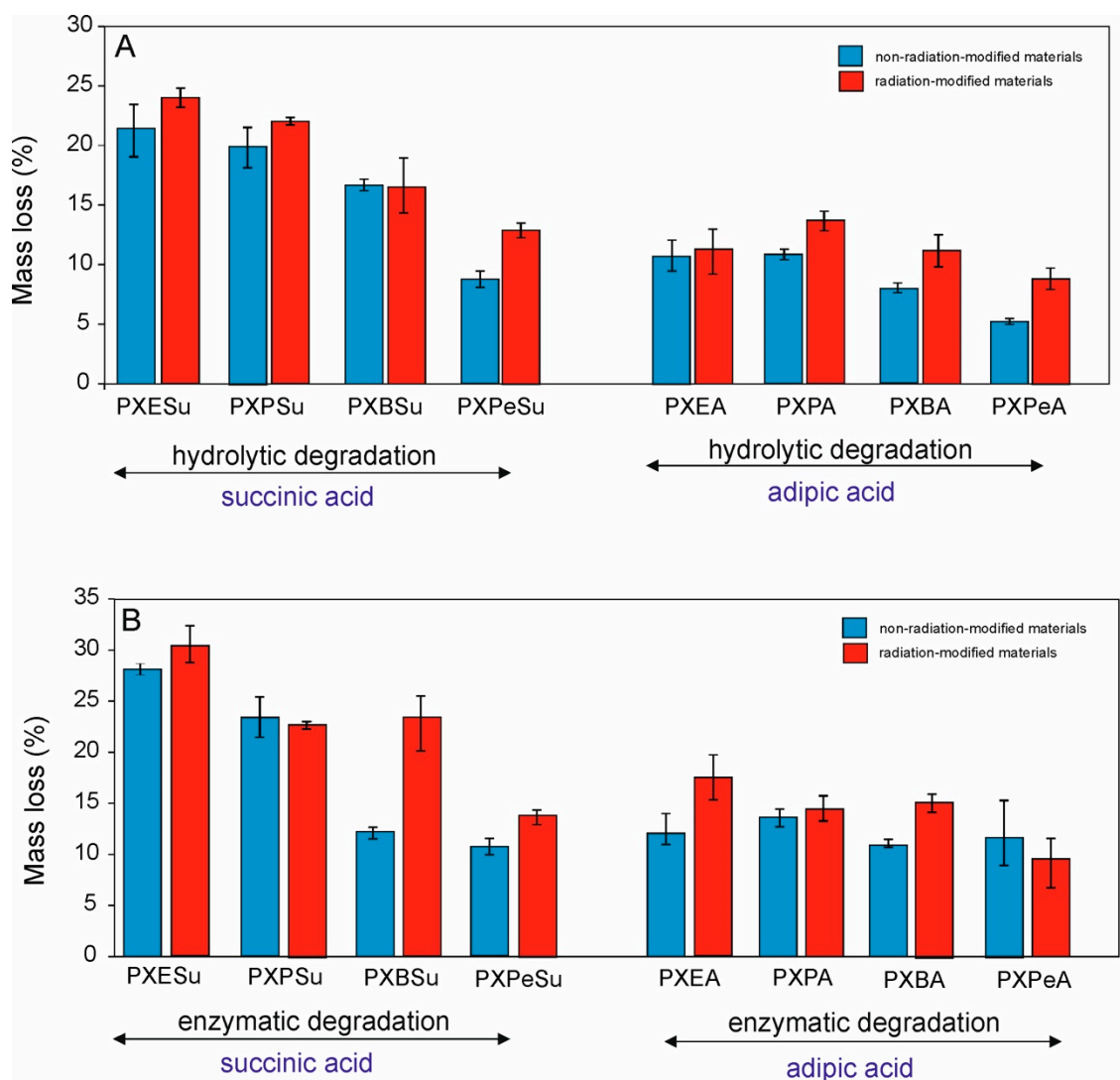
**Figure 14.** Hydrolytic (**A**) and enzymatic degradation (**B**) of PXESu, PXPSu, PXBSu, PXPeSu and PXEA, PXPA, PXBA, and PXPeA nonradiation-modified materials (blue) and radiation-modified materials (red).

### 4.8. Thermogravimetric Analysis (TGA)

To determine the thermal stability of crosslinked elastomers, TGA tests were performed. The results are shown in Figure 15. All materials showed similar slopes of the function curve and had thermal stability up to 250 °C, which is significantly higher than both the synthesis and crosslinking temperature and the foreseeable temperature of use.
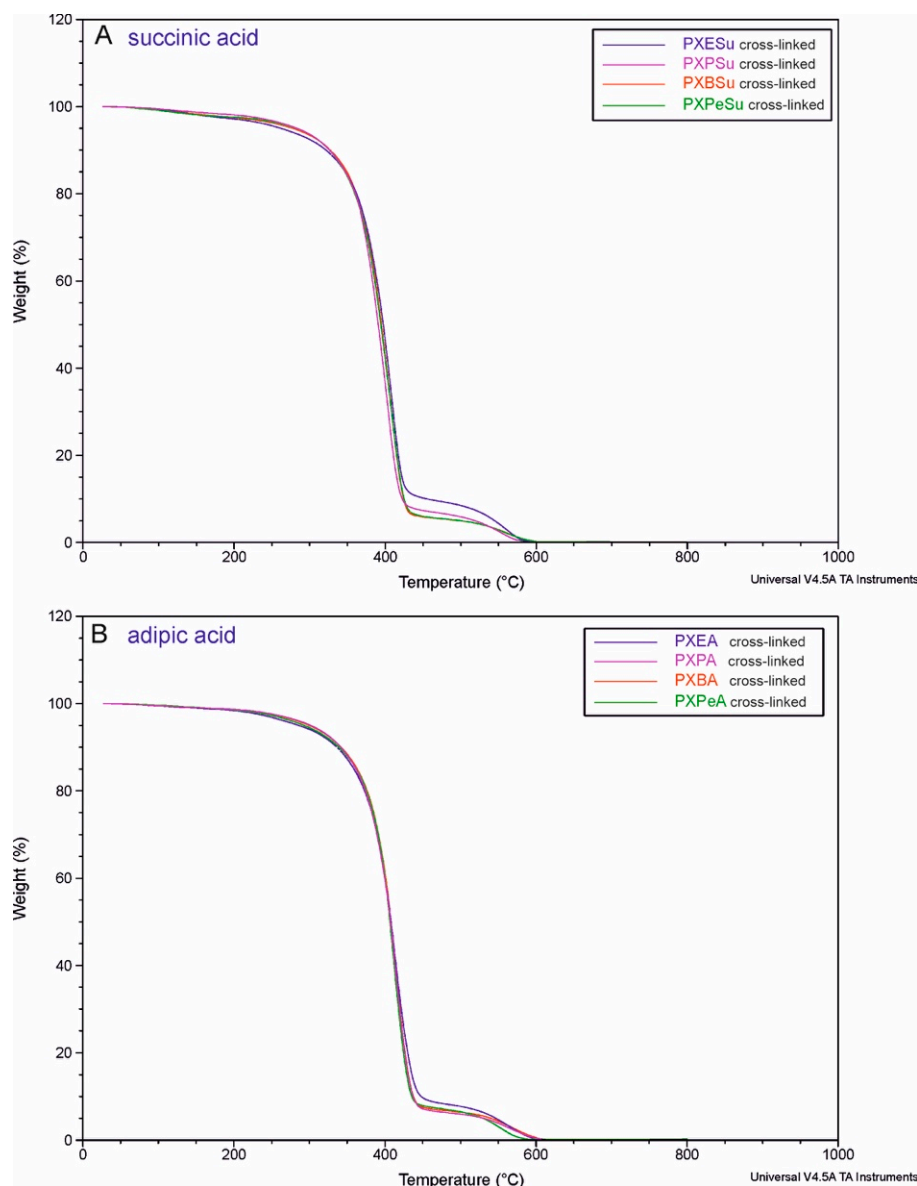
**Figure 15.** Thermogravimetric analysis (TGA) of PXESu, PXPSu, PXBSu, PXPeSu (**A**) and PXEA, PXPA, PXBA, and PXPeA (**B**) after synthesis.

*4.9. Scanning Electron Microscopy (SEM)*

SEM images of polymers before radiation-modification, after radiation-modification, after radiation-modification following hydrolytic degradation, and after radiation-modification following enzymatic degradation were taken to confirm that the physical changes that appeared on the material surface were indeed due to the irradiation process. They are presented in Figure 16.

Physical changes on the material surfaces were present for both PXESu and PXEA. In the case of PXESu, small cracks were visible on the surface, which may have indicated that degradation was taking place. This was mirrored by the reduction of the tensile strength of the material, as determined by tensile tests. Such surface cracks were not present on the surface of PXEA, and this material was characterized improved tensile strength.

Surface hydrolytic and enzymatic degradation was characterized by the presence of salts precipitated from PBS solution and cracking on the surface. This confirmed that the degradation process had taken place in both cases.
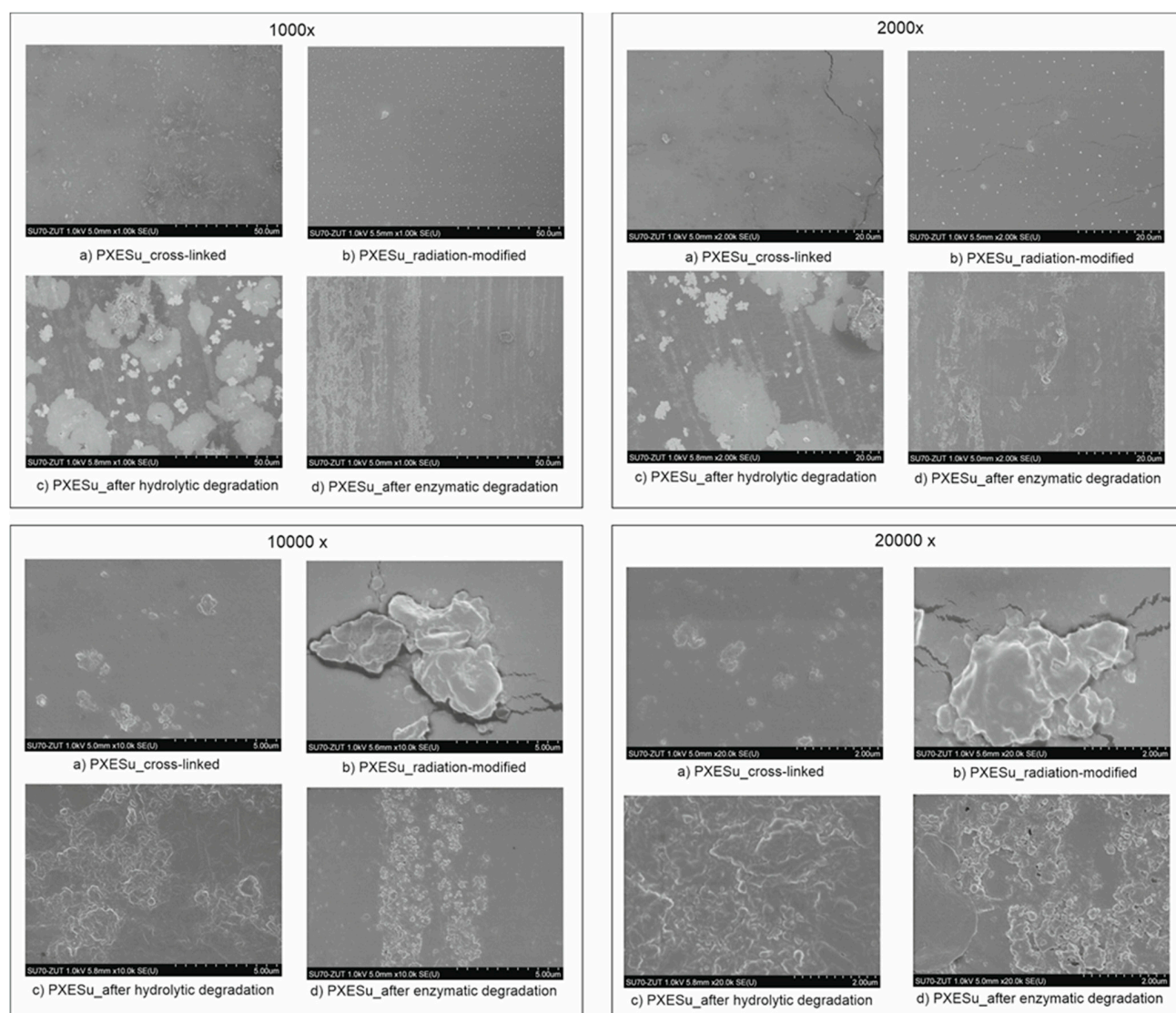
**Figure 16.** Scanning electron microscopy (SEM) images of PXESu crosslinked (**a**); PXESu radiation-modified (**b**); PXESu after hydrolytic degradation (**c**); PXESu after enzymatic degradation (**d**).

## 5. Conclusions

The authors aimed to evaluate the utilization of chain-length monomers to tailor the physicochemical properties of xylitol-based elastomers. With this aim, eight different materials were prepared, and their e-beam treatment was carried out. Their chemical structure was confirmed by both ^{1}H NMR and ^{13}C NMR. FTIR was used to confirm crosslinking and determined that the polymers did not degrade after radiation-modification. The thermal properties of the were tested by DSC, DMTA, and TGA analyses. The DSC test confirmed the amorphous character of the materials, and the results were well complimented by the DMTA analysis. TGA tests confirmed a good thermal stability of the obtained elastomers. Mechanical test results have shown that adipic acid-based materials are better suited for radiation modification, but succinic-acid-based elastomers have overall better mechanical properties. Elastomers were confirmed to be biodegradable, and their susceptibility to hydrolytic degradation increased as the monomer chain length increased. This relationship was further enhanced by radiation modification. Overall, by choosing appropriate monomers, it is possible to obtain elastomers which are similar but with fine-tuned properties for a specific use. Radiation modification further enhances their properties.

## References

1. Bruggeman, J.P.; de Bruin, B.J.; Bettinger, C.J.; Langer, R. Biodegradable poly(polyol sebacate) polymers. *Biomaterials* **2008**, *29*, 4726–4735. [CrossRef]
2. Ning, Z.Y.; Zhang, Q.S.; Wu, Q.P.; Li, Y.Z.; Ma, D.X.; Chen, J.Z. Efficient synthesis of hydroxyl functioned polyesters from natural polyols and sebacic acid. *Chin. Chem. Lett.* **2011**, *22*, 635–638. [CrossRef]
3. Dasgupta, Q.; Chatterjee, K.; Madras, G. Combinatorial approach to develop tailored biodegradable poly(xylitol dicarboxylate) polyesters. *Biomacromolecules* **2014**, *15*, 4302–4313. [CrossRef]
4. Chen, Q.Z.; Bismarck, A.; Hansen, U.; Junaid, S.; Tran, M.Q.; Harding, S.E.; Ali, N.N.; Boccaccini, A.R. Characterisation of a soft elastomer poly(glycerol sebacate) designed to match the mechanical properties of myocardial tissue. *Biomaterials* **2008**, *29*, 47–57. [CrossRef] [PubMed]
5. Sundback, C.A.; Shyu, J.Y.; Wang, Y.; Faquin, W.C.; Langer, R.S.; Vacanti, J.P.; Hadlock, T.A. Biocompatibility analysis of poly(glycerol sebacate) as a nerve guide material. *Biomaterials* **2005**, *26*, 5454–5464. [CrossRef] [PubMed]
6. Zaky, S.H.; Lee, K.W.; Gao, J.; Jensen, A.; Verdelis, K.; Wang, Y.; Almarza, A.J.; Sfeir, C. Poly (glycerol sebacate) elastomer supports bone regeneration by its mechanical properties being closer to osteoid tissue rather than to mature bone. *Acta Biomater.* **2017**, *54*, 95–106. [CrossRef] [PubMed]
7. Motlagh, D.; Yang, J.; Lui, K.Y.; Webb, A.R.; Ameer, G.A. Hemocompatibility evaluation of poly(glycerol-sebacate) in vitro for vascular tissue engineering. *Biomaterials* **2006**, *27*, 4315–4324. [CrossRef]
8. Kemppainen, J.M.; Hollister, S.J. Tailoring the mechanical properties of 3D-designed poly(glycerol sebacate) scaffolds for cartilage applications. *J. Biomed. Mater. Res. Part A* **2010**, *94*, 9–18. [CrossRef] [PubMed]
9. Moorhoff, C.; Li, Y.; Cook, W.D.; Braybrook, C.; Chen, Q.Z. Characterization of the prepolymer and gel of biocompatible poly(xylitol sebacate) in comparison with poly(glycerol sebacate) using a combination of mass spectrometry and nuclear magnetic resonance. *Polym. Int.* **2015**, *64*, 668–688. [CrossRef]
10. Li, Y.; Chen, Q.Z. Fabrication of mechanically tissue-like fibrous poly(xylitol sebacate) using core/shell electrospinning technique. *Adv. Eng. Mater.* **2015**, *17*, 324–329. [CrossRef]
11. Li, Y.; Thouas, G.A.; Chen, Q. Novel elastomeric fibrous networks produced from poly(xylitol sebacate)2:5 by core/shell electrospinning: Fabrication and mechanical properties. *J. Mech. Behav. Biomed. Mater.* **2014**, *40*, 210–221. [CrossRef]
12. Ma, P.; Li, T.; Wu, W.; Shi, D.; Duan, F.; Bai, H.; Dong, W.; Chen, M. Novel poly(xylitol sebacate)/hydroxyapatite bio-nanocomposites via one-step synthesis. *Polym. Degrad. Stab.* **2014**, *110*, 50–55. [CrossRef]
13. Hu, J.; Gao, W.; Kulshrestha, A.; Gross, R.A. "Sweet polyesters": Lipase-catalyzed condensation—Polymerizations of alditols. *Macromolecules* **2006**, *39*, 6789–6792. [CrossRef]
14. Kavimani, V.; Jaisankar, V. Synthesis and Characterisation of Sorbitol Based Copolyesters for Biomedical Applications. *J. Phys. Sci. Appl.* **2014**, *4*, 507–515.
15. Piatek-Hnat, M.; Bomba, K.; Peksiński, J.; Kozłowska, A.; Sośnicki, J.G.; Idzik, T.J. Effect of e-beam irradiation on thermal and mechanical properties of ester elastomers containing multifunctional alcohols. *Polymers* **2020**, *12*, 1043. [CrossRef] [PubMed]
16. Piatek-Hnat, M.; Bomba, K.; Peksiński, J.; Kozłowska, A.; Sośnicki, J.G.; Idzik, T.J.; Piwowarska, D.; Janik, J. Influence of e-beam irradiation on the physicochemical properties of poly(polyol succinate-co-butylene succinate) ester elastomers. *Materials* **2020**, *13*, 3196. [CrossRef] [PubMed]
17. Piatek-Hnat, M.; Bomba, K.; Pęksiński, J. Structure and properties of biodegradable poly (xylitol sebacate-co-butylene sebacate) copolyester. *Molecules* **2020**, *25*, 1541. [CrossRef] [PubMed]

18. Piątek-Hnat, M.; Sładkiewicz, P.; Bomba, K.; Pęksiński, J.; Kozłowska, A.; Sośnicki, J.; Idzik, T. Tailoring the Physico-Chemical Properties of Poly(xylitol-dicarboxylate-co-butylene dicarboxylate) Polyesters by Adjusting the Cross-Linking Time. *Polymers* **2020**, *12*, 1493. [CrossRef] [PubMed]

19. Piatek-Hnat, M.; Bomba, K.; Peksiński, J. Synthesis and selected properties of ester elastomer containing sorbitol. *Appl. Sci.* **2020**, *10*, 1628. [CrossRef]

20. Piątek-Hnat, M.; Bomba, K. The influence of of cross-linking process on the physicochemical properties of new copolyesters containing xylitol. *Mater. Today Commun.* **2020**, *20*, 100734. [CrossRef]

21. Firoozi, N.; Kang, Y. A Highly Elastic and Autofluorescent Poly(xylitol-dodecanedioic Acid) for Tissue Engineering. *ACS Biomater. Sci. Eng.* **2019**, *5*, 1257–1267. [CrossRef]

22. Bruggeman, J.P.; Bettinger, C.J.; Langer, R. Biodegradable xylitol-based elastomers: In vivo behavior and biocompatibility. *J. Biomed. Mater. Res. Part A* **2010**, *95*, 92–104. [CrossRef] [PubMed]

23. Minh Quynh, T.; Mitomo, H.; Yoneyama, M.; Quoc Hien, N. Properties of Radiation-Induced Crosslinking Stereocomplexes Derived From Poly(L-Lactide) and Different Poly(D-Lactide). *Trans. Polym. Eng. Sci.* **2009**, *49*, 970–976. [CrossRef]

24. Nagasawa, N.; Kasai, N.; Yagi, T.; Yoshii, F.; Tamada, M. Radiation-induced crosslinking and post-processing of poly(l-lactic acid) composite. *Radiat. Phys. Chem.* **2011**, *80*, 145–148. [CrossRef]

25. Huang, Y.; Gohs, U.; Müller, M.T.; Zschech, C.; Wiessner, S. Electron beam treatment of polylactide at elevated temperature in nitrogen atmosphere. *Radiat. Phys. Chem.* **2019**, *159*, 166–173. [CrossRef]

26. Changyu, H.; Xianghai, R.; Kunyu, Z.; Zhuang, Y.; Dong, L. Thermal and Mechanical Properties of Poly(e-caprolactone) Crosslinked with g Radiation in the Presence of Triallyl Isocyanurate. *J. Appl. Polym. Sci.* **2010**, *116*, 2658–2667.

27. Zhu, G.; Liang, G.; Xu, Q.; Yu, Q. Shape-memory effects of radiation crosslinked Poly($\varepsilon$-caprolactone). *J. Appl. Polym. Sci.* **2003**, *90*, 1589–1595. [CrossRef]

28. Suhartini, M.; Mitomo, H.; Nagasawa, N.; Yoshii, F.; Kume, T. Radiation crosslinking of poly(butylene succinate) in the presence of low concentrations of trimethallyl isocyanurate and its properties. *J. Appl. Polym. Sci.* **2003**, *88*, 2238–2246. [CrossRef]

29. Ashby, R.D.; Cromwick, A.M.; Foglia, T.A. Radiation crosslinking of a bacterial medium-chain-length poly(hydroxyalkanoate) elastomer from tallow. *Int. J. Biol. Macromol.* **1998**, *23*, 61–72. [CrossRef]

30. Bergmann, A.; Teßmar, J.; Owen, A. Influence of electron irradiation on the crystallisation, molecular weight and mechanical properties of poly-(R)-3-hydroxybutyrate. *J. Mater. Sci.* **2007**, *42*, 3732–3738. [CrossRef]

*Article*

# E-Beam Effects on Poly(Xylitol Dicarboxylate-co-diol Dicarboxylate) Elastomers Tailored by Adjusting Monomer Chain Length

Marta Piątek-Hnat [1,*], Kuba Bomba [1], Janusz P. Kowalski-Stankiewicz [2], Jakub Pęksiński [3], Agnieszka Kozłowska [1], Jacek G. Sośnicki [4], Tomasz J. Idzik [4], Beata Schmidt [5], Krzysztof Kowalczyk [5], Marta Walo [6], Grzegorz Mikołajczak [3] and Agnieszka Kochmańska [7]

1 Faculty of Chemical Technology and Engineering, West Pomeranian University of Technology, Piastów Ave. 42, 71-065 Szczecin, Poland; kubabomba4@gmail.com (K.B.); agak@zut.edu.pl (A.K.)
2 Department of Computer Sciences in Medicine & Education Quality Evaluation, Pomeranian Medical University in Szczecin, Żołnierska St. 54, 71-210 Szczecin, Poland; janus@pum.edu.pl
3 Faculty of Electrical Engineering, West Pomeranian University of Technology, Sikorskiego Ave. 37, 71-313 Szczecin, Poland; jakub.peksinski@zut.edu.pl (J.P.); Grzegorz.Mikolajczak@zut.edu.pl (G.M.)
4 Department of Organic and Physical Chemistry, Faculty of Chemical Technology and Engineering, West Pomeranian University of Technology, Piastów Ave. 42, 71-065 Szczecin, Poland; jacek.sosnicki@zut.edu.pl (J.G.S.); tomasz.idzik@zut.edu.pl (T.J.I.)
5 Department of Chemical Organic Technology and Polymeric Materials, Faculty of Chemical Technology and Engineering, West Pomeranian University of Technology, Piastów Ave. 42, 71-065 Szczecin, Poland; Beata.Schmidt@zut.edu.pl (B.S.); Krzysztof.Kowalczyk@zut.edu.pl (K.K.)
6 Laboratory for Measurements of Technological Doses, Institute of Nuclear Chemistry and Technology, Dorodna St. 16, 03-195 Warsaw, Poland; M.Walo@ichtj.waw.pl
7 Department of Materials Technology, West Pomeranian University of Technology, 70-310 Szczecin, Poland; akochmanska@zut.edu.pl
* Correspondence: marp@zut.edu.pl

**Abstract:** Poly(xylitol dicarboxylate-co-diol dicarboxylate) elastomers can by synthesized using wide variety of monomers with different chain lengths. Obtained materials are all biodegradable, thermally stable elastomers, but their specific properties like glass transition temperature, degradation susceptibility, and mechanical moduli can be tailored for a specific application. Therefore, we synthesized eight elastomers using a combination of two dicarboxylic acids, namely suberic and sebacic acid, and four different diols, namely ethanediol, 1,3-propanediol, 1,4-buanediol, and 1,5-pentanediol. Materials were further modified by e-beam treatment with a dose of 100 kGy. Materials both before and after radiation modification were tested using tensile tests, gel fraction determination, ^{1}H NMR, and ^{13}C NMR. Thermal properties were tested by Differential Scanning Calorimetry (DSC), Dynamic Thermomechanical Analysis (DMTA) and Thermogravimetric Analysis (TGA). Degradation susceptibility to both enzymatic and hydrolytic degradation was also determined.

**Keywords:** xylitol; biodegradable elastomers; radiation modification; e-beam; mechanical and thermal properties

## 1. Introduction

Due to the high consumption of commodity polymers and the difficulty of their recycling, it is of great importance to develop materials that are not only biodegradable but also at least partially based on monomers obtainable from renewable sources. There is an additional advantage if such polymers react well to radiation modification, which allows to improve their properties in a time-, energy-, and space-saving way that is easy to control and operate [1]. Such materials described in the literature are polylactide [2–4], polycaprolacone, [5,6], poly(butylene succinate) [7], poly(hydroxyalkanoate) [8], poly-(R)-3-hydroxybutyrate [9], and sugar-alcohol-based polyesters [10–12]. Materials belonging

to this last group are elastomers synthesized by the polycondensation reaction of a sugar alcohol, such as xylitol, and a dicarboxylic acid, which leads to obtaining poly(polyol dicarboxylate) polyesters [13–15]. The temperature of glass transition, stress and elongation at break, and time of degradation of those materials can be fine-tuned for a specific use, while their most important characteristics, namely biodegradability and elastomeric behavior, are preserved. This can be done by altering the length of dicarboxylic acid used as monomer [15,16], the hydroxyl group content of sugar alcohol [13,14], stoichiometric ratio of monomers [13,17], or reaction temperature [18]. Most extensively described poly(polyol dicarboxylate) polyesters are materials based on sebacic acid and xylitol [19–21], or glycerol [18,22–25].

Glycerol-based elastomers in particular were extensively tested in terms of possible biomedical applications. Other than the possible application of poly(glycerol sebacate) (PGS) as drug carrier [26], a wide range of potential uses in tissue engineering were discussed in the literature. PGS can be used as scaffold for bone tissue regeneration [23,27], myocardial tissue regeneration [18], hollow conduit guides for treatment of neural defects [22], delivering retinal progenitor cell to the subretinal area [28], treatment of defects in cartilage tissue [25], and regeneration of blood vessels [24].

Poly(xylitol sebacate) (PXS) elastomers also hold significant promise in the biomedical field, for example, tissue-like materials obtained by core/shell electrospinning PXS with poly(vinyl alcohol) as a sacrificial component [20,21].

The properties of sugar-alcohol-based elastomers can be further improved by utilizing a diol as a third monomer, which leads to a poly(polyol dicarboxylate-co-diol dicarboxylate) product. The properties of materials belonging to this group can also by tailored by utilizing different polycondensation times [29], by changing the chain length of dicarboxylic acid [30] or diol [12,31] used for the synthesis, or by changing the hydroxyl group content of the polyol [10,32,33]. Further fine-tuning of their properties can be conducted with 50 to 150 kGy e-beam treatment with doses ranging from 50 to 150 kGy, each leading to slightly different end-product [10,32].

Poly(polyol dicarboxylate-co-diol dicarboxylate) elastomers exhibit a wide range of obtainable characteristics, and modifying those materials with radiation leads to beneficial results. Therefore, we decided to synthesize and perform an e-beam treatment on 8 materials based on xylitol, sebacic and suberic acid, and four different diols as monomers. A radiation dose of 100 kGy was chosen based on previous research [10,32]. Most of these materials, to the best of our knowledge, were never synthesized and radiation-modified before. In comparison with our previous work [10,29,30,32,34], an improved synthesis method was used, which allowed to greatly decrease the cross-linking time from 12 days to about 48 h.

Overall, due to the fact that materials presented in this work react well to radiation, they could see a potential application as polymer boluses for radiotherapy [35,36].

## 2. Materials and Methods

### 2.1. Synthesis of Elastomers

Sigma-Aldrich (St. Louis, MO, USA) was the chemical supplier. All ingredients were reagent grade. The 8 poly(xylitol dicarboxylate-diol dicarboxylate) elastomers were synthesized.

Poly(xylitol suberate-co ethylene suberate) (PXESb) was synthesized using xylitol, suberic acid, and ethanediol. Poly(xylitol suberate-co-propylene suberate) (PXPSb) was synthesized using xylitol, suberic acid, and 1,3-propanediol. Poly(xylitol suberate-co-butylene suberate) (PXBSu) was synthesized using xylitol, suberic acid, and 1,4-butanediol. Poly(xylitol suberate-co-pentylene suberate) (PXPeSu) was synthesized using xylitol, suberic acid, and 1,5-pentanediol.

Poly(xylitol sebacate-co-ethylene sebacate) (PXES) was synthesized using xylitol, sebacic acid, and ethanodiol. Poly(xylitol sebacate-co-propylene sebacate) (PXPS) was synthesized using xylitol, sebacic acid, and 1,3-propanediol. Poly(xylitol sebacate-co-butylene sebacate) (PXBS) was synthesized using xylitol, sebacic acid, and 1,4-butanediol.

Poly(xylitol sebacate-co-pentylene sebacate) (PXPeS) was synthesized using xylitol, sebacic acid, and 1,5-pentanediol.

The synthesis process consists of three steps: 9 h esterification reaction at 150 °C in nitrogen atmosphere in a vacuum evaporator, 3 h polycondensation reaction at 150 °C in low-pressure-atmosphere (100 mBar) in a vacuum evaporator, and cross-linking reaction of materials cast into silicone forms at 150 °C in low-pressure-atmosphere (100 mBar) in a vacuum dryer. The molar ratio of dicarboxylic acid:xylitol:diol was 2:1:1. No catalyst was used. Synthesis was performed in melt—no solvent was used.

### 2.2. Irradiation

E-beam treatment of cross-linked elastomers was done in the Institute of Nuclear Chemistry and Technology (Warsaw, Poland) with an Elektronika 10/10 linear electron accelerator (NPO, Torij, Russia). Parameters were 10 MeV beam, 360 mA average set current, 0.368 m/min sample movement speed, and 100 kGy split into doses of 25 kGy.

## 3. Experimental Methods

### 3.1. Nuclear Magnetic Resonance Spectroscopy (NMR)

The prepolymer chemical structure was ascertained by $^1$H NMR (at 400.1 MHz) and $^{13}$C NMR (at 106.6 MHz), with Bruker DPX III HD (Bruker, Rheinstetten, Germany), with 50 mg sample mass, 0.7 mL of CDCl$_3$ solvent (deuterated chloroform), and internal reference (Tetramethylsilane-TMS). The results analysis was performed with MestReNova 12.0.3 (Mestrelab, Santiago de Compostela, Spain).

### 3.2. Fourier Transform Infrared Spectroscopy (FTIR)

The elastomer chemical structure (prepolymers, cross-linked materials, and e-beam-treated materials) was ascertained with Alpha Spectrometer Bruker (Bruker, Germany), with 2 cm$^{-1}$ resolution and 4000 to 400 cm$^{-1}$ range. The results analysis was performed with Omnic 7.3 (Thermo Electron Corporation, Waltham, MA, USA).

### 3.3. Differential Scanning Calorimetry (DSC)

The thermal behavior of the elastomers (prepolymers, cross-linked materials, and e-beam-treated materials) was tested with Q2500 DSC instrument (TA instruments, New Castle, DE, USA), with heating range −100 to 100 °C, heating rate 10 °C/min, and in nitrogen atmosphere. The results analysis was performed with TA Instruments Universal Analysis 2000, 3.9a (New Castle, DE, USA).

### 3.4. Dynamic Thermomechanical Analysis (DMTA)

The thermomechanical behavior of the elastomers (cross-linked materials and e-beam-treated materials) was tested with DMA Q800 (TA Instruments, New Castle, DE, USA) with 2 °C/min rate of heating, 1 Hz frequency, and −100 to 100 °C temperature range. The results analysis was performed with TA Instruments Universal Analysis 2000, 3.9a (New Castle, DE, USA).

### 3.5. Mechanical Properties

The mechanical behavior of elastomers before and after e-beam treatment was tested with Instron 36 (Norwood, MA, USA), with a crosshead speed of 100/mm/min, 500 N load cell, in relative humidity of 50%, and at 25 °C, according to the standard PN-EN-ISO 526/1:1996.

### 3.6. Gel Fraction

Gel fraction determination was performed on polymer samples (cross-linked, 0.5 g mass) immersed for 5 days in solvent (tetrahydrofuran, THF). Samples after drying (des-

iccator, 14 days, 25 °C, lowered pressure) were weighed. The mass-loss calculation was performed with Equation (1):

$$X = \frac{m_1}{m_0} \times 100\% \tag{1}$$

where $m_1$—sample mass after extraction, $m_0$—sample mass before extraction.

### 3.7. Hydrolytic Degradation

Hydrolytic degradation was performed on UV-sterilized (20 min duration, laminar chamber) 10 mm elastomer discs in a 48-well plate, each covered with PBS (phosphate-buffered saline) (Sigma Aldrich, Poznan, Poland) solution (1.5 mL, 7.1 to 7.2 range of pH). The process took 21 days in 37 °C. The solution was changed, and samples were sterilized again every 2 days. Samples after drying (desiccator, 14 days, 25 °C, lowered pressure) were weighed. The mass-loss calculation was performed with Equation (2):

$$D = \frac{(m_0 - m_1)}{m_0} \times 100\% \tag{2}$$

where $m_0$ is the sample mass pre-degradation, $m_1$ is the sample mass post-degradation, and D is the mass loss.

### 3.8. Enzymatic Degradation

Enzymatic degradation was performed on UV-sterilized (20 min duration, laminar chamber) 10 mm elastomer discs in a 48-well plate, each covered with a solution of porcine lipase in PBS (phosphate-buffered saline) (Sigma Aldrich, Poznan, Poland) (1.5 mL, 7.1 to 7.2 range of PH). The process took 21 days, and took place at 37 °C temperature. The solution was changed, and samples were sterilized again every 2 days. Samples after drying (desiccator, 14 days, 25 °C, lowered pressure) were weighed. The mass-loss calculation was performed with Equation (3):

$$D = \frac{(m_0 - m_1)}{m_0} \times 100\% \tag{3}$$

where $m_0$ is the sample mass pre-degradation, $m_1$ is the sample mass post-degradation, and D is the mass loss.

### 3.9. Thermogravimetric Analysis (TGA)

The thermal stability of the non-radiation-modified cross-linked elastomers was tested with Q500 TGA instrument (TA instruments, New Castle, DE, USA), with heating rate of 10 °C/min, heating range of 25 °C to 600 °C and in dry air atmosphere. Instrument was equipped with platinum crucible, and samples weighed about 15 mg each. The results analysis was performed with TA Instruments Universal Analysis 2000, 3.9a (New Castle, DE, USA).

## 4. Results and Discussion

Table 1 summarizes the elastomer properties and composition, and Figure 1 illustrates the polymer structure.

**Table 1.** Properties and molar composition of poly(xylitol dicarboxylate-co-diol dicarboxylate) pre and post e-beam treatment.

| Material | Molar Composition (Ratio of poly(xylitol dicarboxylate) Blocks to poly(diol dicarboxylate) Blocks) Determined by $^1$H NMR for Prepolymers | Stress at Break (MPa) | Elongation at Break (%) | Modulus at 50% Elongation (MPa) |
|---|---|---|---|---|
| PXESb | 1.33 | 1.01 +/− 0.23 | 62.77 +/− 9.34 | 1.08 +/− 0.19 |
| PXESb (radiation-modified) | - | 1.06 +/− 0.22 | 59.1 +/− 14.9 | 1.03 +/− 0.05 |

<div align="center">Table 1. <em>Cont.</em></div>

| Material | Molar Composition (Ratio of poly(xylitol dicarboxylate) Blocks to poly(diol dicarboxylate) Blocks) Determined by $^1$H NMR for Prepolymers | Stress at Break (MPa) | Elongation at Break (%) | Modulus at 50% Elongation (MPa) |
|---|---|---|---|---|
| PXPSb | 0.51 | 0.96 +/− 0.23 | 67.00 +/− 12.54 | 0.92 +/− 0.05 |
| PXPSb (radiation-modified) | - | 1 +/− 0.078 | 63.62 +/− 3.33 | 1.04 +/− 0.05 |
| PXBSb | 0.27 | 0.56 +/− 0.08 | 88.14 +/− 15.77 | 0.40 +/− 0.07 |
| PXBSb (radiation-modified) | - | 0.78 +/− 0.08 | 88 +/− 16.4 | 0.58 +/− 0.05 |
| PXPeSb | 0.47 | 0.70 +/− 0.09 | 81.68 +/− 7.24 | 0.56 +/− 0.09 |
| PXPeSb (radiation-modified) | - | 0.83 +/− 0.12 | 72 +/− 8.4 | 0.764 +/− 0.02 |
| PXES | 1.02 | 0.58 +/− 0.02 | 84.40 +/− 15.43 | 0.45 +/− 0.09 |
| PXES (radiation-modified) | - | 0.94 +/− 0.22 | 82.3 +/− 13.9 | 0.72 +/− 0.05 |
| PXPS | 0.5 | 1.33 +/− 0.34 | 125.53 +/− 23.19 | 0.60 +/− 0.06 |
| PXPS (radiation-modified) | - | 1.06 +/− 0.22 | 89 +/− 23.09 | 0.74 +/− 0.05 |
| PXBS | 0.44 | 0.72 +/− 0.13 | 107.87 +/− 16.06 | 0.39 +/− 0.10 |
| PXBS (radiation-modified) | - | 0.82 +/− 0.13 | 105 +/− 24.9 | 0.45 +/− 0.07 |
| PXPeS | 0.45 | 0.78 +/− 0.13 | 112.9 +/− 15.28 | 0.42 +/− 0.03 |
| PXPeS (radiation-modified) | - | 0.68 +/− 0.07 | 90.65 +/− 19.35 | 0.54 +/− 0.11 |

where E_100%: Modulus at 100% elongation, E_50%: Modulus at 50% elongation, $\varepsilon$: Elongation at break, $\sigma_r$: Stress at break.
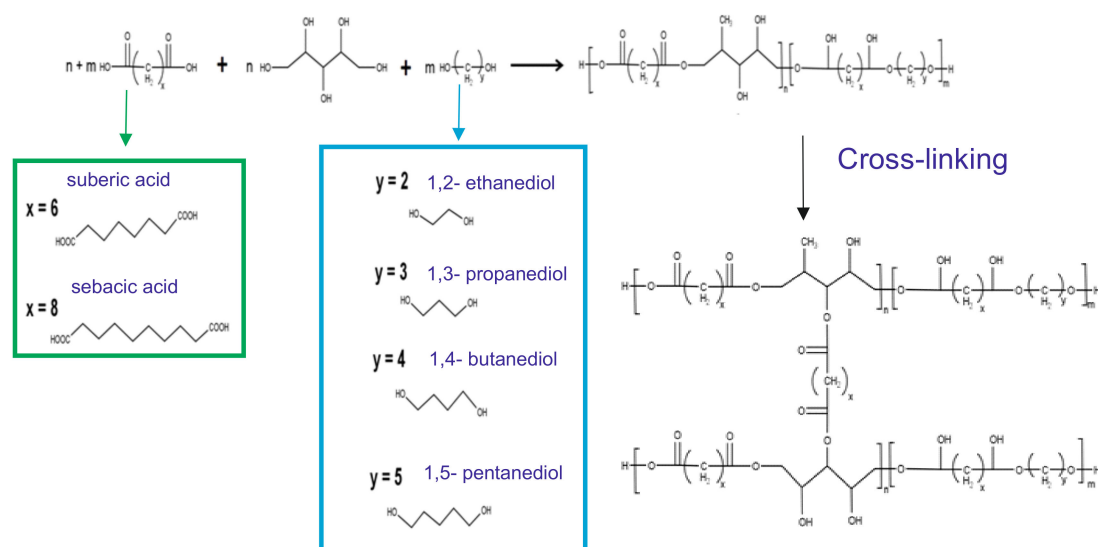


**Figure 1.** Scheme of the poly(xylitol dicarboxylate-co-diol dicarboxylate) synthesis.

### 4.1. Nuclear Magnetic Resonance Spectroscopy (NMR)

The prepolymer chemical structure was ascertained by $^1$H NMR and $^{13}$C NMR. The results are presented in Figure 2, Figure 3, Figure 4, Figure 5.
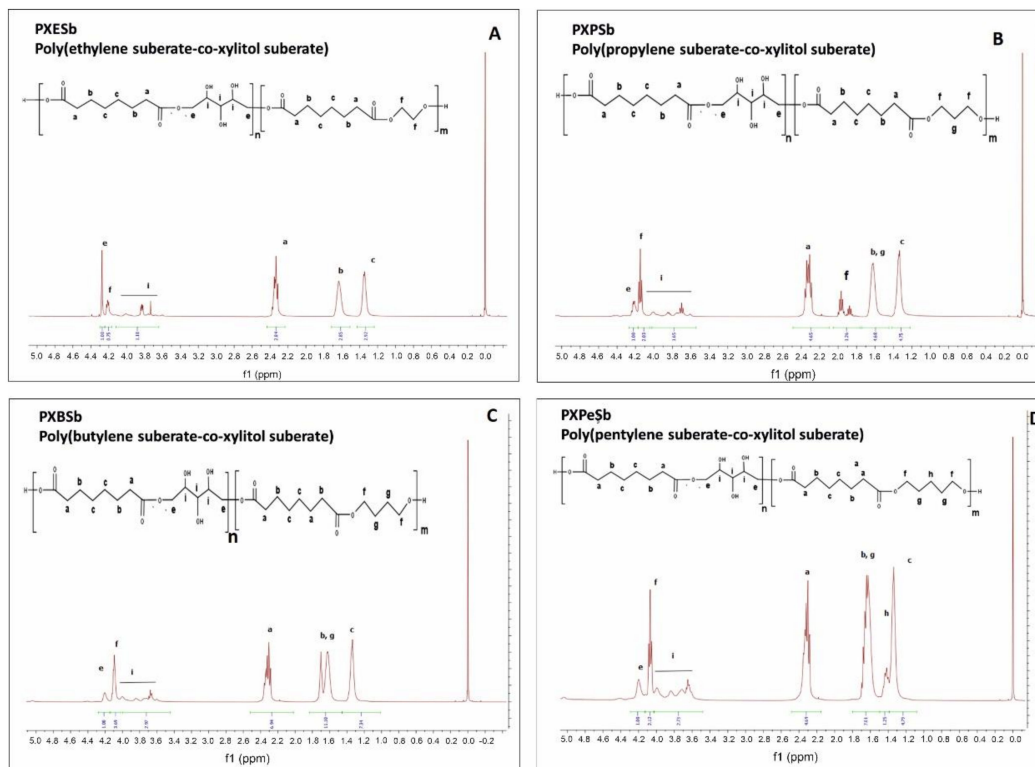


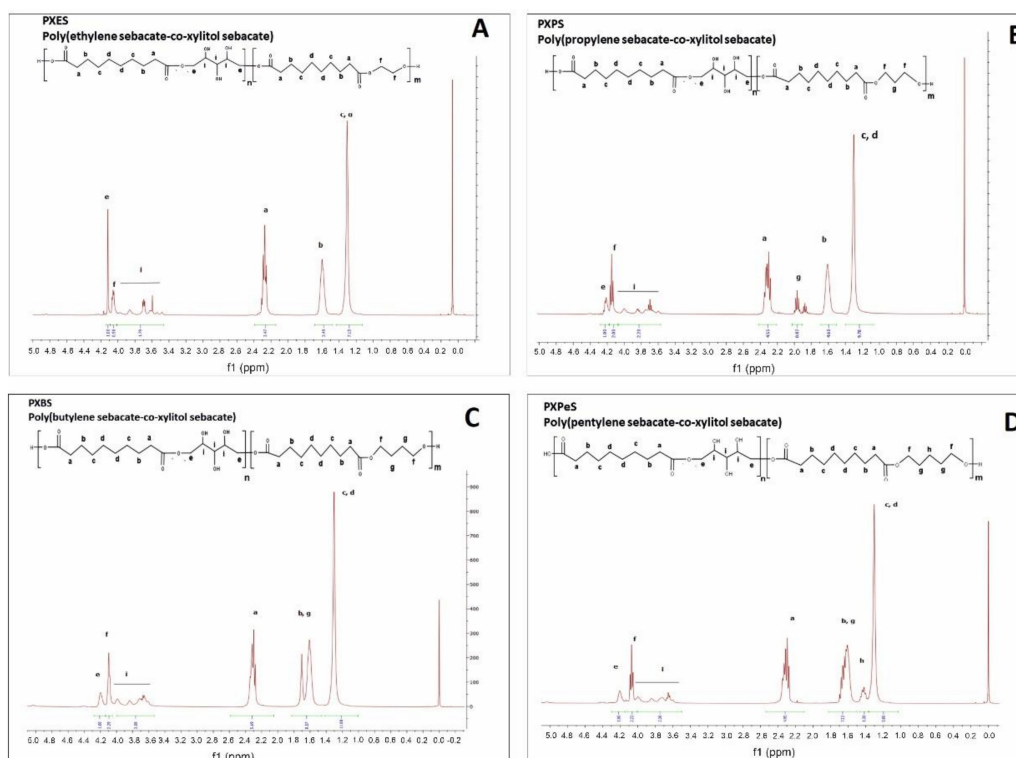**Figure 2.** $^1$H NMR of following prepolymers: PXESb (**A**), PXPSb (**B**), PXBSb (**C**), PXPeSb (**D**).



**Figure 3.** 1H NMR of following prepolymers: PXES (**A**), PXPS (**B**), PXBS (**C**), PXPeS (**D**).
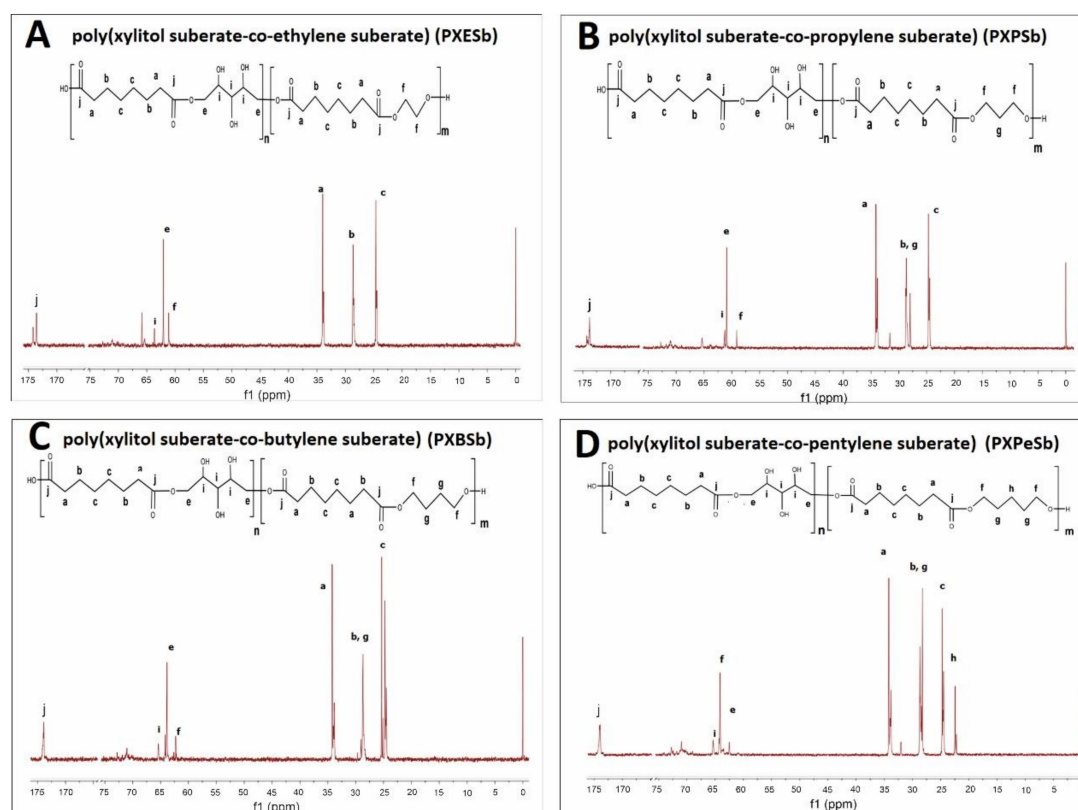
**Figure 4.** $^{13}$C NMR of following prepolymers: PXESb (**A**), PXPSb (**B**), PXBSb (**C**) PXPeSb (**D**) prepolymers.
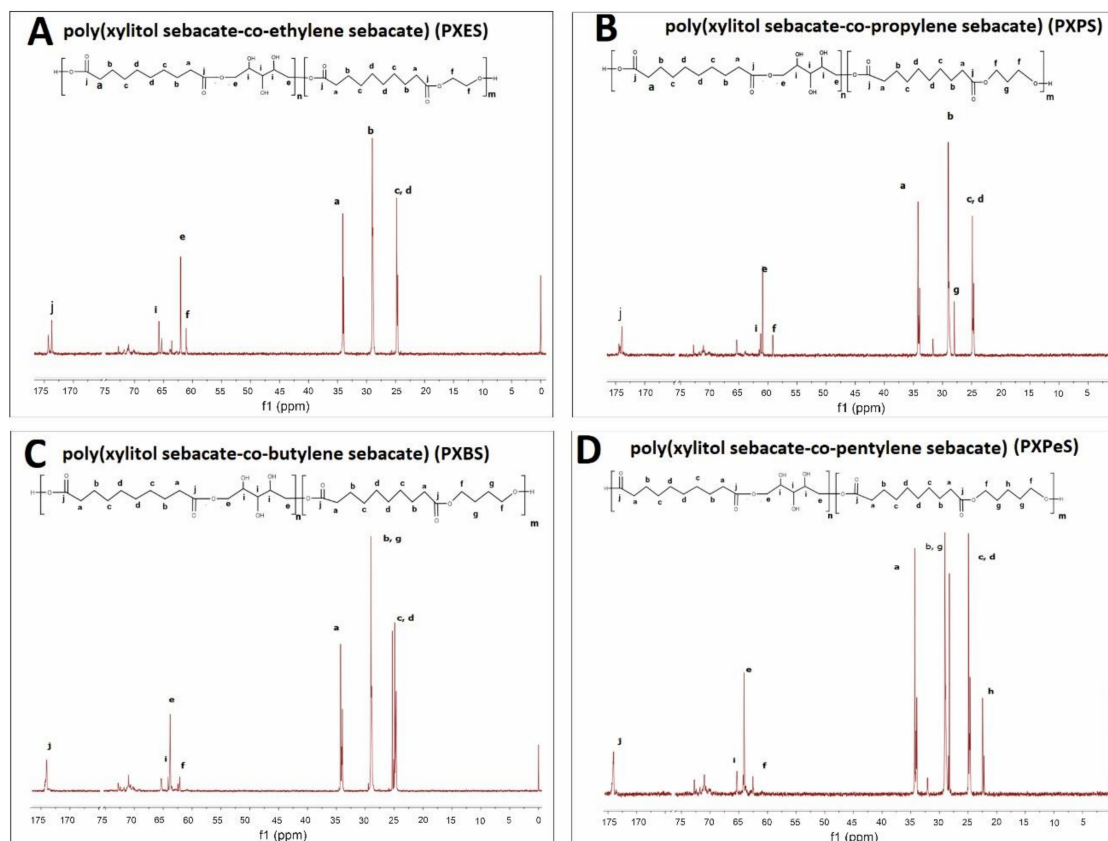


**Figure 5.** $^{13}$C NMR of following prepolymers: PXES (**A**), PXPS (**B**), PXBS (**C**) PXPeS (**D**) prepolymers.

In ${}^1$H NMR, the alkyl groups can be linked to the following signals: 2.4–2.6 ppm—CH2 (a), 1.7 ppm—CH2 (g) and CH2 (b), 1.4 ppm—CH2 (h), 1.2 ppm—CH$_2$ (c) and CH$_2$ (d) Peaks in the range of 3.6 to 4.6 ppm are linked to secondary −OH groups in xylitol. Two signals connected to alkyl groups next to ester bonds can be observed: 4.2 ppm—CH$_2$ (f) (diol-acid ester bond), and 4.4 ppm—CH$_2$ (e) (xylitol-acid ester bond). By dividing the areas of those two signals, the molar composition was calculated.

In ${}^{13}$C NMR, the alkyl groups can be linked to the following signals: 34 ppm—CH$_2$ (a), 29 ppm—CH$_2$ (g) and CH$_2$ (b), 25 ppm—CH$_2$ (c) and CH$_2$ (d), 22 ppm—CH$_2$ (h). The CH$_2$OH (i) groups in xylitol result in a signal at 65 ppm. Two signals connected to alkyl groups next to ester bonds can be observed: 64 ppm—CH$_2$ (f) (diol-acid ester bond), and 62 ppm—CH$_2$ (e) (xylitol-acid ester bond). The carbonyl group results in a signal at 172 ppm.

### 4.2. Fourier Transform Infrared Spectroscopy (FTIR)

The FTIR spectra are presented in Figures 6 and 7. The presence of four groups typical for polyesters based on sugar alcohols can be ascertained: –C–O–C groups give a signal at 1170 cm${}^{-1}$, C=O groups result in a signal at 1725 cm${}^{-1}$, CH$_2$ groups generate a signal at 2930 cm${}^{-1}$, and free –OH groups produce a signal at 3450 cm${}^{-1}$. A lack of polymer-deterioration due to e-beam treatment can be ascertained by the absence of significant differences between the spectra of materials pre and post radiation-modification.
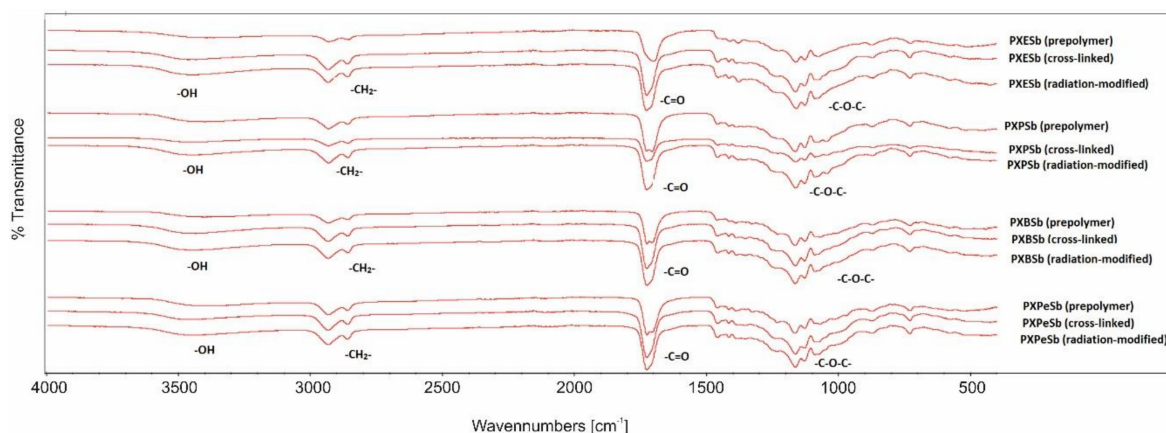


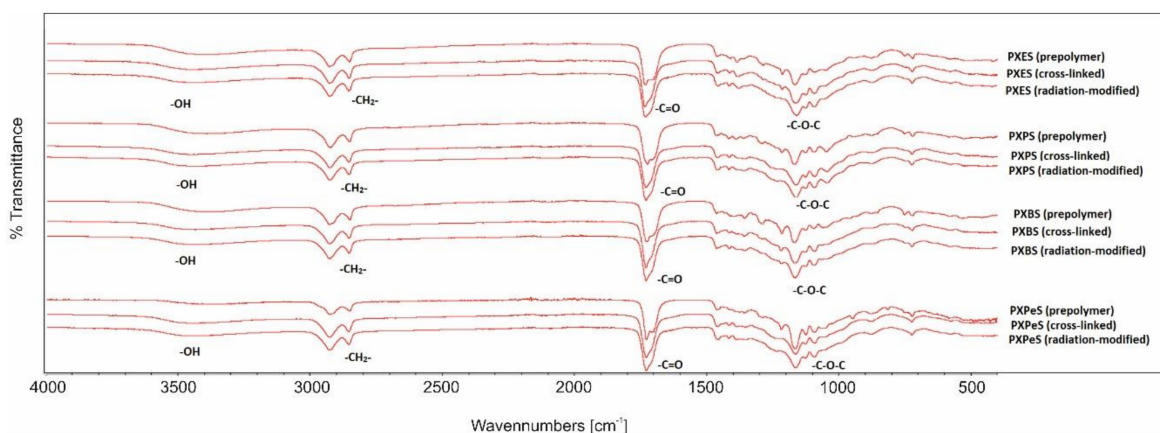**Figure 6.** FTIR spectra of PXESb, PXPSb, PXBSb, PXPeSb prepolymers, cross-linked polymers, and radiation-modified polymers.



**Figure 7.** FTIR spectra of PXES, PXPS, PXBS, prepolymers, cross-linked polymers, and radiation-modified polymers.

The comparison of prepolymer spectra and cross-linked polymers spectra shows a small increase of –C–O–C signal intensities and decrease of –OH signal intensities. This

is due to the formation of ester bonds between –OH groups and unreacted molecules of dicarboxylic acids, which binds the chains together and creates cross-links.

### 4.3. Thermal Properties: Differential Scanning Calorimetry (DSC)

We conducted an analysis and comparison of the thermal properties of elastomers obtained by using different combinations of diols and dicarboxylic acids, and examined how those properties were affected by radiation modification using differential scanning calorimetry. The results are presented in Figures 8 and 9 and in Table 2.
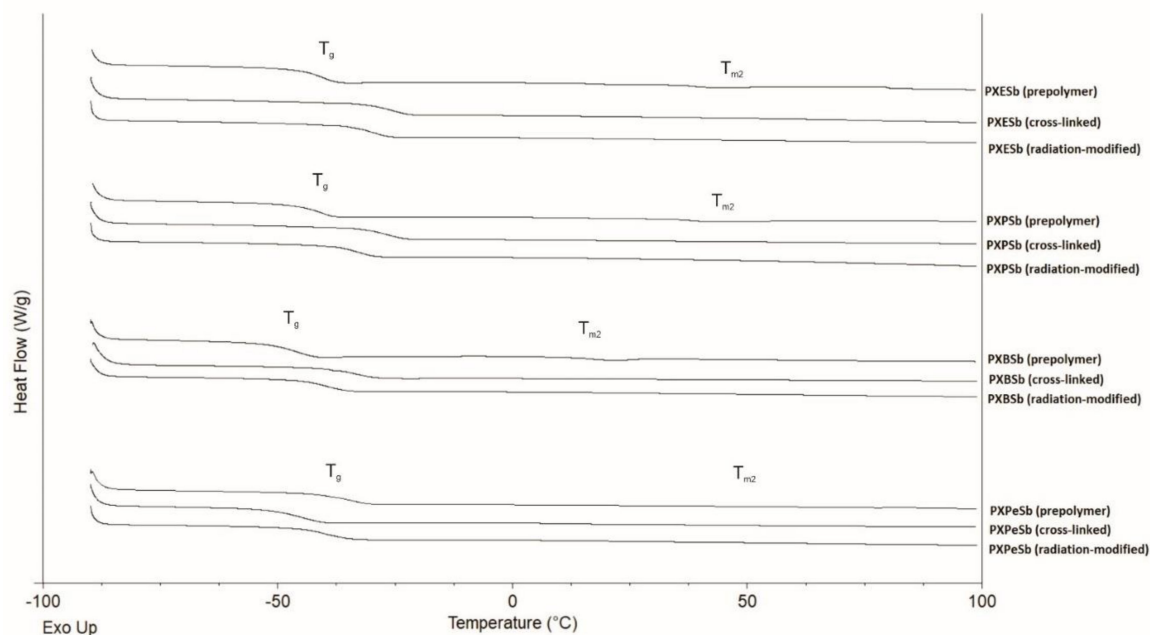


**Figure 8.** DSC thermograms (first-heating) of PXESb, PXPSb, PXBSb, and PXPeSb prepolymers, cross-linked polymers, and radiation-modified polymers.
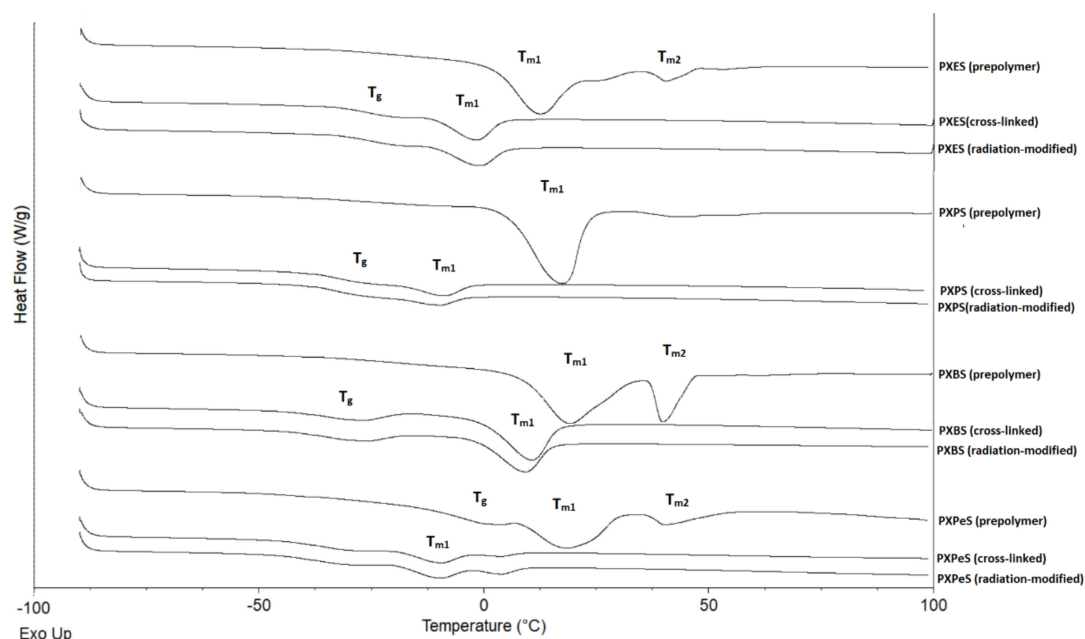


**Figure 9.** DSC thermograms (first-heating) of PXES, PXPS, PXBS, PXPeS prepolymers, cross-linked polymers, and radiation-modified polymers.

**Table 2.** DSC thermal data of poly(xylitol dicarboxylate-co-diol dicarboxylate) before and after irradiation.

| Material | Glass Transition Temperature $T_g$ (°C) | Change in Heat Capacity $\Delta C_p$ (J/g °C) | Melting Temperature $T_{m1}$ (°C) | Melting Enthalpy $H_{m1}$ (J/g) | Melting Temperature $T_{m2}$ (°C) | Melting Enthalpy $H_{m2}$ (J/g) |
|---|---|---|---|---|---|---|
| PXESb prepolymer | −40.3 | 0.69 | - | - | 45.02 | 1.40 |
| PXESb cross-linked | −25.6 | 0.56 | - | - | - | - |
| PXESb (radiation-modified) | −29.3 | 0.57 | - | - | | |
| PXPSb prepolymer | −40.6 | 0.61 | - | - | 44.70 | 2.20 |
| PXPSb cross-linked | −26.3 | 0.51 | - | - | - | - |
| PXPSb (radiation-modified) | −32.9 | 0.53 | - | - | - | - |
| PXBSb prepolymer | −45.9 | 0.67 | - | - | 21.6 | 1.31 |
| PXBSb cross-linked | −32.9 | 0.47 | - | - | - | - |
| PXBSb (radiation-modified) | −39.6 | 0.55 | | | | |
| PXPeSb prepolymer | −34.5 | 0.51 | - | - | 53.9 | 0.42 |
| PXPeSb cross-linked | −44.9 | 0.68 | - | - | - | - |
| PXPeSb (radiation-modified) | −40 | 0.54 | | | | |
| PXES prepolymer | - | - | 12.4 | 33.9 | 40.5 | 3.46 |
| PXES cross-linked | −26 | 0.49 | −1.8 | 10.3 | - | - |
| PXES (radiation-modified) | −25.3 | 0.51 | −1.09 | 9.8 | | |
| PXPS prepolymer | - | - | 17.1 | 45.3 | - | - |
| PXPS cross-linked | −32.5 | 0.40 | −8.4 | 5.1 | - | - |
| PXPS (radiation-modified) | −33.4 | 0.47 | −9.5 | 3.5 | | |
| PXBS prepolymer | - | - | 18.9 | 33.5 | 39.9 | 12.6 |
| PXBS cross-linked | −35.5 | 0.43 | 10.6 | 24.6 | - | - |
| PXBS (radiation-modified) | −34.8 | 0.48 | 9.16 | 17.6 | | |
| PXPeS prepolymer | −4.3 | 0.78 | 19.2 | 20.1 | 40.9 | 5 |
| PXPeS cross-linked | −35.5 | 0.47 | −9.6 | 7.5 | - | - |
| PXPeS (radiation-modified) | −36.2 | 0.50 | −10.5 | 4.2 | 4.3 | 1.4 |

where $\Delta C_p$: Heat capacity change, $T_{m1}$: Melting temperature, $T_g$: Glass transition temperature, $\Delta H_{m1}$: Melting enthalpy.

All samples (except for PXES, PXPS, and PXBS prepolymers) exhibit a glass transition temperature.

Melting temperatures are present for all prepolymers. Although the melting temperature is present, the polymers as a whole do not melt. The melting occurs only in small crystalline regions trapped within the amorphous elastomer network. $T_{m1}$ is the result of the melting of poly(xylitol dicarboxylate) segments, and $T_{m2}$ is the result of the melting of poly(diol dicarboxylate) segments. In all elastomers, the melting temperature $T_{m2}$ disappears after the cross-linking process, In case of sebacic-acid-based elastomers, the melting temperature $T_{m1}$ shifts in the direction of lower values as a result of the cross-linking reaction. the melting enthalpy also decreases.

For elastomers based on suberic acid (except for PXPeSb), glass transition increases due to the cross-linking, and then decreases again as a result of e-beam treatment. This is due to the chain mobility decreasing as a result of cross-linking, and then increasing again as a result of radiation modification. For elastomers based on sebacic acid, glass transition is not present in prepolymers except for PXPeSb.

In sebacic-acid-based elastomers, the glass transition temperature stays within a similar range for both cross-linked and e-beam-treated materials, but the heat capacity increases as a result of radiation modification.

The glass transition temperature also decreases for all the materials with the increase in monomer-chain-length due to the chain mobility decreasing.

### 4.4. Dynamic Thermomechanical Analysis (DMTA)

The relaxation behavior of PXESb, PXPSb, PXBSb, and PXPeSb (Figure 10), and PXES, PXPS, PXBS, and PXPeS (Figure 11), was tested with DMTA. E′ (storage modulus), E″ (loss modulus), and tan delta (loss tangent) were measured as a function of temperature. Materials in a temperature range between −90 and −30 °C are in a glassy state and undergo viscoelastic elastation in a temperature range between −30 and 0 °C. This is associated with glass transition and can be determined by a significant diminishment of storage modulus and presence of loss modulus and loss tangent function maxima. The temperature of glass transition shifts in the direction of lower temperatures with the increase of the diol chain length. Those results coincide with DSC-determined glass transition temperature. PXPeSb material is characterized by substantially higher loss and storage modulus values than other materials, which decrease as a result of radiation modification due to the stabilization of the structure.
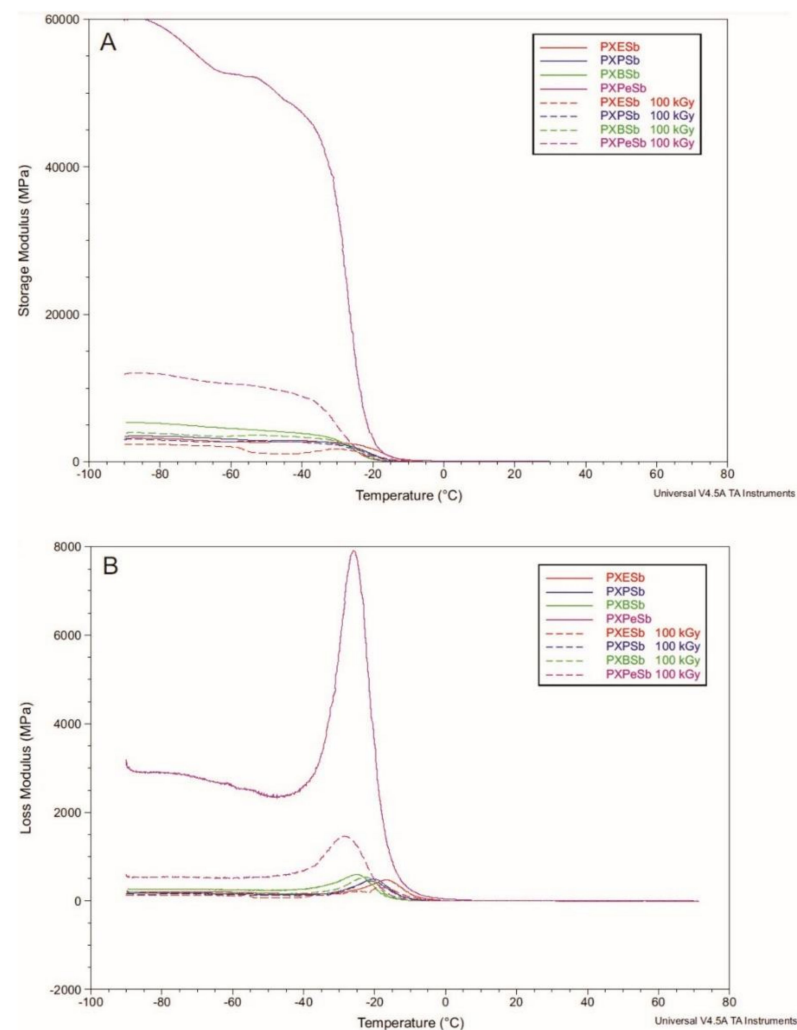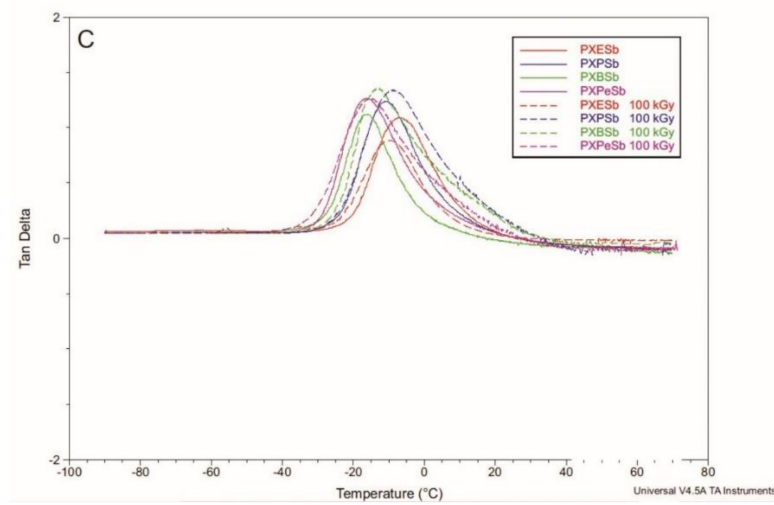


**Figure 10.** *Cont.*

**Figure 10.** (**A**) E′ (storage modulus), (**B**) E″ (loss modulus), and (**C**) loss tangent tested by DMTA for PXESb, PXPSb, PXBSb, and PXPeSb.
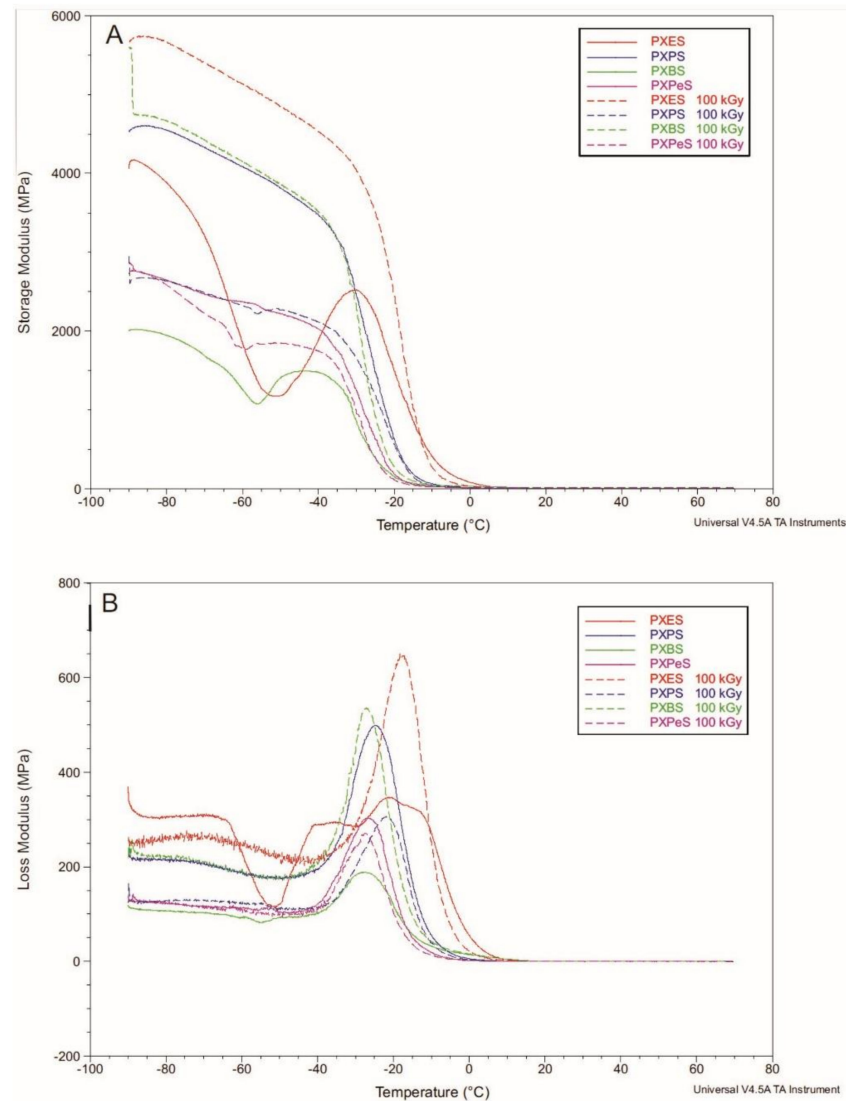


**Figure 11.** *Cont*.

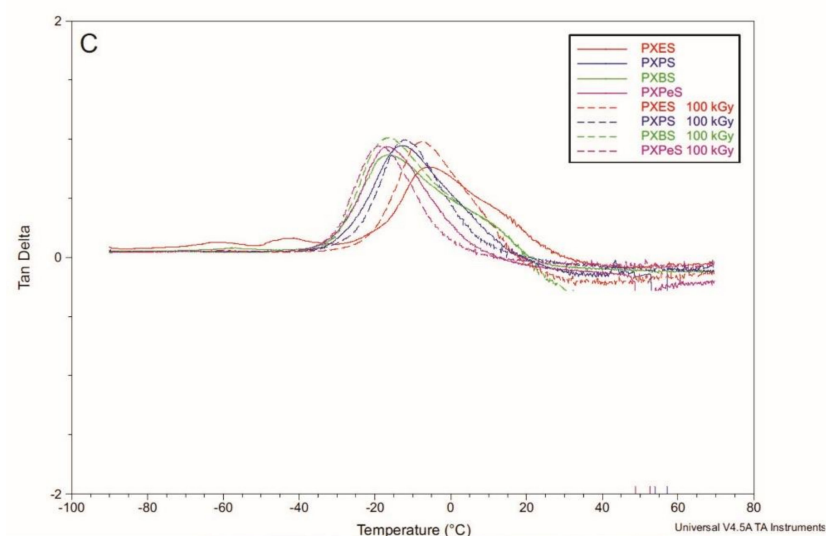**Figure 11.** (**A**) E′ (storage modulus), (**B**) E″ (loss modulus), and (**C**) loss tangent tested by DMTA for PXES, PXPS, PXBS, and PXPeS.

PXES and PXBS materials show a significant decrease followed by an increase of storage modulus at −60 °C, which is before glass transition, and in case of PXES, a second peak of the loss function at −60 °C is present. This can be linked to non-cross-linked end-chain-fragments trapped within an amorphous cross-linked phase. The structure stabilizes after e-beam treatment, and this sharp decrease is no longer present. For radiation-modified PXPS and PXPeS materials, however, a slight decrease of storage modulus before glass transition can be seen, which was not present in non-modified materials. This could be an indication of some degradation of those materials taking place.

This change in storage modulus after e-beam treatment is mirrored by the change in stress at break determined by tensile tests. PXES and PXBS materials, which stabilize as a result of radiation, are also characterized by an increase of stress at break as a result of e-beam treatment. However, for PXPS and PXPeS materials, which show signs of degradation as a result of irradiation, stress at break decreases.

*4.5. Mechanical Properties*

Tensile tests were performed to test and compare mechanical properties of xylitol-based elastomers synthesized with combination of different diols and dicarboxylic acids Another goal was determining whether performing the radiation modification results in a beneficial alteration of elastomer properties. The results of tensile tests are presented in Figure 12 and Table 1. PXPS has the highest elongation at stress at break, while PXESb has the highest modulus at 50% elongation. Radiation modification leads to an increase in modulus at 50% elongation for all the materials with the exception of PXESb, and the increase of stress at break for PXPSb, PXBSb, PXPeSb, PXES, and PXBS. Elongation at break decreases due to e-beam treatment, which is typical for radiation modification [1]. Overall, all materials except for PXESb exhibit some improvement in their properties as a result of e-beam treatment.
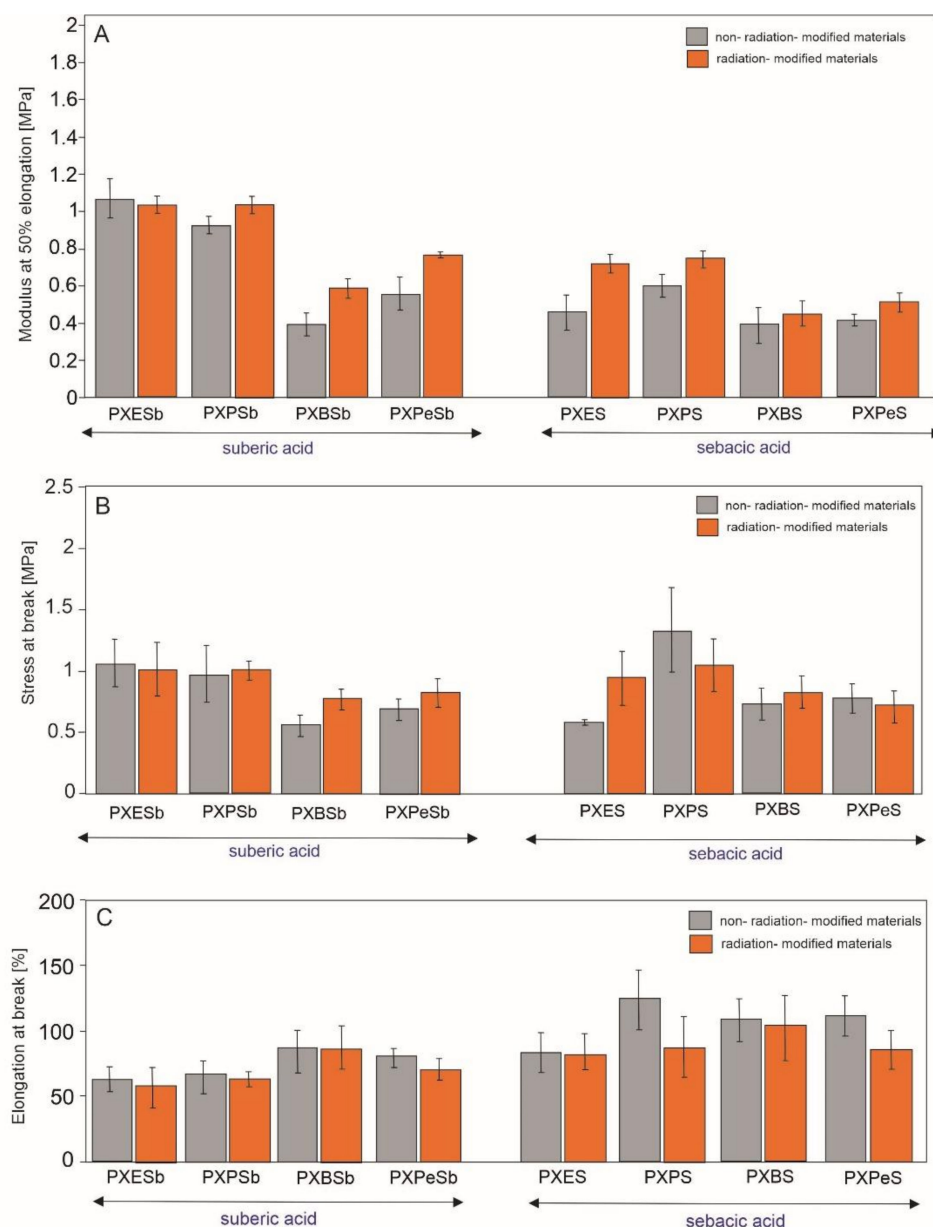
**Figure 12.** Mechanical properties of PXESb, PXPSb, PXBSb, PXPeSu and PXES, PXPS, PXBS, PXPeS non-radiation-modified materials (gray) and radiation-modified materials (orange): tangent modulus at 50% elongation (**A**), stress at break (**B**), and elongation at break (**C**).

*4.6. Gel Fraction*

The results of gel fraction determination are presented in Figure 13. The gel fraction content of non-radiation-modified materials is within a range of 70–88%, with PXESb having the highest gel fraction content. The gel fraction content increases only for PXPSb and PXBSb as a result of radiation modification, while it decreases for the rest of the materials. There is no correlation between the change of gel content and other properties of the elastomers.
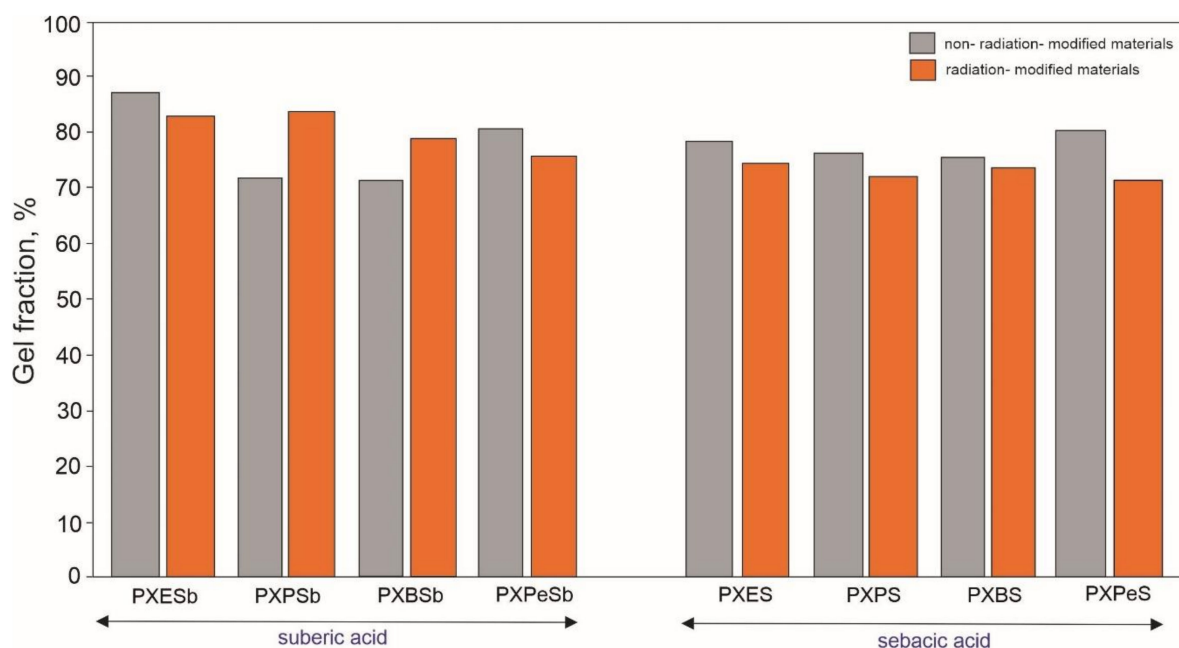
**Figure 13.** Gel fraction results for PXESb, PXPSb, PXBSb, PXPeSb and PXES, PXPS, PXBS, PXPeS non-radiation-modified materials (gray) and radiation-modified materials (orange).

### 4.7. Biodegradation

Biodegradation tests were performed to test how the monomer chain length and subsequent e-beam treatment affect the materials' susceptibility to both enzymatic and hydrolytic degradation. The results are presented in Figure 14. Materials based on suberic acid and ethanediol-1,3-propanediol-, and 1,4-butanediol are most susceptible to hydrolytic degradation, with mass loss in the range of 4–5.5%. Mass loss of the rest of the materials is significantly lower and about 3%. Addition of the enzyme to the degradation solution also leads to significant increase in mass loss. Materials based on 1,4-butanediol are most susceptible to such degradation, while materials based on 1,5-pentanediol are least susceptible. There is a significant increase in the degradation susceptibility of materials due to e-beam treatment.
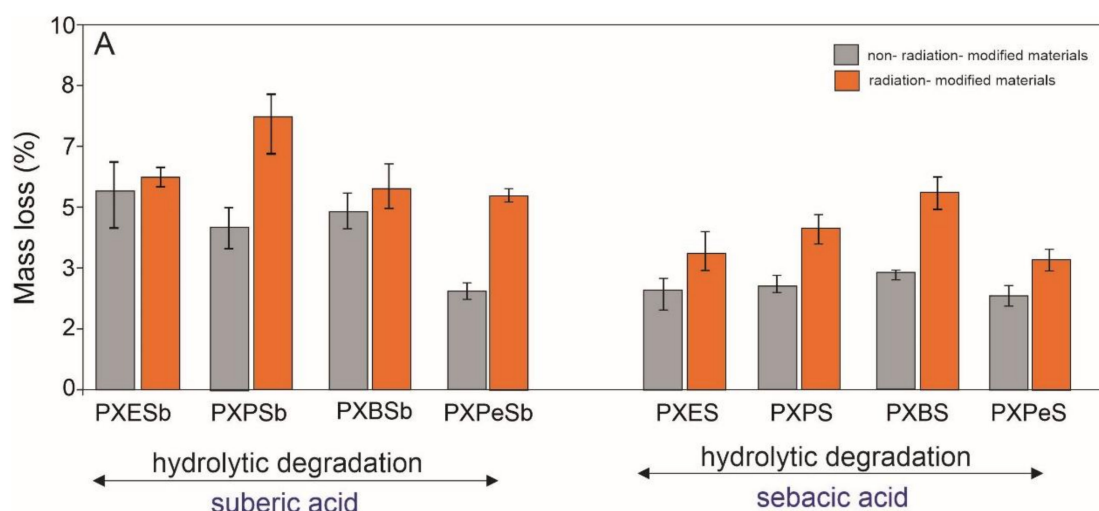


**Figure 14.** *Cont*.
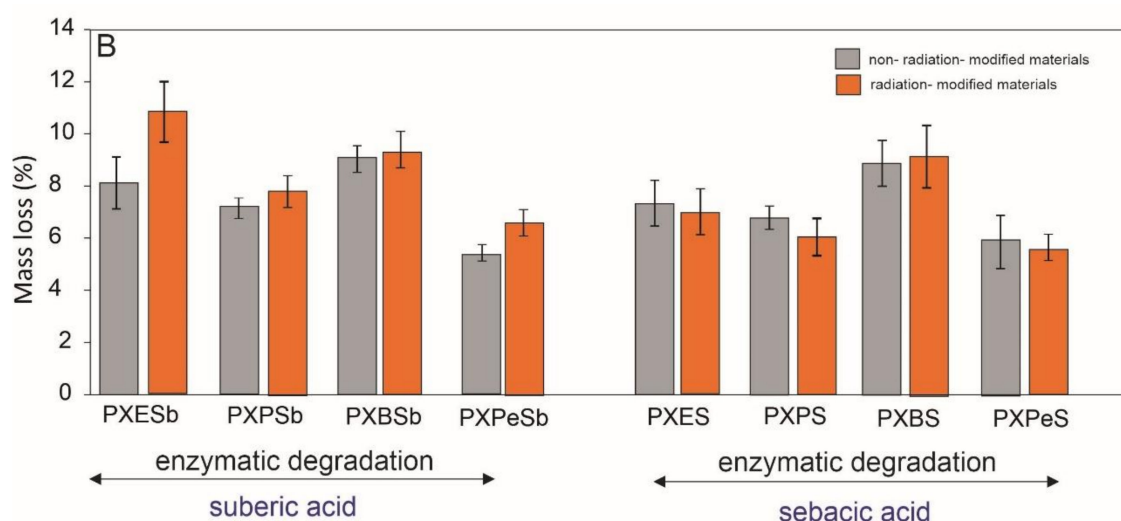
**Figure 14.** Hydrolytic (**A**) and enzymatic degradation (**B**) of PXESb, PXPSb, PXBSb, PXPeSb and PXES, PXPS, PXBS, PXPeS non-radiation-modified materials (gray) and radiation-modified materials (orange).

### 4.8. Thermogravimetric Analysis (TGA)

The thermal stability of the elastomers was tested by TGA. The results are presented in Figure 15. All materials have thermal stability up to 250 °C, which is both significantly higher than the foreseeable temperature of use and the temperature during synthesis and cross-linking. Materials start to degrade above 250 °C. Three steps of material degradation can be observed. Step 1 at about 250–300 °C leads to about 3.2% mass loss and is possibly due to the impurities present in the materials. Step 2 starting at 300 °C and ending at 470 °C is due to the decomposition of the polymer, and leads to 86% mass loss. Charred remains of the polymer remain relatively stable between 470 and 570 °C, and evaporate completely at temperatures between 570 and 600 °C (step 3) The function of mass loss versus temperature is similar for all the materials.
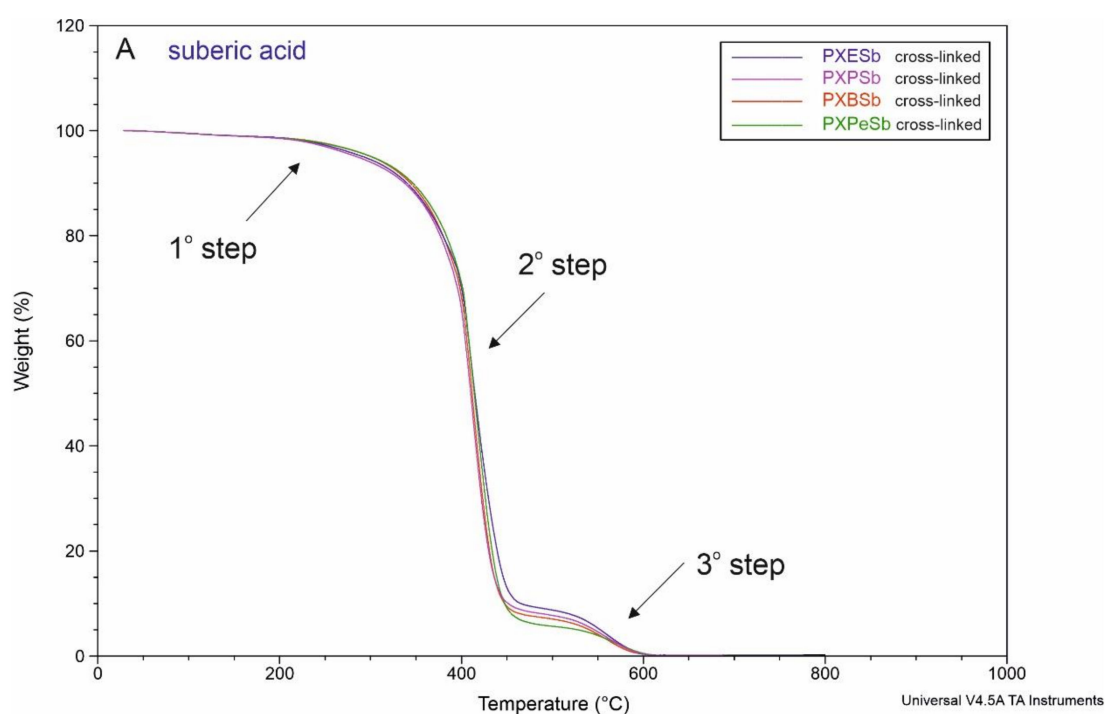


**Figure 15.** *Cont.*
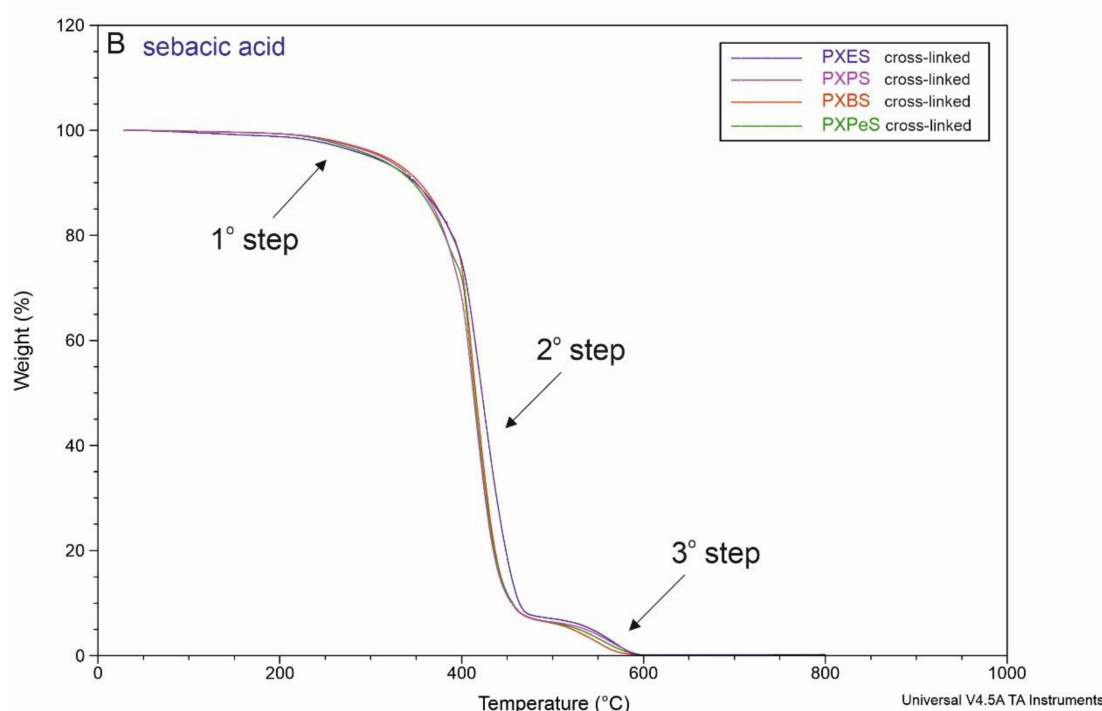
**Figure 15.** Thermogravimetric analysis (TGA) of PXESb, PXPSb, PXBSb, PXPeSb (**A**) and PXES, PXPS, PXBS, PXPeS (**B**) after synthesis.

## 5. Conclusions

Eight elastomers based on two dicarboxylic acids, namely suberic and sebacic acid, and four different diols were synthesized. Materials were modified by e-beam treatment, and a positive effect of such modification on mechanical characteristics was confirmed for all the materials except PXESb. $^{1}$H NMR and $^{13}$C NMR delivered information about the polymer structure and allowed the calculation of a molar composition of poly(xylitol dicarboxylate) to poly(diol dicarboxylate) segments of obtained materials. FTIR was used to confirm the cross-linking process taking place and to determine that the polymer structure does not deteriorate as a result of radiation modification. Thermal properties were tested by DSC and DMTA analyses, and the results obtained from these two methods complement each other well. Elastomers were also determined to have good thermal stability by TGA analysis. Materials were also characterized by good susceptibility to both enzymatic and hydrolytic degradation, which was further enhanced by e-beam treatment. Overall, it was determined that the properties of poly(xylitol-dicarboxylate-co-diol dicarboxylate) can be tailored for a specific application. This application could foreseeably be polymeric boluses for radiotherapy treatment. Materials described in this work are good candidates for such application because of their very good response to the influence of radiation, wide range of possible to obtain mechanical properties, thermal stability, and ease of disposal (due to biodegradability).

**Institutional Review Board Statement:** Not applicable.

**Informed Consent Statement:** Not applicable.

**Data Availability Statement:** The data presented in this study is available on request from the corresponding authors.

**Conflicts of Interest:** The authors declare no conflict of interest.

## References

1. Drobny, J.G. *Ionizing Radiation and Polymers: Principles, Technology, and Applications*; Elsevier: Amsterdam, The Netherlands, 2012.
2. Minh Quynh, T.; Mitomo, H.; Yoneyama, M.; Quoc Hien, N. Properties of Radiation-Induced Crosslinking Stereocomplexes Derived From Poly(L-Lactide) and Different Poly(D-Lactide) Tran. *Polym. Eng. Sci.* **2009**, *49*, 970–976. [CrossRef]
3. Nagasawa, N.; Kasai, N.; Yagi, T.; Yoshii, F.; Tamada, M. Radiation-induced crosslinking and post-processing of poly(l-lactic acid) composite. *Radiat. Phys. Chem.* **2011**, *80*, 145–148. [CrossRef]
4. Huang, Y.; Gohs, U.; Müller, M.T.; Zschech, C.; Wiessner, S. Electron beam treatment of polylactide at elevated temperature in nitrogen atmosphere. *Radiat. Phys. Chem.* **2019**, *159*, 166–173. [CrossRef]
5. Changyu, H.; Xianghai, R.; Kunyu, Z.; Zhuang, Y.; Dong, L. Thermal and Mechanical Properties of Poly(e-caprolactone) Crosslinked with g Radiation in the Presence of Triallyl Isocyanurate. *J. Appl. Polym. Sci.* **2010**, *116*, 2658–2667.
6. Zhu, G.; Liang, G.; Xu, Q.; Yu, Q. Shape-memory effects of radiation crosslinked Poly($\varepsilon$-caprolactone). *J. Appl. Polym. Sci.* **2003**, *90*, 1589–1595. [CrossRef]
7. Suhartini, M.; Mitomo, H.; Nagasawa, N.; Yoshii, F.; Kume, T. Radiation crosslinking of poly(butylene succinate) in the presence of low concentrations of trimethallyl isocyanurate and its properties. *J. Appl. Polym. Sci.* **2003**, *88*, 2238–2246. [CrossRef]
8. Ashby, R.D.; Cromwick, A.M.; Foglia, T.A. Radiation crosslinking of a bacterial medium-chain-length poly(hydroxyalkanoate) elastomer from tallow. *Int. J. Biol. Macromol.* **1998**, *23*, 61–72. [CrossRef]
9. Bergmann, A.; Teßmar, J.; Owen, A. Influence of electron irradiation on the crystallisation, molecular weight and mechanical properties of poly-(R)-3-hydroxybutyrate. *J. Mater. Sci.* **2007**, *42*, 3732–3738. [CrossRef]
10. Piatek-Hnat, M.; Bomba, K.; Peksiński, J.; Kozłowska, A.; Sośnicki, J.G.; Idzik, T.J. Effect of e-beam irradiation on thermal and mechanical properties of ester elastomers containing multifunctional alcohols. *Polymers* **2020**, *12*, 1043. [CrossRef] [PubMed]
11. Piatek-Hnat, M.; Bomba, K.; Peksiński, J.; Kozłowska, A.; Sośnicki, J.G.; Idzik, T.J.; Piwowarska, D.; Janik, J. Influence of e-beam irradiation on the physicochemical properties of poly(polyol succinate-co-butylene succinate) ester elastomers. *Materials* **2020**, *13*, 3196. [CrossRef] [PubMed]
12. Piatek-Hnat, M.; Bomba, K.; Kowalski-Stankiewicz, J.P.; Pęksiński, J.; Kozłowska, A.; Sośnicki, J.G.; Idzik, T.J.; Schmidt, B.; Kowalczyk, K.; Walo, M.; et al. Physical Effects of Radiation Modification of Biodegradable Xylitol-Based Materials Synthesized Using a Combination of Different Monomers. *Polymers* **2021**, *13*, 1041. [CrossRef]
13. Bruggeman, J.P.; de Bruin, B.J.; Bettinger, C.J.; Langer, R. Biodegradable poly(polyol sebacate) polymers. *Biomaterials* **2008**, *29*, 4726–4735. [CrossRef] [PubMed]
14. Ning, Z.Y.; Zhang, Q.S.; Wu, Q.P.; Li, Y.Z.; Ma, D.X.; Chen, J.Z. Efficient synthesis of hydroxyl functioned polyesters from natural polyols and sebacic acid. *Chin. Chem. Lett.* **2011**, *22*, 635–638. [CrossRef]
15. Dasgupta, Q.; Chatterjee, K.; Madras, G. Combinatorial approach to develop tailored biodegradable poly(xylitol dicarboxylate) polyesters. *Biomacromolecules* **2014**, *15*, 4302–4313. [CrossRef]
16. Firoozi, N.; Kang, Y. A Highly Elastic and Autofluorescent Poly(xylitol-dodecanedioic Acid) for Tissue Engineering. ACS Biomater. *Sci. Eng.* **2019**, *5*, 1257–1267.
17. Ma, P.; Li, T.; Wu, W.; Shi, D.; Duan, F.; Bai, H.; Dong, W.; Chen, M. Novel poly(xylitol sebacate)/hydroxyapatite bio-nanocomposites via one-step synthesis. *Polym. Degrad. Stab.* **2014**, *110*, 50–55. [CrossRef]
18. Chen, Q.Z.; Bismarck, A.; Hansen, U.; Junaid, S.; Tran, M.Q.; Harding, S.E.; Ali, N.N.; Boccaccini, A.R. Characterisation of a soft elastomer poly(glycerol sebacate) designed to match the mechanical properties of myocardial tissue. *Biomaterials* **2008**, *29*, 47–57. [CrossRef] [PubMed]
19. Moorhoff, C.; Li, Y.; Cook, W.D.; Braybrook, C.; Chen, Q.Z. Characterization of the prepolymer and gel of biocompatible poly(xylitol sebacate) in comparison with poly(glycerol sebacate) using a combination of mass spectrometry and nuclear magnetic resonance. *Polym. Int.* **2015**, *64*, 668–688. [CrossRef]
20. Li, Y.; Thouas, G.A.; Chen, Q. Novel elastomeric fibrous networks produced from poly(xylitol sebacate)2:5 by core/shell electrospinning: Fabrication and mechanical properties. *J. Mech. Behav. Biomed. Mater.* **2014**, *40*, 210–221. [CrossRef]
21. Li, Y.; Chen, Q.Z. Fabrication of mechanically tissue-like fibrous poly(xylitol sebacate) using core/shell electrospinning technique. *Adv. Eng. Mater.* **2015**, *17*, 324–329. [CrossRef]
22. Sundback, C.A.; Shyu, J.Y.; Wang, Y.; Faquin, W.C.; Langer, R.S.; Vacanti, J.P.; Hadlock, T.A. Biocompatibility analysis of poly(glycerol sebacate) as a nerve guide material. *Biomaterials* **2005**, *26*, 5454–5464. [CrossRef] [PubMed]
23. Zaky, S.H.; Lee, K.W.; Gao, J.; Jensen, A.; Verdelis, K.; Wang, Y.; Almarza, A.J.; Sfeir, C. Poly (glycerol sebacate) elastomer supports bone regeneration by its mechanical properties being closer to osteoid tissue rather than to mature bone. *Acta Biomater.* **2017**, *54*, 95–106. [CrossRef] [PubMed]

24. Motlagh, D.; Yang, J.; Lui, K.Y.; Webb, A.R.; Ameer, G.A. Hemocompatibility evaluation of poly(glycerol-sebacate) in vitro for vascular tissue engineering. *Biomaterials* **2006**, *27*, 4315–4324. [CrossRef]

25. Kemppainen, J.M.; Hollister, S.J. Tailoring the mechanical properties of 3D-designed poly(glycerol sebacate) scaffolds for cartilage applications. *J. Biomed. Mater. Res.—Part A* **2010**, *94*, 9–18. [CrossRef] [PubMed]

26. Sun, Z.J.; Chen, C.; Sun, M.Z.; Ai, C.H.; Lu, X.L.; Zheng, Y.F.; Yang, B.F.; Dong, D.L. The application of poly (glycerol-sebacate) as biodegradable drug carrier. *Biomaterials* **2009**, *30*, 5209–5214. [CrossRef]

27. Zaky, S.H.; Lee, K.W.; Gao, J.; Jensen, A.; Close, J.; Wang, Y.; Almarza, A.J.; Sfeir, C. Poly(Glycerol Sebacate) elastomer: A novel material for mechanically loaded bone regeneration. *Tissue Eng.—Part A* **2014**, *20*, 45–53. [CrossRef]

28. Neeley, W.L.; Redenti, S.; Klassen, H.; Tao, S.; Desai, T.; Young, M.J.; Langer, R. A microfabricated scaffold for retinal progenitor cell grafting. *Biomaterials* **2008**, *29*, 418–426. [CrossRef] [PubMed]

29. Piatek-Hnat, M.; Bomba, K.; Peksiński, J. Synthesis and selected properties of ester elastomer containing sorbitol. *Appl. Sci.* **2020**, *10*, 1628. [CrossRef]

30. Piątek-Hnat, M.; Sładkiewicz, P.; Bomba, K.; Pęksiński, J.; Kozłowska, A.; Sośnicki, J.; Idzik, T. Tailoring the Physico-Chemical Properties of Poly(xylitol-dicarboxylate-co-butylene dicarboxylate) Polyesters by Adjusting the Cross-Linking Time. *Polymers* **2020**, *12*, 1493. [CrossRef] [PubMed]

31. Kavimani, V.; Jaisankar, V. Synthesis and Characterisation of Sorbitol Based Copolyesters for Biomedical Applications. *J. Phys. Sci. Appl.* **2014**, *4*, 507–515.

32. Piątek-Hnat, M.; Bomba, K. The influence of of cross-linking process on the physicochemical properties of new copolyesters containing xylitol. *Mater. Today Commun.* **2020**, *25*, 1541. [CrossRef]

33. Hu, J.; Gao, W.; Kulshrestha, A.; Gross, R.A. "Sweet polyesters": Lipase-catalyzed condensation—Polymerizations of alditols. *Macromolecules* **2006**, *39*, 6789–6792. [CrossRef]

34. Piatek-Hnat, M.; Bomba, K.; Pęksiński, J. Structure and properties of biodegradable poly (xylitol sebacate-co-butylene sebacate) copolyester. *Molecules* **2020**, *25*, 1541. [CrossRef] [PubMed]

35. Lukowiak, M.; Boehlke, M.; Matias, D.; Jezierska, K.; Piatek-Hnat, M.; Lewocki, M.; Podraza, W.; El Fray, M.; Kot, W. Use of a 3D printer to create a bolus for patients undergoing tele-radiotherapy. *Int. J. Radiat. Res.* **2016**, *14*, 287–295. [CrossRef]

36. Jezierska, K.; Sękowska, A.; Podraza, W.; Gronwald, H.; Łukowiak, M. The effect of ionising radiation on the physical properties of 3D-printed polymer boluses. *Radiat. Environ. Biophys.* **2021**. [CrossRef] [PubMed]

# Influence of the addition of citric acid on the physico-chemical properties of poly(sorbitol sebacate-*co*- butylene sebacate)

Marta Piątek-Hnat

**Abstract**— The article presents the results of the physicochemical properties of poly(sorbitol sebacate- co-butylene sebacate) (PSBS) obtained with 0.25; 0.5; 0.75; 1 mol of citric acid (KC). It was shown that PSBS obtained with 0.25 and 0.5 mol KC is characterized by the most optimal mechanical and thermal properties. As a result of the study, it was found that the use of sorbitol and citric acid allows obtaining ester materials with properties that can meet the  material requirements of products for mwdical applications (scaffolds, drug delivery systems). The poly(sorbiotol sebacate- co- butylene sebacate)  are hydrophilic and, despite the high content of the gel fraction (high degree of cross-linking), are susceptible to hydrolytic degradation.

**Index Terms**— ester elastomers, polycondensation, citric acid, physico-chemical properties, sugar alcohol, cross-linking

— — — — — — — — — ◆ — — — — — — — — —

## 1 INTRODUCTION

Poly(sorbitol sebacate- co- butylene sebacate) PSBS is a material obtained as a result of the reaction of sebacic acid 1,4-butanediol with a sugar alcohol - sorbitol. The use of products derived from natural sources for the synthesis of new materials is of great interest, and therefore many scientists conduct research in this direction by modifying the composition of materials and the types of monomers used. PSBS is characterized by good physicochemical properties while being susceptible to hydrolytic degradation, which allows application in the direction of medical applications. The aim of the work was to obtain poly(sorbitol sebacate- co-butylene sebacate) in the mass polycondensation reaction using sebacic acid as a monomer, sugar alcohol-sorbitol, 1,4-butanediol and as a modifier - citric acid with various molar participation. The modifiers used were aimed at improving the properties of poly(sorbitol sebacate- co- butylene sebacate). The resulting polymers with variable molar participation were characterized for changes in physicochemical properties. Due to the multifunctionality of the sorbitol used, the obtained elastomers were characterized by a high degree of cross-linking, also dependent on the molar proportion of citric acid. [1-9].

## 2. MATERIAL AND METHODS

### 2.1 Synthesis of poly(sorbitol sebacate-co-butylenesebacate) with citric acid

The technological process of obtaining ester elastomers is three-stage. In the first stage, an esterification reaction takes place between sebacic acid (Sigma-Aldrich, Poland), sorbitol (Sigma-Aldrich, Poland), butylene glycol (1,4-butanediol) (Sigma-Aldrich, Poland) citric acid (Fluka) catalyzed by Ti(BuO)$_4$ (Fluka), at a temperature of 150- 160 ºC. In the second step, polycondensation occurs under reduced pressure. The

third step leading to obtaining a crosslinked elastomer takes place in a vacuum dryer [10-11].

### 2.2 Methods

Determination of gel fraction of elastomers was made by the extraction method. PN-EN 579: 2001. Material samples (about 1 g) were placed in Schott type P2 crucible and subjected to extraction in boiling tetrahydrofuran (100 cm$^3$) for 3 hours. After extraction, the samples were dried in a vacuum oven at 25 °C for 3 hours and then in a desiccator. Three determinations were made for each elastomer. The content of gel fractions was calculated from formula (1) as the mean of three measurements:

$$X = m1/m0 \ 100\% \tag{1}$$

where: m1 - sample mass after extraction, m0 - sample mass before extraction

Mechanical tests were carried out with an Instron 3366 instrunents equipped with a 500 N load cell in accordance with standard PN-EN-ISO 527/1:1996 (crosshead speed of 100 mm/min, at 25 ºC and 50 % of relative humidity)

The stady of the contact angle of the surface of the materials was made with deionized water using the  Haas Contact Angle Analyzer apparatus on the Phoenix Mini model.

The method involves placing a drop of water on the surface of the material and determining the angle between them. Thermal properties were determined using differential scanning calorimetry (DSC) (Q100, TA Instruments apparatus). The measurement was carried out in a cycle heating in the temperature range from -100 to 150 ºC.
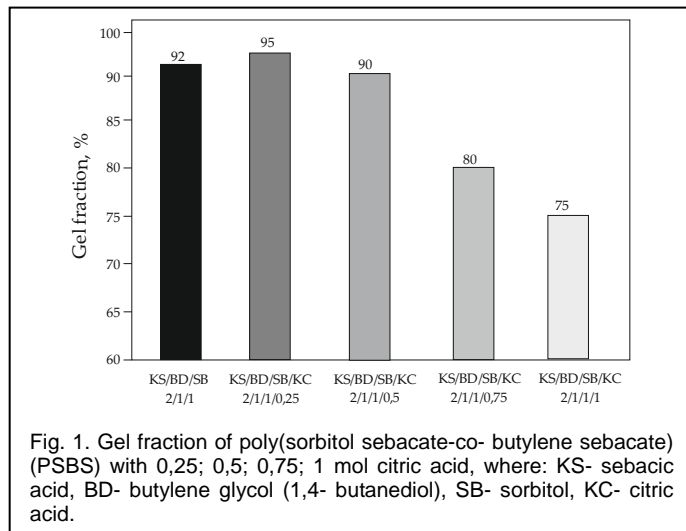
## 3. RESULTS AND DISCUSSION

Figure 1 shows the results of the gel fraction content determination. Gel fraction values for unmodified material and at a content of 0.25 and 0.5 moles of citric acid oscillate between 90-95%. For PSBS containing 0.75 and 1 mole of citric acid we observe a decrease in the gel fraction value

Differential DSC scanning calorimetry was performed to determine the thermal properties of poly(sorbitol sebacate- co-

---

• *Marta Piątek-Hnat, Ph D, West Pomeranian University of Technology Szczecin, Polymer Institute, Division of  Functional Materials and Bio-materials, Poland*
*E-mail: marp@zut.edu.pl*

butylene sebacate). (PSBS) with a different molar content of citric acid.



Fig. 1. Gel fraction of poly(sorbitol sebacate-co- butylene sebacate) (PSBS) with 0,25; 0,5; 0,75; 1 mol citric acid, where: KS- sebacic acid, BD- butylene glycol (1,4- butanediol), SB- sorbitol, KC- citric acid.
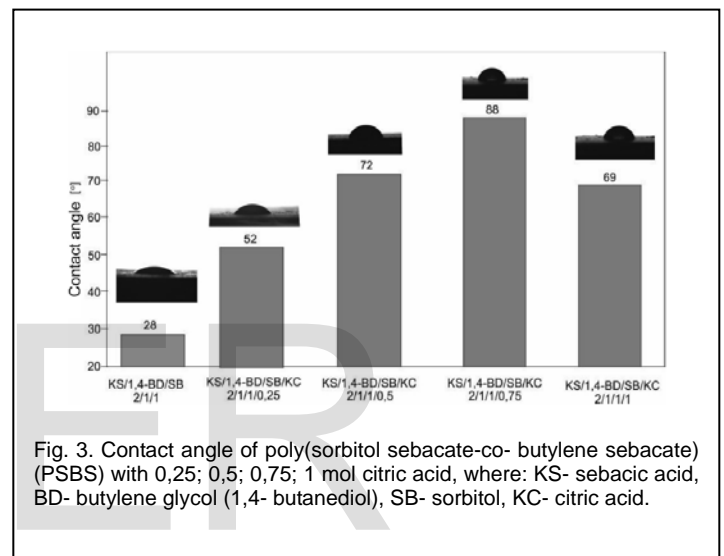
DSC thermograms (Fig. 2) of the obtained materials, a low-temperature transformation can be observed which is associated with the transformation of the glass transition of the amorphous phase. The glass transition temperature ($T_g$) associated with this transformation oscillates between -34 ° C and -17 ° C. It can be seen that as its content increases, its value increases. The DSC thermogram of elastomers with a content of 0.75 and 1 mole of citric acid at 57 °C has an endothermic peak associated with the melting temperature of the crystalline phase probably derived from sebacic acid. The results of these tests correspond very well with the analysis of gel fraction content, where it was observed a decrease in materials with a content of 0.75 and 1 mole of citric acid.
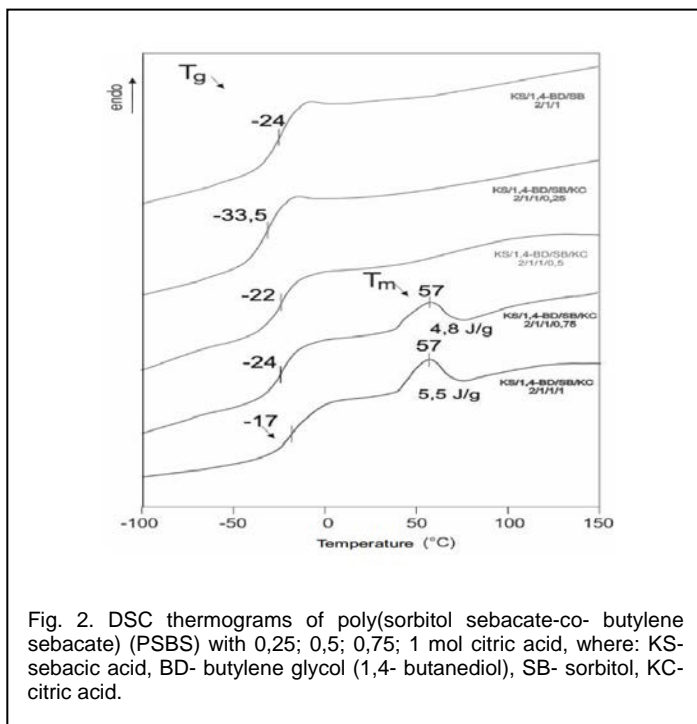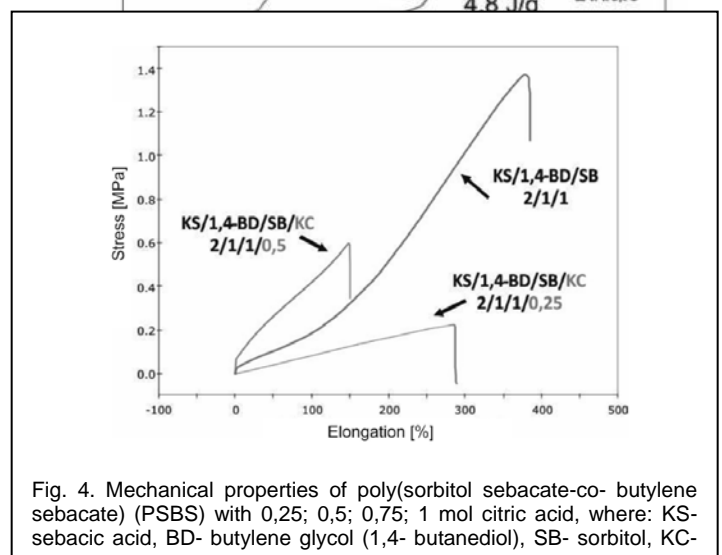
The surface properties (Fig.3.) of poly(sorbitol sebacate- co- butylene sebacate) (PSBS) All obtained elastomers are characterized by the hydrophilic nature of the surface, while the lowest value of the contact angle was observed for unmodified PSBS and containing 0.25 moles of citric acid

Fig. 4 presents the results of tests of mechanical properties for PSBS unmodified and modified with 0.25 and 0.5 moles citric acid. On the basis of the obtained results of mechanical tests, it can be stated that the unmodified material is characterized by stress values up to breakage of 1.4 MPa and elongation to break at the level of approx. 400%. After modification with 0.25 and 0.5 mol of citric acid, the value of both tension and elongation decreases.



Fig. 3. Contact angle of poly(sorbitol sebacate-co- butylene sebacate) (PSBS) with 0,25; 0,5; 0,75; 1 mol citric acid, where: KS- sebacic acid, BD- butylene glycol (1,4- butanediol), SB- sorbitol, KC- citric acid.



Fig. 2. DSC thermograms of poly(sorbitol sebacate-co- butylene sebacate) (PSBS) with 0,25; 0,5; 0,75; 1 mol citric acid, where: KS- sebacic acid, BD- butylene glycol (1,4- butanediol), SB- sorbitol, KC- citric acid.



Fig. 4. Mechanical properties of poly(sorbitol sebacate-co- butylene sebacate) (PSBS) with 0,25; 0,5; 0,75; 1 mol citric acid, where: KS- sebacic acid, BD- butylene glycol (1,4- butanediol), SB- sorbitol, KC- citric acid.

## 4 CONCLUSION

The study examined physicochemical properties (PSBS) with the participation of 0.25-1 molar citric acid. It can be concluded that the PSBS obtained with 0.25 and 0.5 moles of KC is characterized by the most optimal physicochemical properties. As a result of the conducted tests, it was found that the use of sorbitol and variable molar fraction of citric acid allows obtaining ester materials with interesting properties. The ester materials obtained are characterized by high hydrophilicity and, despite the high content of the gel fraction (high degree of cross-linking), they are susceptible to hydrolytic degradation.

## REFERENCES

[1] Sundback, C.A.; Shyu, J.Y.; Wang, Y.; Faquin, W.C.; Langer, R.;Vacanti, J.P.,Hadlock, T.A.; Biomaterials, 2005, 26, 5454-5464

[2] Qi-Zhi Chen, Alexander Bismarck, Ulrich Hansen, Sarah Junaid, Michael Q. Tran, Siân E. Hardingb, Nadire N. Ali, Aldo R. Boccaccini; Biomaterials, 29 (2008) 47–57

[3] Wang YD, Kim YM, Langer R.: J Biomed Mater Res A 2003;66A(1):192–7 Motlagh D, Yang J, Lui KY, Webb AR, Ameer GA.: Biomaterials 2006;27(24):4315–24

[4] Bettinger CJ, Orrick B, Misra A, Langer R, Borenstein JT.: Biomaterials 2006;27(12):2558–65.

[5] Behl M., Lendlein A.: Materials Today, April 2007

[6] Y. Hu, D.W. Grainger, S.R.Winn, O. Hollinger, J. Biomed. Mater. Res. 59,563 (2002)

[7] J. P. Bruggeman, Ch. J. Bettinger, Ch. L. E. Nijst, D. S. Kohane, R. Langer,, Adv. Mater. 2008, 20, 1922–1927

[8] J. P. Bruggeman, Ch. J. Bettinger, R. Langer,, Journal of Biomedical Materials Research, Volume 95A, Issue 1, 2010, 92-104

[9] Paturej M., El Fray M.: Polish Journal of Applied Chemistry LIII, no. 1, (2009) 73-78

[10] M Piątek-Hnat, J. Pilip, K. Gorący, M. Terebelska, E. Kaczmarek, A. Wojciechowska, M. Jędrzejczyk. Tworzywa Sztuczne w Przemyśle, nr 5/2015, 50-52 (in polish)